



HAL
open science

**Commande prédictive distribuée pour la gestion de
l'énergie dans le bâtiment Distributed model predictive
control for energy management in building**

Mohamed Yacine Lamoudi

► **To cite this version:**

Mohamed Yacine Lamoudi. Commande prédictive distribuée pour la gestion de l'énergie dans le bâtiment Distributed model predictive control for energy management in building. Autre. Université de Grenoble, 2012. Français. NNT : 2012GRENT097 . tel-00875593v3

HAL Id: tel-00875593

<https://theses.hal.science/tel-00875593v3>

Submitted on 22 Oct 2013

HAL is a multi-disciplinary open access archive for the deposit and dissemination of scientific research documents, whether they are published or not. The documents may come from teaching and research institutions in France or abroad, or from public or private research centers.

L'archive ouverte pluridisciplinaire **HAL**, est destinée au dépôt et à la diffusion de documents scientifiques de niveau recherche, publiés ou non, émanant des établissements d'enseignement et de recherche français ou étrangers, des laboratoires publics ou privés.

UNIVERSITÉ DE GRENOBLE

THÈSE

Pour obtenir le grade de

DOCTEUR DE L'UNIVERSITÉ DE GRENOBLE

Spécialité : **Automatique-Productique**

Arrêté ministériel : 7 août 2006

Présentée par

Mohamed Yacine LAMOUDI

Thèse dirigée par **Mazen Alamir**

et coencadrée par **Patrick Béguery**

préparée au sein du **Laboratoire GIPSA-Lab** et **Schneider-
Electric/Strategy & Innovation**

et de **L'ecole doctorale EEATS**

Commande prédictive distribuée pour la gestion de l'énergie dans le bâtiment

Distributed model predictive control for energy
management in buildings

Thèse soutenue publiquement le **29 Novembre 2012**,

devant le jury composé de :

Jean-Luc Thomas

Professeur titulaire de chaire au CNAM, Paris, Président

Hervé Guéguen

Professeur, Supelec Rennes, Rapporteur

Sorin Olaru

Professeur, Supelec Paris, Rapporteur

Mazen Alamir

Directeur de recherche, CNRS, Examineur

Patrick Béguery

Schneider-Electric / Strategy & Innovation, Grenoble, Examineur

Oskar Nilsson

Schneider-Electric / Buildings division, Malmö, Examineur



To my wife Kamélia and my parents,
for their love and support

Remerciements

Je tiens à remercier Monsieur Mazen Alamir -Directeur de recherche CNRS- qui a dirigé cette thèse tant pour ses qualités scientifiques et humaines: ses idées, ses conseils et les longues discussions que nous avons eu ont été d'une grande importance pour le bon déroulement du travail. Mes remerciements s'adressent aussi à Monsieur Patrick Béguery - Strategy & Innovation Schneider Electric- pour son appui, ses conseils et son implication au quotidien dans le travail.

Je tiens aussi à remercier Monsieur Jean-Luc Thomas, Professeur de chaire au Conservatoire National des Arts et Métiers d'avoir accepté de présider le jury de thèse. Que messieurs le rapporteurs, Professeur Sorin Olaru et Professeur Hervé Guéguen soient remerciés pour les remarques et questions pertinentes qui ont permis d'améliorer la qualité du travail.

Je tenais aussi à remercier Monsieur Oskar Nilsson - Schneider Electric/Buildings, d'avoir accepté d'examiner la thèse, ses conseils et nos échanges fréquents ont été d'une grande importance tout au long de la thèse.

De même, je tiens à remercier tous les membres de l'équipe HOMES pour la formidable ambiance de travail qui aura régné tout au long de ces années avec une pensée toute particulière pour Messieurs Didier Pellegrin et François Bonnard, Directeurs successifs du programme HOMES qui m'ont offert la chance d'entreprendre ce travail.

Je tiens aussi à remercier Monsieur Claude Le Pape - Schneider Electric, pour ses conseils tant sur la forme et que sur le fond de la thèse. Que monsieur Franck Bernier -Schneider Electric, soit remercié pour implication déterminante dans la partie implantation sur la RoomBox.

Finalement, une pensée toute particulière pour mon épouse Kamélia et mes parents pour leur appui et leur présence tout au long de ces années de travail. Cette thèse leur est dédiée.

*M. Y. Lamoudi
Grenoble, le 1^{er} Décembre 2019.*

Résumé

À l'heure actuelle, les stratégies de gestion de l'énergie pour les bâtiments sont principalement basées sur une *concaténation de règles logiques*. Bien que cette approche offre des avantages certains, particulièrement lors de sa mise en œuvre sur des automates programmables, elle peine à traiter la diversité de *situations complexes* qui peuvent être rencontrées (prix de l'énergie variable, limitations de puissance, capacité de stockage d'énergie, bâtiments de grandes dimension).

Cette thèse porte sur le développement et l'évaluation d'une commande prédictive pour la gestion de l'énergie dans le bâtiment ainsi que l'étude de l'embarcabilité de l'algorithme de contrôle sur une cible temps-réel (Roombox - Schneider-Electric).

La commande prédictive est basée sur l'utilisation d'un modèle du bâtiment ainsi que des prévisions météorologiques et d'occupation afin de déterminer la séquence de commande optimale à mettre en œuvre sur un horizon de prédiction glissant. Seul le premier élément de cette séquence est en réalité appliqué au bâtiment. Cette séquence de commande optimale est obtenue par la résolution *en ligne* d'un problème d'optimisation. La capacité de la commande prédictive à gérer des systèmes multivariables contraints ainsi que des objectifs économiques, la rend particulièrement adaptée à la problématique de la gestion de l'énergie dans le bâtiment.

Cette thèse propose l'élaboration d'un schéma de commande distribué pour contrôler les conditions climatiques dans chaque zone du bâtiment. L'objectif est de contrôler simultanément: la température intérieure, le taux de CO₂ ainsi que le niveau d'éclairage dans chaque zone en agissant sur les équipements présents (CVC, éclairage, volets roulants). Par ailleurs, le cas des bâtiments multi-sources (par exemple: réseau électrique + production locale solaire), dans lequel chaque source d'énergie est caractérisée par son propre prix et une limitation de puissance, est pris en compte. Dans ce contexte, les décisions relatives à chaque zone ne peuvent plus être effectuées de façon indépendante. Pour résoudre ce problème, un mécanisme de coordination basé sur une décomposition du problème d'optimisation centralisé est proposé. Cette thèse CIFRE ¹ a été préparée au sein du laboratoire Gipsa-lab en partenariat avec Schneider-Electric dans le cadre du programme HOMES (www.homesprogramme.com).

¹Convention Industrielle de Formation par la REcherche

Abstract

Currently, energy management strategies for buildings are mostly based on a *concatenation* of logical rules. Despite the fact that such rule based strategy can be easily implemented, it suffers from some limitations particularly when dealing with complex situations. This thesis is concerned with the development and assessment of Model Predictive Control (MPC) algorithms for energy management in buildings. In this work, a study of implementability of the control algorithm on a real-time hardware target is conducted beside yearly simulations showing a substantial energy saving potential. The thesis explores also the ability of MPC to deal with the diversity of *complex* situations that could be encountered (varying energy price, power limitations, local storage capability, large scale buildings).

MPC is based on the use of a model of the building as well as weather forecasts and occupancy predictions in order to find the optimal control sequence to be implemented in the future. Only the first element of the sequence is actually applied to the building. The best control sequence is found by solving, at each decision instant, an *on line optimization problem*. MPC's ability to handle constrained multivariable systems as well as economic objectives makes this paradigm particularly well suited for the issue of energy management in buildings.

This thesis proposes the design of a distributed predictive control scheme to control the indoor conditions in each zone of the building. The goal is to control the following simultaneously in each zone of the building: indoor temperature, indoor CO₂ level and indoor illuminance by acting on all the actuators of the zone (HVAC, lighting, shading). Moreover, the case of multi-source buildings is also explored, (e.g. power from grid + local solar production), in which each power source is characterized by its own dynamic tariff and upper limit. In this context, zone decisions can no longer be performed independently. To tackle this issue, a coordination mechanism is proposed. A particular attention is paid to computational effectiveness of the proposed algorithms. This CIFRE² Ph.D. thesis was prepared within the Gipsa-lab laboratory in partnership with Schneider-Electric in the scope of the HOMES program (www.homesprogramme.com).

²Convention Industrielle de Formation par la REcherche

Notations and acronyms

Notations

$\leq, \geq, =$	element-wise operators
$=:$	definition
$\langle \cdot, \cdot \rangle$	scalar product
$\text{card}\{E\}$	cardinal (number of elements) of the set E
v^T	vector or matrix transpose
$\ v\ $	any norm of the vector v
$\ v\ _\infty$	l_∞ norm of the vector v
$\ v\ _1$	l_1 norm of the vector v
$\ v\ _2$	l_2 norm of the vector v
$ v $	element-wise absolute value of v
$\Pi_j(\mathbf{v})$	selection operator
$\Pi_{[j_0:j_1]}(\mathbf{v})$	selection operator
$\text{diag}\{M_0, \dots, M_j\}$	diagonal (or block-diagonal) concatenation
$M_1 \otimes M_2$	Kronecker product (see below)
$v_1 \odot v_2$	Vectors element-wise product
\mathbf{I}	Identity matrix with appropriate dimension
\mathbf{I}_n	Identity matrix of dimension n
$\mathbf{0}$	zeros matrix with appropriate dimension
$\mathbf{0}_{n_i \times n_j}$	zero matrix of dimension $n_i \times n_j$, $\mathbf{0}_{n_i \times n_j} \in \mathbb{R}^{n_i \times n_j}$
$\mathbf{0}_{n_i}$	zeros matrix of dimension n_i , $\mathbf{0}_{n_i} \in \mathbb{R}^{n_i}$
$\mathbf{1}_{n_i}$	Ones matrix of dimension n_i , $\mathbf{1}_{n_i} \in \mathbb{R}^{n_i}$

Notations and acronyms

∞_{n_i}	Infinity matrix of dimension n_i , $\infty_{n_i} \in \mathbb{R}^{n_i}$
\check{J}	Convex approximation of the function J
\hat{J}	Concave approximation of the function J
g	gradient or subgradient
$\partial J(x)$	Subdifferential of the function J at x ($g(x) \in \partial J(x)$)
\mathfrak{B}	bundle

Kronecker product

Let $M_1 \in \mathbb{R}^{n_m \times n_p}$ and $M_2 \in \mathbb{R}^{n_q \times n_s}$. The Kronecker product $M_1 \otimes M_2$ is defined by:

$$M_1 \otimes M_2 := \begin{bmatrix} M_1(1,1) \cdot M_2 & M_1(1,2) \cdot M_2 & \dots & M_1(1,n_p) \cdot M_2 \\ M_1(2,1) \cdot M_2 & M_1(2,2) \cdot M_2 & \dots & M_1(2,n_p) \cdot M_2 \\ \vdots & \vdots & \vdots & \vdots \\ M_1(n_m,1) \cdot M_2 & M_1(n_m,2) \cdot M_2 & \dots & M_1(n_m,n_p) \cdot M_2 \end{bmatrix} \in \mathbb{R}^{(n_m \cdot n_q) \times (n_p \cdot n_s)}$$

examples: $\mathbf{I}_n \otimes M = \text{diag}\{\underbrace{M, \dots, M}_{n \text{ times}}\}, \quad \mathbf{1}_n \otimes M = \left. \begin{bmatrix} M \\ \vdots \\ M \end{bmatrix} \right\} n \text{ times}$

Acronyms

Building

BEMS	Buildings Energy Management System
BMS	Buildings Management System
D/R	Demand Response
FCU	Fan Coil Unit
HVAC	Heat Cooling and Air Conditioning
IAQ	Indoor Air Quality
OUE	Other Usage of Electricity
R-B	Rule-based control

Optimization

CPLEX	Optimization software (Ilog CPLEX)
GLPK	GNU linear mixed programming programming solver
LP	Linear Programming (optimization problem)
MILP	Mixed Integer Linear Programming (optimization problem)
NLP	Nonlinear Programming (optimization problem)
PWA	Piece Wise Affine (function)
QP	Quadratic Programming (optimization problem)
SOCP	Second Order Cone Programming (optimization problem)
SLP	Sequential Linear Programming (optimization problem)
SQP	Sequential Quadratic Programming (optimization problem)

Control theory

MIMO	Multi Input Multi Output (system)
SISO	Single Input Single Output (system)
LTI	Linear Time Invariant (system)
LTV	Linear Time Variant (system)
PID	Proportional Integral Derivative (controller)
MPC	Model Predictive Control

Notations and acronyms

NMPC Nonlinear Model Predictive Control
DMPC Distributed Model Predictive Control

Other

CSTB Centre Scientifique et Technique du Bâtiment
IEA International Energy Agency
SIMBAD SIMulator of Building And Devices

Contents

Notations and acronyms	xi
List of tables	xxii
List of figures	xxvii
1 General Introduction	1
1.1 The energetic context	1
1.2 Aims of the thesis	5
1.3 Outline of the thesis	7
1.4 List of publications	9
I Background	11
2 Building Energy Management Systems	13
2.1 Introduction	13
2.2 Conventional control	15
2.3 Introduction to Nonlinear Model Predictive Control	16
2.3.1 General notations	17
2.3.2 Nonlinear Model Predictive Control	18
2.3.3 Main features and benefits	20
2.4 MPC in buildings	20
2.4.1 Main benefits	21
2.4.2 MPC in buildings- main variants	24

Contents

2.5	Conclusion	29
3	Introduction to building modeling	31
3.1	Introduction	31
3.2	A brief description of SIMBAD simulation tool	32
3.3	Zone modeling	34
3.3.1	Zone model identification	36
3.3.2	Thermal model	38
3.3.3	CO ₂ model	38
3.3.4	Lighting model	40
3.4	Model identification	40
3.4.1	Identification approach	41
3.4.2	Identification results	42
3.5	Occupancy and Other Usage of Electricity (OUE)	44
3.5.1	Occupancy modeling	44
3.5.2	Other Usage of Electricity (OUE)	44
3.6	Conclusion	45
II	Zone Model Predictive Control	47
4	Zone MPC - Design and Real-Time implementation	49
4.1	Introduction - zone control	49
4.2	About occupants comfort	50
4.3	The Control Problem	52
4.4	Solving the optimization problem	58
4.4.1	Fixed-point algorithm	59
4.5	State and disturbance estimation	60
4.5.1	Model extension	61
4.5.2	Disturbance prediction	62
4.6	Convergence analysis	65
4.7	Input Parametrization and Output checking	67

4.8	Computational study	69
4.9	Simulations - some investigations	72
4.9.1	Zone MPC validation	73
4.9.2	Dealing with variable energy prices	74
4.9.3	Impact of prediction horizon length	76
4.9.4	Introducing uncertainty	77
4.10	Yearly simulation	82
4.10.1	Case study	82
4.10.2	Zone controllers integration in SIMBAD	83
4.10.3	Simulation results	84
4.11	Roombox implementation	88
4.12	Conclusion and further investigations	91
5	Zone Model Predictive Control - Fan Coil Unit management	93
5.1	Context and motivation	93
5.2	Fan Coil Unit (FCU) modeling	94
5.2.1	A general description	95
5.2.2	Zone modeling	97
5.3	The control problem	99
5.4	Solving the optimization problem	100
5.4.1	Piece-wise affine approximation	100
5.4.2	Fixed-point algorithm	102
5.5	Validation	104
5.6	Conclusion	106
III	Distributed Model Predictive Control	109
6	Distributed Model Predictive Control - Theoretical framework	111
6.1	Introduction	111
6.2	Problem statement	113
6.2.1	The subsystems	113

Contents

6.2.2	Resource sharing	115
6.3	Description of the approach	115
6.3.1	Problem Decomposition	116
6.4	Solving the master problem	117
6.4.1	Disaggregated bundle method	117
6.5	Distributing optimization over time	123
6.5.1	The correction mechanism	125
6.6	Theoretical results availability	127
6.7	Conclusion	130
7	Constrained DMPC for building energy management	131
7.1	Context and motivations	131
7.2	Problem description	135
7.3	Zone controllers	137
7.3.1	Zone models	137
7.3.2	Zone Model Predictive Control	138
7.3.3	Introducing local constraints	139
7.4	DMPC - the control problem	141
7.4.1	Global power limitation	142
7.4.2	Global power limitation and shared energy storage	143
7.4.3	Global power limitation, shared energy storage and shared inputs	147
7.5	Distributed Model Predictive Control	148
7.5.1	Solving the master problem	149
7.5.2	The stabilization term	150
7.6	Assessment of the bundle method	153
7.7	Simulations	154
7.7.1	Battery management and global power limitation	154
7.7.2	Computational time	160
7.7.3	Handling shared variables	160
7.7.4	Introducing uncertainty	161

7.8 Conclusion	164
General Conclusion	169
Appendices	175
A Résumé en français	175
A.1 Introduction	175
A.2 Commande prédictive non linéaire - rappels	176
A.2.1 Notations	176
A.2.2 Commande prédictive non linéaire	177
A.2.3 La commande prédictive dans le bâtiment	179
A.3 Commande prédictive de zone	181
A.3.1 Résolution du problème d'optimisation	187
A.3.2 Simulations	188
A.3.3 Implémentation sur contrôleurs temps-réel	190
A.4 Commande prédictive distribuée	190
A.4.1 Mise en œuvre de la commande prédictive distribuée	191
A.4.2 Introduction de contraintes de ressources locales	193
A.4.3 Introduction du mécanisme de coordination	194
A.4.4 Algorithme des plans coupants stabilisé	195
A.4.5 Résultats de simulations	198
A.5 Conclusion générale	199
B Linear programming problem matrices	201
C Prediction errors on d^C and d^L	203
D Yearly estimated disturbances	205
E Computational time for the 20 zones of the building	207

Contents

F C code and equivalent M code	209
Bibliography	211

List of Tables

Chapter 1 General Introduction	1
1.1 Energy dependency - all products (EU-27)	3
1.2 Installed capacity for electricity generation from renewables, EU-27 (GW)	4
Chapter 3 Introduction to building modeling	31
3.1 Description of Inputs/Outputs and exogenous variables related to one zone of the building.	35
Chapter 4 Zone MPC - Design and Real-Time implementation	49
4.1 Impact of parametrization on closed-loop performances	71
4.2 Energy invoice for different values of α	79
4.3 Invoices with the introduction of errors on occupation and weather forecast	81
4.4 Nominal comfort region	83
4.5 Energy consumption / Comfort - Rule-based vs. MPC	85
Chapter 5 Zone Model Predictive Control - Fan Coil Unit management	93
5.1 Fan coil unit parameters	97
5.2 Description of Input/Output and exogenous variables of a zone with a fan coil unit	98
Chapter 6 Distributed Model Predictive Control - Theoretical framework	111
6.1 Summary of optimization variants based on aggregation or not of the bundles and stabilization or not of the master problem.	123

Appendices	175
A.1 Entrées/Sorties et perturbations liées à une zone du bâtiment.	183
A.2 Consommation énergétique/ Confort - Règles expertes vs. MPC	189

List of Figures

Chapter 1 General Introduction	1
1.1 World energy consumption	2
1.2 World energy consumption outlook	3
Chapter 2 Building Energy Management Systems	13
2.1 Receding horizon principle	19
2.2 Model Predictive Control ingredients in buildings	21
2.3 Optimal start time illustration	23
2.4 Illustration of the usage of MPC with variable price energy	24
2.5 Zone representation	25
2.6 Illustration of the main equipment controlled at the energy layer.	26
2.7 Management of polygeneration system with MPC [Houwing et al. 2007]	27
2.8 The MAHAS system	27
Chapter 3 Introduction to building modeling	31
3.1 Building decomposition	33
3.2 Zones in a building. The zones vary in their structure, orientations and usage (occupancy schedules).	34
3.3 Building XML tree	35
3.4 Thermal-electrical analogy - simplified circuit	39
3.5 Simplified CO ₂ model - electrical analogy	40
3.6 Simplified indoor illuminance model - electrical analogy	41
3.7 Test building representation	42
3.8 Step response of the 20-zone building	43

List of Figures

3.9	Step responses of the 20-zone building - first hour	44
3.10	Simulated and identified model	45
3.11	Occupancy schedules in each zone	46
3.12	Other Usage of Electricity (OUE) profiles	46
Chapter 4 Zone MPC - Design and Real-Time implementation		49
4.1	Caption text appearing in lof	51
4.2	Comfort-related bounds on comfort parameters with respect to predicted occupancy profile.	56
4.3	Discomfort function	56
4.4	Estimated disturbances on two weeks	63
4.5	Disturbance prediction principle	64
4.6	Prediction errors comparison	65
4.7	Fixed-point algorithm convergence	66
4.8	Piece-wise constant parametrization of the predicted control profile and undersampling of the optimal predicted output.	67
4.9	Computational time vs. N_u^{par} for increasing horizon lengths	70
4.10	Computational time evolution ($N = 720, N_u^{par} = 20, N_y^{par} = 20$)	72
4.11	Zone predictive controller validation	73
4.12	On-peak/ Off-peak electricity price. parametrized by $\beta_p > 1$	74
4.13	Invoice minimization for different values of β_p	75
4.14	Invoice minimization for different values of β_p - (2)	76
4.15	Impact of horizon length on MPC performance	77
4.16	Mean error distribution on outdoor temperature forecast service for different values of α for a prediction horizon of 12[h].	78
4.17	Simulation results for $\alpha = \{0, 0.5, 1\}$ with perfectly known occupation profile	79
4.18	Presence probability (blue) and corresponding generated stochastic occupancy profile (green).	80
4.19	Markov chain of occupancy in a zone	81
4.20	Simulation results with uncertainties on weather ($\alpha = \{0, 0.5, 1\}$) and occupation profile	82
4.21	MPC integration in SIMBAD - workflow	84

4.22 MPC vs. RB monthly energy consumptions	85
4.23 MPC vs. Rule-based control - temperature profiles in an office during the two first weeks	86
4.24 MPC vs. Rule-based control - temperature profile in a meeting room during the two first weeks	86
4.25 MPC vs. RB- yearly building average temperature	87
4.26 MPC vs. Rule-based control	88
4.27 Office Roombox (Schneider-Electric)	88
4.28 Roombox - memory and CPU usage	90
4.29 RoomBox implementation steps	91
Chapter 5 Zone Model Predictive Control - Fan Coil Unit management	93
5.1 Zone fan coil units. The FCUs are parallel-connected.	94
5.2 Fan Coil Unit representation	95
5.3 Heat emission characteristic function ϕ^N of an FCU	96
5.4 Piece-wise affine approximation of ϕ^N with $n_a = 5$ regions	101
5.5 Subgraph of $\hat{\phi}(u_w, u_f)$	105
5.6 Energy price profiles used in simulations	105
5.7 Zone #18 - Boiler.	107
5.8 Zone #18 - Heat Pump (COP=2).	107
5.9 Zone #18 - Heat Pump (COP=3.5).	107
5.10 Zone #1 - Boiler.	108
5.11 Zone #1 - Heat Pump (COP=2).	108
5.12 Zone #1 - Heat Pump (COP=3.5).	108
Chapter 6 Distributed Model Predictive Control - Theoretical framework	111
6.1 Hierarchical Distributed Model Predictive Control	116
6.2 Representation of J_ℓ and its piece-wise linear approximation $\check{J}_\ell^{(3)}$. . .	119
6.3 Stabilization terms. (a): quadratic stabilization term. (b): trust region. (c): stabilized trust region.	121
6.4 Effect of the memory factor on the first approximation of the function .	125
6.5 Hierarchical Distributed Model Predictive Control scheme.	127
6.6 Illustration of the DMPC algorithm	129

List of Figures

Chapter 7 Constrained DMPC for building energy management	131
7.1 Illustration of the current electricity grid.	132
7.2 Power dependant energy rating	134
7.3 Constrained Distributed Model Predictive in a multi-zone building . .	136
7.4 Zone layer and Energy layer	144
7.5 Stabilization term ($\Delta \mathbf{r}_\ell = \mathbf{r}_\ell - \bar{\mathbf{r}}_\ell^{(s)}$).	150
7.6 Illustration of the coordination mechanism in the building	152
7.7 Bundle algorithm assessment	155
7.8 Comparison of performance of the DMPC algorithm with and without distributed-in-time feature	156
7.9 DMPC with a battery management and power limitation	158
7.10 Centralized control with battery management and power limitation on a 20-zone building	159
7.11 Computation time- DMPC	161
7.12 Shared ventilation system	162
7.13 DMPC with a shared input actuator	163
7.14 Performance comparison between DMPC with and without memory for different values of maximum number of iterations.	165
Appendices	175
A.1 Commande à horizon glissant	178
A.2 Décomposition du bâtiment- niveau énergie et niveau zone	180
A.3 Commande prédictive dans le bâtiment - les ingrédients	181
A.4 Représentation d'une zone du bâtiment	182
A.5 Bornes de confort.	185
A.6 Fonction d'inconfort	185
A.7 Validation du contrôleur prédictif de zone	189
A.8 Office Roombox (Schneider-Electric)	190
A.9 Commande prédictive distribuée - Mise en œuvre sur un bâtiment mul- tizonne équipé d'un système de stockage électrique et soumis à une con- trainte de puissance consommée.	193
A.10 Approximation par plans coupants de la fonction J_ℓ	196
A.11 Stabilization term ($\Delta \mathbf{r}_\ell = \mathbf{r}_\ell - \bar{\mathbf{r}}_\ell^{(s)}$).	197

A.12	Commande prédictive distribuée - schéma fonctionnel	198
A.13	Simulation de la commande distribuée sur un bâtiment de 20 zones . .	199
C.1	Prediction errors comparison d^C	203
C.2	Prediction errors comparison d^L	204
D.1	Estimated disturbances 1 year	206
E.1	Computational burden - 20 zones	208

Chapter 1

General Introduction

" Other factors remaining constant, culture evolves as the amount of energy harnessed per capita per year is increased, or as the efficiency of the instrumental means of putting the energy to work is increased. ... We may now sketch the history of cultural development from this standpoint ".

–Leslie White, "White's Law", 1949.

1.1 The energetic context

Overview

Exploitation of fossil fuels has led to tremendous transformations in society. It is probably responsible for more changes, from the end of the 19th century to the present day, than throughout the rest of the history of humanity.

Energy is at the heart of our *modern civilization*. Transport, communication, industry, ... belong to the numerous examples that show our extreme dependence on energy. Indeed, its availability largely determines the sustainability of human civilization.

For decades, abundant and cheap energy resources have led to extraordinary advances and profound changes in our civilization. However, this era is now over. Accessible fossil energy stocks are dramatically decreasing, creating more and more geopolitical and economic tensions. Moreover, global warming is a major issue today, which, in the last fifteen years, has aroused the attention and concern of the international community and public opinion regarding energy stakes and greenhouse gas

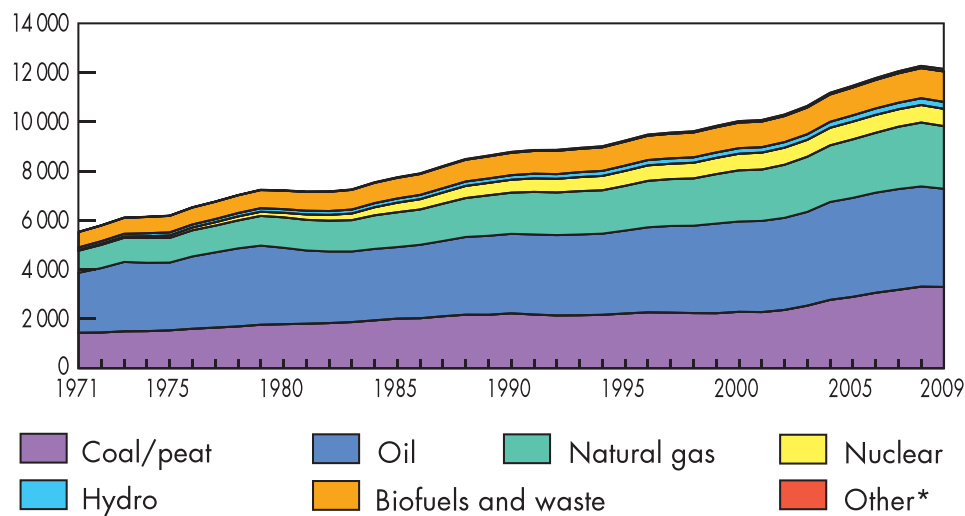


Figure 1.1 World energy consumption (source [IEA 2011a])

emission.

Reduction in energy consumption has now been proved to be *vital* as witnessed by numerous scientific researches conducted in recent decades, attesting clearly the direct impact of human activity on climate change. Indeed, current investigations are highlighting the critical issues that shape the energetic challenge of the 21th century:

- i. For environmental considerations, greenhouse gases emission needs to decrease,
- ii. Current energy mix is largely dominated by fossil resources (80%) (figure 1.1) which are responsible for 65% of greenhouse gases emissions. Moreover, current projections of IEA [IEA 2011b] show that this dependency remains stable until 2035;
- iii. Fast growth of *new* economies implies an increasing energy consumption in the next decades (figure 1.2). Actually, according to IEA, energy consumption growth from 2009 to 2035 is estimated to over 40% (figure 1.2). 90% of this increase is due to non-OECD¹ countries (23% to China alone) [IEA 2011b].

Beside these considerations, the supply of European energy is largely dependent on importations. Currently, Europe produces less than half of its energy. Moreover, European energetic dependency² (EU-27) has constantly increased as reported by EuroStat [EuroStat 2010] at a rate of 9% from 1998 to 2008 to reach 54.8% (table 1.1).

¹OECD: Organization for Economic Co-operation and Development

²energetic dependency = $\frac{\text{energy importation}}{\text{energy consumption}} [\%]$

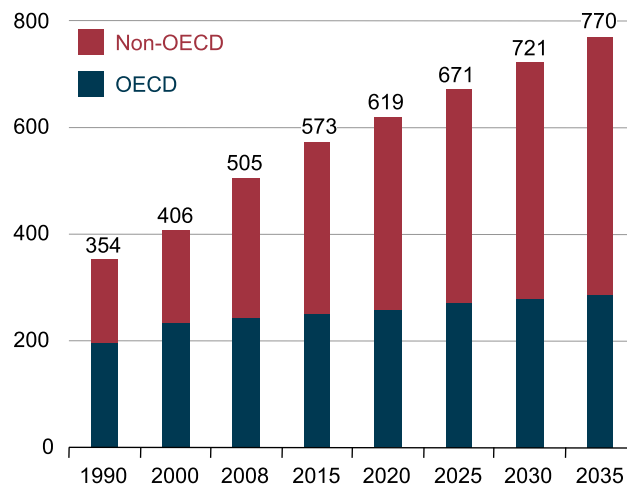


Figure 1.2 World energy consumption outlook [quadrillion btu]. (source [IEA 2011b])

Year	1998	1999	2000	2001	2002	2003	2004	2005	2006	2007	2008
E.D [%]	46.1	45.2	46.8	47.5	47.6	49.0	50.3	52.6	53.8	53.1	54.8
O.D [%]	77.0	73.0	75.8	77.5	76.0	78.5	79.9	82.4	83.7	82.5	84.3
G.D [%]	45.6	47.9	48.9	47.3	51.2	52.5	54.0	57.7	60.8	60.3	62.3

Table 1.1 Energy dependency - all products (EU-27) - E.D: total energy dependency - O.D: oil dependency - G.D: gas dependency (source: Eurostat online data code: nrg_100a [IEA 2011b])

All these arguments fully justify the EU’s 20-20-20 commitments (20% increase in energy efficiency, 20% reduction of CO₂ emissions, and 20% renewables by 2020 compared to 1990 levels).

To meet these goals, *greener* alternatives to fossil resources are gradually being introduced. It is a fact that the EU-27 experienced a continual growth rate (6.4%) of installed renewables between 1998 and 2008 (table 1.2).

Nevertheless, even if the total contribution of renewables to electricity in Europe increased by 45% during this period, its impact on total consumption is fairly moderate³. As a matter of fact, renewables alone are not sufficient to solve the energy issue [European Commission 2003].

³a growth of only 3% (from 13.4% in 1998 to 16.7% in 2008).

Year	1998	2000	2002	2004	2006	2008	change (98-08)
Total	150	161	177	191	216	245	+64%
Hydro	134	136	141	138	140	143	+6%
Wind	6	13	23	34	48	64	+935%
Wood	5	6	6	8	12	14	+168%
Other	4	6	7	10	16	24	+487%

Table 1.2 Installed capacity for electricity generation from renewables, EU-27 (GW) (Source: Eurostat online data code: nrg_113a). Wind generation capacity undergone the most growth ($\times 10$).

Building energy consumption issue

According to [IEA 2011b], buildings (combining households and tertiary) account for 40% of world-wide⁴ primary energy consumption⁵. Moreover, IEA forecasts that it will experience a world-wide yearly growth of 1.1% in future decades [IEA 2011b].

The above accounts for the concern with building energy consumption and the attention paid to its key role in the future. Policy makers are extremely aware of the importance of this issue [European Commission 2010, U.S. Congress 1992]. In fact, implementation of legislation specific to buildings has led to a renewed interest in this issue by both the industrial and the academic communities. Consequently, the large number of research projects concerning energy management of buildings driven by continuous advances and deployment of energy-aware solutions make this issue a particularly strategic and competitive sector for industrial firms.

Several approaches have been investigated to enhance energy performance of buildings. In short, *passive energy efficiency* basically consists in acting on the intrinsic characteristics of the building, both at the design stage and during the building life by refurbishments. However building refurbishments are extremely costly. In *active energy efficiency* better control strategies are implemented to reduce utilization of energy without decreasing comfort.

Although energy efficiency of buildings continues to be the first goal, buildings represent inherently a huge energy stock from the grid perspective. Their ability to store energy in a thermal form (passive storage) as well as in dedicated equipment (active storage) makes them undeniably a crucial component of the so called smart grids (discussed in chapter 7).

Hence, electricity grid managers can make use of this huge *storage feature* by send-

⁴40% also in EU, [European Commission 2010].

⁵It increased by 39% between 1973 and 2003 in IEA countries [IEA 2011b].

ing some Demand/Response (D/R) signals to adjust their consumption. Roughly speaking, buildings provide a great opportunity of implementing *smarter* utilization strategies of energy if they can be *responsive*⁶ to such D/R signals.

Therefore, the building energy issue is not only about saving energy by deploying increasingly more energy efficiency solutions, but also by making them smart grid aware.

1.2 Aims of the thesis

This work is concerned with the development and assessment of Model Predictive Control algorithms (MPC) for energy management in buildings. Furthermore, a study on implementability of the control algorithm on a real-time hardware target is conducted. In light of the above discussion, the thesis explores the ability of MPC to deal with the diversity of *complex* situations that could be encountered (varying energy price, power limitations, local storage capability, large scale buildings).

Currently, energy management strategies for buildings are mostly based on a *concatenation* of logical rules. Despite the fact that such rule-based strategies can be easily implemented, they suffer from some major drawbacks (a) each rule involves some internal parameters that need to be adjusted (b) it becomes quickly complicated to ensure the consistency of the control algorithm when it implements a large number of such rules (c) this approach is not suited to deal explicitly with economic objectives (d) buildings are becoming more complex, incorporating more equipment and capabilities than before.

Despite the fact that many control strategies have been investigated, no real solution has yet been found for the problem of energy management in buildings. Nevertheless, Mode Predictive Control clearly emerges as a promising technology for building control.

MPC is based on use of a building model as well as on weather forecasts and occupancy predictions in order to find the optimal control sequence to be implemented in the future. Only the first element in the sequence is actually applied to the building. At the next decision instant, a new optimal control sequence is computed, as so on. The best control sequence is found by solving, at each moment in the decision process, an *on line optimization problem*. MPC's ability to handle constrained multivariable systems as well as economic objectives makes this paradigm particularly well suited for the issue of energy management in buildings.

Model predictive control for building energy management has been widely stud-

⁶in chapter 7, more detailed explanations are provided.

ied. However, most studies:

- Focused generally on the thermal aspect;
- Do not consider equipment with nonlinear characteristics;
- Generally consider only one zone of a building and thus do not include in the decision process the possible couplings that may occur;
- Generally propose a centralized control scheme, which is quite unrealistic and unsafe when there is a large number of zones in the building.

To overcome the above-mentioned limitations, this thesis proposes the design of a distributed predictive control scheme to control the indoor conditions in each zone of the building while meeting global power limitations as well as managing storage equipment and shared actuators among zones. The goal is to control the following simultaneously in each zone of the building: indoor temperature, indoor CO₂ level and indoor illuminance by acting on all the actuators of the zone (HVAC, lighting, shading).

Moreover, the case of multi-source buildings (e.g.: power from grid + local solar production), in which each power source is characterized by its own dynamic tariff and upper limit, is considered. In this context zone decisions can no longer be performed independently. To tackle this issue a coordination mechanism based on a primal decomposition of the centralized optimization problem is proposed. A particular attention is paid to computational effectiveness of the proposed algorithms. Moreover, a new *distributed-in-time optimization* feature is proposed to limit the communication rates and computational burden between the agents in the building and therefore to propose a real-time implementable solution. To the best of our knowledge, such a feature has not been proposed before. The originality of our contribution lies in the simultaneous handling of these features.



www.homesprogramme.com

This Ph.D. thesis was prepared within the Gipsa-lab and Schneider-Electric in the scope of the HOMES program (www.homesprogramme.com). Led by Schneider-Electric, this collaborative industrial research program targets energy efficiency in buildings.

1.3 Outline of the thesis

The manuscript is organized as follows⁷:

Part I Background

This first part presents some basics of building modeling followed by an introduction to energy management systems in buildings and model predictive control for building applications.

Chapter 2 Building Energy Management Systems

This chapter briefly sets out the main solutions related to predictive control for energy management in buildings. Following a short presentation of the general principle of predictive control with emphasis on its critical features, the main reasons for adopting this paradigm in buildings are then described along with the major variants identified.

Chapter 3 Introduction to building modeling

The main aim of this chapter is to give a concise overview of building models and the simulation environment SIMBAD used in this work. As the focus of this thesis is the design of model-based controllers, emphasis is placed on structural features of the models as they will be used later on in the second part to design predictive controllers.

Part II Zone Model Predictive Control

In this part, two control layers will be proposed to implement MPC in buildings. The goal here is the design of the zone controllers (low layer) further integrated in part III to the control structure as a whole.

⁷A french abstract of thesis is provided in appendix A.

Chapter 4 Zone MPC - Design and Real-Time implementation

Focusing on one zone of the building, the goal is to ensure comfort of occupants at minimum operational cost. Since the whole set of available actuators in a given zone is controlled to ensure multi-variable comfort, this chapter shows that the MPC-related optimization problem is a non-convex optimization problem that has to be solved efficiently. **Simulations on a 20-zone building show that energy savings could achieve 16 % for perfectly known temperature forecast and 14 % when forecast is uncertain. Real-time implementability of the proposed control algorithm is also validated on a Schneider-Electric controller (Roombox).**

Chapter 5 Zone Model Predictive Control - Fan Coil Unit management

This chapter extends the previously designed zone model predictive controller to manage fan coil units. As will be discussed, a fan coil unit exhibits a nonlinear heat emission characteristic. It will be shown that this characteristic can be approximated by a PWA function that can be easily handled through linear programming.

Part III Distributed Model Predictive Control

When dealing with medium/large scale buildings, designing a centralized solution is impractical. In this part, a distributed model predictive control strategy is presented, with in particular, the design of the higher control layer (coordinator).

Chapter 6 Distributed Model Predictive Control - Theoretical framework

This chapter presents a hierarchical model predictive control framework for a network of subsystems submitted to general resource sharing constraints. The method is based on a primal decomposition of the centralized problem over several subsystems. A coordination agent is responsible for adjusting the parameters of the problems that are to be solved by each subsystem to ensure that some global resource constraint on the whole system is respected. Our main contribution consists of the introduction of a new distributed-in-time feature combined with a bundle algorithm. The aim here is to ensure sufficient performance at a fairly cheap communication cost by reducing

the number of exchanges in order to enable real-time implementation of the proposed approach.

Chapter 7 Constrained DMPC for building energy management

The control scheme presented in chapter 6 is then applied in this chapter on an energy coordination problem in a multi-zone building in which the zones have to share a limited amount of power as well as centralized energy storage equipment (electric battery) and shared actuators. Effectiveness of the scheme to deal with these issues is illustrated.

General conclusion

The general conclusion gathers the most pertinent results and the main contribution of the thesis. The main challenges facing implementation of Model Predictive Control in buildings are then presented with some related works regarding each of these issues.

1.4 List of publications

Conferences

1. M. Y. Lamoudi, M. Alamir, and P. Béguery. Distributed constrained model predictive control based on bundle method for building energy management. In *50th IEEE Conference on Decision and Control and European Control Conference- Orlando, 2011*.
2. M. Y. Lamoudi, M. Alamir, and P. Béguery. Unified NMPC for multi-variable control in smart buildings. In *IFAC 18th World Congress, Milano, Italy, 2011*.
3. M. Y. Lamoudi, M. Alamir, and P. Béguery. Model predictive control for energy management in buildings- part 1: zone model predictive control. In *IFAC conference on Nonlinear Model Predictive Control, 2012*.
4. M. Y. Lamoudi, M. Alamir, and P. Béguery. Model predictive control for energy management in buildings- part 2: Distributed model predictive control. In *IFAC conference on Nonlinear Model Predictive Control, 2012*.

Chapter 1. General Introduction

5. M. Y. Lamoudi, P. Béguery, and M. Alamir. Use of simulation for the validation of a predictive control strategy. In *12th International IBPSA Conference , Sydney, Australia, 2011.*
6. P. Béguery, M. Y. Lamoudi, O. Cottet, O. Jung, N. Couillaud, and D. Destruel. Simulation of smart buildings HOMES pilot sites. In *12th International IBPSA Conference , Sydney, Australia, 2011.*

Book chapter

1. M. Y. Lamoudi, M. Alamir, and P. Béguery. A distributed-in-time NMPC-based coordination mechanism for resource sharing problems. Chapter in *Distributed Model Predictive Control made easy. Springer Verlag, 2012.* (to appear)

Schneider-Electric white papers

1. M. Y. Lamoudi, P. Béguery, O. Nilsson and B. Leida. Model Predictive Control - toward smarter energy management systems. *White paper, Schneider-Electric, Jan. 2012.*

Patents

1. M. Y. Lamoudi, P. Béguery, and M. Alamir. Procédé de commande pour gérer le confort d'une zone d'un bâtiment selon une approche multicritères et installation pour la mise en œuvre du procédé, 2011.
2. C. Guyon, M. Y. Lamoudi and P. Béguery, Procédé et dispositif de répartition de flux d'énergie électrique et système électrique comportant un tel dispositif, 2012.

Part I

Background

Chapter 2

Building Energy Management Systems

Abstract

This chapter gives a concise state of the art of the main control solutions proposed for the energy management in buildings. This overview starts with a succinct presentation of conventional building control strategies. Then, the general principle of predictive control with emphasis on its critical benefits for our application is given. The main benefits of implementing this paradigm for Building Energy Management Systems (BEMS) are then exposed along with the major variants identified in the most pertinent references dealing with this topic.

2.1 Introduction

The thermostat, that was invented at the very early XXth century to control coil boilers, can be considered as the first *automated* thermal regulation system in buildings. Indeed, its introduction and its widespread usage makes it probably one of the most common control systems.

It can be disappointing to note that from that time and despite huge technological evolutions of control systems as well as large penetration of automation in buildings, thermal management systems have not seen spectacular evolutions from the purely algorithmic aspect as it has been the case in other areas like automotive industry for instance, in which the introduction of electronic drove much more algorithmic control developments.

The reasons of that are certainly numerous, but one may say that this is mainly due to the following facts:

- a. Buildings thermal systems, from a purely control aspect, are not challenging. Therefore simple controllers are sufficiently efficient when focusing exclusively on

thermal regulation;

- b. Energy management systems target energy reduction. Since for many decades energy costs were low, no real energetic policies have been carried-out, hence no real interest of both industrials and academics regarding building's energy consumption has been noticed;
- c. Unlike to production industry, each building is unique. This uniqueness makes the design of control algorithms that are simultaneously efficient and largely deployable extremely challenging.

Nevertheless, instead of thermal management, nowadays buildings include much more equipment and capabilities as lifts, fire alarms and much more complex HVAC¹ systems. This is basically the reason of the existence of Building Management Systems (BMS).

In the context of the present work, only BEMSs are targeted. BEMSs, which are generally part of BMS, are control systems dedicated to energy management in buildings.

BEMS refers both to the hard and the soft parts of the control system. It is mainly found in large buildings and largely dedicated to HVAC control, hot/chilled water production and storage management. More rarely, a BEMS can include lighting and blinds control.

Due to the huge consumption of the building area, which represents no less than 40% of total primary energy consumed in the world, and the widely carried out CO₂ emission reduction policy (see chapter 1), a great interest of the research community -especially in the last decade- led to a better understanding of the issues related to building energy management.

In spite of the fact that many control strategies have been investigated, the problem of energy management in buildings remains essentially open, as it is attested by [Dounis & Caraiscos 2009] where a good overview of the main advanced control techniques studied until now and a discussion on conventional control are presented.

It goes without saying that an exhaustive review of the existing control strategies and the ones proposed in literature goes beyond the scope of this chapter. Nevertheless it is important to point-out the emergence of model predictive control as a particularly adapted approach for building energy management [Cooperman et al. 2010]. Some crucial benefits of this paradigm are presented in this chapter.

Before an introduction to model predictive control in buildings which is at the heart of the present work in section 2.3, the section 2.2 first gives, for completeness of

¹HVAC: Heating Ventilation and Air Conditioning.

the presentation, an overview of the conventional control systems. In section 2.4, the major benefits arising from the implementation of MPC in buildings are introduced as well as the main identified variants of this technology in buildings. Section 2.5 concludes the chapter.

2.2 Conventional control

Conventional control methods are essentially based on a stack of control rules acting in a more or less coordinated fashion.

This kind of control systems, generally referred as *rule based control*, consists of a high logical control layer in which a set of rules of the type :

if *< condition >* then *< action >*

are implemented. These rules provide set points and/or control modes to low control loops that ensure local references tracking. The local controllers consist generally in PIDs or On/Off controllers.

As a major advantage of this approach, one may cite the "apparent" simplicity of such paradigm. Indeed, this set of rules is generally implemented by an expert that defines, based on a priori knowledge of the building, both the set of rules involved in the decision systems and the tuning parameters and thresholds involved in each rule (an example is given further in section 2.4.1). Furthermore, their implementation on real targets is extremely easy and fully adapted to current commercialized controllers. Beside these important advantages, many drawbacks of this approach can be enumerated:

1. The concatenation of a large number of rules leads to a large decision tree, it becomes therefore difficult to ensure the consistency of the proposed control system;
2. The number of tuning parameters involved in such schemes is high, which has the effect of complicating commissioning step,
3. The buildings are likely to become structurally more complex, incorporating more and more systems: possibilities of production/storage/resale and in a varying energy price context. For these complex situations a logical rule-based system reaches its limits given the "quantitative" and "proactive" specificity of the control decisions to be undertaken.

To overcome these limitations, many authors advocate to address the issue from a radically different perspective. The idea is not to find the best action (rule) to be undertaken in a given situation, but to model the building while expressing an objective (minimize energy and maximize comfort) as an optimization problem.

The resolution of the latter optimization problem leads to an optimal plan of action which is regularly updated thanks to new measurements and predictions of the most pertinent variables acting on the building.

It turns out that this paradigm called Model Predictive Control (MPC) is particularly suitable for our purpose, as evidenced in the multitude of works referenced around this issue that will be exposed throughout the chapter. The following section introduces Model Predictive Control.

2.3 Introduction to Nonlinear Model Predictive Control

This section is an introduction to model predictive control. It provides only the essential material required in the sequel.

Model Predictive Control (also referred to as Receding Horizon Control) is an advanced control methodology relying on the use of a *internal model* of the process.

This internal model (also called control model) synthesizes the dynamics of the process to be controlled. In MPC, this representation is used to find the optimal control sequence to be applied to the model in order to minimize some objective function beside respecting a set of operational constraints. The constraints may be related for instance to limitations on the actuators and/or the states of systems.

Model Predictive Control has experienced in the past twenty years remarkable progress [Mayne et al. 2000] both from theoretical aspects and regarding practical issues giving rise to thousands of successful industrial applications (chemical processes, food industry, automotive etc.). In [Qin & Badgwell 2003] an overview of the main referenced applications of MPC is given.

Numerous variants of this technique have emerged in the recent decades: starting from the classical MPC applied to linear systems with quadratic objective functions to much more complex variants where the resulting optimization problem is no longer complying with the convexity properties of the first case and for which more advanced optimization methods must be implemented. The latter case results from situations in which the model of the process is nonlinear, it is more commonly known as Nonlinear Model Predictive Control (NMPC).

2.3.1 General notations

Consider the following general nonlinear dynamical system, given in its discrete-time form:

$$x_{k+1} = f(x_k, u_k, w_k) \quad (2.3.1a)$$

$$y_k = h(x_k, u_k, w_k) \quad (2.3.1b)$$

where:

- $(x, u, w, y) \in \mathbb{R}^{n_x} \times \mathbb{R}^{n_u} \times \mathbb{R}^{n_w} \times \mathbb{R}^{n_y}$ are respectively the state, input, disturbance and output vectors,
- $x_k \equiv x(k \cdot \tau)$, where τ is the sampling period and k is the time index,
- $x^+ \equiv x_{k+1}$ is the state vector at the next sampling time.

Let us introduce the following notation for any predicted profile of a vector $v \in \mathbb{R}^{n_v}$ over a prediction horizon of length N at instant k :

Notation 2.1. Predicted trajectory

$$\mathbf{v}_k := [v_{k|k}^T, v_{k+1|k}^T, \dots, v_{k+N-1|k}^T]^T \in \mathbb{R}^{N \cdot n_v} \quad (2.3.2)$$

where $v_{k'|k}$ is the prediction of $v_{k'}$ at instant k . Furthermore, when no ambiguity results, \mathbf{v}_k is simply noted \mathbf{v} .

for instance : $\mathbf{u}_k := [u_{k|k}^T, u_{k+1|k}^T, \dots, u_{k+N-1|k}^T]^T \in \mathbb{R}^{N \cdot n_u}$ is the predicted input profile over the prediction horizon $[k, k + N - 1]$.

◇

Moreover, let us define the selection operator denoted $\Pi_j(\cdot)$ of any predicted profile \mathbf{v}_k as follows:

Notation 2.2. Selection operator

$$\Pi_j(\mathbf{v}_k) := v_{k+j|k} \quad (2.3.3)$$

The operator $\Pi_j(\cdot)$ simply selects the $(j+1)^{\text{th}}$ vector v in the sequence \mathbf{v}_k (e.g: $\Pi_0(\mathbf{v}_k) = v_{k|k}$).

In addition, let us consider the following notation:

$$\Pi_{[j_0:j_1]}(\mathbf{v}_k) := [v_{k+j_0|k}^T, \dots, v_{k+j_1|k}^T]^T, \quad j_1 > j_0 \quad (2.3.4)$$

◇

2.3.2 Nonlinear Model Predictive Control

In model predictive control the representation of the system (2.3.1) as well as the predicted disturbance profile \mathbf{w}_k are used jointly to find at each decision instant k the best open-loop control sequence noted \mathbf{u}_k^* , minimizing some objective function J . Thus, at each instant k , the following optimization problem has to be solved:

Optimization Problem 2.1. Generic NMPC-related optimization problem

$$\mathbf{u}_k^* = \underset{\mathbf{u}}{\text{Argmin}} J(\mathbf{u}, \mathbf{y}) \quad (2.3.5a)$$

Subject to:

$$\begin{cases} \forall j = 0, \dots, N - 1 \\ \Pi_{j+1}(\mathbf{x}) = f(\Pi_j(\mathbf{x}), \Pi_j(\mathbf{u}), \Pi_j(\mathbf{w})) \\ \Pi_j(\mathbf{y}) = h(\Pi_j(\mathbf{x}), \Pi_j(\mathbf{u}), \Pi_j(\mathbf{w})) \end{cases} \quad (2.3.5b)$$

$$\Pi_0(\mathbf{x}) = x_k \quad (2.3.5c)$$

$$\mathcal{C}^{\text{st}}(\mathbf{y}, \mathbf{w}, \mathbf{u}, \mathbf{x}) \leq 0 \quad (2.3.5d)$$

In the optimization problem 2.1:

- The set of equality constraints (2.3.5b) are the consistency constraints,
- The constraint (2.3.5c) enforces the first component of the state trajectory to the current measured (or observed) state vector (feedback),
- \mathcal{C}^{st} represents a set of operational constraints that has to be satisfied.

Once the problem 2.1 has been solved, only the first component of the optimal control sequence i.e: $\Pi_0(\mathbf{u}_k^*) = u_{k|k}^*$ is applied during the time interval $[k \cdot \tau, (k + 1) \cdot \tau]$. The whole procedure is repeated at the next sampling time $k + 1$, based on new measurement or observation of the state x_{k+1} and new predictions of the disturbance \mathbf{w}_{k+1} . This leads to the so called *receding horizon principle* illustrated on figure 2.1.

In fact, NMPC consists of an implicit feedback-feedforward scheme of the form $u_k = K(x_k, \mathbf{w}_k)$, where:

$$K(x_k, \mathbf{w}_k) = \Pi_0(\mathbf{u}_k^*) \quad (2.3.6)$$

In closed-loop, the system evolution is then given by:

$$x_{k+1} = f(x_k, \Pi_0(\mathbf{u}_k^*), w_k) \quad (2.3.7a)$$

$$y_k = h(x_k, \Pi_0(\mathbf{u}_k^*), w_k) \quad (2.3.7b)$$

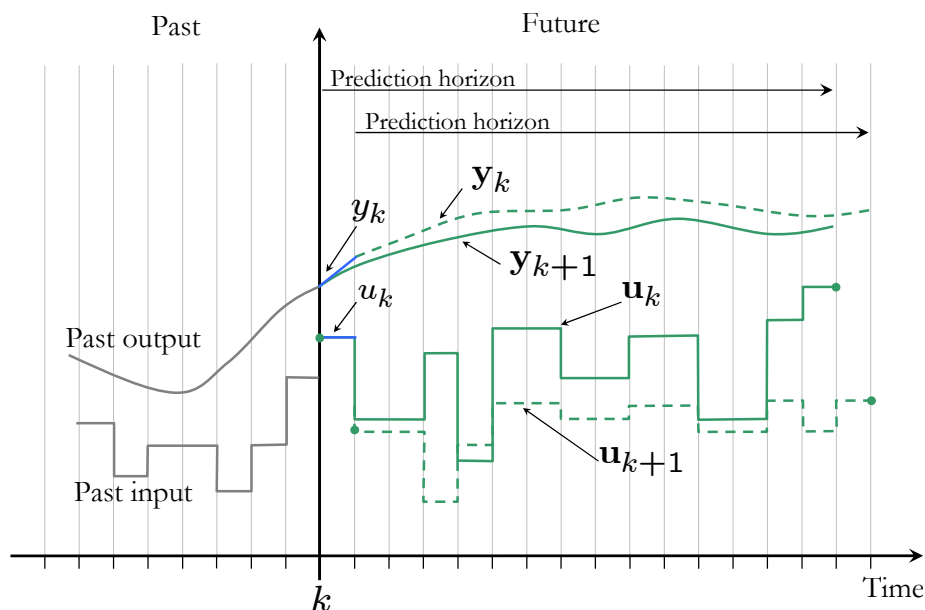


Figure 2.1 Receding horizon principle: at each decision instant a new optimal control trajectory \mathbf{u}_k is computed, only the first element of the sequence (u_k) is implemented, and so on.

The feedforward feature of the scheme results from the direct inclusion of the predicted disturbance profile \mathbf{w}_k into the process of decision making, i.e, the optimization problem (2.1). This offers on one hand an anticipation capability to the controller and on the other better disturbance rejection capabilities.

Thus, unpredicted and unmeasured disturbances are corrected thanks to the *feedback* but also *anticipated* thanks to *feedforward*. This gives to the controller both a *reactive* and a *proactive* behavior -if future disturbances can be predicted-.

This latter feature is of great interest in the present work, since -as it will be shown throughout the manuscript- the inclusion of an a priori knowledge of future disturbances considerably enhances the performance of the controller.

It goes without saying that the complexity of the optimization problem (2.3.5) is one of the most important issues one faces in model predictive control, since this optimization procedure has to be carried-out on line at each decision instant. Therefore, the implementation of MPC algorithms is essentially conditioned by the real-time feasibility of the optimization problem (2.1). The reader may find more details on MPC in [Mayne et al. 2000].

2.3.3 Main features and benefits

It turns out that one of the major benefits associated to the use of the MPC lies in its intuitiveness. Indeed, the control problem is somehow *reduced* to an optimization problem, making this paradigm a powerful abstraction tool which allows treating processes of very different natures. This is obviously conditioned by the existence of adequate optimization tools allowing to solve efficiently the resulting optimization problems.

Note that handling MIMO systems is another strong point arising from this paradigm. Moreover, note that MPC enables to handle explicitly saturations on inputs and states of the system since they are directly included in the formulation of the optimization problem. This is also true for economical objectives. However, in practice, several implementation difficulties are encountered which are mainly related to: (a) the larger computational burden induced by such on-line optimization based control technique and (b) the availability of a sufficiently precise yet simple model the process.

2.4 MPC in buildings

The main necessary ingredients for MPC implementation in buildings can be summarized on figure 2.2. They gather:

- a. the model of the building, which consists of a dynamical description of the part of the building to be controlled,
- b. the forecast on the most pertinent exogenous variables that impact the behavior of the building (weather, energy rate, occupancy),
- c. the objective function describing the criterion to be optimized (energy or invoice minimization while meeting comfort requirements),
- d. the mathematical solver enabling to solve the underlying optimization problems.

A variety of MPC and MPC-like solutions for energy related issues in buildings have been proposed in the literature. Furthermore, the recent marketing of predictive solutions for buildings demonstrates the feasibility and economic benefits of implementing such techniques for buildings energy management².

This section presents the main identified MPC variants for building application as well as the crucial benefits of implementing such control strategy in buildings.

²see BuildingIQ website: <http://www.buildingiq.com/>.



Figure 2.2 Model Predictive Control ingredients in buildings. In building, MPC lies on using a model of the building as well as prediction on disturbances to formulate and solve at each decision instant an optimization problem to find the best sequence of actions which minimizes the cost function (energy, invoice, etc.) and ensure occupant comfort.

2.4.1 Main benefits

As mentioned in the introduction, MPC for building application attracted the interest of many researchers and industrials. Here, the crucial motivations of using MPC in buildings are presented.

Building's inertia

Thermal inertia is one of the main features of buildings. Indeed, for such inertial systems the need to anticipate some actions is desirable for several reasons. For the sake of illustration, let us give two examples:

Optimal start

The optimal time to begin heating (or optimal start time) is the instant at which the heating must be switched on to reheat the building (or the zone) after a vacancy period in order to meet the comfort temperature at occupants arrival. Actually, starting heating too late prevents achieving the desired temperature at the right moment resulting in discomfort, while starting in advance results in an unnecessary energy consumption given that the temperature reaches its set point too quickly, requiring more energy to maintain it or reheat the building again. This is illustrated on figure

2.3.

The optimal start time (generally in early morning) depends not only on the dynamic characteristics of the building but also on weather conditions, and of course of the predicted occupants arrival time. Therefore, an inclusion of these considerations is crucial. Moreover, the set-back temperature (see figure 2.3) needs to be also determined according to the same considerations (a too low set-back temperature causes discomfort since the heating system, if the optimal start time is not carefully adjusted, may not be able to rise the temperature to the comfort set-point).

In conventional energy management systems, a basic rule is given by algorithm 2.1. In practice, one can notice a certain conservativeness in choosing $time^{opt}$ and T^{sb} (high set-back temperature and early heating). Obviously, this is clearly to privilege comfort.

Algorithm 2.1 Optimal start - rule based control

```
1: if  $time \leq time^{opt}$  then  
2:   regulate temperature at  $T^{sb}$   
3: else  
4:   if  $T \leq T^c$  then  
5:     heating ON  
6:   else  
7:     regulate temperature at  $T^c$   
8:   end if  
9: end if
```

Variable price of energy

Now, assume that energy tariff is time varying. In such context, it is clear that shifting some consumption to cheaper energy periods would be far beneficial. This can be performed by using some energy buffer (overheating the building, storing energy in electrical batteries if available or hot water tanks) (see figure 2.4, page 24). Nevertheless, the *optimal amount of energy* to be stored depends on the storage efficiency which is in this case linked to characteristics of the building and the available other storage capabilities. Moreover, the shape of the price signal may be quite complex and the *optimal* decision in this case is not trivial.

Nevertheless, the inertial character of buildings is not the only feature to consider as explained hereafter.

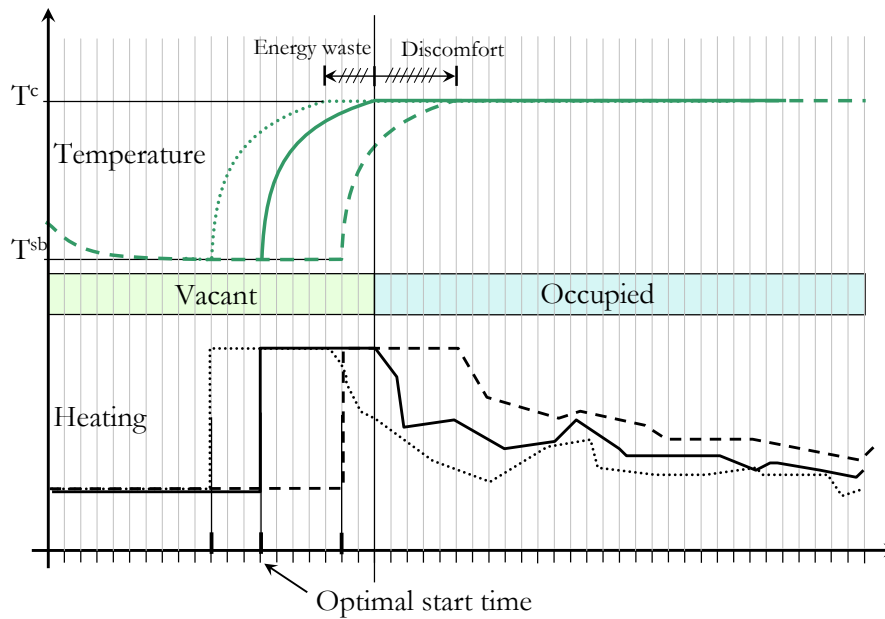


Figure 2.3 Optimal start time illustration. Starting heating too late produces occupant discomfort while starting too early generates energy losses.

Physical couplings

Explicit handling of couplings between certain phenomena can result in important energy savings. As previously, let us give a brief example: blinds position impacts both temperature and indoor illuminance. In summer, the blinds positions have a prominent impact on the heat introduced in the building and therefore on the energy consumption of the building since cooling system should compensate this heat introduction. In this situation, is it more interesting to close the blinds (introduce less heat) and turn on the light if necessary or not? remembering that artificial lighting system produces also heat. It goes without saying that a *universal rule* for this situation is also difficult to find.

It turns out that taking into account coupling between these phenomena leads to consider MIMO systems, which are most often of high dimension particularly in large-scale buildings. The multiplicity of outputs is explained by the fact that temperature must be controlled in each zone, but also air quality and indoor illuminance.

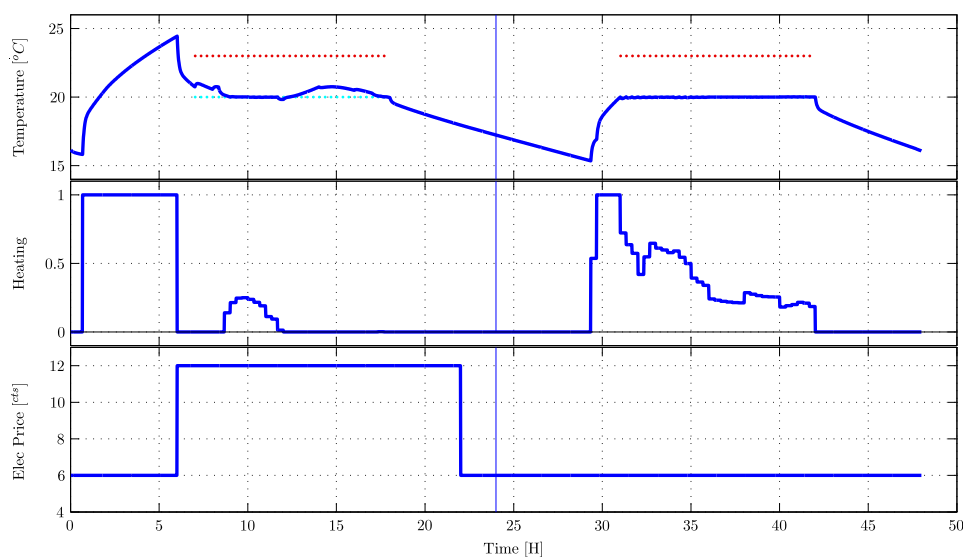


Figure 2.4 Illustration of the usage of MPC with variable price energy. Note that during the first day the building is overheated during the off-peak period (before 6 a.m.), the second day the energy price is constant and therefore no overheating is performed (an optimal start is implemented).

Demand Response capability

Demand/Response is an important concept in *smart grids*. Basically, it means that the building is able to adapt its consumption to some energy market conditions (varying energy rate, dynamical power limitations,...). The market conditions are adjusted by grid managers -possible in advance- in order to reflect the current energy mix and grid status and encourage some power consumption shifting. Due to their huge consumption, buildings are likely to play a crucial role in that sense. This feature is discussed more deeply in section 7.1.

2.4.2 MPC in buildings- main variants

This section introduces the main identified variants of MPC in buildings.

Zone predictive control

Figure 2.5 illustrates the *integrated* zone controller (also called: IRA³ in [Gyalistras & Gwerder 2010]). The problem here, consists of addressing the issue related to only

³IRA: Integrated Room Automation

one zone of building in which a set of actuators has to be controlled in order to ensure comfort of occupants. The comfort refers to thermal and/or air quality and/or indoor illuminance and/or humidity. This comfort has to be obviously ensured at the minimal energetic cost.

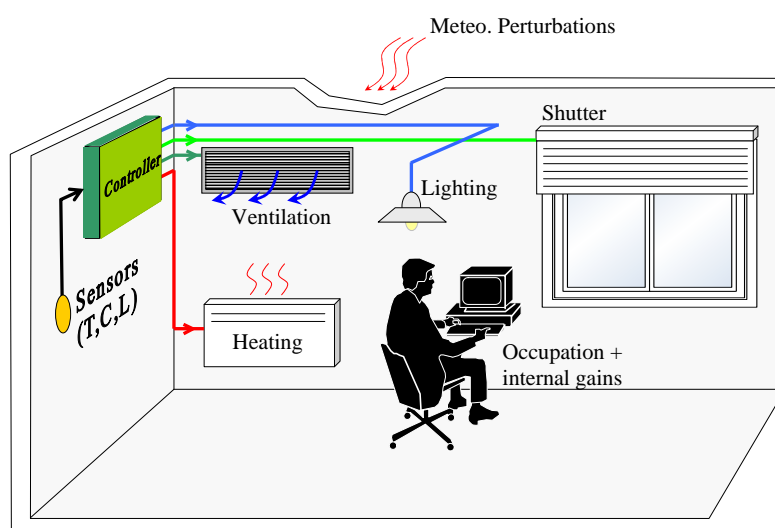


Figure 2.5 Typical zone representation. A zone is defined as contiguous part of the building, it includes several actuators (HVAC, lighting, shutters)

The main advantages of integrated zone control lie in managing the couplings between physical phenomena beside exploiting the thermal inertia of zone. These couplings, as discussed previously may have an important impact on energy consumption.

The works related to the study of zone controllers are also intended to simplify the problem arising in the whole building by restricting the study to a single part of it⁴. One of the difficulties lies in the bilinear model (discussed later in chapter 3, see equation (3.3.1)). This induces a nonlinear optimization problem which will be further discussed in chapters 4 and 5.

The reader may refer to [Oldewurtel et al. 2010, Gwerder & Tödli 2007, Gwerder & Tödli 2009, Freire et al. 2008, Freire et al. 2005] or [Candanedo & Athienitis 2009, Chen 2001, Chen 2002] for more literature on the topic.

⁴This last approach has been adopted for instance in [Parisio 2009].

Model predictive control for global energy flows managements

Some authors focus on the only part of the building related to production/storage energy. The goal here is to manage the purchased/sold/stored power given some prediction on building consumption. The perimeter includes all or part of the systems shown in figure 2.6.

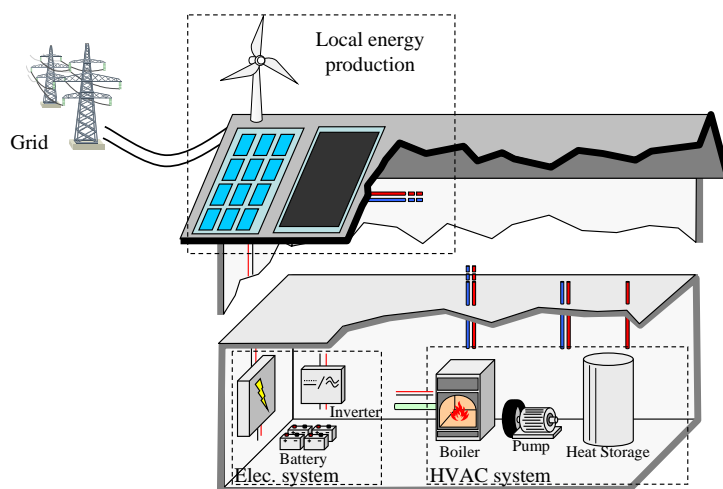


Figure 2.6 Illustration of the main equipment controlled at the energy layer.

For instance, control of thermal energy storage in building cooling systems has been proposed in [Borrelli et al. 2009] while [Collazos et al. 2009] proposed a management of polygeneration systems with predictive technique.

This approach was also studied by [Negenborn et al. 2009, Houwing et al. 2007] that, additionally to the equipment shown in figure 2.6, treated the co-generation equipment electrical/thermal (figure 2.7). Generally, the models used, in this case, are restricted to an overall description of power flows. However, some studies include also simple models of the building's envelope ([Awad et al. 2009, Borrelli et al. 2009]), obviously inducing more complex problems. An interesting application of energy flows management in buildings with thermal storage capacity (active and/or passive) is presented by [Henze & Krarti 2005]. Other examples can be found in [Le 2008, Maor & Reddy 2008].

Remark 2.1.

Note that the distinction above (zone MPC/ Global energy flows management) is only intended

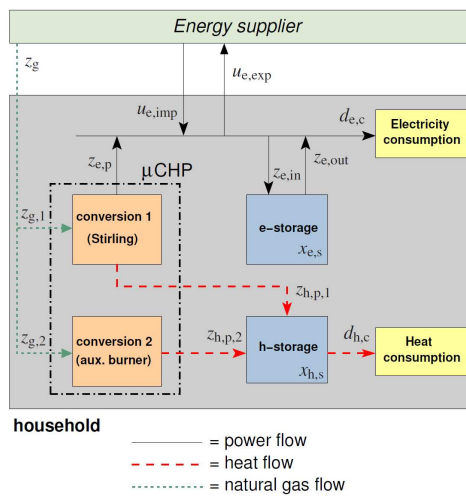


Figure 2.7 Management of polygeneration system with MPC [Houwing et al. 2007]

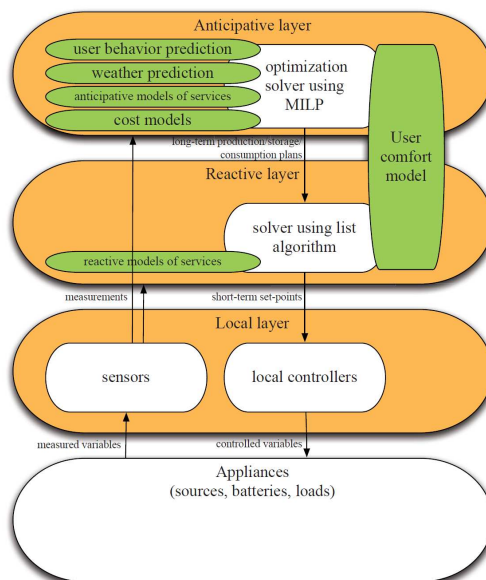


Figure 2.8 MAHAS system: the system has 3 layers, the highest layers correspond to slower dynamics [Ha et al. 2008]

to structure the presentation. Indeed, some studies lie beyond this categorization. Actually, this distinction expresses the fact that the study under consideration focuses on one of the two perimeters, simplifying (sometimes excessively) the other. For instance, in [Siroky et al. 2010], the description of a representative zone is used to manage the heating system of the entire building⁵. Some authors do not attach to specify an application scope and combine predictive control to other approaches. For instance, [Abrás 2009, Abrás et al. 2007, Ha et al. 2008] propose a service-oriented model of the building. Each service (heating, cooking, etc.) requires the availability of some resource to become active. Therefore a resource allocation plan on long time horizons (predictive control) needs to be introduced (figure 2.8). \diamond

Stochastic predictive control

This trend clearly reflects the fact that meteorological forecast data are uncertain. Therefore, meteorological uncertainty should be explicitly handled in the process of decision making.

The first recorded work in this area has been proposed in [Nygård-Ferguson 1990] to deal with overheating issue in winter season with a zone equipped with a heating floor (a large inertia). Such overheating occurs particularly during sunny days and not only generates discomfort but also significant energy losses. [Nygård-Ferguson 1990] showed that a predictive stochastic controller was particularly appropriate in this case and could generate, on some days, substantial energy savings while improving occupant comfort.

Within the OptiControl project [Gyalistras & Team 2010], this approach has been widely investigated. Instead of using strict bounds on comfort variables, [Gyalistras & Team 2010, Parisio 2009] propose to characterize occupant comfort by a probability of violation of constraints on these parameters. Even if this study provides an evident pertinence of this approach when compared to certainty equivalent formulation (no inclusion of the uncertainty), these considerations lead to much more computationally demanding optimization algorithms as explained in more detail in [Oldewurtel et al. 2008], in which some techniques of reducing such an important computational burden are presented. For more literature on the topic, the reader is referred to [Zavala et al. 2009].

Distributed Model Predictive Control

Most of the works cited before implement a *centralized* MPC, i.e: where the decision process is centralized in a unique entity. It goes without saying that in large

⁵In this experiment an energy saving estimation of 17-24% is announced.

scale buildings, such an approach could fail because of the high dimensionality of the underlying optimization problems. Moreover, it leads to non modular architectures which are unsuitable for extensibility and maintainability concerns. Distributed Model Predictive Control (DMPC) has been studied in [Moroşan et al. 2011, Ma et al. 2011] where a distributed predictive control strategy is applied to the thermal regulation of buildings. Deeper discussion on Distributed MPC is provided in part III of the manuscript since this part is exclusively dedicated to this issue.

2.5 Conclusion

Although the problem of building energy consumption is still very largely open, research works conducted in recent years showed that it is difficult to achieve the expected energy performances in building using conventional control approaches. It is now clear that the renewed interest in advanced control methods for energy management in buildings highlighted MPC as a particularly adapted approach, since it enables to:

- Take explicitly into account dynamical characteristics as well as weather forecast, price variations, constraints on resource limitation, multi-sources systems, etc. to optimally schedule actuators operations in building.
- Handle multi-inputs multi-outputs systems, which is the case in buildings.
- Give coherence in the process of decision making. Indeed, conventional rule-based approach leads generally to a complex logical tree structure, which becomes intractable when the number of rules and tuning parameters becomes large.
- Handle explicitly economic objectives (variable energy price for example), which can be very difficult and impractical using a rule-based approach.

In the next chapter, some elements on building modeling are provided, after which parts II and III are dedicated to the design of model predictive controllers for buildings.

Chapter 3

Introduction to building modeling

Abstract

The main aim of this chapter is to give a concise overview of building models and the SIMBAD simulation environment used in this work. As the focus of this work is the design of a model-based controller, emphasis is placed on its structural features. Moreover, since SIMBAD has been provided as a black box Simulink model, an off-line identification procedure has been designed to identify the zone models used later to design the zones local controllers.

3.1 Introduction

Building simulation is a crucial component during the development of control strategies as it provides valuable information regarding building *behavior*, when submitted to different internal or external conditions. Moreover, it enables assessment (to a certain extent) and the successive enhancements of different energy management strategies, which would be rather unrealistic to implement on real buildings for obvious economic and time consumption reasons.

A large range of simulation software are dedicated to building modeling and simulation. To cite only a few: TRNSYS¹, ENERGY+², IDA-ICE³. Although they implement relatively precise models, they are mainly dedicated to global energy estimation and sensitivity analysis regarding construction materials and HVAC dimensioning etc. Therefore, they include only a few basic controllers such as PIDs or ON/OFF controllers. In most cases, existing interfaces with other software are quite unreliable and do not enable extensive control development.

¹<http://www.trnsys.com> last access 09/15/2012.

²<http://apps1.eere.energy.gov/buildings/energyplus/> last access 09/15/2012.

³<http://www.equa.se/eng.ice.html> last access 09/15/2012.

This is particularly unsuited when designing *advanced* control algorithms, which may be quite hard (or even impossible in some cases) to implement on such simulation tools.

These considerations led the HOMES program to adopt SIMBAD (SIMulator of Building And Devices) as a simulation tool for the assessment of control strategies. SIMBAD is a Matlab/Simulink toolbox developed by CSTB⁴ and dedicated to building simulation. It enables simulation of the main physical phenomena coexisting in a building (thermal, IAQ⁵, lighting), and is used to evaluate the potential of control algorithms that have been developed within this collaborative program. One of the main motivations is its implementation in Matlab/Simulink and its quite large HVAC library.

Buildings are generally split into two layers: energy and zone layers. The energy layer gathers energy supply, storage and transformation, while the zone layer gathers several zones. Each zone is a contiguous part of the building in which occupant comfort must be guaranteed by managing several available actuators (heating, shading, ventilation, etc.).

This chapter focuses on the zone layer by providing the main features of the zone models, since the design of the control algorithm presented further on in chapter 4, is precisely based on these models.

This chapter is organized as follows: in section 3.2 a brief presentation of SIMBAD is provided. Section 3.3 provides the main features of the zone models. In section 3.4, the zone models are identified. Some elements on occupancy modeling and the other usage of electricity (OUE) are provided in section 3.5. Section 3.6 concludes the chapter.

3.2 A brief description of SIMBAD simulation tool

This section provides a brief description of the simulation tool. Readers can find more information in [Riederer 2001, Riederer et al. 2000] or (<http://kheops.champs.cstb.fr/Simbadhvac/index.html>).

Remark 3.1.

The version of SIMBAD used during the HOMES program was specifically developed by the CSTB in the scope of the HOMES program. Indeed, the major difference in this version compared to the commercialized one, is the fact that involves a C-coded (compiled) Simulink

⁴Centre Scientifique et Technique du Bâtiment, France.

⁵Indoor Air Quality

3.2. A brief description of SIMBAD simulation tool

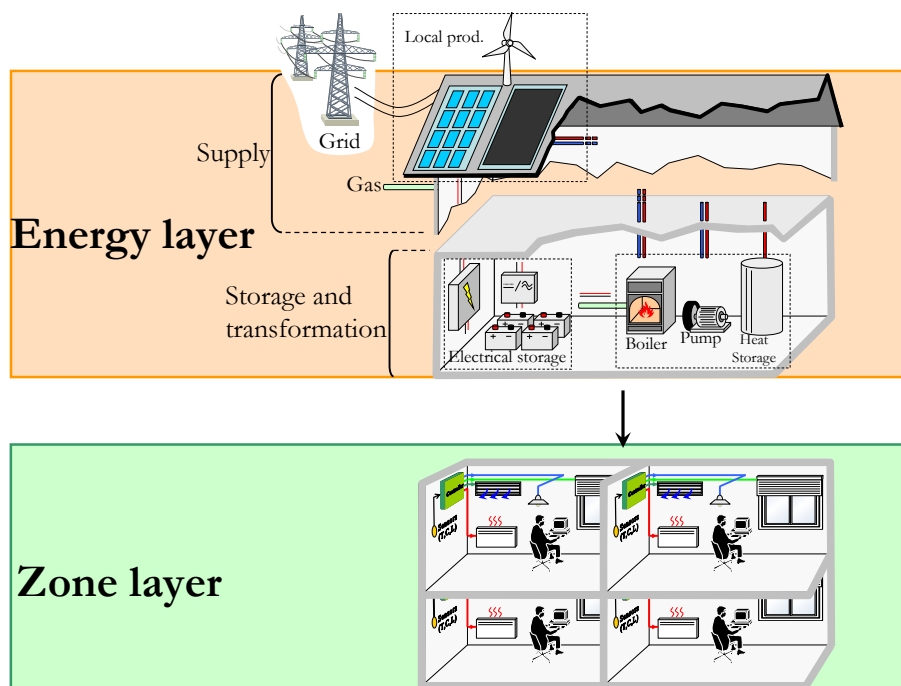


Figure 3.1 Building decomposition

model. Moreover, the whole parameters of the building are grouped in an XML file (see figure 3.3). ◇

In SIMBAD, each building is described by an XML file (figure 3.3) containing all the information related to:

- **the architecture** of the building in terms of physical characteristics of the envelope, physical interconnections between zones (common walls), facade and window orientations of each building zone;
- **the systems** involved in the building, including HVAC systems and lighting as well as all auxiliary systems (pumps, valves, etc.) and their respective dimensioning;
- **the occupation** described by brief information related to the utilization of the zone (for instance: "office");
- **the location** which is mainly used to determine the related weather station, it is also used for calculation of the solar position.

This knowledge related to building architecture is essential to determine:

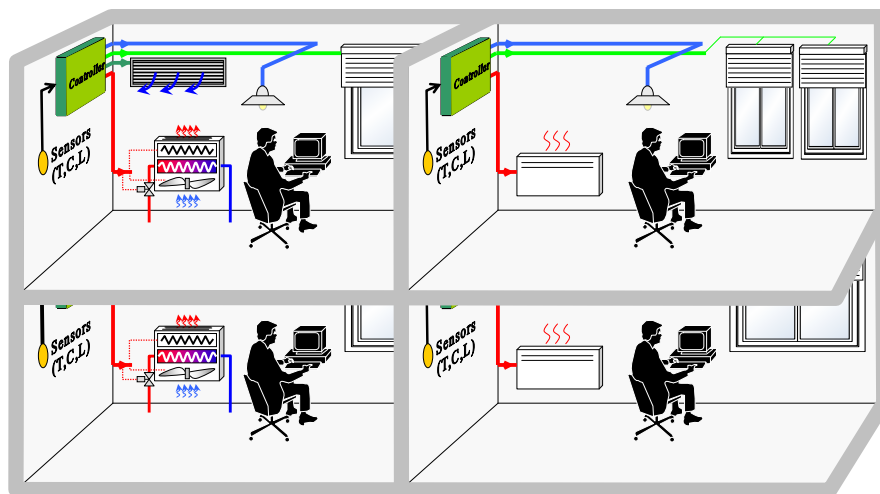


Figure 3.2 Zones in a building. The zones vary in their structure, orientations and usage (occupancy schedules).

- all temperatures impacting the zone concerned (determination of the physically linked zones),
- number and nature of each actuator in each zone as well as the corresponding power consumptions of each equipment item,
- disturbances impacting each zone (orientation of each facade, number and orientations of windows).

This information enables to build the structure of the model of each zone in terms of inputs/outputs. Table 3.1 shows a typical zone inputs/outputs description.

In the following, an identification procedure is used to derive the dynamical model of each zone on a building described in SIMBAD. These models will be used in the sequel to design the corresponding predictive controllers of each zone.

3.3 Zone modeling

In the present work, a building zone refers to a contiguous part of the building in which at least one actuator and one sensor are available. A building zone may re-

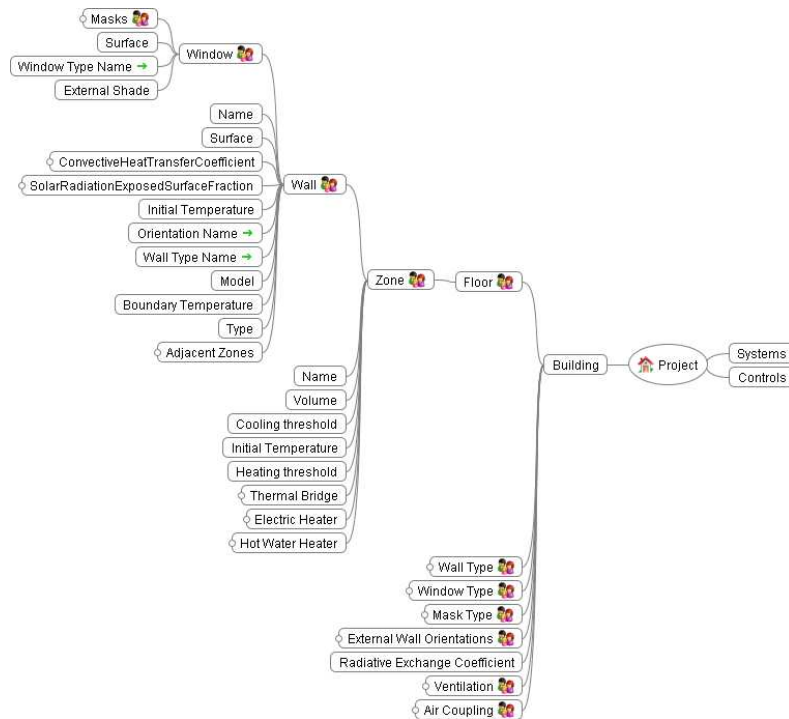


Figure 3.3 Building XML tree. Each building in SIMBAD is defined by an XML file containing information related to physical characteristics of the building as well as zones interconnections.

	Variables	Description	Unit
Inputs	u_h	Heating ctrl	[–]
	u_v	Ventilation control	[–]
	u_l	Lighting control	[–]
	$\{u_b^i\}_{i=1,\dots,N_f}$	Blind ctrl facade i	[–]
Disturbances	T_{ex}	Outdoor temperature	[°C]
	$\{T_{adj}^i\}_{i \in N_{adj}}$	Adjacent zone temp.	[°C]
	$\{\phi_g^i\}_{i=1,\dots,N_f}$	Global irr. flux facade i	[W/m ²]
	Occ	Number of occupants	[–]
	C_{ex}	Outdoor CO ₂ level	[ppm]
Outputs	T	Indoor air temperature	[°C]
	C	Indoor CO ₂ level	[ppm]
	L	Indoor illuminance	[Lux]

Table 3.1 Description of Inputs/Outputs and exogenous variables related to one zone of the building.

fer to a "real" zone of the building (e.g. an office) but can also group several zones aggregated from a control point of view (e.g. several adjacent offices).

In this section, only the key structural features of the dynamic model of a building zone are presented since they are needed to understand the algorithm used further on to derive the solution of the MPC-related optimization problem. The entire building thermal model (multi-zone building) is obtained by interconnecting individual zones models. All details concerning physical modeling of the zone are omitted. However, the reader can refer to [Riederer et al. 2001, Virk & J.Y.M.Cheung 1995, Kolokotsa et al. 2009, Jaluria 2007] and the references therein for more information regarding building modeling.

3.3.1 Zone model identification

SIMBAD is delivered as a black-box simulink library. Therefore, the building mathematical model is not explicitly accessible and has to be deduced from this simulation tool in order to be integrated in the Model Predictive Controllers.

However, the embedded model has only to represent input/output transfers and therefore any dynamical representation capturing the behavior of the building can be used. It is thus unnecessary to derive a physical model from SIMBAD, thereby greatly simplifying the task since physical models are generally more difficult to identify than non physical ones even in simple cases.

A key point in system identification is the choice of an appropriate mathematical structure. This choice is generally linked to the form of the first principle equations used to describe the system.

Once this structure has been defined, an identification procedure can be carried out to find the set of parameters involved in the parametrization of the model structure.

According to the modeling hypotheses considered in SIMBAD that result from classical arguments [Riederer et al. 2000, Mustafaraja et al. 2010, Kolokotsa et al. 2009, Freire et al. 2005, Romanos 2007], it comes out that the dynamical model of each zone can be expressed by the following bilinear state-space representation:

$$M(\theta) : \begin{cases} x^+ &= A_\theta x + [B_\theta(y, w)]u + G_\theta w \\ y &= C_\theta x + [D_\theta(w)]u + F_\theta w \end{cases} \quad (3.3.1)$$

where:

- $A_\theta, B_\theta, C_\theta, D_\theta, G_\theta, F_\theta$ are matrices of appropriate sizes parameterized by a set of parameters θ ;
- x is the state vector of the identified model and has a priori no physical meaning (during simulation, it is recovered using a Kalman observer);
- $y := (T, C, L)^T \in \mathbb{R}^3$ is the output vector (see table 3.1);
- $u := (u_h, u_v, u_l, u_b^1, \dots, u_b^{N_b})^T$ regroups all the controlled inputs (see table 3.1);
- $w := (T^{ex}, \{T_{adj}^i\}_{i \in N_{adj}}, \{\phi^j\}_{j \in N_f}, Occ, C^{ex})^T$ is the vector of exogenous variables (see table 3.1);

Remark 3.2.

- a. The term $[B_\theta(y, w)]u$ is a bilinear term ($B_\theta(y, w)$ is affine in y and w) and is explained by the fact that the temperature and CO_2 level depend not only on the actuator position u but also on the difference between indoor and outdoor quantities ($T - T^{ex}$) (convective heat introduced by mechanical ventilation) and $(C - C^{ex})$. Moreover, the blinds positions impact zone temperature via the terms $(T^{ex} - T)u_b^1, \dots, (T^{ex} - T)u_b^{N_b}, \phi^1 u_b^1, \dots, \phi^{N_b} u_b^{N_b}$.
- b. In SIMBAD, radiative exchanges are linearized. This accounts for the fact that the terms on the form T^4 are non-existent in (3.3.1).
- c. The global fluxes on each facade of the zone $\phi_g^i, i = 1, \dots, N_f$ are obtained by summing the diffuse and the projected direct parts of the solar flux. This implements classical solar projection formulas that can be found in existing references (e.g. [Jung 2009]).

◇

For the given model structure $M(\theta)$, the identification problem consists in finding the best set of parameters denoted θ^* so that the error between the output of the identified model $M(\theta)$ noted y_{Id}^θ and the output of the simulator y_{sim} for the same inputs is minimized. This is expressed by the following optimization problem:

$$\theta^* = \underset{\theta}{\text{Argmin}} \sum_{k=0}^{k=k_{sim}} \|(y_{sim})_k - (y_{Id}^\theta)_k\|_2 \quad (3.3.2)$$

where $k_{sim} \cdot \tau$ is the simulation duration and τ is the sampling period.

$M(\theta)$ is a Multi-Input/Multi-Output dynamic system with coupled dynamics. In order to simplify the identification task, this system is (virtually) split into three Multi-Input/Single-Output systems, where each one corresponds to an output (temperature, CO_2 rate, indoor illuminance).

3.3.2 Thermal model

Thermal-electrical analogy is the most common way to represent thermal phenomena in buildings. Building thermal models can be seen as RC networks (see figure 3.4) in which the values of resistors and capacitances depend on construction materials. Their number is closely linked to the accuracy of the thermal model (number of thermal nodes considered) [Deng et al. 2010, Riederer et al. 2002, Bacher & Madsen 2011]. In Simbad:

- Each external wall is represented by 3 resistors and two capacitances,
- Internal walls are represented by two resistors and one capacitance,
- Air volume is represented by one capacitance.

Temperature behavior can be described using the following Multi-Input/Single-Output Nonlinear Auto Regressive model (which is strictly equivalent to the dynamical relation linking T and u, w expressed by $M(\theta)$):

$$T = \sum_i^{n_v} \frac{\mathbf{B}_i^{\text{Th}}}{1 + \mathbf{A}^{\text{Th}}} \cdot \mathbf{v}_i^{\text{Th}} \quad (3.3.3a)$$

with:

$$\mathbf{v}^{\text{Th}} := [u_h, (T^{\text{ex}} - T)u_v, u_l, \phi^1 u_b^1, \dots, \phi^{n_f} u_b^{n_f}, (T^{\text{ex}} - T)u_b^1, \dots, (T^{\text{ex}} - T)u_b^{n_f}, T^{\text{ex}}, \phi_1, \dots, \phi_{n_f}, \text{Occ}] \quad (3.3.3b)$$

where:

- \mathbf{v}_i^{Th} is the i^{th} component of the vector \mathbf{v}^{Th} ;
- $\mathbf{A}^{\text{Th}}(q^{-1}) := a_1^{\text{Th}}q^{-1} + \dots + a_{n_a}^{\text{Th}}q^{-n_a}$ is a polynomial of order n_a ;
- $\mathbf{B}_i^{\text{Th}}(q^{-1}) := b_{i,1}^{\text{Th}}q^{-1} + \dots + b_{i,n_b^i}^{\text{Th}}q^{-n_b^i}$ is the input polynomial related to the i^{th} component of vector \mathbf{v}^{Th} and is of order n_b^i ;
- q^{-1} is the delay operator defined for any time dependent \mathbf{x}_k by: $q^{-n}\mathbf{x}_k := \mathbf{x}_{k-n}$.

Notice that the vector \mathbf{v}^{Th} gathers all affine contributions on temperature (i.e. such that the transfer between each input \mathbf{v}_i^{Th} and the output T is linear).

3.3.3 CO₂ model

The CO₂ level model is a first order accumulation model, in which the CO₂ produced by occupants is exhausted naturally (infiltration) or mechanically (mechanical venti-

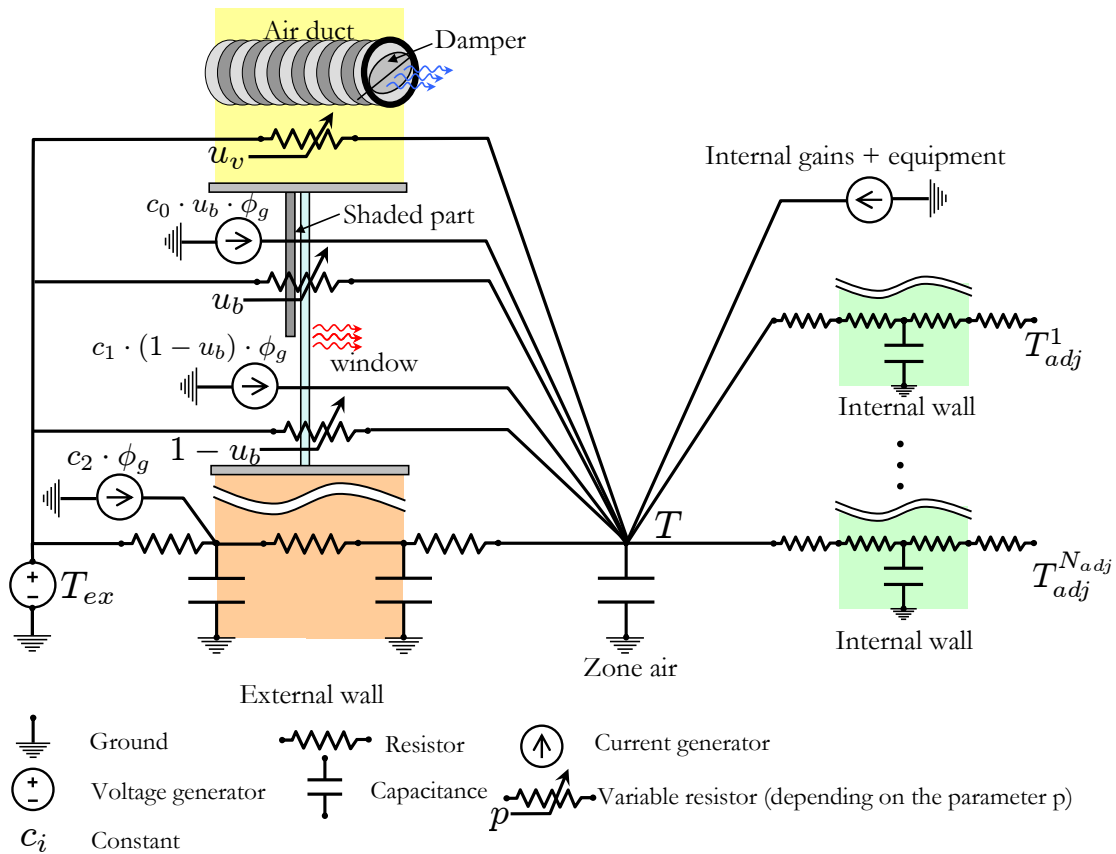


Figure 3.4 Thermal-electrical analogy - simplified circuit. The bilinearity of the model is due the varying resistors involved in the model (ventilation u_v and blind position u_b) as well as the products involved in the window heat transfer model ($u_b \cdot \phi_g$).

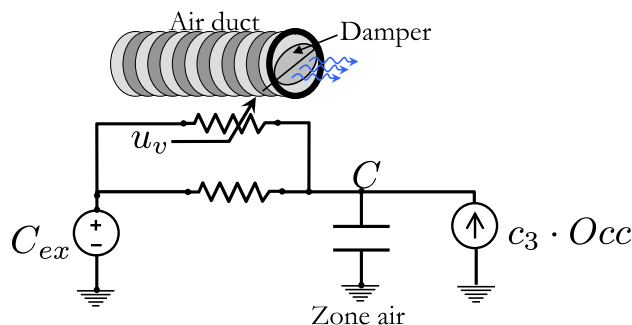


Figure 3.5 Simplified CO₂ model - electrical analogy. The model is bilinear due to the existence of input-output product $u_v \cdot (C - C^{ex})$.

lation), see figure 3.5.

Using the same notations for indoor CO₂ level, it comes that:

$$C = \sum_i^{n_v} \frac{\mathbf{B}_i^C}{1 + \mathbf{A}^C} \cdot \mathbf{v}_i^C \quad (3.3.4)$$

where $\mathbf{v}^C := [(C - C^{ex})u_v, Occ]^T$

3.3.4 Lighting model

Indoor illuminance is impacted both by artificial lighting and blind positions: the model is static. The following static model is assumed (see figure 3.6):

$$L = a_L u_l + \sum_{j=1}^{j=N_b} b_L^j \phi_j u_b^j + \sum_{j=1}^{j=N_f} \bar{b}_L^j \phi_j (1 - u_b^j) \quad (3.3.5)$$

3.4 Model identification

In this section an identification procedure is used to identify the zone models.

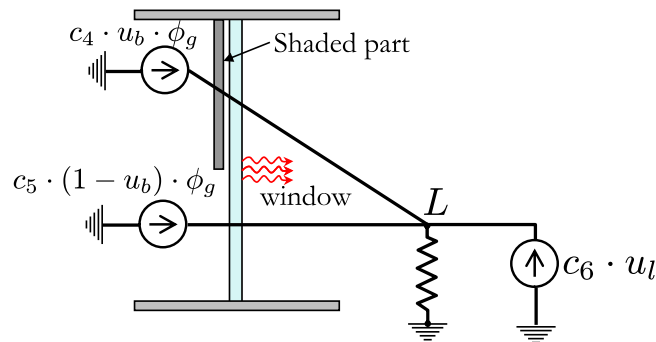


Figure 3.6 Simplified indoor illuminance model - electrical analogy

3.4.1 Identification approach

With the mathematical model structure now, one can identify the polynomials A^{Th} , B_i^{Th} , A^C , B_i^C and constants a_L , b_L^j , \bar{b}_L^j in order to fully describe the model. Noting the set of the unknown coefficients cited above θ , it is easy to recover the model $M(\theta)$.

In fact, this problem can be solved using a dedicated identification tool (we used Matlab's identification toolbox). Actually three transfer functions are identified and then grouped to form the whole model of the zone.

Even if this identification problem seems to be quite simple given that no noise affects the measurements and no unmeasured disturbance is present. The following precautions must be taken in order to ensure a successful identification:

1– Appropriately chosen excitation signals have to be injected in the simulator. This in order to ensure that inputs are not correlated. Moreover each excitation signal has to be sufficiently rich in frequencies to excite all the modes of the simulation model [Landau & Zito 2006];

2– The meteorological data file has been replaced by a virtual one including fully controlled excitation signals.

3– The solar direct flux has been set to zero. The identified model has then been extended by adding the direct flux to the diffuse solar flux (with appropriate projections on each facade) to reduce the number of considered inputs during the identification.

4– The initial state of the process (SIMBAD) is forced to zero (equilibrium). This also simplifies the task as the initial state does not need to be determined;

5– Finally, concerning thermal aspect, note that adjacent zones air temperatures are considered as disturbances from the point of view of the zone concerned, therefore local zone controllers must be inserted in each adjacent zone in order to control each adjacent zone temperature.

3.4.2 Identification results

The identification procedure described above was applied on a 20-zone building that will be used as a throughout this thesis. This virtual building represents a typical French tertiary building equipped with electrical heaters⁶. This building represents a typical small office building which corresponds to nowadays construction standards (2006) consisting of 20 zones. Its area is approximatively 540 m². The external walls are composed of a layer of thermal insulation and a layer of concrete, see figure 3.7.



Figure 3.7 Test building representation. This building represents a typical small office building. It consists of 20 zones, its area is approximately 540 m².

It has been noted that the simulation model (SIMBAD) can be identified with a good fit ($\approx 98\%$) for sufficiently high model orders (typical values $n_a = n_b = 6$ concerning temperature and a first order for CO₂ level, see relations (3.3.3a) and (3.5)).

⁶The version of SIMBAD used during the HOMES program experienced constant enhancements. These results have been obtained on SIMBAD release of 6 June 2011. Next releases introduced some corrections and modifications regarding thermal and lighting aspects. In this light, the models identified in this chapter should be seen as rather good approximations but not exact models of SIMBAD since the yearly simulations launched later have been performed on latest version of SIMBAD.

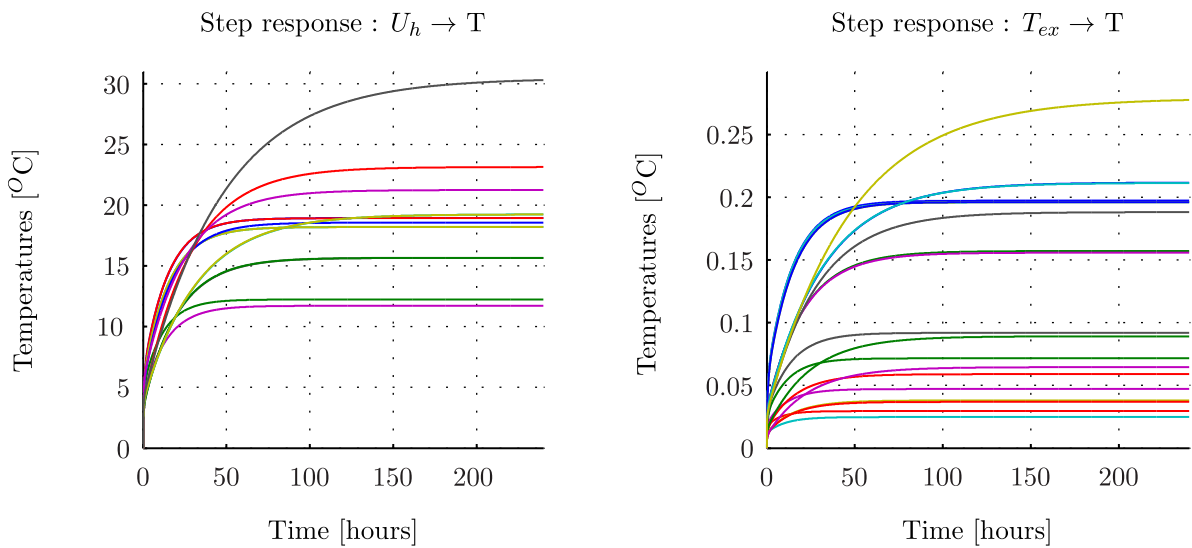


Figure 3.8 Step response of the 20-zone building. Note that temperature responses exhibit two phases: a fast increase due to air dynamic (clearer on figure 3.9) and a very slow dynamic due to walls dynamic. This generally leads to very ill conditioned problems during identification (see [Malisani et al. 2010]).

Figure 3.10 shows the temperature response. Figure 3.8 shows the temperature step responses of the 20 zones of the building. Note that:

- Even for the same building, zone dynamics are rather different. Note also that the static gain of ($T_{ex} \rightarrow T$) determines the insulation of the zone (the lower it is the better the insulation is).
- Note that the step response (figure 3.8) has roughly two dynamics: a rather fast one due to air dynamic and a very slow one resulting from walls dynamics. (figure 3.9). Therefore, a good characterization of the system should take into account the fast dynamics (note: a step on the heater induces an increase of (4-6 [°C]) depending on the zones after one hour). Remark also the time delay introduced by the electrical heaters (≈ 2 [min]), figure 3.9.

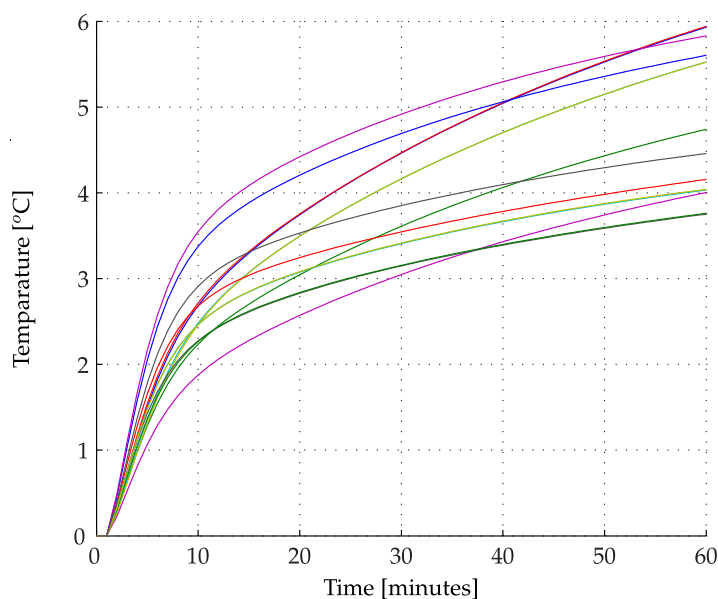


Figure 3.9 Step responses ($U_h \rightarrow T$) during the first hour (figure 3.8). Note that electrical heaters may generate a temperature increase comprised between 4 and 6 [°C] after one hour.

3.5 Occupancy and Other Usage of Electricity (OUE)

3.5.1 Occupancy modeling

Each zone has its own occupancy schedule. Figure 3.11 shows the weekly occupancy profiles of three zones. Each schedule is a fifteen-minutes based schedule. The two first zones are offices, the last zone is a meeting room.

3.5.2 Other Usage of Electricity (OUE)

Other Usage of Electricity (OUE) refers to non-controllable equipment mostly designating white appliances, brown appliances, computer, etc. Their integration in the simulation tool is of particular importance, since their heat production is non-negligible. Figure 3.12 shows the non-controllable electricity consumption in three different zones of the building.

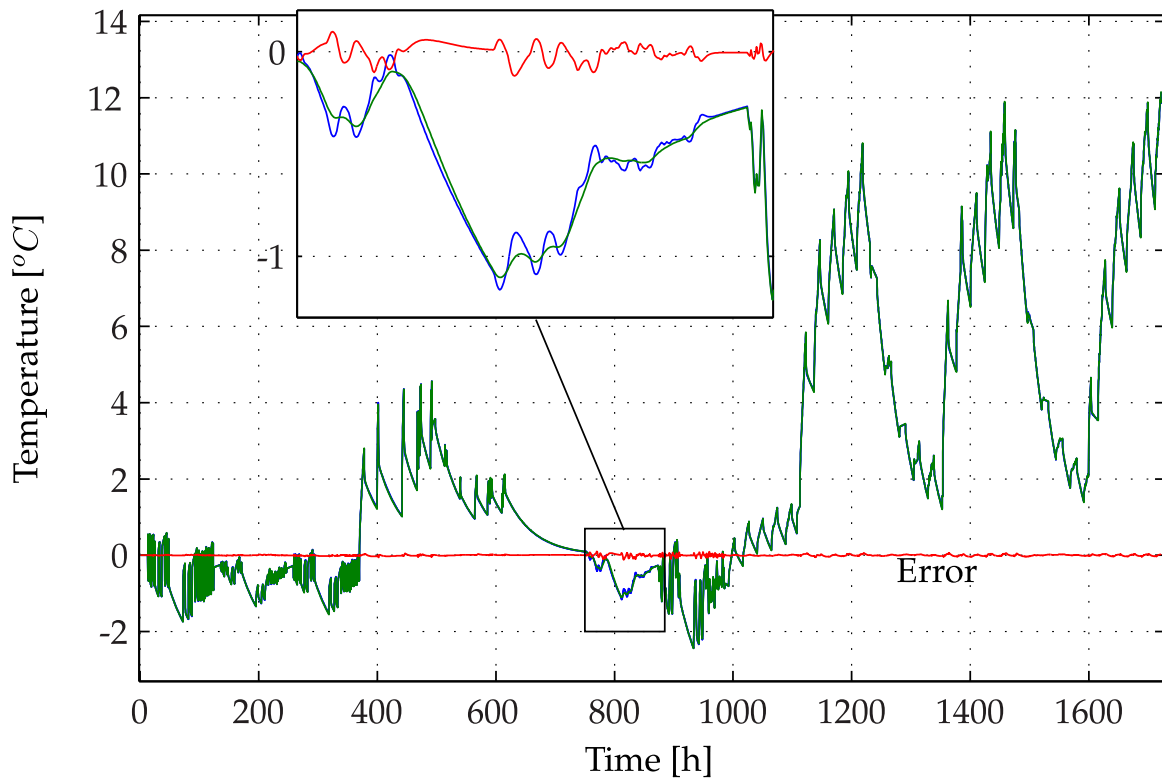


Figure 3.10 Simulated and identified outputs (blue: SIMBAD, green: Identified model, red: error): note that the models are quasi-similar.

3.6 Conclusion

In this chapter, a presentation of the simulation environment and the main features of the models used in this work has been provided. Moreover, an off-line identification procedure has been implemented to deduce the control models used in the next chapters to derive the predictive controllers. Therefore, assumption is made in the sequel that the zones models are available in the building. Even if this assumption can be rather strong in real life, it is considered in the framework of the present work that some identification techniques can be implemented to recover them using real data measurements. The interested reader may refer to [Balan et al. 2011, Malisani et al. 2010] for information on building model identification techniques.

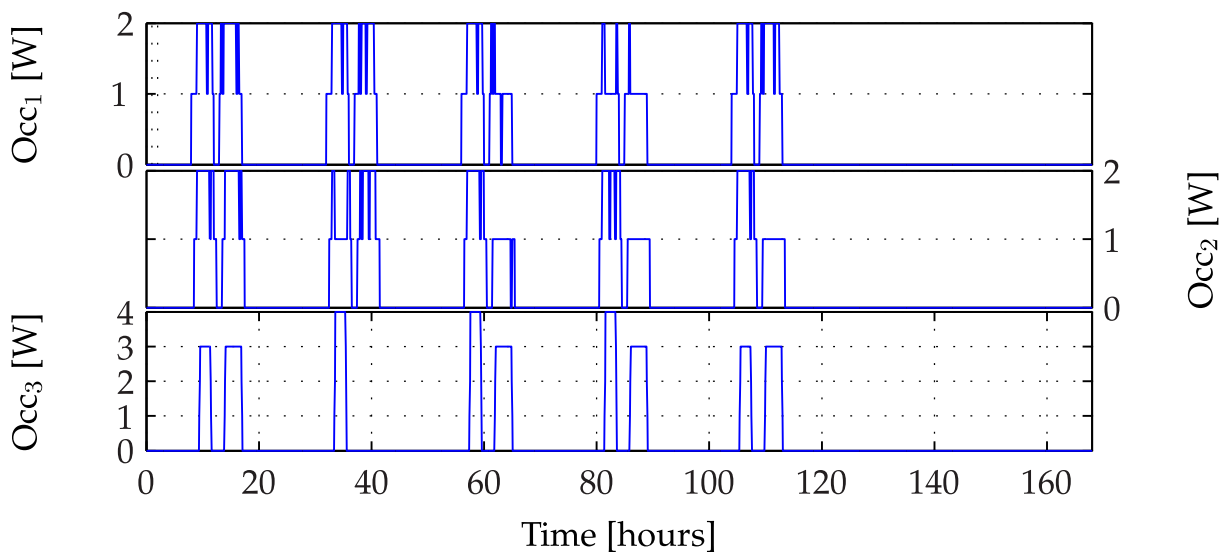


Figure 3.11 The occupancies tend to differ from one zone to the other. First two zones are offices while the third zone is a meeting room.

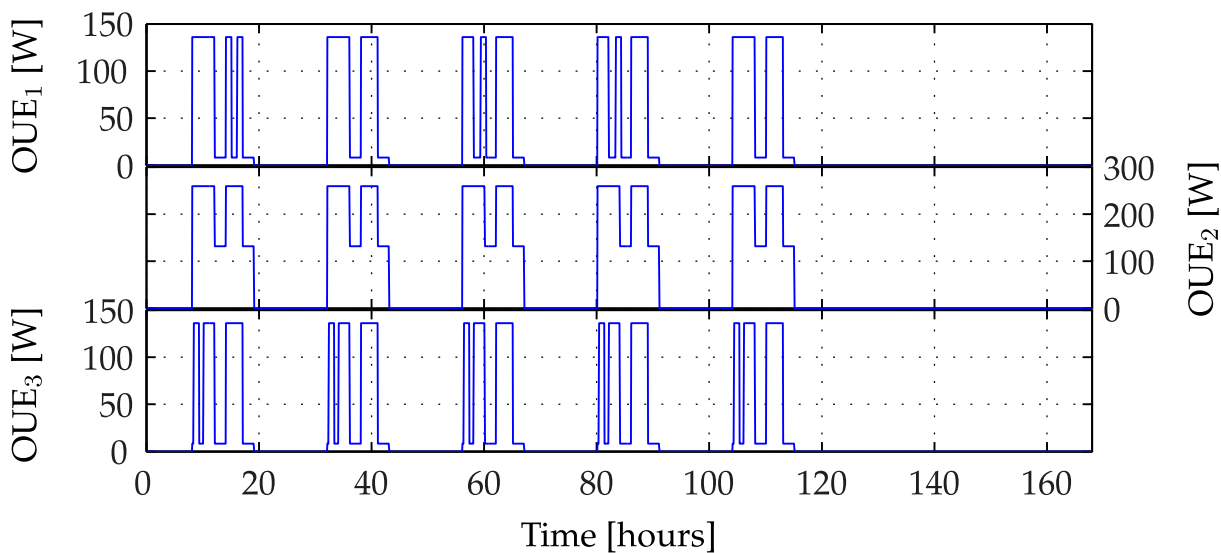


Figure 3.12 Other Usage of Electricity (OUE) profiles. OUE consist of non-controllable electric consumption in the zone, their integration in the simulation tool is of particular importance for their heat production.

Part II

Zone Model Predictive Control

Chapter 4

Zone MPC - Design and Real-Time implementation

Abstract

A hierarchical control structure is generally used in building control. It can be split into two decision layers: energy and zone layers. Energy layer is concerned with high level decisions. Zone layer is concerned with regulation of environmental conditions in one zone of the building. In this chapter a MIMO¹ zone controller is designed to control comfort

4.1 Introduction - zone control

In this chapter, the problem of minimizing energy consumption of a building zone under pre-assigned multi-variable comfort conditions and varying energy tariffs is addressed.

Roughly speaking, the aim at the zone layer is to provide comfort to occupants at the lower energetic cost. The energetic cost has to be interpreted depending on the context, to be the total amount of energy consumed in the case of the constant price tariffication or to be the energetic invoice in the case of variable energy tariffication. In this chapter, a model predictive controller intended to control zone environmental conditions is designed, namely: indoor temperature, CO₂ level and indoor illuminance are controlled.

Although the idea of using MPC to address this problem is not new (for instance, [Nygård-Ferguson 1990] proposed a predictive controller for high inertia buildings where a stochastic approach has been used that led to remarkable results), the recent strategic emergence of this topic renewed the interest in this solution, [Oldewurtel

¹MIMO: Multi-input/Multi-output.

et al. 2010]. This is witnessed by the many recent works adopting such predictive solutions that have been discussed in chapter 2.

The controller, contrarily to the conventional decoupled controllers currently implemented for zone control, takes into account all the interactions between physical phenomena in the zone, as well as predicted disturbances in order to ensure occupant comfort during occupied hours.

This is possible, thanks to the direct inclusion of the zone model as well as predicted disturbances and predicted occupancy of the zone into the process of decision. Moreover, a careful attention is paid to the computational burden of the nonlinear programming problem resulting from such considerations since the algorithm is intended to be integrated in a real hardware, namely the Roombox.

The chapter is organized as follows: in section 4.2, brief recalls on comfort concept are provided. In section 4.3, the control problem is derived, then solved in section 4.4. The design of the state observer is performed in section 4.5. Convergence of the fixed-point algorithm is analysed in section 4.6. Parametrization techniques are used in section 4.7 to reduce the computational burden of the optimization problem. In section 4.8, a computational study of the proposed algorithm is proposed. Simulations performed on SIMBAD are gathered in sections 4.9 and 4.10. Real hardware implementation on the Roombox controller is described in section 4.11. Finally, section 4.12 summarizes the main results.

4.2 About occupants comfort

Before designing the controller, let us first give some elements on comfort *measurement*.

Roughly speaking, comfort conditions mean that satisfactory indoor environmental conditions are ensured during occupied periods. In the present framework, the parameters defining comfort are the indoor temperature (T), indoor CO₂ level (C) and indoor illuminance (L). Concerning indoor illuminance and CO₂ levels, comfort related to these indicators is ensured when the indoor illuminance is larger than a lower bound (generally 500 [lux] in offices) and when the CO₂ level is lower than a prescribed value (generally 1000 [ppm]²). Since it appeared during simulations that comfort related to these aspects is always provided, no indicator is considered.

Concerning thermal aspect, the comfort estimation is more complex. Indeed, for the thermal comfort, the so called Predicted Mean Vote/Predicted Percentage Dissat-

²ppm: parts per million.

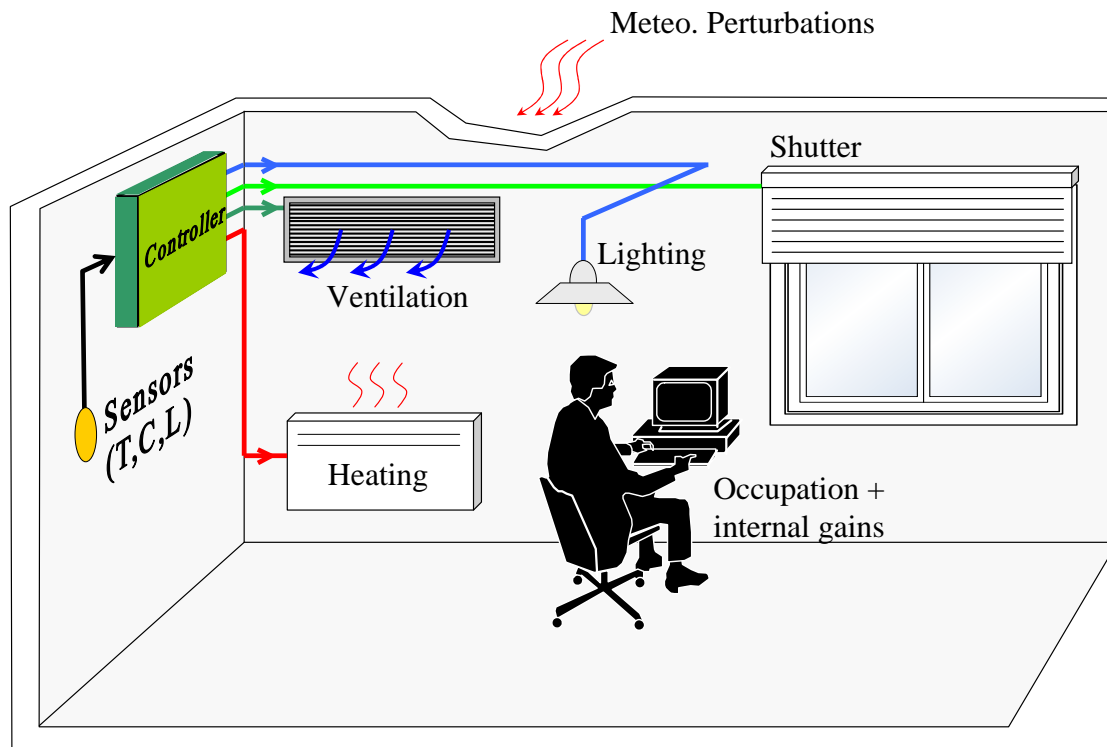


Figure 4.1 Typical zone representation. A zone is defined as contiguous part of the building, it includes several actuators(HVAC, lighting, shutters).

ified (PMV/PPD)³ is the most common way to describe thermal comfort. Nevertheless, it turns out in practice that the required parameters to estimate this comfort index are too complex to obtain. The set of the involved parameters gather, among others, air flow speed, radiant temperature, indoor humidity, clothing, human activity, etc. Therefore, the most common description of thermal comfort is, in practice, reduced to a prescribed range of temperatures $[T, \bar{T}]$ to which the temperature has to belong (see standards [ASHRAE55 2004], [EN15251 2005] and [ISO7730 2006]). This is precisely the comfort criterion used by the designed controller seen later.

Nevertheless, for assessment purpose, the PMV index is used for the yearly simulations presented later as a global thermal indicator.

Therefore, two kinds of comfort criteria are used in the sequel to evaluate the closed performances of the designed controllers. The first one should be seen as a *quality of control* criterion. Basically, the integral of constraints violation on tempera-

³see [ASHRAE55 2004] for a precise definition and [Jung 2009] for some discussions on the usage of this thermal comfort indicator for regulation purposes.

ture is computed over the whole simulation time. Namely, one defines the Thermal Constraint Violation (TCV) [$^{\circ}C \cdot h$] by:

$$\text{TCV} := \frac{1}{60} \left(\sum_k \max(T_k - \bar{T}_k, 0) - \sum_k \min(T_k - \underline{T}_k, 0) \right) \quad (4.2.1)$$

where \bar{T} , \underline{T} are respectively upper and lower bounds on indoor temperature.

As discussed before, this criterion does not actually provide a *real* estimation of thermal comfort. Therefore, for yearly simulations, a global thermal comfort (GTC [%]), which is the most critical indicator⁴, is defined based on PMV/PPD measures. Even if such measure is in real-life quite complex to perform, assumption is made on the availability of the whole parameters involved in. This provides a comparison base-line during the assessment of the several control strategies (and their variants) designed in the scope of the HOMES program. Basically GTC [%] represents the fraction of time spent in comfort conditions during the whole year and is defined by:

$$\text{GTC} [\%] := \frac{\text{card}\{k | \text{PPD}_k \leq \overline{\text{PPD}} \wedge \text{Occ}_k \neq 0\}}{\text{card}\{k | \text{Occ}_k \neq 0\}} := \frac{\text{comfort time}}{\text{occupation time}} \quad (4.2.2)$$

where PPD_k is the PPD computed as instant k and the threshold on the PPD value (here $\overline{\text{PPD}} = 15\%$) is considered to reflect a reasonable comfort degradation.

4.3 The Control Problem

In this section, the control problem is formulated. As discussed in chapter 3, the identification of a structured model involving the key zone quantities leads to the following bilinear state space representation :

$$\begin{cases} x^+ &= A \cdot x + [B(y, w)] \cdot u + F \cdot w \\ y &= C \cdot x + D(w) \cdot u \end{cases} \quad (4.3.1)$$

Let us also introduce the simulator form of (4.3.1) denoted \mathcal{Z} and defined by:

$$\mathbf{y}_k := \mathcal{Z}(\mathbf{u}_k, \mathbf{w}_k, x_k) \quad (4.3.2)$$

which simply means that the output trajectory \mathbf{y}_k is obtained when the zone starts from initial state x_k and submitted to the input and disturbance trajectories \mathbf{u}_k and \mathbf{w}_k .

⁴when compared to indoor air quality and indoor illuminance in usual conditions

Assumption 4.1. *The following quantities are available:*

- *The current state x_k of the system model (obtained via dynamic observer, this is detailed further in section 4.5),*
- *The predicted utility cost Γ corresponding to each power source,*
- *The prediction of the exogenous inputs profile \mathbf{w}_k (outdoor temperature, solar irradiation, occupancy, etc.),*
- *The comfort related bounds profiles $\underline{\mathbf{y}}_k$ and $\bar{\mathbf{y}}_k$ which are implicitly given by the prediction on occupancy \mathbf{Occ}_k .*

◇

Moreover, assume that power consumption of electrical equipment is linear in u and define the total instantaneous power consumption of the zone p_k by:

$$p_k = E \cdot u_k \in \mathbb{R} \quad (4.3.3)$$

where the matrix $E \in \mathbb{R}^{1 \times n_u}$ gathers the maximal power consumption of all equipment:

$$E := \begin{bmatrix} \alpha_h & \alpha_v & \alpha_l & 0 & \dots & 0 \end{bmatrix} \quad (4.3.4)$$

where α_h , α_v and α_l stand respectively for maximal power associated to electrical heating and ventilation system and lighting.

Hence, the power profile consumption over the prediction horizon of length N (resulting from all the actuators) is given by:

$$\mathbf{p}_k = \mathbf{E} \cdot \mathbf{u}_k, \quad \mathbf{p}_k \in \mathbb{R}^N \quad (4.3.5)$$

with:

$$\mathbf{E} := \mathbf{I}_N \otimes E \quad (4.3.6)$$

Adding saturations on inputs ($u_k \in [0, 1]^{n_u}$), the NMPC-related optimization problem at instant k becomes:

Optimization Problem 4.1. Zone optimization problem

$$\mathbf{u}_k^* = \underset{0 \leq \mathbf{u} \leq 1}{\mathbf{Argmin}} \quad J^E(\Gamma_k, \mathbf{p}_k) + J^C(\mathbf{y}_k) + J^D(\mathbf{u}_k) + J_F(\Pi_{(N-1)}(\mathbf{y}_k)) \quad (4.3.7)$$

Subject to:

$$\mathbf{p}_k = \mathbf{E} \cdot \mathbf{u}_k \quad (4.3.8)$$

$$\mathbf{y}_k = \mathcal{Z}(\mathbf{u}_k, \mathbf{w}_k, x_k) \quad (4.3.9)$$

where:

- J^E corresponds to the integral energy criterion over the horizon and is defined as follows :

$$J^E(\mathbf{\Gamma}_k, \mathbf{p}_k) = (\mathbf{\Gamma}_k^T \cdot \mathbf{E})^T \cdot \mathbf{u}_k \quad (4.3.10)$$

It depends on the consumed power profile \mathbf{p} and the utility cost $\mathbf{\Gamma}$. Note that J^E is affine in \mathbf{u}_k ,

- $J^C(\mathbf{y}_k)$ is the discomfort criterion and depends only the outputs \mathbf{y}_k . As it has been discussed in section 4.2, the discomfort function enforces the output to belong to the comfort region. Obviously, comfort is only required when occupants are present (figure 4.2). The function J^C is parametrized via the two positive scalars ρ_0, ρ_1 and $\delta_y \in \mathbb{R}^{n_y \cdot N}$ (see figure 4.3) to introduce some *smoothness* if a constraint violation cannot be avoided.

- $J^D(\mathbf{u}_k)$ represents the cost on rate variations of actuators:

$$J^D(\mathbf{u}_k) = \langle \Delta, |\Pi_0(\mathbf{u}_k) - u_{k-1}| \rangle + \sum_{j=1}^{j=N} \langle \Delta, |\Pi_j(\mathbf{u}_k) - \Pi_{(j-1)}(\mathbf{u}_k)| \rangle \quad (4.3.11)$$

Recall that $\Pi_j(\mathbf{u}_k)$ selects the j^{th} component in the predicted profile \mathbf{u}_k . $|\cdot|$ is the element-wise absolute value.

Note, that it is mandatory to keep a memory, from one sampling time to the next one, of the last applied control u_{k-1} . The parameter $\Delta \in \mathbb{R}^{n_u}$ ($\Delta \geq 0$) is a design parameter. Indeed, the objective of introducing J^D is twofold:

- Ensuring the uniqueness of the solution of the optimization problem (4.1),
 - Avoiding excessive variations of the control inputs u , as it is the case with LP formulation (compared to QP formulations).
- $J_F(\Pi_{(N-1)}(\mathbf{y}_k))$ is the final cost. It indicates here the fact that at the end of the prediction horizon the comfort of the zone should be provided (the zone is assumed always occupied at the end of the horizon).

Remark 4.1.

In practice, Δ is chosen so that J^D remains relatively small compared to J^E , for the well known reasons presented in [Rao & Rawlings 2000]. Actually, if $\|\Delta\|$ is too large an idle control may results (the control input remains constant). If $\|\Delta\| \rightarrow 0$ a dead-beat control may appear. \diamond

Remark 4.2.

- a. The variables ρ_0 and ρ_1 (figure 4.3) can be used as tuning parameters to trade-off energy (J^E) and comfort (J^C) (see [Moroşan et al. 2010a]). In this work, they are chosen large enough to focus on comfort. Therefore, the introduction of the discomfort function should be seen a "soft-constrained" formulation of the problem in which comfort violation is never permitted ($\rho_0 = \rho_1 = \infty$). In this last situation, the optimization problem (4.1) may be infeasible.
- b. Note that the comfort related bounds are not necessarily infinite during vacancy hours. This is related to the fact that, upper and lower bounds on temperature have to be respected during vacancy hours, this to meet standard requirements [EN15251 2005] (see figure 4.2).
- c. Anti glare and noise reduction are also integrated for comfort requirements. They are integrated as hard constraints on inputs during occupancy periods. Nevertheless, they are intentionally omitted in formulations for the sake of simplicity.

Anti-glare:

$$(\phi_g^i > \bar{\phi} \wedge occ \neq 0) \Rightarrow u_b^i = 0$$

ϕ_g^i is the global solar irradiance of the facade i . Which simply means that the blind on facade i is fully closed if the global irradiance on the corresponding facade is larger then a predifine threshold $\bar{\phi}$.

Noise reduction:

$$occ \neq 0 \Rightarrow u_v \leq 0.5$$

meaning that ventilation is reduced during occupancy period to reduce the noise resulting from air circulation in ducts.

◇

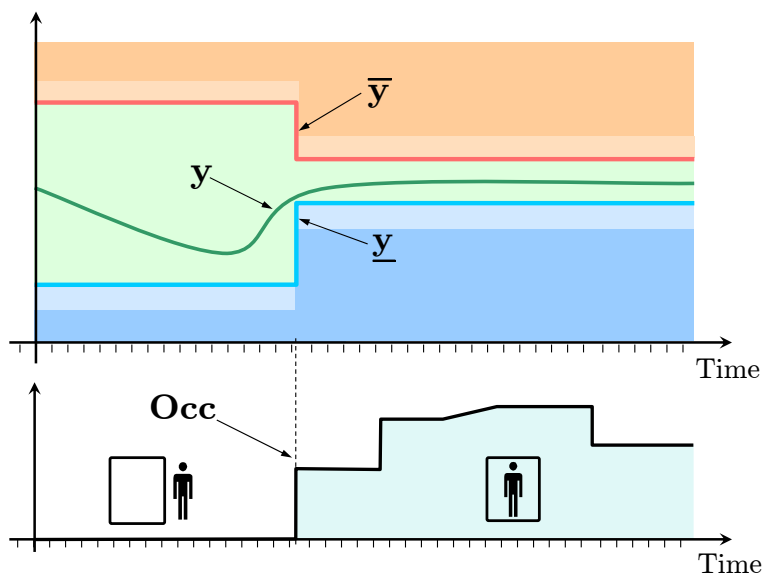


Figure 4.2 Comfort-related bounds on comfort parameters with respect to predicted occupancy profile.

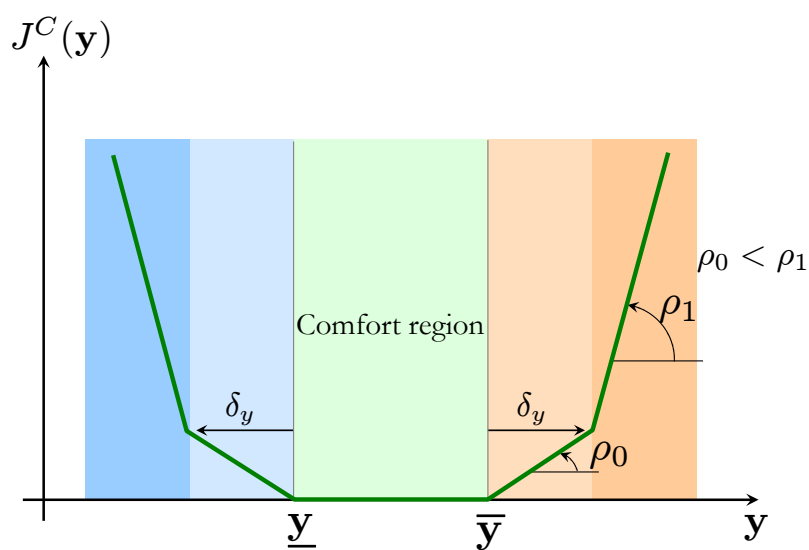


Figure 4.3 Discomfort function used in the optimization problem 4.1: The discomfort function is parametrized by ρ_0, ρ_1 and δ_y which represents a reasonable bound violation.

One can see that the zone optimization problem 4.1 can be expressed on the following form:

Optimization Problem 4.2. Nonlinear optimization problem

$$\text{NLP}_k: \underset{\mathbf{u}_k, \delta_0, \delta_1, \delta_d, \mathbf{y}_k}{\text{Minimize}} J(\mathbf{u}_k, \mathbf{y}_k, \Gamma_k) \quad (4.3.12a)$$

Subject To :

$$[\Phi(\mathbf{y}_k, \mathbf{w}_k)]\mathbf{u}_k + \delta_0^- + \delta_1^- \geq \underline{\mathbf{y}}_k - \Psi x_k - \Xi \mathbf{w}_k \quad (4.3.12b)$$

$$[\Phi(\mathbf{y}_k, \mathbf{w}_k)]\mathbf{u}_k - \delta_0^+ - \delta_1^+ \leq \bar{\mathbf{y}}_k - \Psi x_k - \Xi \mathbf{w}_k \quad (4.3.12c)$$

$$\mathbf{D} \cdot \mathbf{u}_k - \delta_d^+ + \delta_d^- = \mathbf{a} \quad (4.3.12d)$$

$$\mathbf{0} \leq \mathbf{u}_k \leq \mathbf{1} \quad (4.3.12e)$$

$$\delta_0 \geq \mathbf{0}, \delta_d \geq \mathbf{0}, \mathbf{0} \leq \delta_1 \leq \begin{bmatrix} \delta_y \\ \delta_y \end{bmatrix} \quad (4.3.12f)$$

$$\mathbf{y}_k = \mathcal{Z}(\mathbf{u}_k, \mathbf{w}_k, x_k) \quad (4.3.12g)$$

where:

- $\delta_0 := \begin{bmatrix} \delta_0^+ \\ \delta_0^- \end{bmatrix} \in \mathbb{R}^{2 \cdot N \cdot n_y}$, $\delta_1 := \begin{bmatrix} \delta_1^+ \\ \delta_1^- \end{bmatrix} \in \mathbb{R}^{2 \cdot N \cdot n_y}$ are slack variables introduced in order to describe the function $J^C(\mathbf{y})$ (figure 4.3);
- $\delta_d := \begin{bmatrix} \delta_d^+ \\ \delta_d^- \end{bmatrix} \in \mathbb{R}^{2 \cdot N \cdot n_u}$ are slack variables introduced to describe the function $J^D(\mathbf{y})$;
- The notations $\mathbf{1}$ and $\mathbf{0}$ indicate vectors (or matrices) of ones and zeros respectively with appropriate sizes if not indicated,
- $\Phi(\mathbf{y}_k, \mathbf{w}_k)$, Ψ and Ξ are the prediction matrices, they are defined as follows:

$$\Psi := \begin{bmatrix} C \\ CA \\ CA^2 \\ \cdot \\ CA^{N-1} \end{bmatrix}, \quad \Phi(\mathbf{y}_k, \mathbf{w}_k) := \begin{bmatrix} D_k & \mathbf{0} & \cdot & \mathbf{0} \\ CB_k & D_{k+1} & \cdot & \cdot \\ CAB_k & CB_{k+1} & \cdot & \cdot \\ \cdot & \cdot & \cdot & \mathbf{0} \\ CA^{N-2}B_k & CA^{N-3}B_{k+1} & \cdot & D_{k+N-1} \end{bmatrix} \quad (4.3.13)$$

where $B_k := B(y_k, w_k)$ and $D_k := D(w_k)$.

- The matrices \mathbf{D} and \mathbf{a} are defined as follows:

$$\mathbf{D} := \begin{bmatrix} \mathbf{I}_{n_u} & \mathbf{0} & \mathbf{0} & \dots & \dots & \mathbf{0} \\ \mathbf{I}_{n_u} & -\mathbf{I}_{n_u} & \mathbf{0} & \dots & \dots & \mathbf{0} \\ \mathbf{0} & \mathbf{I}_{n_u} & -\mathbf{I}_{n_u} & \dots & \dots & \mathbf{0} \\ \dots & \dots & \dots & \dots & \dots & \dots \\ \mathbf{0} & \dots & \dots & \mathbf{0} & \mathbf{I}_{n_u} & -\mathbf{I}_{n_u} \end{bmatrix}, \mathbf{a} := \begin{bmatrix} u_{k-1} \\ \mathbf{0} \\ \mathbf{0} \\ \dots \\ \mathbf{0} \end{bmatrix}, \quad (4.3.14)$$

Defining the decision variables \mathbf{z} so that it gathers all the decision variables involved in the optimization problem, namely :

$$\mathbf{z} := \left[\mathbf{u}_k^T \quad \delta_0^T \quad \delta_1^T \quad \delta_d^T \right]^T \quad (4.3.15)$$

one can see that the optimization problem 4.2 is a nonlinear optimization problem of the form :

Optimization Problem 4.3.

$$\text{Minimize } \mathbf{L} \cdot \mathbf{z} \quad (4.3.16)$$

$\underline{\mathbf{z}} \leq \mathbf{z} \leq \bar{\mathbf{z}}, \mathbf{y}_k$

Subject To:

$$\mathbf{A}(\mathbf{y}_k) \cdot \mathbf{z} \leq \mathbf{b} \quad (4.3.17)$$

$$\mathbf{y}_k = \mathcal{Z}(\mathbf{u}_k, \mathbf{w}_k, x_k) \quad (4.3.18)$$

The matrices \mathbf{L} , $\mathbf{A}(\mathbf{y})$, \mathbf{b} , $\bar{\mathbf{z}}$, $\underline{\mathbf{z}}$ are defined in appendix B.

The presence of product terms between the variables \mathbf{y} and \mathbf{z} prevents the optimization problem (4.2) from being an LP. Actually, this problem is a non-convex optimization problem that could be difficult to solve. In the next section a sequential optimization procedure is presented in order to deal with this issue.

Remark 4.3.

In the optimization problem 4.3, the matrix \mathbf{A} is assumed to depend only on the output trajectory \mathbf{y}_k given that at a decision instant k , the disturbance trajectory \mathbf{w}_k is given. \diamond

4.4 Solving the optimization problem

In this section, the algorithm used to solve the optimization problem 4.3 is presented.

4.4.1 Fixed-point algorithm

As discussed before, the major difficulty in solving the optimization problem 4.2 lies in the presence of product terms of the form $u \cdot y$ in the inequalities (4.3.12b) and (4.3.12c). To tackle this issue, an iterative procedure is proposed hereafter.

Assume that, at any iteration s , of the procedure an output trajectory $y_k^{(s)}$ is given *a priori*. Therefore, one can form the following *fictitious* Linear Time Varying system:

$$\text{LTV}^{(s)} : \begin{cases} x^+ &= A \cdot x + [B(y^{(s)}, w)] \cdot u + F \cdot w \\ y &= C \cdot x + D(w) \cdot u \end{cases} \quad (4.4.1)$$

and subsequently the following linear programming problem $\text{LP}_k^{(s)}$, in which the output trajectory y is no longer a decision variable, can be defined:

Optimization Problem 4.4. Linear programming

$$\underset{\mathbf{z} \leq \mathbf{z} \leq \bar{\mathbf{z}}}{\text{Minimize}} \mathbf{L} \cdot \mathbf{z} \quad \text{s.t.} : \quad \mathbf{A}(y_k^{(s)}) \cdot \mathbf{z} \leq \mathbf{b} \quad (4.4.2)$$

The solution of the optimization problem 4.4 gives the optimal control sequence $\mathbf{u}_k^{(s)}$:

$$\mathbf{u}_k^{(s)} \leftarrow \text{LP}_k^{(s)} \quad (4.4.3)$$

$\mathbf{u}_k^{(s)}$ is the optimal control sequence related to the LTV system (4.4.1) but not to the original system (4.3.1). Nevertheless, assume now that the control sequence $\mathbf{u}_k^{(s)}$ is injected in the nonlinear system, namely:

$$\mathbf{y}_k^{(s+1)} = \mathcal{Z}(\mathbf{u}_k^{(s)}, \mathbf{w}_k, x_k) \quad (4.4.4)$$

where \mathcal{Z} is the simulator form of the zone (see eq. (4.3.2)). Therefore the output trajectory $y_k^{(s+1)}$ can be used to form the fictitious system $\text{LTV}^{(s+1)}$ and so on.

The fixed point algorithm consists of successively repeating these two steps until a convergence of the solution is achieved. This leads to algorithm 4.1.

Algorithm 4.1 Fixed-point algorithm

```

1:  $s \leftarrow 1$ 
2:  $\mathbf{u}_k^{(0)} \leftarrow [\Pi_1(\mathbf{u}_{k-1}^*)^T, \dots, \Pi_{(N-1)}(\mathbf{u}_{k-1}^*)^T, \Pi_{(N-1)}(\mathbf{u}_{k-1}^*)^T]^T$  ▷ Warm start
3:  $\mathbf{y}_k^{(1)} \leftarrow \mathcal{Z}(\mathbf{u}_k^{(0)}, \mathbf{w}_k, x_k)$ 
4:  $e^{(0)} \leftarrow \infty$ 
5: while  $e^{(s-1)} \geq \eta$  and  $s \leq s_{max}$  do
6:    $\mathbf{u}_k^{(s)} \leftarrow \text{LP}_k^{(s)}$ 
7:    $\mathbf{y}_k^{(s+1)} = \mathcal{Z}(\mathbf{u}_k^{(s)}, \mathbf{w}_k, x_k)$ 
8:    $e^{(s)} \leftarrow \text{Max}(\|\mathbf{y}_k^{(s+1)} - \mathbf{y}_k^{(s)}\|_\infty, \|\mathbf{u}_k^{(s+1)} - \mathbf{u}_k^{(s)}\|_\infty)$ 
9:    $s \leftarrow s + 1$ 
10: end while
11:  $\mathbf{u}_k^* \leftarrow \mathbf{u}_k^{(s-1)}$ 

```

where: $\eta > 0$ is a small threshold and s_{max} is the maximal number of iterations allowed. The step (2:) of the algorithm is the warm-start strategy, it consists of initializing the optimal control profile with the one found at last iteration with the convenient shifting. A convergence analysis as well as a computational study are provided in section 4.6.

Remark 4.4.

The fixed point algorithm can be seen as a form of Sequential Linear Programming (SLP) (a well known optimization technique proposed in the early sixties [Griffith & Stewart 1961]). In fact, the algorithm 4.1 consists of successively approximating the nonlinear optimization problem 4.3 by the linear one 4.4 which is the basic idea in SLP. The main difference between a standard SLP procedure and the algorithm 4.1 lies in the fact that the output trajectory \mathbf{y} is not part of the set of decision variables of the LP 4.4. Instead, the simulation step (7:) is used to update it from one iteration to next one. In standard SLP procedures, this step is non-existent as it is compensated by the fact that the output trajectory \mathbf{y} is included in the set of decision variables. The constraints of the optimization problem 4.2 are linearized at each step around a trajectory $(\mathbf{u}_k^{(s)}, \mathbf{y}_k^{(s)})$. This has the effect however of enlarging the number of decision variables, which is not the case in algorithm 4.1. ◇

4.5 State and disturbance estimation

In order to deal with unpredicted disturbances as well as model mismatch, it is essential to design some state observer able on one hand to estimate the state $x \in \mathbb{R}^{n_x}$ of the system as well as some modeling errors here aggregated and modeled as fluxes, as explained in the present section.

4.5.1 Model extension

Let us consider the following state space representation, where the disturbance vector $d \in \mathbb{R}^{n_d}$ has been introduced in order to model any error on the system. The disturbance vector d gathers, heat flux, CO₂ flux and light flux:

$$d = \begin{bmatrix} d^{Th} \\ d^C \\ d^L \end{bmatrix} \in \mathbb{R}^3 \quad (4.5.1)$$

$$\begin{cases} x^+ &= A \cdot x + [B(y, w)] \cdot u + F \cdot w + F_d \cdot d \\ y &= C \cdot x + D(w) \cdot u + D_d \cdot d \end{cases} \quad (4.5.2)$$

The components of the disturbance vector $d \in \mathbb{R}^3$ are respectively analogous to:

- # d^{Th} [W] is analogous to a heat flux,
- # d^C [-] is analogous to a CO₂ production of one occupant with no heat emission,
- # d^L [lux] is analogous to a lighting system with no heat emission.

They are intended to model the errors resulting from:

- **Unmeasured disturbances:** measurements are assumed available only for local comfort parameters (temperature, CO₂, illuminance) and weather conditions. Thus, the exact number of occupants as well as internal heat gains (resulting for instance from appliances) are unknown.
- **Heat exchange between zones:** which is both due to heat conduction (walls) and air exchange between zones. Notice that, from the zone perspective, the adjacent zone temperatures are unknown. Moreover, air exchanges between zones are unknown.
- **Model mismatch** resulting from identification errors and the non modeled phenomena cited above.
- **Measurement errors** : essentially corrupting the measurements on outdoor conditions since the outdoor conditions (outdoor temperature and external irradiance) are generally provided by the nearest weather station and therefore do not reflect exactly the weather conditions on site.

Starting from the assumption that the disturbance d has a slow dynamic. One can consider the simplistic disturbance model (constant dynamic) which is intended to describe the disturbance dynamics:

$$d^+ = d \quad (4.5.3)$$

one can easily deduce, according to (4.5.3) and (4.5.2), the extended system by forming the matrices $A^{obs} \in \mathbb{R}^{(n_x+n_d) \times (n_x+n_d)}$, $B^{obs}(y, w) \in \mathbb{R}^{(n_x+n_d) \times n_u}$, $F^{obs} \in \mathbb{R}^{(n_x+n_d) \times n_w}$, $C^{obs} \in \mathbb{R}^{n_y \times (n_x+n_d)}$ and $D^{obs}(w) \in \mathbb{R}^{n_y \times n_u}$. This leads to the following state space representation :

$$\begin{cases} \begin{pmatrix} x \\ d \end{pmatrix}^+ = \underbrace{\begin{bmatrix} A & F_d \\ \mathbf{0} & \mathbf{I} \end{bmatrix}}_{A^{obs}} \cdot \begin{pmatrix} x \\ d \end{pmatrix} + \underbrace{\begin{bmatrix} B(y, w) \\ \mathbf{0} \end{bmatrix}}_{B^{obs}(y, w)} \cdot u + \underbrace{\begin{bmatrix} F \\ \mathbf{0} \end{bmatrix}}_{F^{obs}} \cdot w \\ y = \underbrace{\begin{bmatrix} C & D_d \end{bmatrix}}_{C^{obs}} \cdot \begin{pmatrix} x \\ d \end{pmatrix} + \underbrace{\begin{bmatrix} D(w) \end{bmatrix}}_{D^{obs}(w)} \cdot u \end{cases} \quad (4.5.4)$$

In fact, it can be checked that the pair (A^{obs}, C^{obs}) is observable. Therefore, one can easily design a state observer which is capable of estimating on-line the state and the disturbance acting on the system. Hence, a classical Kalman observer has been designed to this end. The estimation of state vector x and the disturbance d are abusively denoted \hat{x} , \hat{d} in the sequel (no distinction is made between estimated and real values).

4.5.2 Disturbance prediction

In the previous section, the extended model (4.5.4) has been used in order to design a state observer to recover the state variables x as well as the disturbance vector d . Here, the use of these disturbance by the control algorithm is described. Basically, a prediction mechanism of these disturbance is presented.

The most common way to treat this issue consists of extrapolating the current observed value of d over the whole prediction horizon. This is mainly performed to ensure an off-set free control. Namely, given an estimation \hat{d} of the disturbance acting on the zone, one would simply use as prediction model for the disturbance the model (4.5.3) in order to build \hat{d} :

$$\Pi_j(\hat{d}_k) = \hat{d}_k, \forall j = 0, \dots, N - 1 \quad (4.5.5)$$

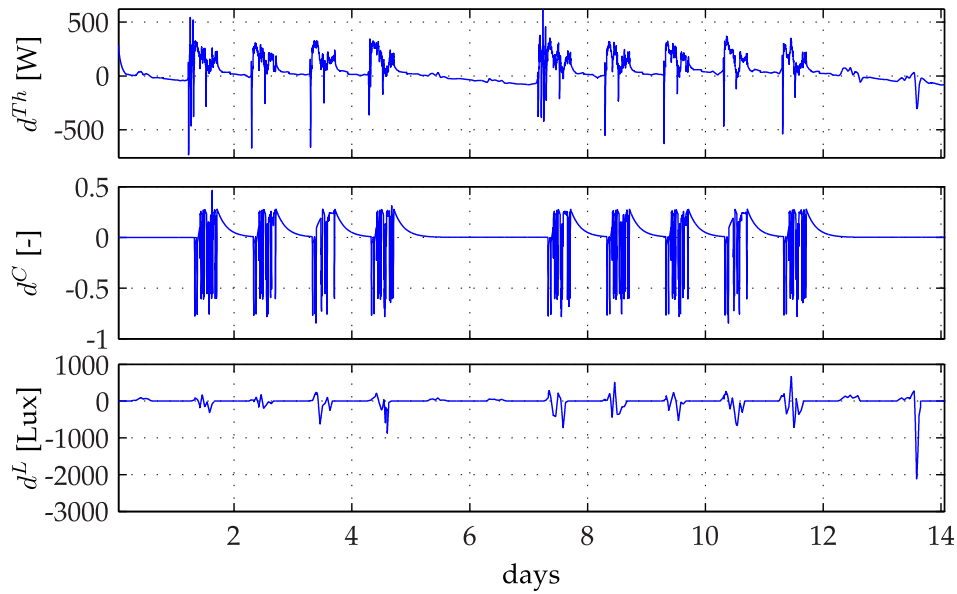


Figure 4.4 Estimated disturbances on two weeks. Note the periodicity of the disturbances. The flat parts (d^{Th} and d^C) correspond to week-ends. The other parts correspond to occupied periods. The daily shape of estimated heat flux is due to occupants and equipment heat production, as well as heat exchanges between zones.

However, an inspection of simulation results⁵ (see figure 4.4) reveals a certain periodicity of the estimated disturbances d (particularly d^{Th} and d^C), which represent respectively the unmodeled heat and CO₂ fluxes observed in the zone.

This result is quite simple to interpret given the investigated kind of buildings. Indeed, in tertiary buildings, occupancy as well as activity are somehow repetitive. Moreover, as the zones follow approximately the same temperatures -for the same reasons-, it is quite evident that the resulting estimated fluxes exhibit the periodicity shown on figure 4.4.

As a result, one can propose the following prediction model of the disturbance over the whole prediction horizon:

$$\begin{aligned} \forall j = 0, \dots, N - 1 \\ \Pi_j(\mathbf{d}_k) = d_k \cdot G(j) + \Pi_{\text{mod}(k+j, N_d)}(\tilde{\mathbf{d}}^{(t)}) \cdot (1 - G(j)) \end{aligned} \quad (4.5.6a)$$

where the function G is a Gaussian function:

⁵In this simulations the designed MPC algorithm has been used. Nevertheless, for the sake of explanations the estimated disturbances are presented first in this section.

$$G(j) = e^{-\alpha_p \cdot j^2} \quad (4.5.7)$$

with:

$$\tilde{\mathbf{d}}^{(t+1)} = \alpha_d \cdot \tilde{\mathbf{d}}^{(t)} + (1 - \alpha_d) \cdot \tilde{\mathbf{d}}^{(t-1)} \quad (4.5.8)$$

where:

- N_d corresponds to 24 hours ($N_d = 24 \cdot 60$), it designates the period over which the disturbance has been recorded,
- t is the current day,
- $0 < \alpha_p$ is a tuning parameter enabling to consider that the observed disturbance will remain constant over a more or less long period of time, which is necessary to ensure a good disturbance rejection, ($(\alpha_p = 0) \Rightarrow (\Pi_j(\mathbf{d}_k) = d_k, j = 1, \dots, N)$) and then starts behaving like the averaged disturbance observed during the last days $\tilde{\mathbf{d}}^{(t)}$.
- The parameter α_d here designates the update coefficient of $\tilde{\mathbf{d}}^{(t)}$ from the day t to the day $t + 1$.

Figure 4.5 illustrates the prediction principle.

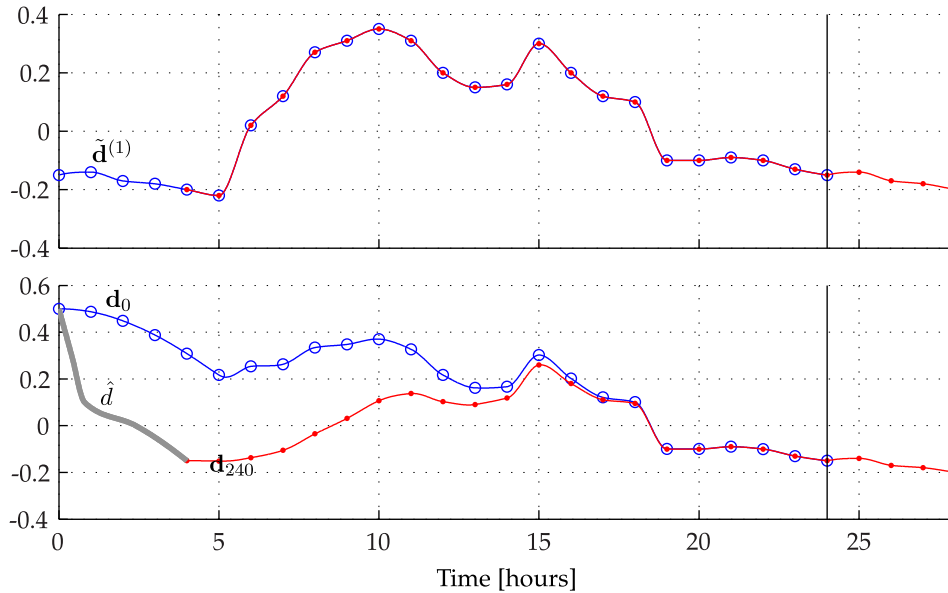


Figure 4.5 Disturbance prediction principle. The predicted disturbance is based on the current estimation of the disturbance provided by the state observer (d) (see the extended system (4.5.4)) as well as past observed disturbances during previous days $\tilde{\mathbf{d}}^{(1)}$.

Figure 4.6 presents a yearly comparison between the mean prediction errors obtained by using the prediction mechanism (red curve) presented here and a simple extrapolation of the current value (blue curve) (see (4.5.5)) for d^{Th} (predictions errors on d^C and d^L exhibit quite similar behaviors as it can be seen in appendix C). Here, the prediction error designates the mean error between the prediction and the real disturbance over the whole prediction horizon. Figure 4.6 presents the results obtained for $\alpha_p = 10^{-4}$ and $\alpha_d = 0.8$ for a prediction horizon of 24 hours.

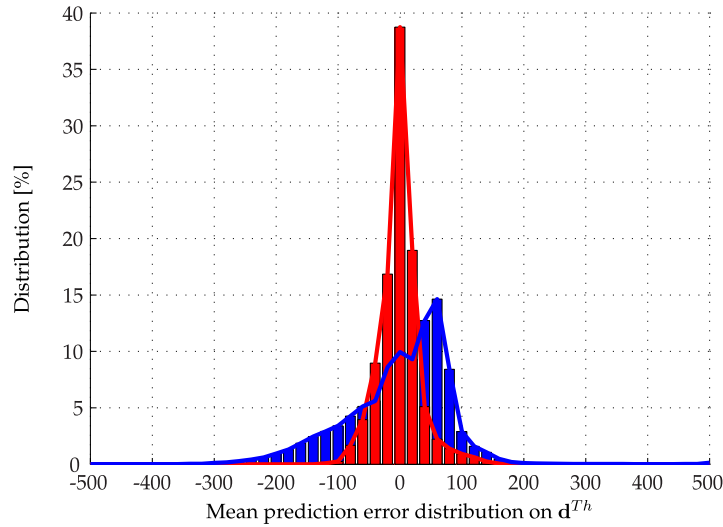


Figure 4.6 Prediction errors comparison between the proposed prediction mechanism (red). In blue: employing the current observed value over the whole prediction horizon ($d^+ = d$). One can note that prediction is improved.

The estimated disturbances over a year are presented in appendix D.

4.6 Convergence analysis

Even if no formal proof of convergence of the algorithm 4.1 is provided, a set of simulations is performed in this part. Figure 4.7 shows the evolution of the error $e^{(s)}$ starting from 100 random initial guesses on input trajectory profiles ($\mathbf{u}_k^{(0)}$). One clearly sees that $e^{(s)} := \text{Max}(\|\mathbf{y}_k^{(s+1)} - \mathbf{y}_k^{(s)}\|_\infty, \|\mathbf{u}_k^{(s+1)} - \mathbf{u}_k^{(s)}\|_\infty)$ decreases very quickly, even when starting from very unrealistic initial guesses. It is important to recall that a warm start (starting from last solution with convenient shifting) is crucial: using a reasonable tolerance η , convergence is achieved generally in one or two iterations.

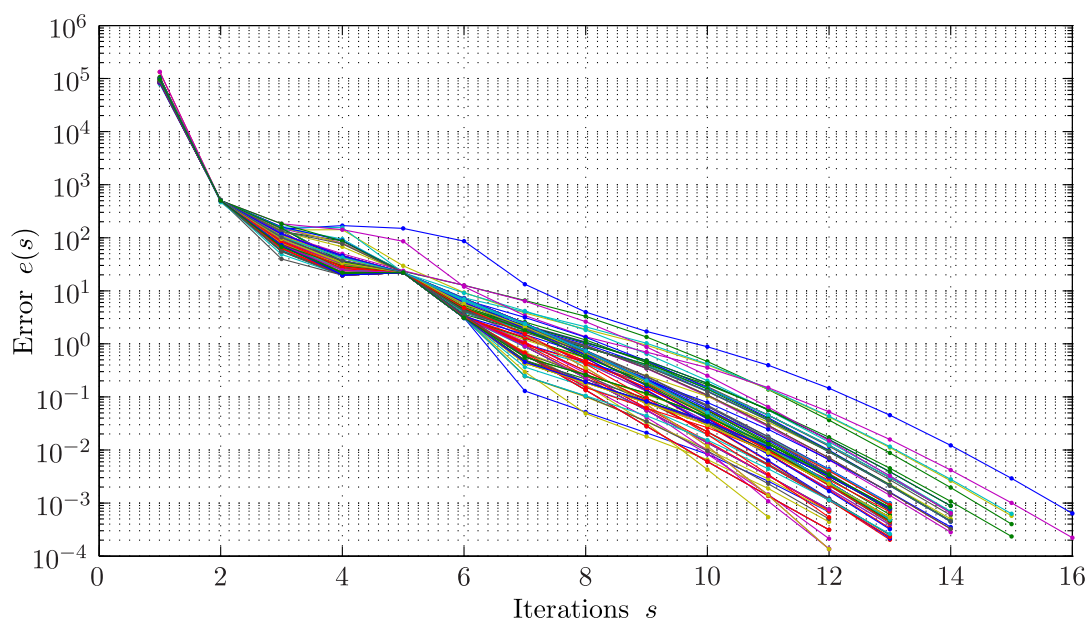


Figure 4.7 Fixed-point algorithm convergence. Evolution of the error $e(s)$ for 100 randomly generated initial guesses $\mathbf{u}_k^{(0)}$. The threshold parameter $\eta = 10^{-4}$. One can see that even when starting from quite unrealistic profiles, the algorithm always converges. Moreover, the error decreases monotonically.

4.7 Input Parametrization and Output checking

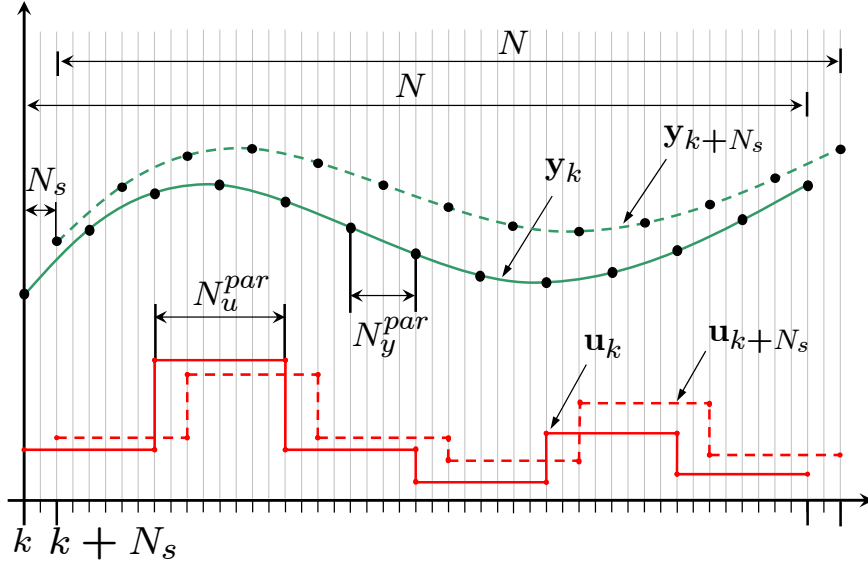


Figure 4.8 Piece-wise constant parametrization of the predicted control profile and undersampling of the optimal predicted output.

It is well known that the computational burden due to the resolution of $\text{LP}_k^{(s)}(\mathbf{y}_k)$ (opt. problem 4.4) is tightly linked to the number of constraints and decision variables involved in.

Since the problem (5.4.11) is high dimensional (a sampling period $\tau = 1\text{min}$ and a prediction horizon length N corresponding to many hours), it is crucial to reduce its size.

In order to reduce the number of decision variables on inputs, a common strategy consists of parametrizing the optimal control sequence \mathbf{u}_k . Basically, instead of looking for arbitrary optimal input profiles \mathbf{u}_k , one restricts the set of admissible optimal solutions to those remaining constant per period of N_u^{par} (see figure 4.8). Namely, the new decision variables $\boldsymbol{\vartheta}_k \in \mathbb{R}^{\frac{N}{N_u^{\text{par}}} \cdot n_u}$ is introduced such that:

$$\mathbf{u}_k = \mathcal{P}_{N_u^{\text{par}}} \cdot \boldsymbol{\vartheta}_k \quad (4.7.1)$$

where the input parametrization matrix $\mathcal{P}_{N_u^{\text{par}}} \in \mathbb{R}^{N \cdot n_u \times \frac{N}{N_u^{\text{par}}} \cdot n_u}$ is defined as follows:

$$\mathcal{P}_{N_u^{\text{par}}} := \mathbf{I}_{\frac{N}{N_u^{\text{par}}}} \otimes [\mathbf{1}_{N_u^{\text{par}} \times 1} \otimes \mathbf{I}_{n_u}] \quad (4.7.2)$$

Moreover, the predicted output profile is under-sampled. This means that the predicted output profile \mathbf{y}_k is checked each N_y^{par} samples, see figure 4.8. The parameter N_s is the refreshing period, it means that the control is updated each N_s time steps. Notice that N_s is in general smaller than N_u^{par} , therefore let us highlight that a N_u^{par} piece-wise constant profile does not mean that the closed-loop control profile is constant per period of N_u^{par} . Actually the input profile is constant per period of N_s , see figure 4.8.

More formally, instead of solving the optimization problem 4.4, the following reduced optimization problem is considered:

Optimization Problem 4.5.

$$\text{LP}^{\text{red}}: \underset{\boldsymbol{\vartheta}_k, \delta_0, \delta_1, \delta_d}{\text{Minimize}} J(\mathcal{P}_{N_u^{\text{par}}} \cdot \boldsymbol{\vartheta}_k, \mathbf{y}_k, \Gamma_k) \quad (4.7.3a)$$

Subject To :

$$\mathcal{C}_{N_y^{\text{par}}} \cdot [\Phi(\mathbf{y}_k^{(s)}, \mathbf{w}_k)] \cdot \mathcal{P}_{N_u^{\text{par}}} \cdot \boldsymbol{\vartheta}_k + \delta_0^- + \delta_1^- \geq \underline{\mathbf{y}}_k - \Psi x_k - \Xi \mathbf{w}_k \quad (4.7.3b)$$

$$\mathcal{C}_{N_y^{\text{par}}} \cdot [\Phi(\mathbf{y}_k^{(s)}, \mathbf{w}_k)] \cdot \mathcal{P}_{N_u^{\text{par}}} \cdot \boldsymbol{\vartheta}_k - \delta_0^+ - \delta_1^+ \leq \bar{\mathbf{y}}_k - \Psi x_k - \Xi \mathbf{w}_k \quad (4.7.3c)$$

$$\mathbf{D} \cdot \mathcal{P}_{N_u^{\text{par}}} \cdot \boldsymbol{\vartheta}_k - \delta_d^+ + \delta_d^- = \mathbf{a}' \quad (4.7.3d)$$

$$\mathbf{0} \leq \boldsymbol{\vartheta}_k \leq \mathbf{1} \quad (4.7.3e)$$

$$\delta_0 \geq \mathbf{0}, \delta_d \geq \mathbf{0}, \mathbf{0} \leq \delta_1 \leq \begin{bmatrix} \delta_y \\ \delta_y \end{bmatrix} \quad (4.7.3f)$$

where \mathbf{a}' and $\mathcal{C}_{N_y^{\text{par}}}$ are given by:

$$\mathbf{a}' := [u_{k-1}^T, \mathbf{0}_{1 \times \frac{N-1}{N_u^{\text{par}}} \cdot n_u}]^T \quad (4.7.4)$$

The output selection matrix $\mathcal{C}_{N_y^{\text{par}}}$ is given by:

$$\mathcal{C}_{N_y^{\text{par}}} := \left[\begin{array}{cc} \mathbf{0}_{n_y \times N_s \cdot n_y} & \mathbf{I}_{n_y} & \mathbf{0}_{n_y \times (N-N_s-1) \cdot n_y} \\ \mathbf{I}_{\frac{N}{N_y^{\text{par}}}} \otimes \left[\mathbf{0}_{n_y \times (N_y^{\text{par}}-1) \cdot n_y} & \mathbf{I}_{n_y} \right] \end{array} \right] \in \mathbb{R}^{n_y \cdot (\frac{N}{N_y^{\text{par}}} + 1) \times N \cdot n_y} \quad (4.7.5)$$

Notice that $\mathcal{C}_{N_y^{\text{par}}}$ selects in the output trajectory \mathbf{y}_k the outputs which correspond to instants $k + N_y^{\text{par}} - 1, \dots, k + 2 \cdot N_y^{\text{par}} - 1, \dots, k + N - 1$, but also the output at instant $k + N_s$. This is to enforce the output of the system to belong to the desired domain at the next decision instant ($y_{k+N_s} \in [\underline{y}_{k+N_s}, \bar{y}_{k+N_s}]$). Otherwise, the output of system could never reach the desired domain.

Remark 4.5.

Notice that the matrices $\mathcal{P}_{N_u^{\text{par}}}$, $\mathcal{C}_{N_y^{\text{par}}}$ and $[\Phi(\mathbf{y}_k^{(s)}, \mathbf{w}_k)]$ are actually never computed on this form. Instead, to render the code efficient, one should note that the parametrization matrix $\mathcal{P}_{N_u^{\text{par}}}$ simply sums successive blocks of columns (of width n_u) of the matrix $[\Phi(\mathbf{y}_k^{(s)}, \mathbf{w}_k)]$. Then the matrix $\mathcal{C}_{N_y^{\text{par}}}$ selects the outputs corresponding to instants $k + N_y^{\text{par}} - 1, \dots, k + 2 \cdot N_y^{\text{par}} - 1, \dots, k + N - 1$. Furthermore, only those rows of the matrix at which some constraint prevails are computed. Hence, the problem 4.5 is actually size-varying over time. This, to render the code more efficient (faster) and to avoid excessive memory usage due to the full computation of the matrix $[\Phi(\mathbf{y}_k^{(s)}, \mathbf{w}_k)]$. \diamond

4.8 Computational study

In this section, a computational study of the predictive control algorithm 4.1 is provided.

Impact of parametrization on computational burden and performances

Here, the objective is to study the computational impact of the parameters N_u^{par} and N_y^{par} involved in the parametrization scheme presented in section 4.7. It goes without saying that the more N_u^{par} and N_y^{par} are large (here taken equal for simplicity), the lower the computational burden is. This is clear on figure 4.9. Actually, one may note that for large prediction horizons, the computational time may become prohibitive if no parametrization is implemented (10 [s]).

Nevertheless, one should also note that larger N_u^{par} and N_y^{par} induce also a decrease of performance (see table 4.1) for obvious reasons (here the simulations have been performed on the first zone of the building). In this monthly simulation, a parameter $N_u^{\text{par}} = 20$ provides nearly the same results as $N_u^{\text{par}} = 5$, while increasing this parameter to $N_u^{\text{par}} = 60$ gives 10% of additional energy consumption and an increase of 102% of TCV (Thermal Constraint Violation).

Actually, this is to illustrate the trade-off between better performance and larger computational burden. Furthermore, for the real-time implementation, the hardware characteristics provide an upper bound on the computational burden which enables to choose adequately the parameters N_u^{par} and N_y^{par} ⁶.

Here, a good compromise was to use a prediction horizon of 12[h] ($N = 720$) with a parametrization $N_u^{\text{par}} = N_y^{\text{par}} = 20$ [min]. Since, as it can be seen on table 4.1-(a),

⁶Indeed, the computational time obtained on the desktop computer used for these simulations is $\approx 1000\times$ lower than the one obtained on a Roombox (discussed in section 4.11)

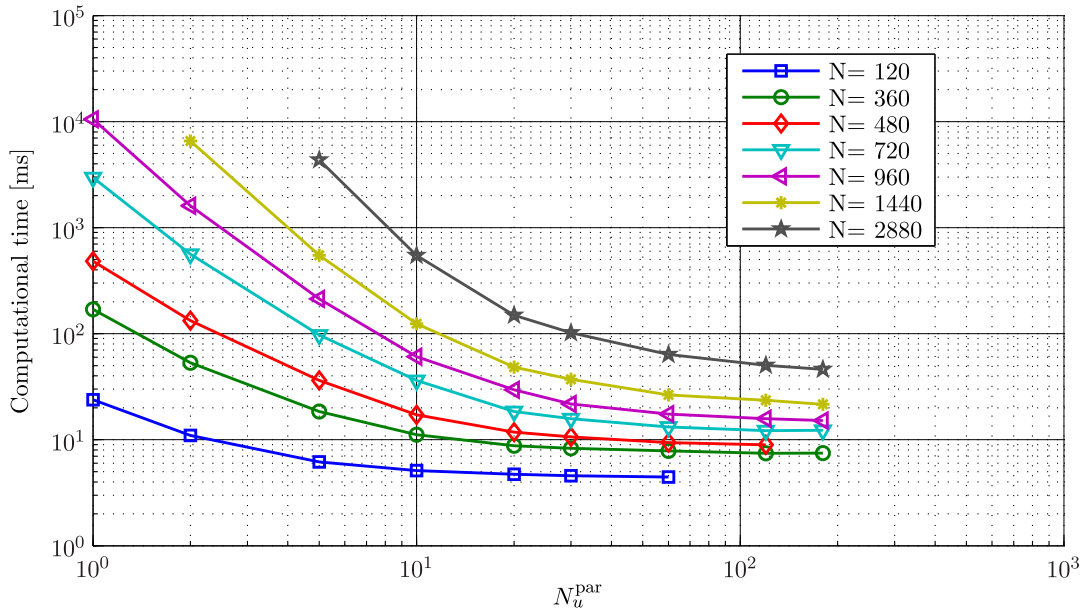


Figure 4.9 Computational time vs. N_u^{par} for increasing horizon lengths ($N_u^{\text{par}} = N_y^{\text{par}}$). Note that the computational burden obviously decreases with increasing N_u^{par} . However this leads to a loss in performance (see table 4.1, page 71), illustrating the trade-off between performance and computational burden.

it actually provides the same results as those for $N_u^{\text{par}} = N_y^{\text{par}} = 5$ with a reasonable computational time.

Evolution of the computational-time in closed-loop

The computation time observed during two weeks is provided. This computational time is extremely low (an average of 14 [ms]) compared to the system dynamics (recall that the parametrization used here is $N_u^{\text{par}} = N_y^{\text{par}} = 20$ for $N = 720$). One can also mention that most of the time is spent in problem preparation (i.e: computation of Φ , see eq. (4.3.13)), the figure 4.10 shows the evolution of computation time. The periodicity of the computational time is due to the fact that the more important is the number of constraints on outputs (which are linked to predicted occupancy of the zone), the more computational effort is needed to build-up the matrix $\Phi(\cdot)$ and to solve the problem 4.5. Moreover, the only rows of $\Phi(\cdot)$ which are computed are those corresponding to outputs where a constraint prevail and the zone is occupied (see remark 4.5). This explains the periodicity of the computation time (the flat parts correspond to decision instants in which the major prediction horizon includes week-ends and therefore no output constraint is introduced on CO₂ and indoor illuminance). Note also that the

4.8. Computational study

N_u^{par}	Invoice(€)	Invoice increase [%]	TCV* [°C·h]	TCV increase [%]
5	36.55	+ 1.90 %	0.177	0 %
10	35.87	+ 0 %	0.183	+ 3.39%
20	36.96	+ 3.04 %	0.190	+ 7.34%
30	37.82	+ 5.44 %	0.188	+ 6.21%
60	39.61	+ 10.43 %	0.359	+ 102.82 %
120	42.72	+ 19.10 %	0.377	+ 112.99 %

(a): N=720 (12H)

N_u^{par}	Invoice(€)	Invoice increase [%]	TCV* [°C·h]	TCV increase [%]
5	35.13	+1.20	0.169	+2.83 %
10	34.71	+0 %	0.165	+ 0 %
20	35.32	+1.76 %	0.172	+ 4.44 %
30	36.30	+4.59 %	0.175	+ 6.36 %
60	37.70	+8.60 %	0.306	+ 85.67 %
120	38.92	+12.11 %	0.400	+ 142.28 %

(b): N=1440 (24H)

Table 4.1 Impact of parametrization on closed-loop performances (N=720) and (N=1440). Note that the minimal energy cost is achieved for $N_u^{\text{par}} = 10$ and the best comfort is achieved for $N_u^{\text{par}} = 5$, even if the differences are quite insignificant. Similar remarks can be made when N=1440. (here $N_y^{\text{par}} = N_u^{\text{par}}$. *TCV: Thermal comfort violation)

allowed number of iterations is set to only one in this case. The same kind of results has been observed on the 20 zones composing the building (see appendix E).

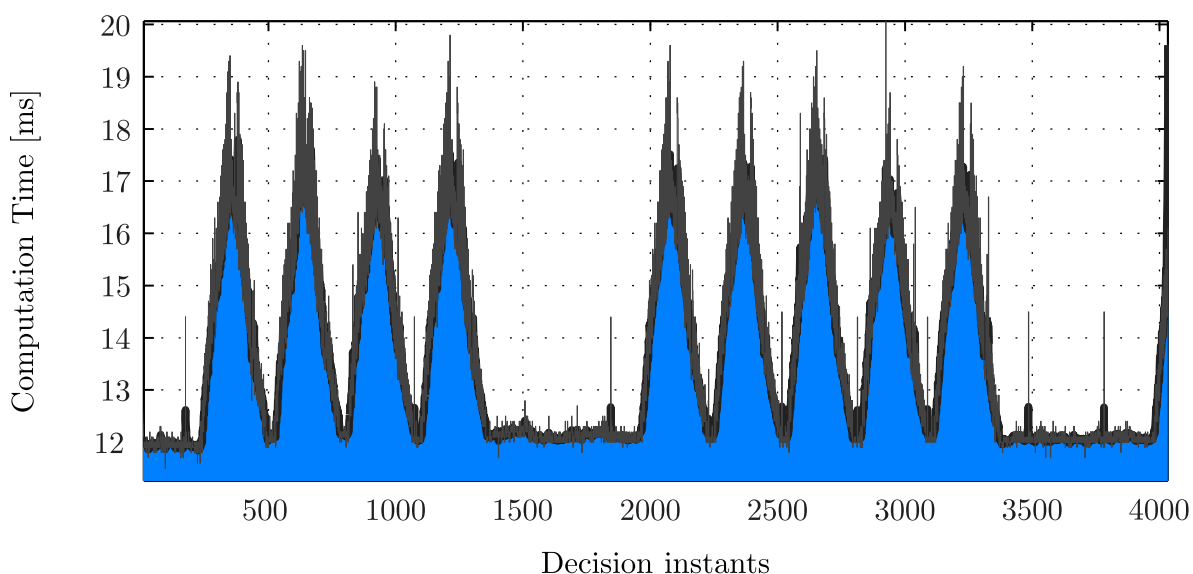


Figure 4.10 Computational time evolution ($N = 720$, $N_u^{par} = 20$, $N_y^{par} = 20$). Note the clear periodicity of the computational time. Indeed, the high computational times (19 [ms]) correspond to decision instants at which occupancy takes a large part of the prediction horizon leading to more constraints in the optimization problem (see remark 4.5). Results obtained on an Intel[®] Xeon[®] @ 2.67 GHz, 3.48 Go RAM. ILOG CPLEX 12.1 is used to solve the linear programming problems.

4.9 Simulations - some investigations

In this section, some simulation results regarding only one zone of the building are provided to illustrate the main features of the proposed controller. Then, a yearly simulation is performed on a complete building in the next section to assess the proposed controller. The investigations that have been conducted are the following ones:

- Zone MPC validation, in subsection 4.9.1,
- Dealing with variable energy prices, in subsection 4.9.2,
- Impact of prediction horizon length, in subsection 4.9.3,
- Introducing uncertainty, in subsection 4.9.4,

4.9.1 Zone MPC validation

This first simulation aims to illustrate the behavior of the proposed controller, and concerns a unique zone of the building (here zone # 1 simulated on 48[h], figure 4.11). The objective here is to minimize energy consumption. Notice that the controller enables to ensure comfort by respecting the prescribed bounds. Here, an optimal start is implemented each day. Notice also, that lighting is used as a heat complement during the optimal-start period. Remark also, that blinds are closed during night ($Ub_1^W = Ub_1^N = 0$) to ensure less heat losses and opened during day to introduce heat as well as natural light(solar). Remark also, that the management of the west blind is different from the one on the north façade. This is due to the fact that no solar irradiance exists on the west façade during morning. Therefore, the blind remains closed to ensure less heat losses.

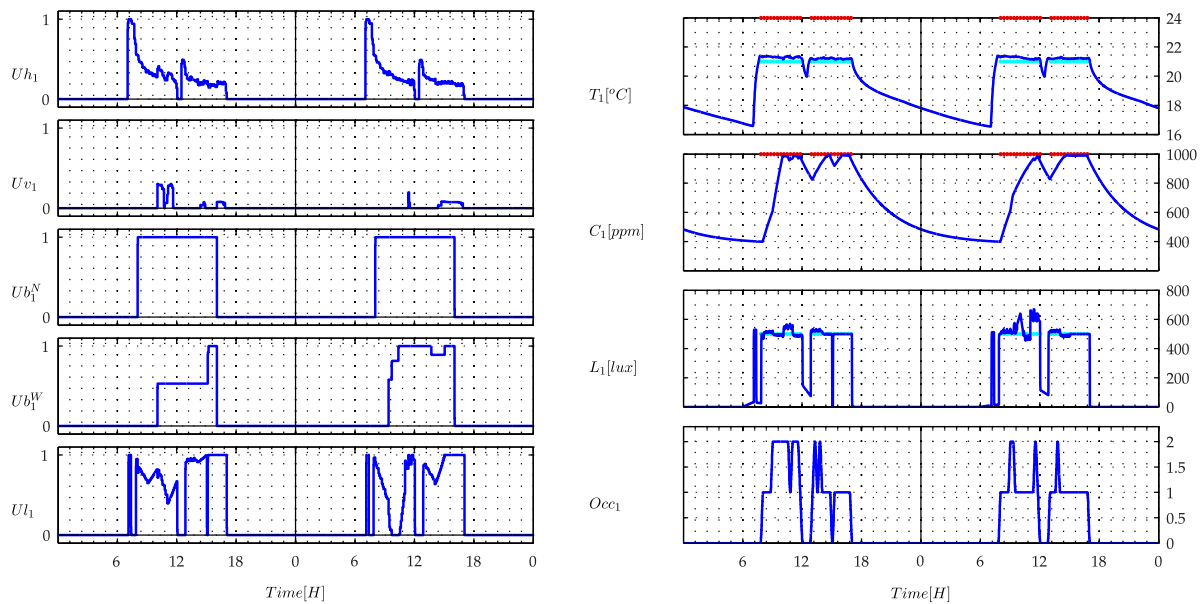


Figure 4.11 Zone model predictive controller validation - illustrative behavior in an office. Note that temperature bounds, CO₂ and lighting bounds are respected.

4.9.2 Dealing with variable energy prices

As mentioned before, dealing with variable energy prices is one of the most interesting features when using MPC. Here, a study is performed on two different zones provided as illustrations. The objective is to study the benefit of taking into account price signals. Namely, one considers the price signal depicted on figure 4.12, where β_p designates a multiplicative coefficient between off-peak period electricity price (γ_{off}) and on-peak period electricity price ($\gamma_{\text{on}} = \beta_p \cdot \gamma_{\text{off}}$). For β_p fixed, MPC is used to minimize the energy invoice. The invoice is then compared to invoice if one minimizes energy instead.

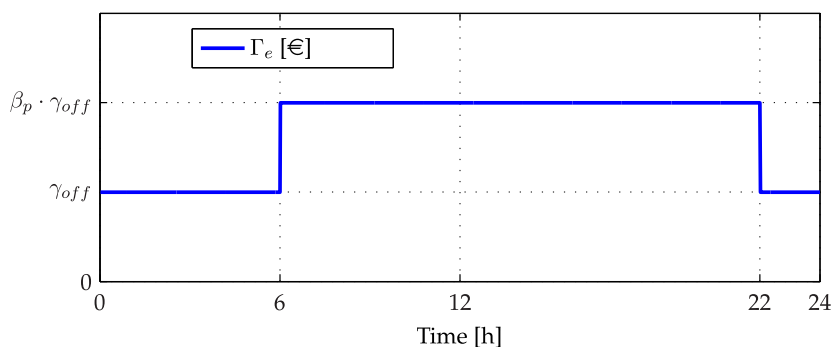


Figure 4.12 On-peak/ Off-peak electricity price. parametrized by $\beta_p > 1$.

Results of two zones are provided on figure 4.13. The first sub-plot corresponds to the invoice when minimizing energy (blue) when applying the price signal (figure 4.12) and when minimizing electricity cost (green), the second sub-plot corresponds to the relative differences and third one to the corresponding optimal temperature trajectories for each value of β_p . (when $\beta_p = 1 \Rightarrow$ energy minimization).

It can be noticed that the more β_p is large, the more important becomes the inclusion of the price signal during the heating scheduling, which is quite evident. Notice however, that the corresponding temperature profiles between the two zones are rather different.

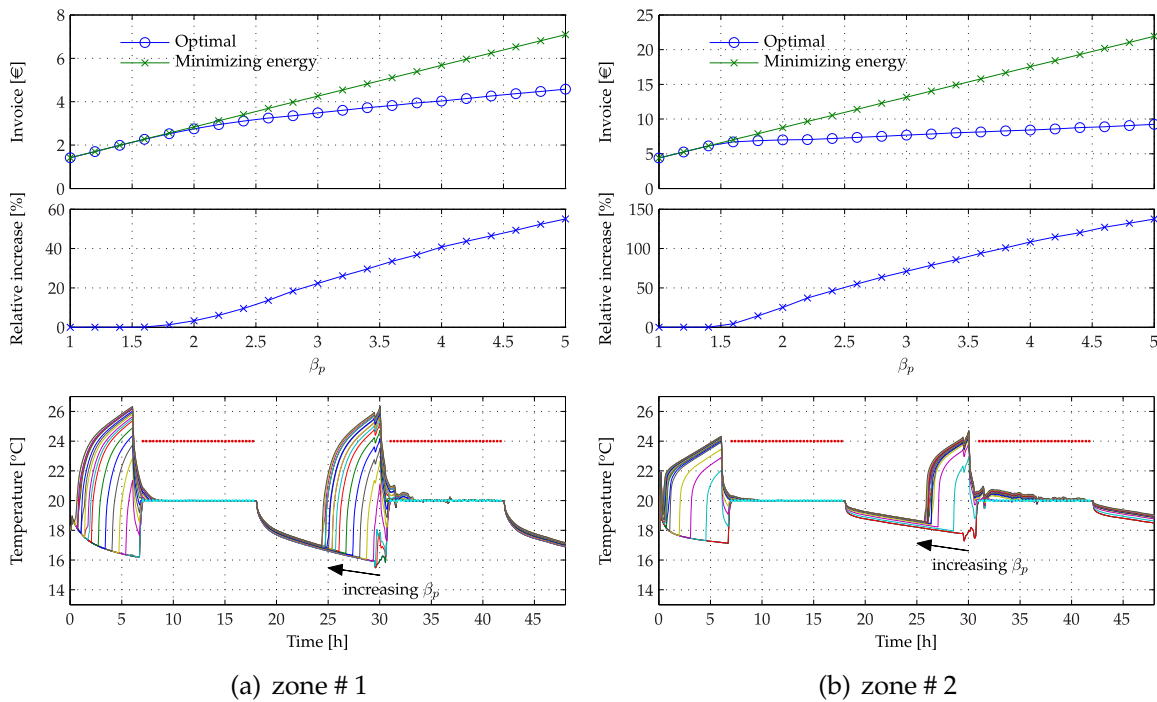


Figure 4.13 Invoice minimization for different values of β_p . The first sub-plot corresponds to the invoices obtained for different values of β_p (optimal) and the corresponding invoice if minimizing energy. The last sub-plot corresponds to the optimal temperature trajectories.

Note that, for the first zone (zone # 1) when $\beta_p = 2$, minimizing energy instead of minimizing invoice results in an increase of $\approx 5\%$ in the total invoice while in the zone # 2 this results in an increase of $\approx 25\%$. The zones are submitted exactly to the same outdoor conditions. Furthermore, notice that the temperature trajectories followed by the zones are different in the two cases and moreover, note that it could be difficult, even in this simple situation to design some rule able to deal with this case. Furthermore, notice on figure 4.14, the same simulation is performed, but with a different heating system (heaters are half dimensioned), the results are also different.

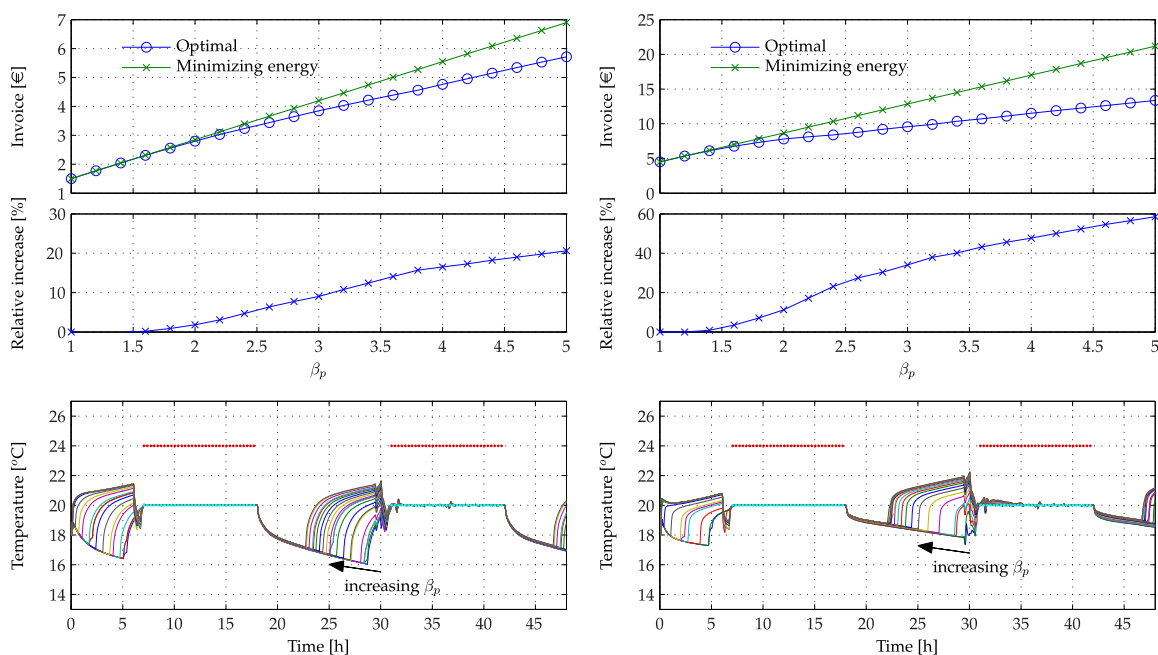


Figure 4.14 Invoice minimization for different values of β_p with the same zones but with a different heater dimensioning (heaters powers is reduced by 50 %). The first sub-plot corresponds to the invoices obtained for different values of β_p (optimal) and the corresponding invoice if minimizing energy. The last sub-plot corresponds to the optimal temperature trajectories.

4.9.3 Impact of prediction horizon length

Taking two zones of the building, let us now study the impact of the prediction horizon on the performances of the scheme (figure 4.15). Here a weekly simulation on two zones has been performed. In this case, notice that the prediction horizon length has a significant impact on the performance of scheme.

Indeed, for the first zone, small horizon lengths leads to impossibility to provide comfort. Furthermore, an increase of the horizon length produces a significant decrease in the invoice ($\approx 13\%$). For the second zone, the invoice decreases also significantly ($\approx 21\%$) but comfort is always provided.

Nevertheless, one clearly sees that the larger the horizon is, the better the performances are until a 24 [h] prediction horizon length over which no improvement is possible.

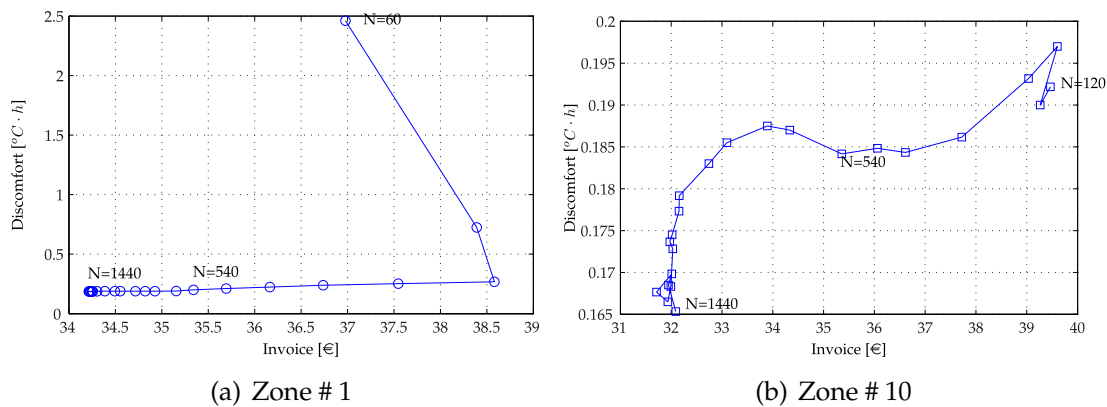


Figure 4.15 Impact of horizon length on performances for two zones in a building. Notice that sensitivity of the zones regarding horizon length is sensibly different. For the first zone small horizon lengths lead to discomfort while for the second, this only reduces energy usage.

4.9.4 Introducing uncertainty

It is worth underlining that within the MPC framework, it is crucial to take into account uncertainties on predictions during the assessment of this control strategy, since predictions are directly integrated in the process of decision making. This is the reason why we propose to study the effect of uncertainties related to weather and occupancy.

It is difficult to model exactly the errors introduced by meteorological forecast services. Therefore, let us assume that a meteorological forecast service (with in situ correction feature⁷) can be modeled by:

$$\mathbf{w}_k = \alpha \cdot \mathbf{w}_k^P + (1 - \alpha) \cdot \mathbf{w}_k^F \quad (4.9.1)$$

where:

- \mathbf{w}_k^P is the perfect prediction profile, \mathbf{w}_k^F is the prediction given by the n_d -bin predictor defined hereafter by (4.9.2),
- $\alpha \in [0, 1]$ defines the quality of weather forecast. Indeed, it is used to weight the perfect prediction and the false one. This way, we can easily control the error on forecast (if $\alpha = 1$ the weather is perfectly known).
- The n_d -bin predictor that we use is a slightly modified version of the one given by [Henze et al. 2004], namely:

⁷The current weather forecast is corrected based on in situ measurements

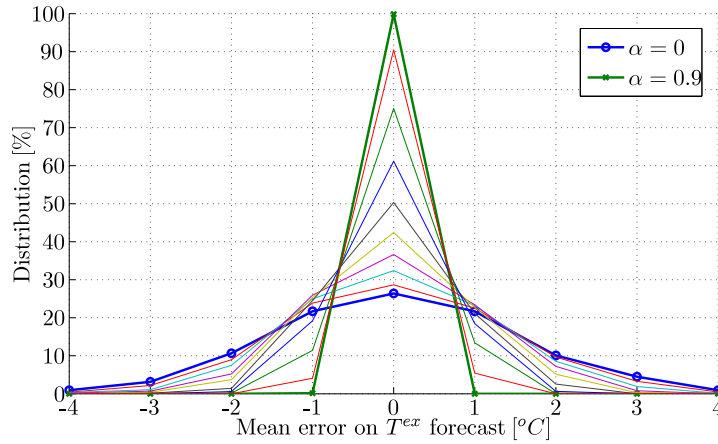


Figure 4.16 Mean error distribution on outdoor temperature forecast service for different values of α for a prediction horizon of 12[h].

$$\Pi_j(\mathbf{w}_k^F) := \frac{1}{n_d} \sum_{d=1}^{d=n_d} w_{(k+j-24\cdot 60\cdot n_d)} + \left(w_k - \frac{1}{n_d} \sum_{d=1}^{d=n_d} w_{(k-24\cdot 60\cdot d)} \right) \quad (4.9.2)$$

This simply means that the predicted temperature for the next 24hours is the mean temperature profiles observed on the n_d previous days and adjusted to fit the current measured temperature (this explains the term $w_k - \frac{1}{n_d} \sum_{d=1}^{d=n_d} w_{(k-24\cdot 60\cdot d)}$). Remark that the first temperature is always perfectly known.

This procedure is used for the prediction of outdoor temperature. Figure 4.16 shows the mean error distribution with a 20-bin predictor (prediction horizon of 12[h]) for Trappes (near Paris) weather station for one year. It is interesting to notice that the proposed simple model (4.9.1) gives unbiased predictions with Gaussian-like error distribution.

We propose in this section some simulations performed on a simple case study. The zone in consideration is a 20 m² office and has two facades (west and south), each of them has a window equipped with blinds. The controlled actuators consist of a heater (u_h), a mechanical ventilation (u_v), a lighting system (u_l) and two blinds u_{b1}, u_{b2} . Their respective power consumptions are (1.5, .15, .5, 0, 0) [kW].

The nominal number of occupants is $N_{occ} = 3$. MPC prediction horizon is 24 hours and a new optimal solution is computed each five minutes. The energy rate is two times higher between 6a.m and 10p.m (Fig. 4.17).

α	0	.5	1
Invoice (€)	10.17	9.88	9.78
%	104%	101%	100 %

Table 4.2 Energy invoice for different values of α . Note in this case that the most uncertain weather predictions induce an increase of 4 % compared to the ideal case (no error on forecast).

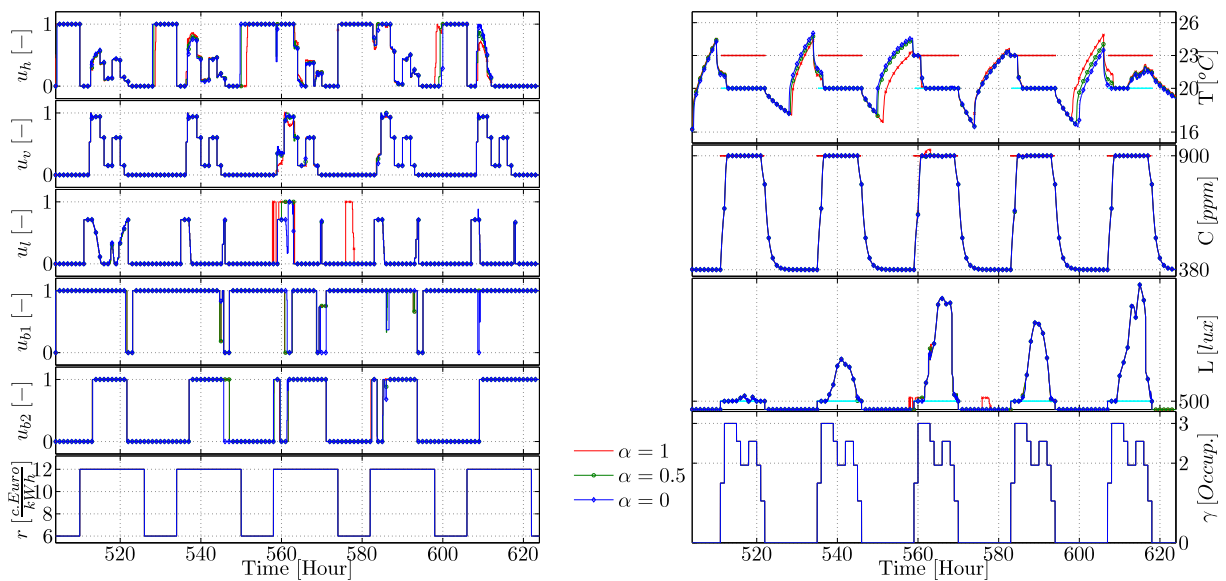


Figure 4.17 Simulation results for $\alpha = \{0, 0.5, 1\}$ with perfectly known occupation profile. Remark that uncertainties on predictions mainly induce a bad estimation of the heating optimal start time (top-left). Comfort bounds are always respected.

Perfectly known occupation

In this first simulation, only uncertainties on weather conditions are introduced. This leads to the results depicted on fig. 4.17. Simulations for 3 values of α has been conducted (0, 0.5, 1). Unsurprisingly, degradation of weather forecast quality generates an increase of the invoice (table 4.2). In this case study, a maximum of 4% of increase (corresponding to $\alpha = 0$) has been noted. Let us notice that, independently of the energy invoice, comfort is maintained since temperature, CO₂ level and indoor illuminance are kept within their respective prescribed bounds (red and cyan).

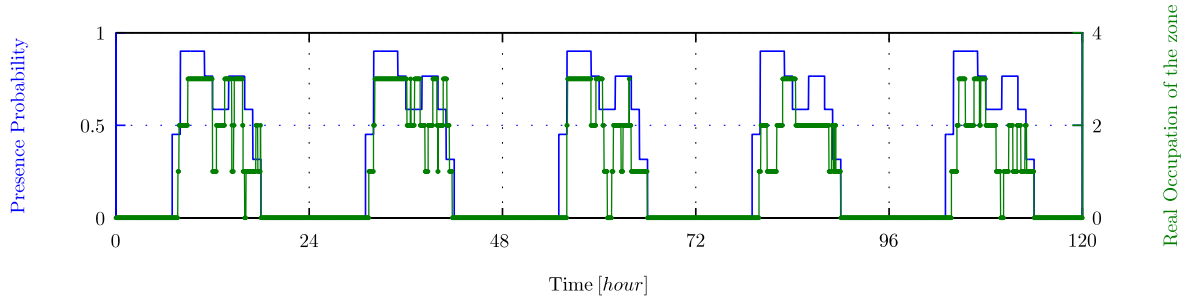


Figure 4.18 Presence probability (blue) and corresponding generated stochastic occupancy profile (green).

Occupancy Modeling

It is well known that occupancy presence has a great impact on energy consumption [Mahdavi & Pröglhöf 2009]. Therefore, it is necessary to inject more realistic occupation profiles that may reveal unobserved behaviors with classical occupation schedules. In order to enrich the occupancy profiles, the following Markov chain based model is used to describe the presence of each occupant in a given zone. This model has been proposed in [Page 2007] and is defined by its transition matrix $\mathcal{T}(k)$:

$$\mathcal{T}(k) = \begin{bmatrix} T_{00}(k) & T_{01}(k) \\ T_{10}(k) & T_{11}(k) \end{bmatrix} \quad (4.9.3)$$

where $\{T_{ij}(k)\}_{(i,j) \in \{0,1\}^2}$ are time dependent transition probabilities of the Markov chain describing the presence/absence of the occupant in the zone (0:absent,1:present), and are given by:

$$T_{01}(k) = \frac{\mu - 1}{\mu + 1} \cdot P(k) + P(k + 1) \quad (4.9.4a)$$

$$T_{11}(k) = \frac{P(k) - 1}{P(k)} \cdot \left[\frac{\mu - 1}{\mu + 1} \cdot P(k) + P(k + 1) \right] + \frac{P(k + 1)}{P(k)} \quad (4.9.4b)$$

$$T_{00}(k) = 1 - T_{01}(k) \quad (4.9.4c)$$

$$T_{10}(k) = 1 - T_{11}(k) \quad (4.9.4d)$$

where μ is the parameter of mobility and is used to adjust the moving frequency of the occupant. $P(k)$ is the presence probability of the occupant in the zone. Given a nominal number of occupants in each zone N_{occ} , one can define for each occupant a presence/absence model. Fig. 4.18 depicts a typical result given by 4.9.3. The presence probability profile (blue curve) is defined in accordance with the occupation schedule of the zone. One can refer to [Page 2007, Mahdavi & Pröglhöf 2009] to find some elements regarding appropriate choices of μ and $P(k)$.

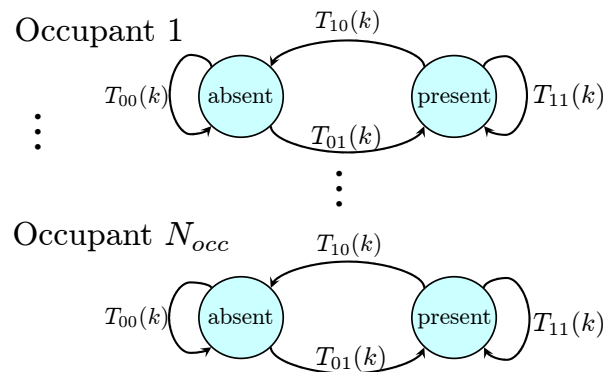


Figure 4.19 Markov chain of occupancy in a zone. The transition probabilities are time varying. Each occupant is characterized using its own Markov chain.

α	0	.5	1	*
Invoice (€)	9.57	8.98	8.92	8.13
%	118 %	110	109 %	100 %

*: weather and occupancy perfectly known.

Table 4.3 Invoices with the introduction of errors on occupation and weather forecast

Uncertainty on both weather and occupation

Let us now introduce in addition uncertainties on the number of occupants in the zone. In this case, the predicted number of occupants (used by the MPC) corresponds to occupancy schedule used in the previous simulation, however the real number of occupants in the zone (injected in SIMBAD) is generated using the stochastic procedure cited above. Notice in this case that the invoice is enlarged comparing to the "perfectly known forecast" case by 18% (table 4.3). This enables us to give a quite realistic potential gain given a known quality of weather forecast for a realistic occupancy profile. Let us finally mention that comfort requirement is always ensured (Fig. 4.20) attesting the robustness of the control strategy in providing comfort for occupants.

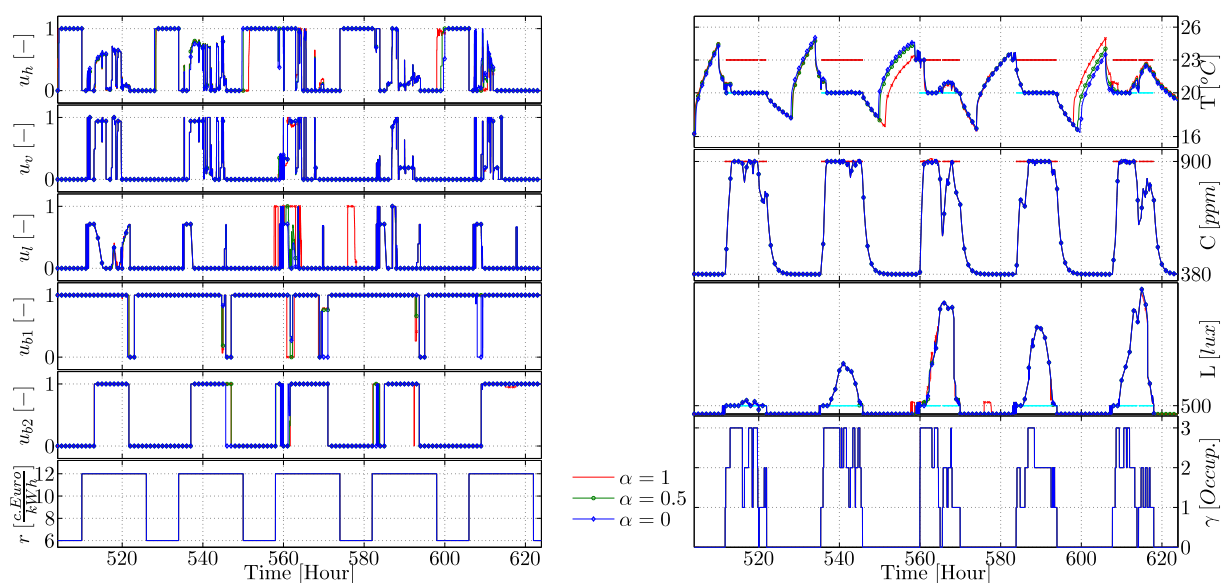


Figure 4.20 Simulation results with uncertainties on weather ($\alpha = \{0, 0.5, 1\}$) and occupation profile. Notice that comfort bounds on the three controlled variables are always respected.

4.10 Yearly simulation

In this section a yearly simulation is performed. Let us first describe the case study and give some technical details regarding the interface between the controller and the simulator before discussing the simulation results.

4.10.1 Case study

The NMPC strategy has been assessed on a multizone building. The chosen building is a typical small office building which corresponds to nowadays construction standards (2006). Its area is approximatively 540 m^2 and is divided in 20 zones. It is located at Trappes (near Paris). The external walls are composed of a layer of thermal insulation and a layer of concrete. Each zone of the building is controlled by a zone NMPC controller. Let us emphasize that the zones are both structurally and dynamically different (see chapter 3). The prediction horizon is 12[h] and the update period $N_s = 5[\text{min}]$. Concerning comfort requirements, they are summarized in table 4.4. Here, the MPC has only access to occupancy schedules. Concerning weather forecast an uncertainty is introduced using the procedure described above. We consider here the two extreme cases. No error on forecast ($\alpha = 1$) and the maximal error on forecast ($\alpha = 0$). See figure 4.16.

	T [$^{\circ}C$]		C [ppm]		L [lux]	
	<i>min</i>	<i>max</i>	<i>min</i>	<i>max</i>	<i>min</i>	<i>max</i>
Occupied	21	24	–	1000	500	–
Vacant	5	35	–	–	–	–

Table 4.4 Nominal comfort region

4.10.2 Zone controllers integration in SIMBAD

Even if SIMBAD is a Simulink based toolbox. Integration of zone MPC controllers appeared to be challenging. This results essentially from:

- a. A large computational burden induced by such optimization-based control strategy. For the targeted building consisting of 20 zones, an update period of 5 [min] results for a yearly simulation in $\approx 2.100.000$ optimization problems, which is quite large. Actually, each simulation takes at least 18 hours for quite moderate prediction horizons (12 hours). These simulation times were obtained after optimizing the controllers code and employing when appropriate C-code. This was for instance the case for the zones models as they are used on-line by the controller (see algo. 4.1, page 60). Indeed, before code optimization the interface with SIMBAD was far unrealistic as the MPC code was approximately ten times slower.
- b. The whole building number of inputs is 89 and controlled outputs 60. Moreover, each zone has its own structure depending on its own configuration (heaters, ventilation, number and orientation of blinds, adjacent zones, etc.).

To tackle these issues, Object-Oriented Programming (OOP) has been used to manage zone controllers. Furthermore, a C-code model file describing both the structure and the dynamic model of each zone has been generated (based on the zone models identified on chapter 3). This offered to the whole code a coherent structure that could be *easily adapted* to the structure of the building and represents a first attempt for an MPC toolbox dedicated to building management systems. The interface between the Simulink model and the Matlab-based controller has been performed by a Simulink S-function. These steps are summarized on figure 4.21.

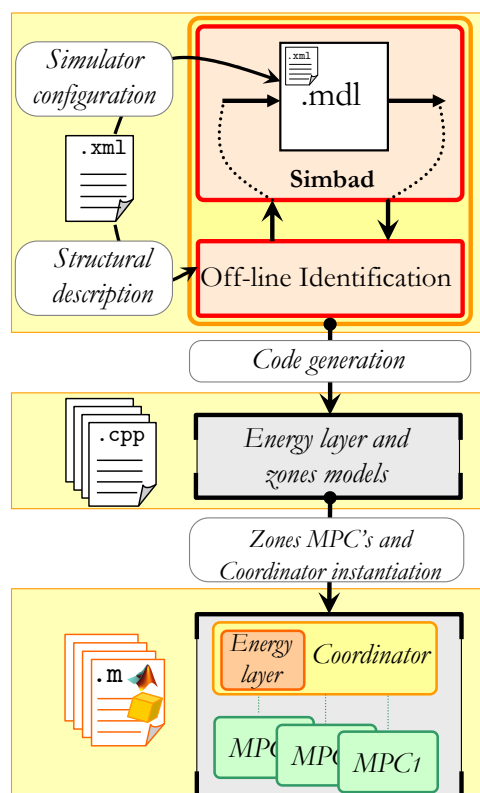


Figure 4.21 MPC integration in SIMBAD - workflow. The off-line identification procedure is described in chapter 3. Coordinator and energy layer will be discussed in chapter 7.

4.10.3 Simulation results

Table 4.5 summarizes the yearly consumptions obtained by the designed rule based controller and the proposed NMPC controller. Figure 4.22 provides the monthly consumptions resulting when implementing a rule-based strategy (left) and the predictive strategy (right). It has to be noticed that the designed controller corresponds to most advanced rule-based controller designed during the HOMES program. Indeed, it does not correspond to nowadays practice as it integrates much more capabilities (as adaptive optimal strategy for instance, more advanced blind management, etc.). The results show that the global comfort is nearly the same in the two situations. The total amount of constraints violation (sum over all the zones) is however lower with a model predictive control (295 [k^oC·h]) compared to a rule based controller (322 [k^oC·h]). In this study, one should note that MPC enabled $\approx 16\%$ of energy savings. Energy savings are essentially due to a better overall management of interactions between actuators as well as some anticipation concerning optimal start. Let us take two situations (office and meeting room) to illustrate the main differences.

	Energy cons. [kWh/m ²]	GTC [%]	TCV [k·°C·h]
Rule based	142	91.6	322
MPC ($\alpha = 1$)	119 (-16%)	91.8	295
MPC ($\alpha = 0$)	122 (-14%)	88.1	310

Table 4.5 Energy consumption / Comfort - Rule-based vs. MPC

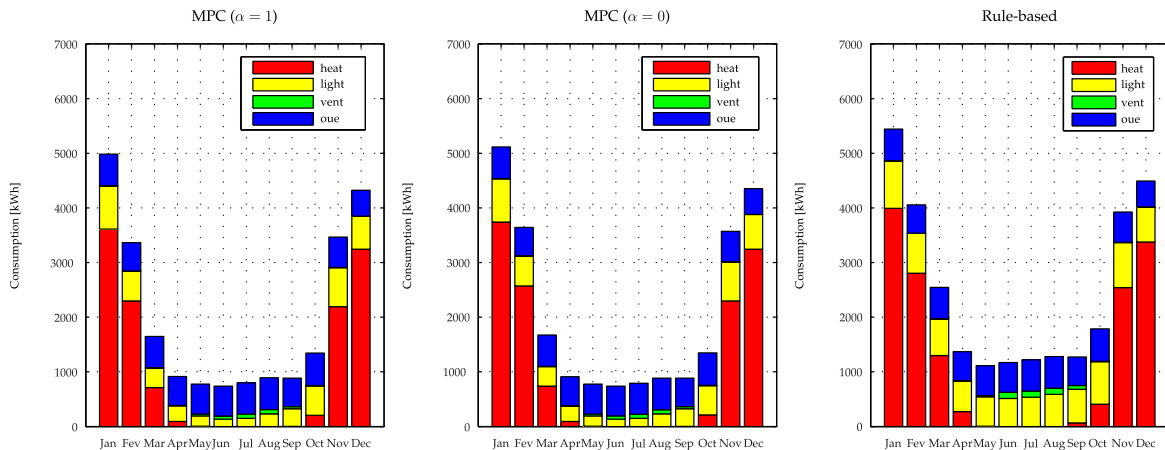


Figure 4.22 MPC vs. RB monthly energy consumptions. Note that introducing uncertainty in forecast induces more energy consumption but still less than with rule-based control.

In a typical office for instance (figure 4.23), one clearly sees that MPC enables a much better optimal start determination compared to rule based strategy (see the two rectangles on figure 4.23 which correspond to an occupancy after a long vacancy period). Remark also (figure 4.23) that for rule based strategy a set-back temperature is implemented at 16 [°C] (first rectangle). Moreover, remark that optimal start is in this case quite inefficient during all working days as temperature fails to achieve the minimal temperature at occupants arrival.

Figure 4.24 shows the temperature profiles obtained by the two strategies in a meeting room. Notice that in the case of the rule-based control temperature is quasi-systematically under the reference.

Nevertheless, it is important to highlight that due to some modeling errors (on solar flux projections) the average temperature in whole building (figure 4.25) can violate the upper constraint during summer. Notice also that a rule-based strategy could lead (particularly during middle-season) to an inappropriate behavior (days 130-150). Indeed, the temperature is in this case largely over the upper constraint as the cooling season does not start yet, then it is decreased (day 150) when the cooling season starts

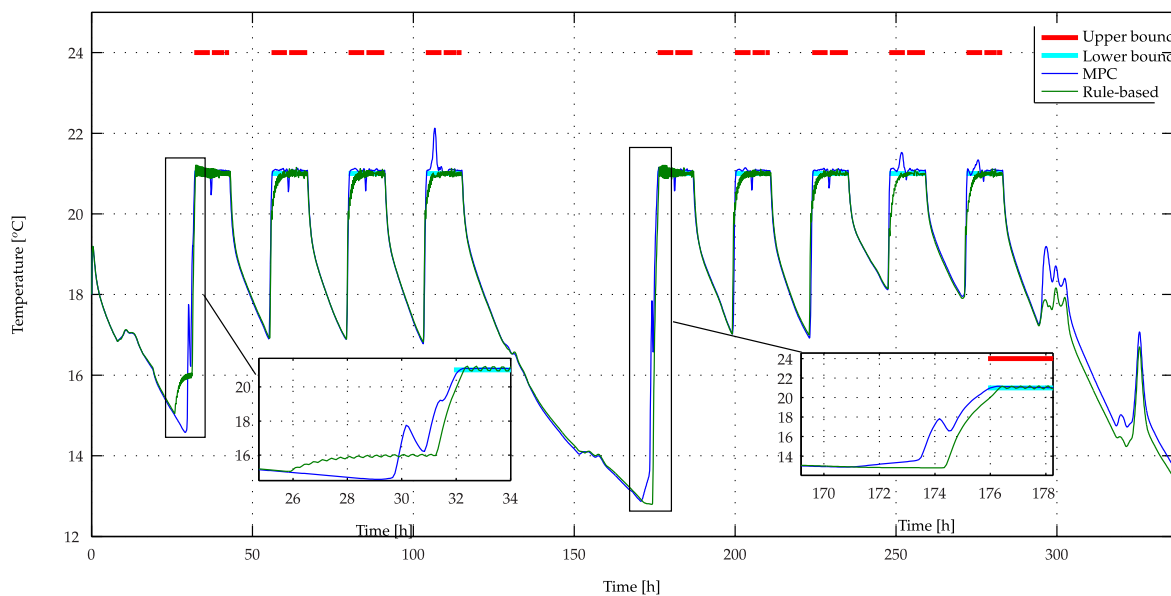


Figure 4.23 MPC vs. Rule-based control - temperature profiles in an office during the two first weeks. The two rectangles correspond to optimal starts after a long vacancy period.

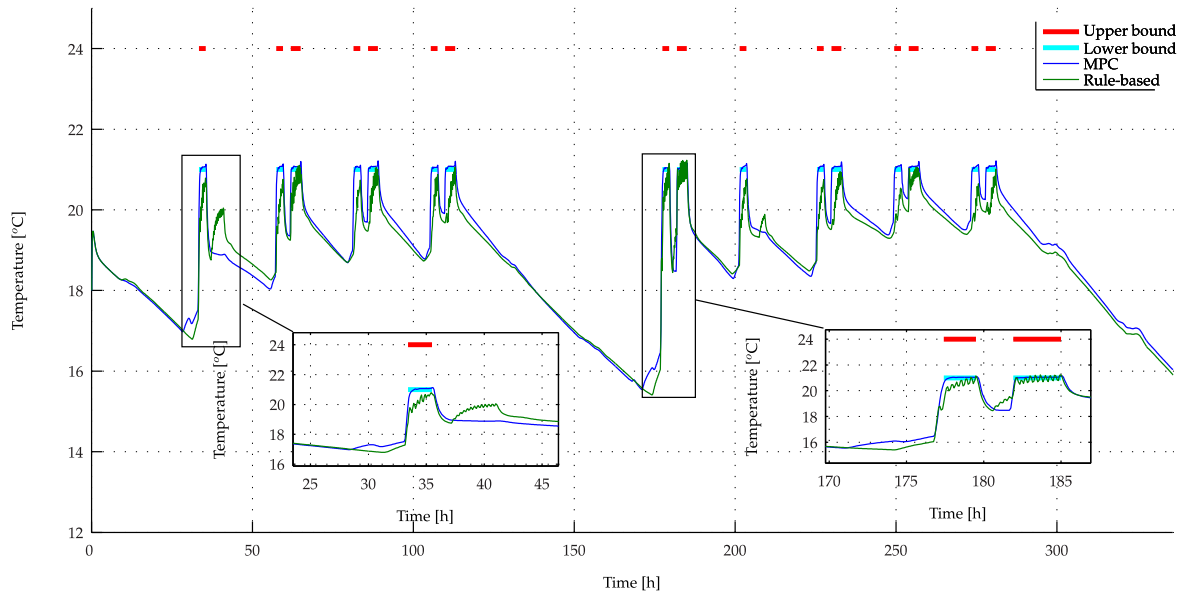


Figure 4.24 MPC vs. Rule-based control - temperature profile in a meeting room during the two first weeks. Observe that control performances with MPC are much better.

and leads to a cold discomfort during the beginning of May. This illustrates the difficulty of managing temperature using some schedule-based heating/cooling seasons. The same behavior can be observed at the end of cooling season.

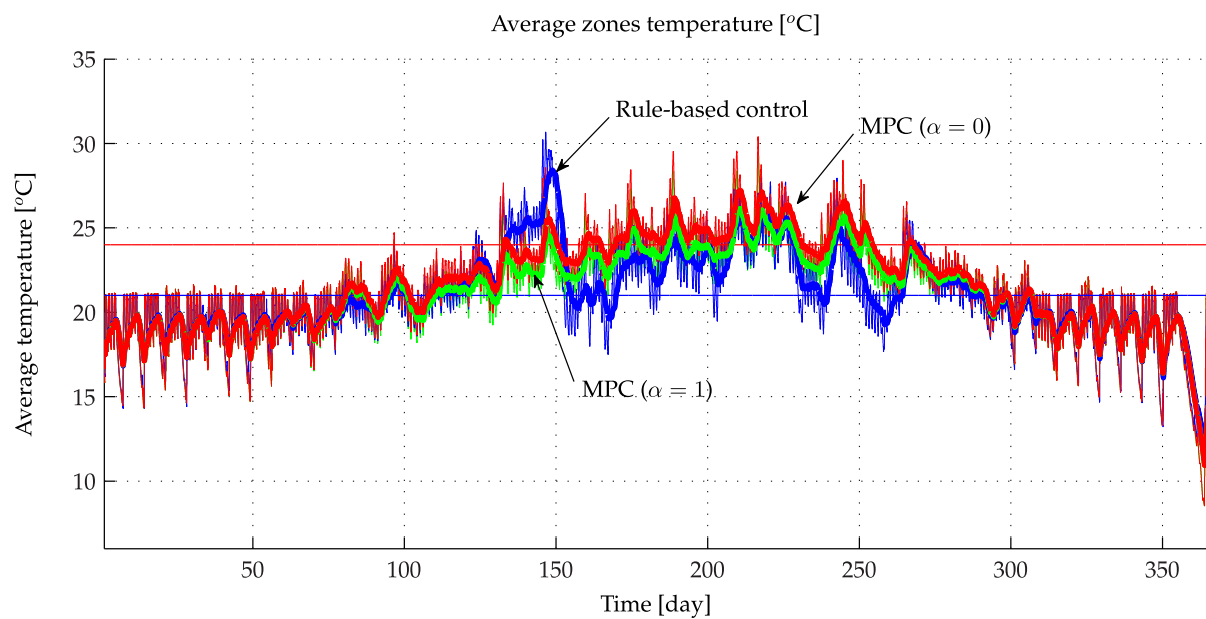


Figure 4.25 MPC vs. RB- yearly building average temperature. The figure only illustrates the global thermal behavior of the building during the year.

Figure 4.26 shows the simulation results obtained over the year for all the zones of the building (only the zones in which temperature is regulated). Note that in some zones, applying the MPC strategy leads to less energy but also less comfort. This discomfort is almost occurring during summer season.

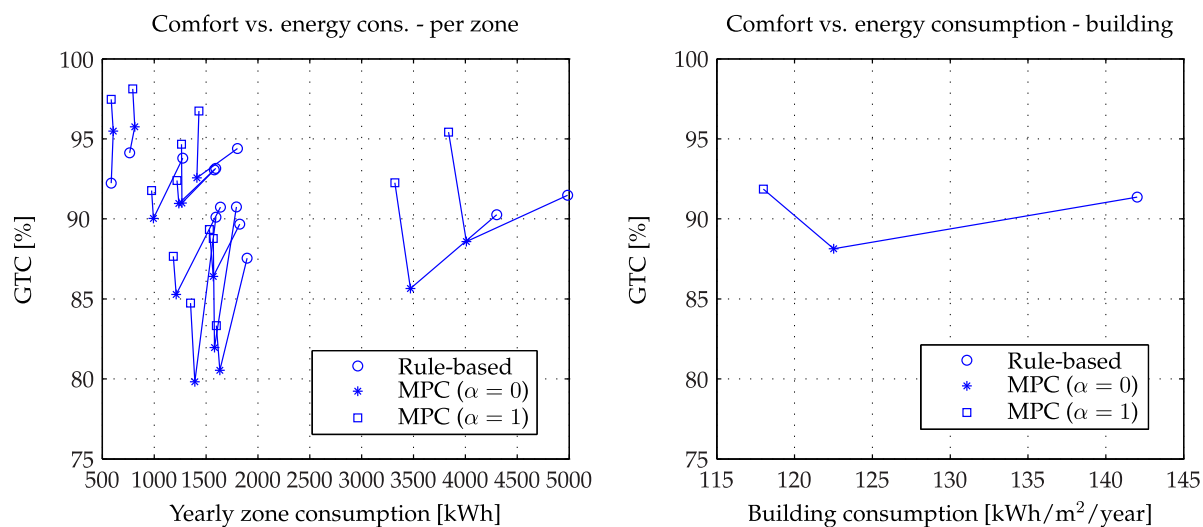


Figure 4.26 MPC vs. Rule-based control. Notice that bad weather forecast ($\alpha = 0$) mainly induces less comfort in the zones and generally more energy consumption.

4.11 Roombox implementation



Figure 4.27 The office Roombox (Schneider-Electric) controls several actuators, ensures power measurement and protection.

The aim here is to study the implementability of the proposed algorithm on the office Roombox. The office Roombox (see figure 4.27) is a Multi-applicative⁸ controller de-

⁸Dedicated to HVAC, lighting and Indoor Air Quality equipment control.

signed for office environmental control. It enables to control several actuators (heating, lighting, shutters and blinds) and equipped with several sensors (temperature, CO₂ level, lighting, etc.). Moreover, in addition to physical quantities, power metering is also available.

Thanks to a sufficiently powerful hardware (bi-CORE ARM9 @ 133 Mhz with 128 Mo RAM) and its embedded Linux operating system, it is an adequate target for investigations and integration of advanced control features. In the scope of the HOMES program, the predictive control algorithm described above has been developed in Matlab language. Therefore, a translation from Matlab to C++ language was required in order to obtain an embeddable code on the real target.

Our choice was to translate this code in C++ instead of an automatic code generation directly from Matlab. This choice is motivated by evident reasons of maintainability and efficiency of the code. The translation operation has been performed thanks to the usage of a matrix library which enables to conduct the matrix operations required by the MPC algorithm in a Matlab-like syntax⁹. This clearly simplified the code translation (see the example in appendix F).

The C++ code has been validated and compiled in eclipse environment in order to be embedded in the Roombox (see figure 4.27). It has to be noticed that some technical issues related to the choice of the mathematical solver and parameterization of the MPC algorithm in terms of number of decision variables have been resolved in order to make the algorithm sufficiently efficient. The chosen solver was GLPK¹⁰, which is a GNU MILP solver. It has the advantage of being free, maintained and quite efficient for small/medium size¹¹ LPs.

The operations described above (figure 4.29) have been conducted with success and the integration of the control algorithm in the hardware showed that the memory occupation and the computation time were much lower than what has been expected. More precisely, the memory occupation (only the MPC algorithm) was approximately 10Mo and the mean CPU load was about 25% (integrating all the other tasks). Indeed, this enables several MPC algorithms to run in parallel on the same Roombox and controlling several zones.

This clearly shows the compatibility of the computational burden with the targeted kind of hardware while exhibiting in our case a mean computational time of 10 [s] which is much less than the required control refreshing period (from one to several minutes). Indeed, for one iteration of algorithm with $N = 720$ and $N_u^{\text{par}} = N_y^{\text{par}} = 20$, the mean computational time is approximately 6 [s].

⁹The matrix library is developed and maintained by P. Bellemain (Gipsa-lab). It is coded in C++ and used in internal developments within the Gipsa-lab.

¹⁰www.gnu.org/software/glpk/

¹¹few hundred of decision variables and few hundred constraints

Chapter 4. Zone MPC - Design and Real-Time implementation

```

Telnet 10.194.0.123
→ Mem: 31664K used, 95020K free, 0K shrd, 32K buff, 12132K cached
CPU:  4.2% usr  3.5% sys  0.3% nic  91.0% idle  0.0% io  0.0% irq  0.0% sirq
→ Load average: 0.33 0.36 0.31 3/71 3320
1110 1110 root      S  7688  6.0  0.0  /usr/bin/noshell
1226 1221 root      R  37336 29.4  0  2.1 /usr/bin/iseReGalx ORBL6D4S2HW-IT70 192.168.1.1 2
3251 3246 root      R  3152  2.4  0  1.7 top
791  1 root      S  3152  2.4  0  0.7 /bin/telnetd -l /bin/login
1222 1221 root      S  37336 29.4  0  0.3 /usr/bin/iseReGalx ORBL6D4S2HW-IT70 192.168.1.1 2
1815  975 root      S  N  9140  7.2  0  0.3 /ion_stack -l 800000108582 -p
1229 1221 root      R  37336 29.4  0  0.1 /usr/bin/iseReGalx ORBL6D4S2HW-IT70 192.168.1.1 2
976  975 root      S  N  9140  7.2  0  0.1 /ion_stack -l 800000108582 -p
983  975 root      S  N  9140  7.2  0  0.1 /ion_stack -l 800000108582 -p
1003 975 root      S  N  9140  7.2  0  0.1 /ion_stack -l 800000108582 -p
1140 1138 root      S  7688  6.0  0.0  /usr/bin/noshell
1113  1 root      S  37336 29.4  0  0.0 /usr/bin/iseReGalx ORBL6D4S2HW-IT70 192.168.1.1 2
1250 1221 root      S  37336 29.4  0  0.0 /usr/bin/iseReGalx ORBL6D4S2HW-IT70 192.168.1.1 2
1249 1221 root      S  37336 29.4  0  0.0 /usr/bin/iseReGalx ORBL6D4S2HW-IT70 192.168.1.1 2
1251 1221 root      S  37336 29.4  0  0.0 /usr/bin/iseReGalx ORBL6D4S2HW-IT70 192.168.1.1 2
1227 1221 root      S  37336 29.4  0  0.0 /usr/bin/iseReGalx ORBL6D4S2HW-IT70 192.168.1.1 2
1225 1221 root      S  37336 29.4  0  0.0 /usr/bin/iseReGalx ORBL6D4S2HW-IT70 192.168.1.1 2
1252 1221 root      S  37336 29.4  0  0.0 /usr/bin/iseReGalx ORBL6D4S2HW-IT70 192.168.1.1 2
1253 1221 root      S  37336 29.4  0  0.0 /usr/bin/iseReGalx ORBL6D4S2HW-IT70 192.168.1.1 2
1255 1221 root      S  37336 29.4  0  0.0 /usr/bin/iseReGalx ORBL6D4S2HW-IT70 192.168.1.1 2
1221 1113 root      S  37336 29.4  0  0.0 /usr/bin/iseReGalx ORBL6D4S2HW-IT70 192.168.1.1 2
1254 1221 root      S  37336 29.4  0  0.0 /usr/bin/iseReGalx ORBL6D4S2HW-IT70 192.168.1.1 2
→ 3210 2563 root      S  10436  8.2  0  0.0 /Programme_roombox_fpi
3211 3210 root      S  10436  8.2  0  0.0 /Programme_roombox_fpi
3212 3211 root      S  10436  8.2  0  0.0 /Programme_roombox_fpi
3216 3211 root      S  10436  8.2  0  0.0 /Programme_roombox_fpi
981  975 root      S  N  9140  7.2  0  0.0 /ion_stack -l 800000108582 -p
960  1 root      S  N  9140  7.2  0  0.0 /ion_stack -l 800000108582 -p
989  975 root      S  N  9140  7.2  0  0.0 /ion_stack -l 800000108582 -p
975  960 root      S  N  9140  7.2  0  0.0 /ion_stack -l 800000108582 -p
998  975 root      S  N  9140  7.2  0  0.0 /ion_stack -l 800000108582 -p
1139 1138 root      S  7688  6.0  0.0  /usr/bin/noshell
961  1 root      S  7688  6.0  0.0  /usr/bin/noshell
1130  961 root      S  7688  6.0  0.0  /usr/bin/noshell
934  1 root      S  5940  4.6  0  0.0 /usr/bin/audspars.txt -w MCCNCCNCCNCCN
945  934 root      S  5940  4.6  0  0.0 /usr/bin/audspars.txt -w MCCNCCNCCNCCN
946  945 root      S  5940  4.6  0  0.0 /usr/bin/audspars.txt -w MCCNCCNCCNCCN
939  934 root      S  5932  4.6  0  0.0 /usr/bin/audspars.txt -w MCCNCCNCCNCCN
940  944 root      S  5932  4.6  0  0.0 /usr/bin/audspars.txt -w MCCNCCNCCNCCN
944  939 root      S  5932  4.6  0  0.0 /usr/bin/audspars.txt -w MCCNCCNCCNCCN
935  1 root      S  5888  4.6  0  0.0 /hmiio -k 0 PRIG20.txt
940  935 root      S  5888  4.6  0  0.0 /hmiio -k 0 PRIG20.txt
941  940 root      S  5888  4.6  0  0.0 /hmiio -k 0 PRIG20.txt
959  1 root      S  5844  4.6  0  0.0 /daliio
965  965 root      S  5844  4.6  0  0.0 /daliio
955  959 root      S  5844  4.6  0  0.0 /daliio
947  1 root      S  3708  2.9  0  0.0 /ionconf -b SLDWDCSLDWDGCRDCHUVR8CHU
873  1 root      S  3236  2.5  0  0.0 /ende
2563 901 root      S  3152  2.4  0  0.0 -ash
3246 901 root      S  3152  2.4  0  0.0 -ash
1  0 root      S  3148  2.4  0  0.0 /bin/syslogd -l7 -b2 -s300 -l -0 /mnt/log -R 192.168.1.1
890  1 root      S  1952  1.5  0  0.0 /rt
3320 765 root      S  1952  1.5  0  0.0 /rt
904  1 root      S  1788  1.3  0  0.0 /bin/httpd -d
673  1 root      SU  0  0.0  0  0.0 [ntcdblockd]
5  1 root      SUC  0  0.0  0  0.0 [kheiper]
8  1 root      SUC  0  0.0  0  0.0 [ksoftirqd/0]
3  1 root      SU  0  0.0  0  0.0 [watchdog/0]
4  1 root      SUC  0  0.0  0  0.0 [events/0]
6  1 root      SUC  0  0.0  0  0.0 [kthreadd]
42  6 root      SUC  0  0.0  0  0.0 [kblockd/0]
43  6 root      SUC  0  0.0  0  0.0 [kcsuend_usbd]

```

Figure 4.28 Roombox - memory and CPU usage. Note that the MPC algorithm accounts for 8.2 % of the memory usage (see Programme_roombox_fpi). Note also that only 33 % of the memory is used in fact, which enables to implement several MPC algorithms running in parallel on the same hardware. Concerning CPU, note that only one of the two cores is turned-on, in this case it is still sufficient. One iteration of the algorithm takes approximately 6 [s].

The code has been validated thanks to fictitious signals sent via the Ethernet port of the Roombox (see figure 4.28). Further step consists of operational validation of the proposed MPC algorithm. This step, requiring a model calibration of the zone, has not been conducted in this work, since the main objective of this study was to validate the real-time feasibility of the control algorithm and not the effectiveness of the control algorithm in real-life situations.

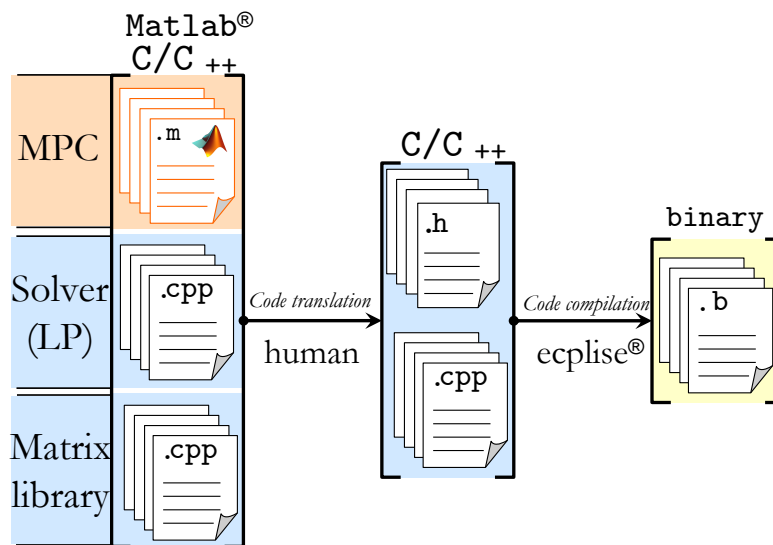


Figure 4.29 RoomBox implementation steps. The code developed on Matlab has been translated to C⁺⁺, then compiled in Eclipse environment.

4.12 Conclusion and further investigations

In this chapter, a MIMO nonlinear model predictive controller has been presented. The algorithm is able to manage several actuators in the zone in order to ensure occupants comfort. Beside handling actuators effects on the temperature, CO₂ level and indoor illuminance, the algorithm is able to take into account varying energy tariff. The simulation results shows its computational efficiency. This enabled us to conduct investigations regarding its implementation on real time target. This experiment showed the compatibility of this algorithm with respect of our target.

Moreover, the integration of the controller in SIMBAD has been conducted. On the investigated building, this showed a an energy potential saving of 16% with quite similar comfort level compared to a well-tuned rule-based control strategy. Uncertainty on forecast reduces the energy saving to 14% but induces also a decrease of comfort (from 91,6 % to 88.1 %), which is quite reasonable. Nevertheless, these simulations are only illustrative and conclusions cannot be generalized. Actually, further development steps should focus on a large scale simulation in several case studies. Indeed, it is important to highlight that other related studies [Oldewurtel 2011] show a clear dependency of performances of MPC on weather forecast quality. Furthermore, including those uncertainties in the process of decision making leading to the so called stochastic MPC can improve the performances of the controller.

Chapter 4. Zone MPC - Design and Real-Time implementation

Moreover, experimentations of the algorithm should be conducted in real-life situations to practical issues related to model identification for instance.

In the next chapter, an extension of the algorithm to handle fan coil units is provided. In the next part of the manuscript, a distributed approach is proposed to tackle the high computational burden induced in the case of multi-zone buildings submitted to power limitations in which several sources of different natures are available.

Chapter 5

Zone Model Predictive Control - Fan Coil Unit management

Abstract

In this chapter, an extension of the previously designed zone model predictive controller is presented. The aim of this chapter is to include the management of fan coils units. It is shown that fan coil units exhibit nonlinear heat emission characteristics, that can be approximated by a Piece Wise Affine (PWA) function and therefore directly included in the LP formulation.

5.1 Context and motivation

Fan coil units are widespread heat/cold emission equipment, particularly in tertiary buildings. This is due to their relative robustness and simplicity of operation. Moreover, they have lower installation cost when compared to air duct systems.

Fan coil units are used to modulate the heat/cold quantity injected in the zone thanks to the existence of two coils (figure 5.2, page 95):

- A heat exchanger in which a fluid (generally water) circulates: the heat quantity extracted from water and injected into the zone depends on the water flowrate (controlled locally by the position of a valve) and the speed of the fan that will affect the air velocity and thus modifies the heat exchange coefficient;
- An electrical coil that behaves like a classical electrical heater.

This chapter proposes an extension of the previously designed controller in order to handle fan coil unit systems. In this case, the main problem lies in the nonlinear emission characteristic of the fan coil unit.

To the best of our knowledge, this problem has not been studied before. This chapter is organized as follows: firstly, the fan coil unit model is provided in section 5.2. In section 5.3, the control problem is derived, then it is solved in section 5.4 which is the main contribution of this chapter. Finally, the controller is simulated in section 5.5. The section 5.6 concludes the chapter.

5.2 Fan Coil Unit (FCU) modeling

This section presents the FCU model. Let us first introduce some assumptions regarding the thermal power distribution network:

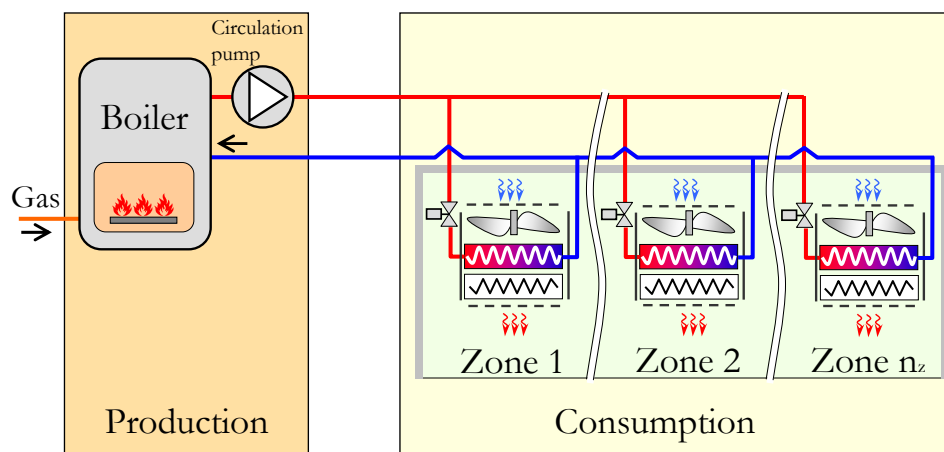


Figure 5.1 Zone fan coil units. The FCUs are parallel-connected.

Assumption 5.1. Hot water distribution network topology

The fan coil units are assumed to be parallel-connected (figure 5.1). Moreover, heat losses and head losses¹ in the network are not taken into account. ◇

Assumption 5.2. Circulation pump

The circulation pump ensures a constant pressure drop between the water inlet and the water outlet of the fan coil units. Moreover, its electrical consumption is linear with respect to the waterflow passing through it. ◇

Assumptions 5.1 and 5.2 enable to consider that the fan coil units are mutually independent as the valve position of any fan coil unit has no impact on the water network pressure drops and therefore no influence on the other fan coil units (figure 5.1). It is thus possible to focus only on one zone part.

¹Reduction in the total head of the liquid as it moves through the water pipes.

5.2.1 A general description

Figure 5.2 is a schematic of a fan coil unit. The system is made up of two heating coils: an electrical heating coil and a heat exchanger which enables heat transfer between the hot water and zone air.

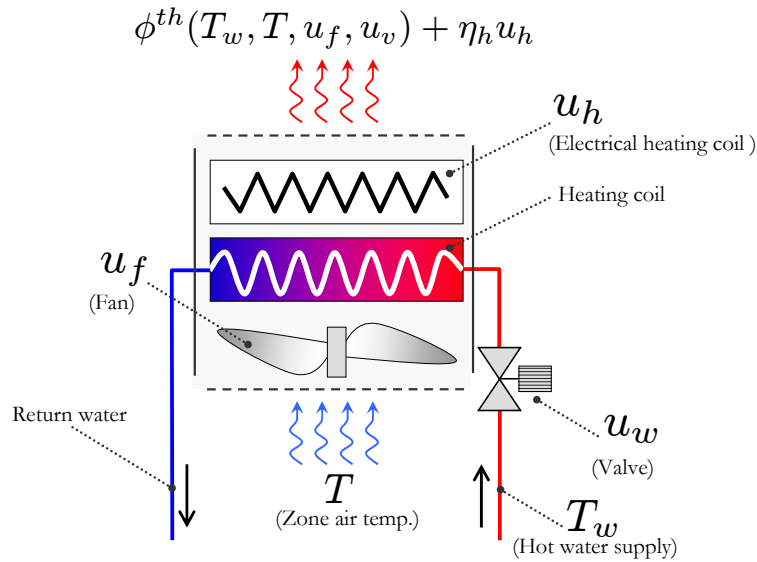


Figure 5.2 Fan Coil Unit representation. There are two heating coils: an electrical heating coil and a heat exchanger. The fan speed and the valve opening define the heat exchange coefficient ϕ^N (see eq. (5.2.1)).

The amount of heat exchanged between the coil and the zone is given by the following relation:

$$\phi^{th}(T_w, T, u_f, u_w) = (T_w - T) \cdot \phi^N(u_w, u_f) \quad (5.2.1)$$

where:

- $(u_w, u_f) \in [0, 1]^2$ are the valve opening and the fan speed,
- $\phi^N(u_w, u_f)$ is the normalized heat emission characteristic, depending on valve opening and fan speed.

In other words, the heat extracted from hot water and injected in the zone $\phi^{th}(\cdot)$ is indirectly controlled by the position of actuators u_w and u_f via the normalized heat

transfer function $\phi^N(u_w, u_f)$ and the difference between the hot water temperature (T_w) and the zone temperature (T). An example of this characteristic function is depicted in figure (5.3).

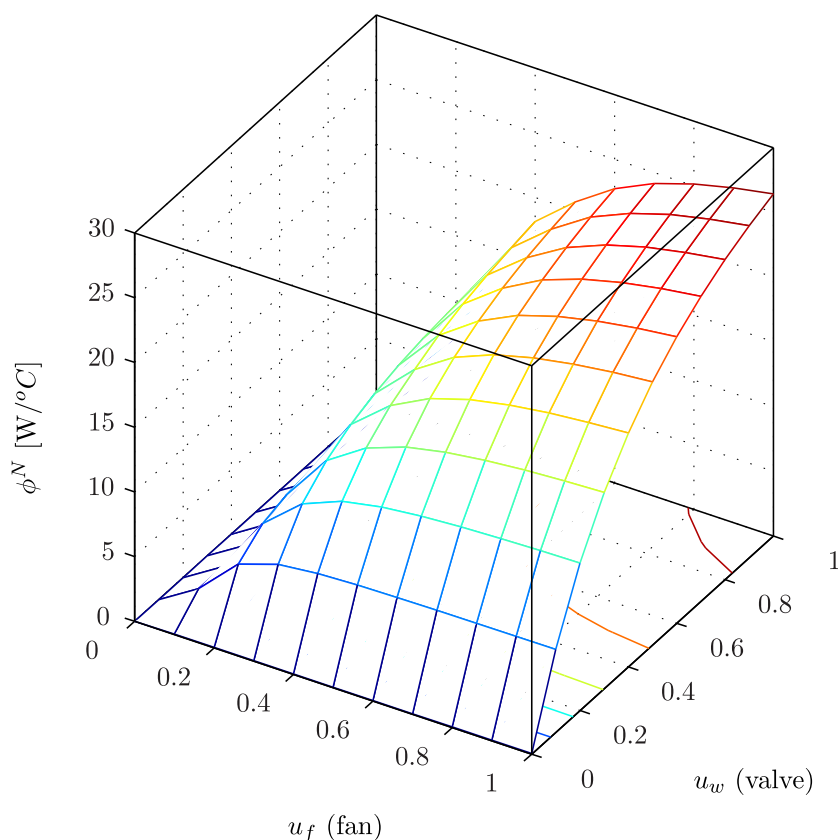


Figure 5.3 Heat emission characteristic function ϕ^N of an FCU (see eq. (5.2.1)).

The characteristic function $\phi^N(u_w, u_f)$ has been obtained² from the building simulation tool SIMBAD. The set of physical characteristics of the FCU determining such an emission characteristic is listed in table 5.1.

It is worth noting that the fan coil unit model is a static model. This modeling assumption results from the fact that the dynamic of the fan coil unit is very fast compared to the zone dynamics. Moreover, note that the heat emission characteristic is valid for a given pressure drop between water inlet/outlet (assumption 5.2).

²To be able to derive the heat emission characteristic of the fan coil unit, an off-line identification has been performed on SIMBAD.

Parameter	unit	e.g
Tube outside diameter	[m]	0.009
Number of tube rows	-	2
Number of tubes per row	-	10
Number of parallel water circuits	-	1
Tube thickness	[m]	0.0005
Tube material	-	copper
Fin spacing	[m]	0.002
Fin thickness	[m]	0.0002
Fin material	-	aluminium
Fan coil mass flow	[kg/s]	0.02804

Table 5.1 Fan coil unit parameters. These parameters determine the FCU heat emission characteristic (see figure 5.3).

5.2.2 Zone modeling

Given the heat emission characteristic of the fan coil unit, the zone model can be built. For the sake of clarity, we shall first recall the list of I/Os related to one zone. Table 5.2 lists the inputs, outputs and exogenous variables related to a zone equipped with a fan coil unit. Note that, from a zone perspective, the water temperature (T_w) is considered as an exogenous variable as it is adjusted by an upper control layer.

Consider first that one is interested only in the transfer from the heat extracted from hot water (injected in the zone) ϕ^{th} to the zone temperature. This transfer can be modeled by a SISO linear state space representation of the form:

$$\begin{cases} x_{th}^+ &= A_{th} \cdot x_{th} + B_{th} \cdot \phi^{th} \\ T &= C_{th} \cdot x_{th} \end{cases} \quad (5.2.2)$$

Based on (5.2.1), the system (5.2.2) can be written as follows:

$$\begin{cases} x_{th}^+ &= A_{th} \cdot x_{th} + \bar{B}_{th}(T_w - T) \cdot \phi^N(u_w, u_f) \\ T &= C_{th} \cdot x_{th} \end{cases} \quad (5.2.3)$$

Introducing now the new control vector $v \in \mathbb{R}^{n_u+1}$:

$$v = [\phi^N(u_w, u_f), u_w, u_f, u_h, u_v, u_l, u_b^1, \dots, u_b^{N_f}]^T \quad (5.2.4)$$

one can easily see that the zone model (introducing the other control variables) can be modeled by :

	Variables	Description	Unit
Inputs	u_w	FCU valve opening	[–]
	u_f	FCU fan speed	[–]
	u_h	Heating ctrl	[–]
	u_v	Ventilation control	[–]
	u_l	Lighting control	[–]
	$\{u_b^i\}_{i=1,\dots,N_f}$	Blind ctrl facade i	[–]
Disturbances	T_w	Inlet FCU water temp.	[°C]
	T_{ex}	Outdoor temperature	[°C]
	$\{T_{adj}^i\}_{i \in N_{adj}}$	Adjacent zones temp.	[°C]
	$\{\phi_g^i\}_{i=1,\dots,N_f}$	Global irr. flux facade i	[W/m ²]
	O_{cc}	Number of occupants	[–]
	C_{ex}	Outdoor CO ₂ level	[ppm]
Outputs	T	Indoor air temperature	[°C]
	C	Indoor CO ₂ level	[ppm]
	L	Indoor illuminance	[Lux]

Table 5.2 Description of Input/Output and exogenous variables of a zone with a fan coil unit

$$x^+ = A \cdot x + \left[B(y, w) \right] \cdot v + F \cdot w \quad (5.2.5a)$$

$$y = C \cdot x + D(w) \cdot v \quad (5.2.5b)$$

$$v \in \mathbb{V} \quad (5.2.5c)$$

where:

$$\mathbb{V} := \{q = [q(1), \dots, q(n_v)]^T \in \mathbb{R}^{n_v} \mid \dots$$

$$q(1) = \phi^N(q(2), q(3)) \wedge q(j) \in [0, 1], j = 2, \dots, n_v\} \quad (5.2.6)$$

The relation (5.2.6) simply indicates that the constrained control v must verify the consistency constraint on emitted power flux, see figure 5.3.

In the sequel, the notation $\mathbf{v} \in \mathbf{V}$ is used to indicate the fulfilment of (5.2.5c) over the entire prediction horizon, namely:

$$\mathbf{v} \in \mathbf{V} \leftrightarrow \Pi_j(\mathbf{v}) \in \mathbb{V}, \forall j = 0, \dots, N - 1 \quad (5.2.7)$$

Moreover, let us note the simulator form of (5.2.5) by:

$$\mathbf{y}_k := \mathcal{Z}(\mathbf{v}_k, \mathbf{w}_k, x_k) \quad (5.2.8)$$

Note that:

- The system described by (5.2.5) is a nonlinear system,
- As was the case in chapter 4, the matrices $B(y, w)$ and $D(w)$ are affine in their arguments. Moreover the respective columns of $B(y, w)$ and $D(w)$ corresponding to u_w and u_f are equal to zero;
- The system described by (5.2.5) is a constrained system.

5.3 The control problem

In this section, only the main features of the optimization problem related to the zone are given as they have been extensively explained in the section 4.3 for the case of a zone without a fan coil unit.

There are two differences between the model (5.2.5) representing a zone with a fan coil unit and the model of a zone without this device (presented in chapter 4):

1. The control variables v (see (5.2.4)) are mutually dependent (ϕ^N, u_w, u_f) ,
2. The power consumption of the zone is also linked to the output y (more precisely to the temperature of the zone).

These are the only reasons that prevent using the algorithm proposed in the previous chapter to solve the resulting optimization problem recalled below:

Optimization Problem 5.1. Zone with FCU optimization problem

$$\mathbf{v}_k^* = \underset{\mathbf{v}_k \in \mathbf{V}}{\text{Argmin}} \quad J^E(\Gamma_k, \mathbf{p}_k) + J^C(\mathbf{y}_k) + J^D(\mathbf{v}_k) + J_F(\Pi_{(N-1)}(\mathbf{y}_k)) \quad (5.3.1)$$

Subject to:

$$\mathbf{p}_k = \mathbf{E}(\mathbf{y}_k, \mathbf{w}_k) \cdot \mathbf{v}_k \quad (5.3.2)$$

$$\mathbf{y}_k = \mathcal{Z}(\mathbf{v}_k, \mathbf{w}_k, x_k) \quad (5.3.3)$$

Note that $p_k \in \mathbb{R}^2$, which is the instantaneous power consumption of the zone grouping in this case both electrical and thermal powers. Moreover, as the thermal power consumption of the zone is linked to the zone temperature and water temperature ($\phi^{th} = (T_w - T) \cdot \phi^N(u_w, u_f)$), then $p_k \in \mathbb{R}^2$ is given by:

$$p_k = E(y_k, w_k) \cdot v_k \in \mathbb{R}^2 \quad (5.3.4)$$

where the matrix $E(y_k, w_k) \in \mathbb{R}^{2 \times n_u}$ gathers the marginal power consumption of all equipment:

$$E(y, w) := \begin{bmatrix} 0 & \alpha_w & \alpha_f & \alpha_h & \alpha_v & \alpha_l & 0 & \dots & 0 \\ \alpha_{th} \cdot (T - T_w) & 0 & 0 & \dots & \dots & \dots & \dots & \dots & 0 \end{bmatrix} \quad (5.3.5)$$

where α_w is the maximum electricity consumption resulting from circulation pump consumption due to valve opening. α_f , α_h and α_v are, respectively, the maximum power consumption resulting from the fan, electrical heating and ventilation system (indirectly controlled at zone level via dumper position). α_{th} is related to thermal power consumption of the FCU.

Consequently, the profile of instantaneous power consumption of the zone (resulting from all the actuators) is given by:

$$\mathbf{p}_k = \mathbf{E}(y_k, \mathbf{w}_k) \cdot \mathbf{v}_k \quad (5.3.6)$$

where:

$$\mathbf{E}(y_k, \mathbf{w}_k) := \text{diag}\{\alpha(y_k, w_k), \dots, \alpha(y_{k+N-1}, w_{k+N-1})\} \in \mathbb{R}^{2 \cdot N \times N \cdot n_u} \quad (5.3.7)$$

5.4 Solving the optimization problem

This section presents the optimization algorithm used to solve the optimization problem 5.1. In order to be able to solve efficiently the problem 5.1, two main steps are needed:

1. Piece-wise linear approximation of the nonlinear relation, $\phi^N(\cdot)$. This step is performed off-line,
2. Resolution of the resulting optimization problem using a sequence of linear programming problems.

5.4.1 Piece-wise affine approximation

The key idea is to approximate the nonlinear function $\phi^N(\cdot)$ by a piece-wise affine approximation noted $\hat{\phi}^N(\cdot)$. The advantage of this kind of approximation will appear in the next section.

To describe approximately $\phi^N(\cdot)$, n_a regions $\mathbf{D}_i, i = 1, \dots, n_a$, in which the function $\phi^N(\cdot)$ can be approximated by a linear function, are introduced. Namely:

$$\hat{\phi}^N(u_w, u_f) = \begin{cases} a_1 u_w + b_1 u_f + c_1 & \text{if } (u_f, u_w) \in \mathbf{D}_1 \\ \vdots & \\ a_{n_a} u_w + b_{n_a} u_f + c_{n_a} & \text{if } (u_f, u_w) \in \mathbf{D}_{n_a} \end{cases} \quad (5.4.1)$$

The approximation $\hat{\phi}^N(\cdot)$ as well as the regions $\mathbf{D}_i, i = 1, \dots, n_a$ are depicted on figure 5.4. Moreover, let us note analogously to (5.2.7) the fulfilment of (5.4.1) over the entire prediction horizon by:

$$\mathbf{v} \in \hat{\mathbf{V}} \quad (5.4.2)$$

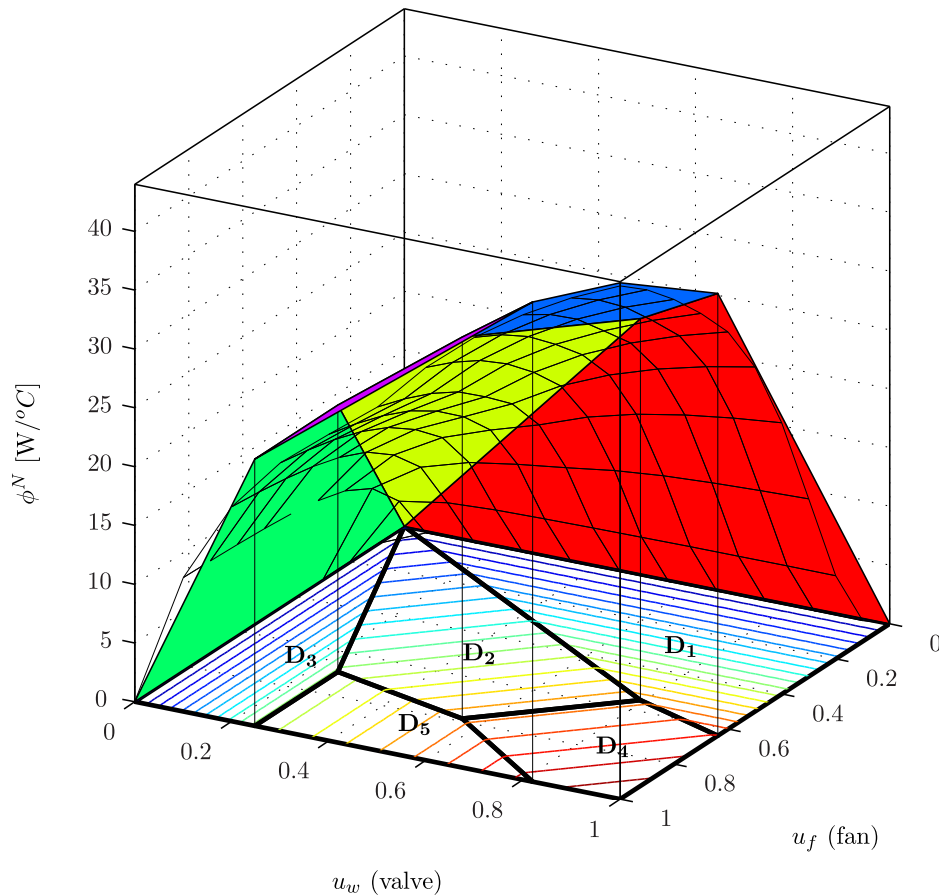


Figure 5.4 Piece-wise affine approximation of ϕ^N with $n_a = 5$ regions. Notice that the approximation is strictly concave.

Note that this kind of approximation can be introduced in the LP problem formulation using some integer variables. However, this generally induces a very large computational burden, as the resulting optimization problem may include a large number of integer variables. As it will be shown below, a MILP formulation can be avoided in this case.

At this step, notice that the heat emission characteristic $\phi^N(u_w, u_f)$ is approximately concave and that its approximation $\hat{\phi}^N$ is (by construction) strictly concave. This fact will greatly simplify the optimization task as shown in the next section.

5.4.2 Fixed-point algorithm

Let us recall the basic idea of the proposed fixed-point algorithm proposed in chapter 4. Its principle is to successively approximate the nonlinear inequalities (5.4.3b)-(5.4.3c) and the cost (5.4.3a) given a candidate output trajectory $\mathbf{y}_k^{(s)}$, where $s = 0, \dots, s_{max}$ is the iteration counter. This output trajectory is updated by simulating the nonlinear system describing the zone, leading to a new optimization problem, and so on.

Hence, at iteration s , the following Mixed Integer Linear Programming (MILP) problem³ must be solved:

Optimization Problem 5.2. Mixed Integer Linear Programming

$$\text{MILP}_k^{(s)} \underset{\mathbf{v}_k, \delta_0, \delta_1, \delta_d}{\text{Minimize}} J(\mathbf{v}_k, \mathbf{y}_k^{(s)}, \Gamma_k, \mathbf{w}_k) \quad (5.4.3a)$$

Subject To :

$$[\Phi(\mathbf{y}_k^{(s)}, \mathbf{w}_k)]\mathbf{v}_k + \delta_0^- + \delta_1^- \geq \underline{\mathbf{y}}_k - \Psi x_k - \Xi \mathbf{w}_k \quad (5.4.3b)$$

$$[\Phi(\mathbf{y}_k^{(s)}, \mathbf{w}_k)]\mathbf{v}_k - \delta_0^+ - \delta_1^+ \leq \bar{\mathbf{y}}_k - \Psi x_k - \Xi \mathbf{w}_k \quad (5.4.3c)$$

$$\mathbf{D} \cdot \mathbf{v}_k - \delta_d^+ + \delta_d^- = \mathbf{a} \quad (5.4.3d)$$

$$\mathbf{v}_k \in \hat{\mathbf{V}} \quad (5.4.3e)$$

$$\delta_0 \geq \mathbf{0}, \delta_d \geq \mathbf{0}, \mathbf{0} \leq \delta_1 \leq \begin{bmatrix} \delta_y \\ \delta_y \end{bmatrix} \quad (5.4.3f)$$

Remark 5.1.

Actually, the optimization problem 5.2 is a MILP because of the existence of the relation (5.4.3e) which implies a set of relations of type $(\hat{\phi}^N(u_w, u_f) = a_i u_w + b_i u_f + c_i \text{ if } (u_f, u_w) \in \mathbf{D}_i, i = 1, \dots, n_a)$, see eq. (5.4.1). The interested reader can refer to [Bemporad & Morari 1999] for more explanations. \diamond

The optimal input profile $\mathbf{v}_k^{(s)}$ obtained from the resolution of the problem 5.2 is then injected in the nonlinear system to update the current candidate output profile $\mathbf{y}_k^{(s+1)}$, namely:

$$\mathbf{y}_k^{(s+1)} = \mathcal{Z}(\mathbf{v}_k^{(s)}, \mathbf{w}_k, x_k) \quad (5.4.4)$$

³The MILP can be derived using the big-M technique presented in [Bemporad & Morari 1999].

These two steps are repeated until convergence is achieved. Note that the main issue in this framework relates to the prohibitive computational burden resulting from the resolution of the MILP 5.2. To overcome this issue, note that:

- 1– **The approximation $\hat{\phi}^N(\cdot)$ is strictly concave.** Therefore:

$$\hat{\phi}^N(u_w, u_f) = \mathbf{Inf}_{i=1, \dots, n_a} [a_i \cdot u_w + b_i \cdot u_f + c_i] \quad (5.4.5)$$

Moreover, the subgraph of $\hat{\phi}^N(\cdot)$, which is the region under the surface defined by (5.4.5) (figure 5.5), is given by the following set of linear inequalities:

$$\begin{bmatrix} 1 & -a_1 & -b_1 \\ 1 & -a_2 & -b_2 \\ \vdots & \vdots & \vdots \\ 1 & -a_{n_a} & -b_{n_a} \end{bmatrix} \cdot \begin{bmatrix} \hat{\phi}^N \\ u_w \\ u_f \end{bmatrix} \leq \begin{bmatrix} c_1 \\ c_2 \\ \vdots \\ c_{n_a} \end{bmatrix} \quad (5.4.6)$$

In addition, $S \in \mathbb{R}^{n_a \times n_v}$ and $h \in \mathbb{R}^{n_a \times 1}$ can be defined such that:

$$S \cdot v \leq h \quad (5.4.7)$$

where:

$$S := \begin{bmatrix} 1 & -a_1 & -b_1 & 0 & \dots & 0 \\ \vdots & \vdots & \vdots & 0 & \dots & 0 \\ 1 & -a_{n_a} & -b_{n_a} & 0 & \dots & 0 \end{bmatrix}, \quad h := \begin{bmatrix} c_1 \\ \vdots \\ c_{n_a} \end{bmatrix} \quad (5.4.8)$$

- 2– **The function $\hat{\phi}^N(\cdot)$ depends exclusively on u_f and u_w and the objective $J(\cdot)$ is positive definite with respect to these two variables.**

Given that the two conditions (1-2) hold, it can be easily shown that the problem 5.2 is equivalent to the following linear programming problem, in which (5.4.3e) has been replaced by the set of linear inequalities (5.4.9e) (subgraph of $\hat{\phi}^N$):

Optimization Problem 5.3. Linear programming

$$\text{LP}_k^{(s)} \underset{\mathbf{v}_k, \delta_0, \delta_1, \delta_d}{\text{Minimize}} J(\mathbf{v}_k, \mathbf{y}_k^{(s)}, \Gamma_k, \mathbf{w}_k) \quad (5.4.9a)$$

Subject To :

$$[\Phi(\mathbf{y}_k^{(s)}, \mathbf{w}_k)]\mathbf{v}_k + \delta_0^- + \delta_1^- \geq \underline{\mathbf{y}}_k - \Psi x_k - \Xi \mathbf{w}_k \quad (5.4.9b)$$

$$[\Phi(\mathbf{y}_k^{(s)}, \mathbf{w}_k)]\mathbf{v}_k - \delta_0^+ - \delta_1^+ \leq \bar{\mathbf{y}}_k - \Psi x_k - \Xi \mathbf{w}_k \quad (5.4.9c)$$

$$\mathbf{D} \cdot \mathbf{v}_k - \delta_d^+ + \delta_d^- = \mathbf{a} \quad (5.4.9d)$$

$$\mathbf{S} \cdot \mathbf{v}_k \leq \mathbf{h} \quad (5.4.9e)$$

$$\delta_0 \geq \mathbf{0}, \delta_d \geq \mathbf{0}, \mathbf{0} \leq \delta_1 \leq \begin{bmatrix} \delta_y \\ \delta_y \end{bmatrix} \quad (5.4.9f)$$

where:

$$\mathbf{S} := \mathbf{I}_N \otimes S \quad \text{and} \quad \mathbf{h} := \mathbf{1}_N \otimes h \quad (5.4.10)$$

The LP problem 5.3 can be written in the following compact form:

$$\text{LP}_k^{(s)} : \underset{\underline{\mathbf{z}} \leq \mathbf{z} \leq \bar{\mathbf{z}}}{\text{Minimize}} \quad \mathbf{L}_k^{(s)} \cdot \mathbf{z}_k \quad \text{s.t.} : \quad \mathbf{A}_k^{(s)} \cdot \mathbf{z}_k \leq \mathbf{b}_k \quad (5.4.11)$$

Where the involved matrices: $\mathbf{L}_k^{(s)}, \mathbf{A}_k^{(s)}, \mathbf{b}_k, \underline{\mathbf{z}}, \bar{\mathbf{z}}$ can be defined based on the relations (5.4.9b)-(5.4.9f).

5.5 Validation

This section proposes simulations of the designed controller. Two case studies are considered:

- Heat is produced by a boiler: in this case the heat energy price is linked only to the price of gas and boiler efficiency. The marginal cost of heat is 5c€/kW.
- The heat production is ensured by a heat pump: in this case the marginal cost of heat is linked to electricity price and the COP (COefficient of Performance) of the heat pump. We consider that the COP of the heat pump is either 2 or 3.5. The heat pump coefficient of performance (dimensionless) defines the ratio between the consumed electrical power and the produced heat power.

However, in both cases the electricity price is considered to have an off-peak period from 10 p.m to 6 a.m., this is summarized on figure 5.6.

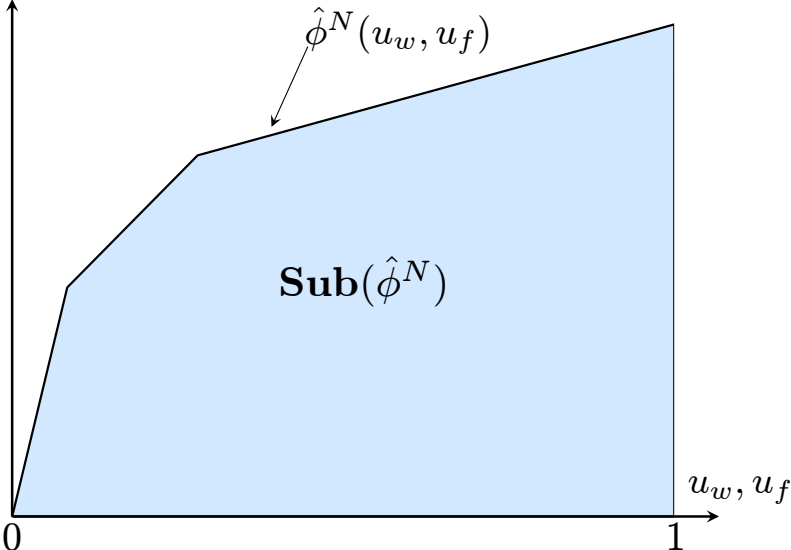


Figure 5.5 Subgraph of $\hat{\phi}(u_w, u_f)$. The subgraph of the function $\hat{\phi}(u_w, u_f)$ is the blue area.

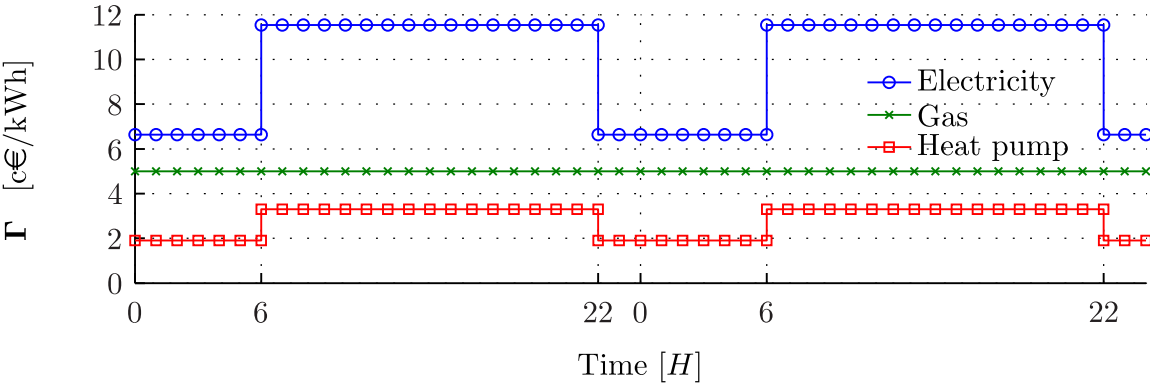


Figure 5.6 Energy price profiles used in simulations. Simulation results are available on figures 5.7 to 5.12.

Discussion

Figures 5.7, 5.8 and 5.9 clearly show that occupant comfort is respected regarding thermal, air quality and light aspects. However note that the anticipative effect of the controller ensures that the zone is preheated before occupants arrival at 8 a.m. However, it should be noted that the behavior differs considerably in the two case studies described (boiler/heat pump). In the first case (boiler), the optimal behavior is to start heating at approximately 1h30 (first and second day), the electrical heating system is used, before 6 a.m (off peak period) in order to preheat the zone and during the day to compensate heat losses when necessary.

In the second case (heat pump) the behavior is totally different since heating is turned on at 10 p.m. the day before (this matches the shift to off-peak period) and temperature is maintained at nearly $18^{\circ}C$. The electrical heating is turned on much less than it was in the first situation since it is exclusively used to compensate heat losses. However, note that in both cases the electrical heating system is used exclusively when the thermal source is saturated, simply because it is always cheaper to use the heat source (see figure 5.6).

Note also that ventilation is used at the minimum necessary level to ensure a good air quality level to introduce as less as possible of fresh air and minimize energy consumption. These results have to be compared with the one obtained on the second zone (see figures 5.10, 5.11 and 5.12) in which the optimal behavior is different (different optimal trajectories and usage of electrical heaters).

5.6 Conclusion

This chapter provides an extension of the zone predictive controller for handling fan coil unit (FCU) systems. The main advantage of the proposed controller is its ability to handle the emission characteristic of the fan coil unit. Indeed, the concavity of the PWA approximation enables an LP formulation of the open loop optimization problem. This drastically simplifies the complexity of the proposed controller.

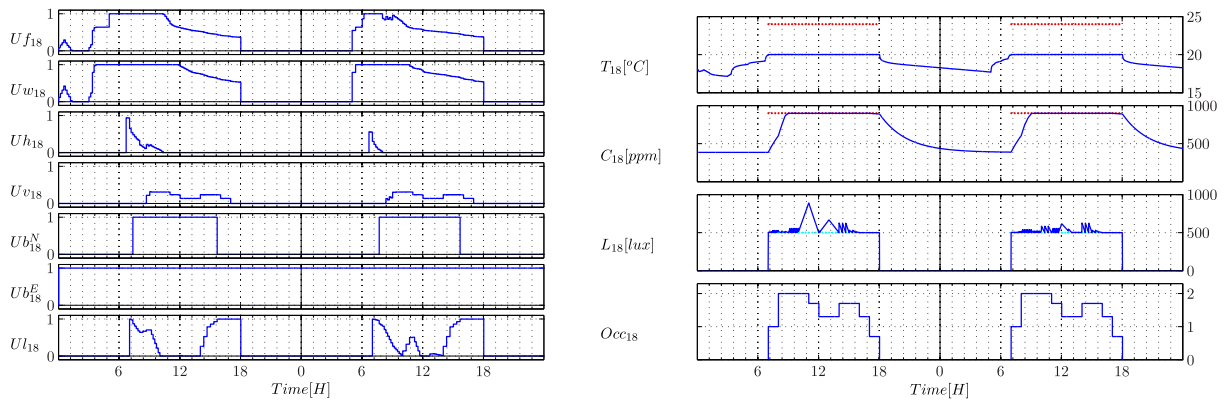


Figure 5.7 Zone #18 - Boiler.

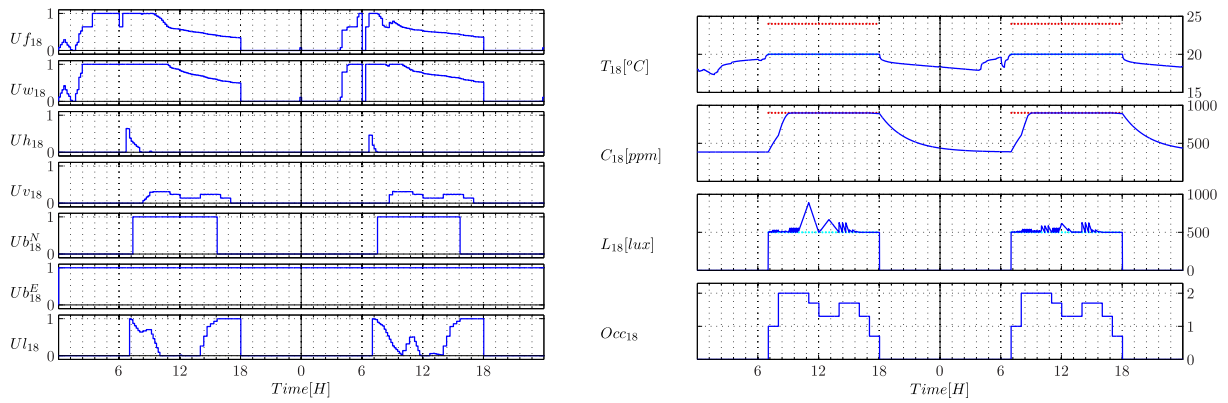


Figure 5.8 Zone #18 - Heat Pump (COP=2).

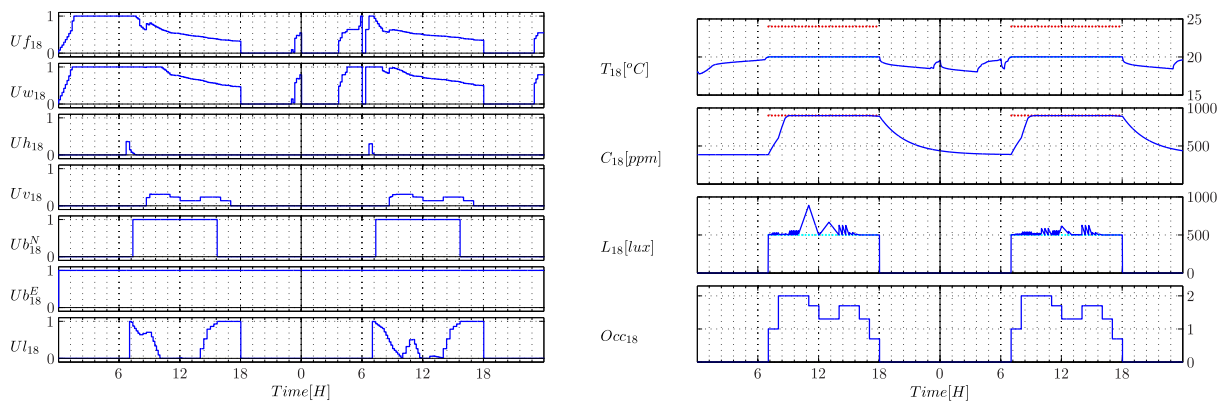


Figure 5.9 Zone #18 - Heat Pump (COP=3.5).

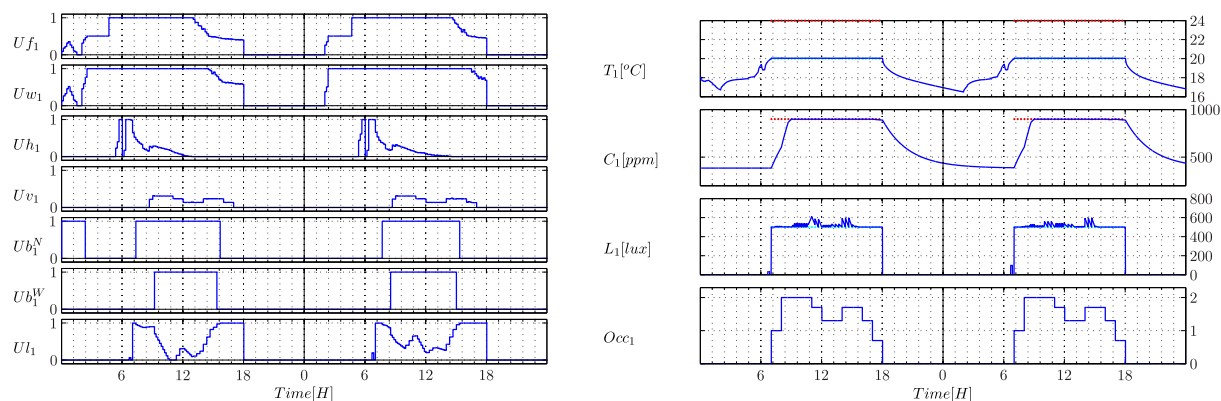


Figure 5.10 Zone #1 - Boiler.

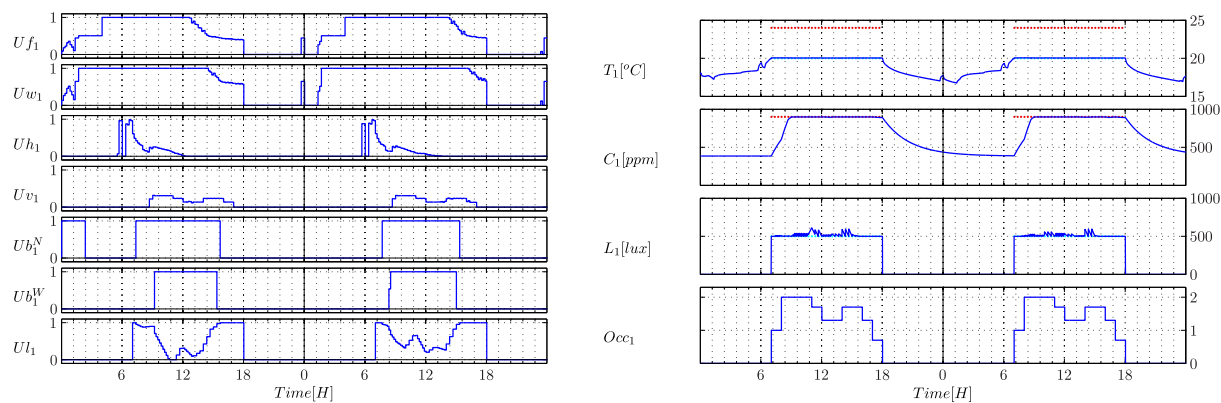


Figure 5.11 Zone #1 - Heat Pump (COP=2).

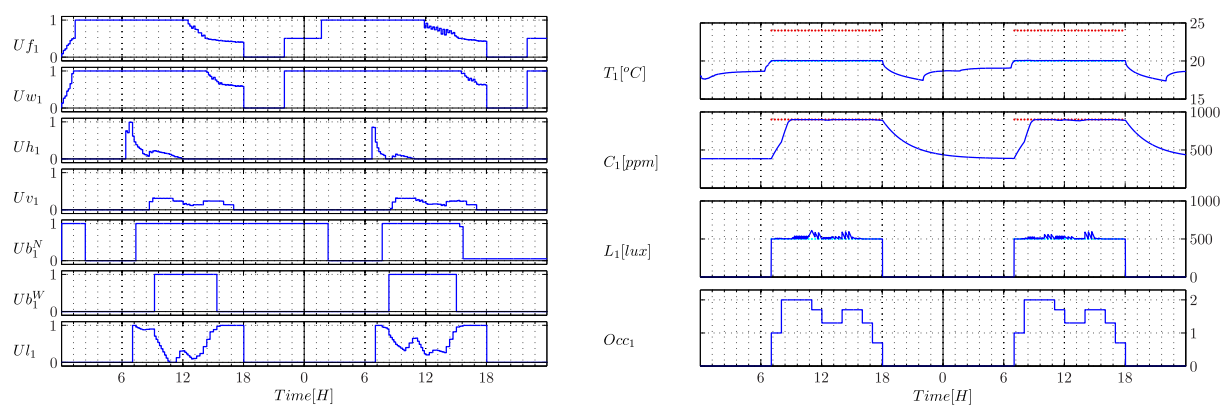


Figure 5.12 Zone #1 - Heat Pump (COP=3.5).

Part III

Distributed Model Predictive Control

Chapter 6

Distributed Model Predictive Control - Theoretical framework

" Il faut oublier, tout peut s'oublier, qui s'enfuit déjà ... "

–Jacques Brel, "Ne me quitte pas", 1959.

" We must forget, all can be forgotten. It is already fleeing... "

–Jacques Brel, "Don't leave me", 1959.

Abstract

In this chapter a hierarchical model predictive control framework is presented for a network of subsystems that are submitted to general resource sharing constraints. The method is based on a primal decomposition of the centralized open-loop optimization problem over several subsystems. A coordination agent is responsible for adjusting the parameters of the problems that are to be solved by each subsystem. A distributed-in-time feature is combined with a bundle method at the coordination layer enhancing performance and the real-time implementability of the proposed approach. Scheme performance is assessed in the next chapter on an energy coordination problem in a building involving several zones that have to share actuators and a limited amount of total power.

6.1 Introduction

The principle of Distributed Model Predictive Control (DMPC) [Camponogara et al. 2002, Negenborn et al. 2004, Rawlings & Stewart 2008] is to design local predictive controllers (also called local agents) responsible for the management of local variables.

Depending on the kind of issues encountered, the agents can share a common goal and/or resources and/or be dynamically coupled. Therefore, it is required to ensure a certain level of coordination between their respective actions in order to achieve a good system-wide performance, which is precisely the aim of DMPC.

Almost all distributed model predictive control strategies are based on successive information exchange [Scheu et al. 2009, Scheu & Marquardt 2009, Scheu et al. 2010]. In such iterative schemes, these local controllers have to come up with an agreement throughout "negotiation" iterations in order to introduce some kind of coordination between their respective actions or, more precisely, to recover the solution (or to achieve a relevant suboptimal solution) of the original centralized problem.

DMPC appears to be a suitable approach for large scale systems. Indeed, for such systems the centralized optimization problem is generally very hard (or even impossible) to solve given restrictions on computational and communication resources.

Moreover, the non scalability of the centralized solution is not the only reason of making the distributed approach interesting, indeed centralizing the decision process on one physical controller is generally unsafe because any failure affects the whole system.

Furthermore, contrary to centralized approaches, DMPC leads to modular schemes which are suitable for many large scale applications.

Several DMPC approaches have been proposed in recent literature. They are generally based either on a primal or a dual decomposition of the centralized optimization problem [Scheu et al. 2009]. They generally proceed by splitting the centralized optimization problem into several subproblems and then, using some structural features of the problem, to design distributed optimization algorithms able to deal with such problems.

Nevertheless, as pointed out in [Diehl 2009], convergence of the distributed solution towards the solution of the centralized problem generally requires a large number of iterations even for simple case studies. This may be prohibitive for real-time implementability issues and for network communication concern. Consequently, despite the apparent similarity of the many distributed MPC-based solutions, a relevant comparison should focus, among other indicators, on the specific issue of communication and computation time.

To deal with this issue, a general framework based on the combination of an efficient distributed optimization technique (*disaggregated bundle method*) and an original *distributed-in-time computation* feature is presented. The technique is based on a primal decomposition of the centralized optimization problem and leads to a hierarchical structure.

The original works leading to the scheme proposed here are intended to address the issue of energy management in buildings with a large number of zones and limited communication rate. As far as the building case is concerned, the results will be reported in the next chapter. In the present chapter, a general setting of the underlying framework is proposed and some properties of the resulting algorithms are analyzed in greater details.

The chapter is organized as follows: section 6.2 presents succinctly the kind of problems are dealt with the presented approach. Section 6.3 provides a step by step description of the approach. In sections 6.4 and 6.5, the resolution of the master problem is presented. Section 6.6 presents the main available theoretical results. Section 6.7 concludes the chapter and describes future research directions. Notice, that numerical studies are presented further on in chapter 7.

6.2 Problem statement

In this section a general description of the class of problems targeted by the proposed scheme is given. Roughly speaking, a network of subsystems sharing limited resources is considered. This is detailed in the present section.

6.2.1 The subsystems

Consider a set of N_s dynamically uncoupled subsystems¹. Each subsystem $\ell \in \mathcal{S} := \{1, \dots, N_s\}$ is governed by the following general nonlinear dynamic:

$$x_{\ell,k+1} = f(x_{\ell,k}, u_{\ell,k}) \quad (6.2.1)$$

where:

- $x_{\ell,k} \in \mathbb{R}^{n_x^\ell}$ is the state vector of the subsystem ℓ at instant k ,
- $u_{\ell,k} \in \mathbb{R}^{n_u^\ell}$ is the input vector of the subsystem ℓ at instant k ,

In the sequel, the following notation is extensively used:

¹Potential coupling can be handled via dedicated observers as is shown for instance in chapter 4 regarding the building energy management context

Notation 6.1. profile notation

Given a vector quantity $v_\ell \in \mathbb{R}^{n_v}$ related to the subsystem ℓ , the boldfaced vector $\mathbf{v}_{\ell,k}$ represents the future profile of v_ℓ over the prediction horizon of length N , namely:

$$\mathbf{v}_{\ell,k} := [v_{\ell,k}^T, \dots, v_{\ell,k+N-1}^T]^T \quad (6.2.2)$$

when no ambiguity results, the time index k is dropped and the predicted profile $\mathbf{v}_{\ell,k}$ is simply denoted by \mathbf{v}_ℓ .

Moreover, all the quantities indexed $\cdot_{\ell,k}$ refer to quantities related to subsystem ℓ at instant k . ◇

Let us now define for each subsystem $\ell \in \mathcal{S}$ the resource vector $r_{\ell,k} \in \mathbb{R}^{n_r}$ and its future profile $\mathbf{r}_{\ell,k}$. The resource limitation for subsystems $\ell \in \mathcal{S}$ over the prediction horizon is expressed via the following local inequality constraint :

$$\forall k, \forall \ell \in \mathcal{S}, \quad \mathbf{h}_\ell(\mathbf{x}_{\ell,k}, \mathbf{u}_{\ell,k}, \mathbf{r}_{\ell,k}) \leq 0 \quad (6.2.3)$$

It is assumed that each subsystem $\ell \in \mathcal{S}$ is locally controlled by a model predictive controller referred to hereafter by $\text{MPC}_\ell(\mathbf{r}_{\ell,k})$, where $\mathbf{r}_{\ell,k}$ is the available resource profile allocated to subsystem ℓ over the prediction horizon.

Therefore, at each sampling time k and given a prescribed available resource profile $\mathbf{r}_{\ell,k}$ over the prediction horizon, the system ℓ has to solve the following optimization problem:

Optimization Problem 6.1. Local optimization problem

$$\text{MPC}_\ell(\mathbf{r}_{\ell,k}) : \quad \underset{\mathbf{x}_{\ell,k} \in \mathcal{X}_{\ell,k}, \mathbf{u}_{\ell,k} \in \mathcal{U}_{\ell,k}}{\text{Minimize}} \quad L_\ell(\mathbf{x}_{\ell,k}, \mathbf{u}_{\ell,k}) \quad (6.2.4a)$$

$$\text{Subject to:} \quad \mathbf{h}_\ell(\mathbf{x}_{\ell,k}, \mathbf{u}_{\ell,k}, \mathbf{r}_{\ell,k}) \leq 0 \quad (6.2.4b)$$

where $L_\ell(\mathbf{x}_{\ell,k}, \mathbf{u}_{\ell,k}) \geq 0$ is the cost function related to the subsystem ℓ , and the domains $\mathcal{X}_{\ell,k}$ and $\mathcal{U}_{\ell,k}$ denote respectively state and input constraints and are possibly time-varying.

Once the problem 6.1 is solved at time k , the optimal predicted input and state trajectories $\mathbf{u}_{\ell,k}^*$ and $\mathbf{x}_{\ell,k}^*$ are obtained. The first component $u_{\ell,k}^*$ of $\mathbf{u}_{\ell,k}^*$ is applied to the subsystem during the time interval $[k, k + 1]$. This operation is repeated at the next instant $k + 1$ based on new measurement or estimation of the state $x_{\ell,k+1}$ and so on. The next section describes how the profile $\mathbf{r}_{\ell,k}$ is managed by a coordination level.

6.2.2 Resource sharing

Consider now a global constraint on the available resource for the whole network of subsystems. Assume that it is expressed via the following inequality:

$$\mathbf{H}(\mathbf{r}_{1,k}, \dots, \mathbf{r}_{N_s,k}) \leq 0 \quad (6.2.5)$$

The centralized formulation of the optimization problem becomes:

Optimization Problem 6.2. Centralized optimization problem

$$\underset{\{\mathbf{x}_{\ell,k} \in \mathcal{X}_{\ell,k}, \mathbf{u}_{\ell,k} \in \mathcal{U}_{\ell,k}\}_{\ell \in \mathcal{S}}}{\text{Minimize}} \quad \sum_{\ell \in \mathcal{S}} L_{\ell}(\mathbf{x}_{\ell,k}, \mathbf{u}_{\ell,k}) \quad (6.2.6a)$$

Subject to:

$$\mathbf{H}(\mathbf{r}_{1,k}, \dots, \mathbf{r}_{N_s,k}) \leq 0 \quad (6.2.6b)$$

$$\mathbf{h}_{\ell}(\mathbf{x}_{\ell,k}, \mathbf{u}_{\ell,k}, \mathbf{r}_{\ell,k}) \leq 0, \quad \forall \ell \in \mathcal{S} \quad (6.2.6c)$$

When there is a large number of subsystems N_s , the centralized optimization problem 6.2 becomes a large scale optimization problem which may become intractable. A coordination layer is thus introduced to keep the global constraint (6.2.5) satisfied (figure 6.1) despite the fact that each subsystem still solves its own optimization problem.

The coordinator is responsible for adjusting the available resources $\{\mathbf{r}_{\ell,k}\}_{\ell \in \mathcal{S}}$ of each agent $\ell \in \mathcal{S}$. Communication is assumed to be possible between each agent and the coordinator agent but is not available between the local agents. The kind of information exchanged between these entities as well as the algorithmic description of the optimization procedure taking place at the coordination layer are presented in the next section.

Remark 6.1.

Note that, although the derivation of control scheme has been largely inspired from the issue of energy management in buildings, the optimization problem 6.2 may refer to a large broad of optimization problems (e.g. distributed production/consumption systems). \diamond

6.3 Description of the approach

To coordinate the local agents, an efficient iterative procedure is designed in this section². Throughout the negotiation iterations between the coordinator and local agents,

²For a global overview of decomposition techniques and distributed optimization algorithms, the reader may refer to [Doan et al. 2009, Grothey 2001].

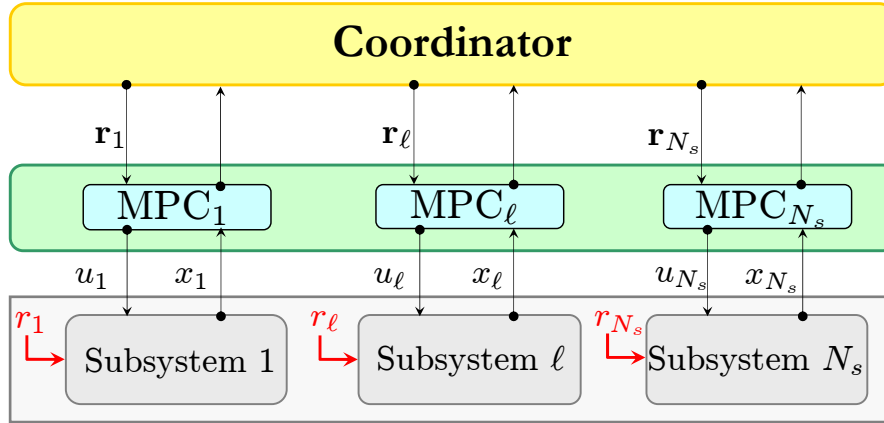


Figure 6.1 Hierarchical Distributed Model Predictive Control: the coordinator manages the subsystems allowable resource profiles $\{\mathbf{r}_{\ell,k}\}_{\ell \in \mathcal{S}}$ to ensure that the global constraint (6.2.5) is always verified.

the coordinator recomputes the optimal resource allocation in order to achieve a suitable repartition of resources between agents that meets the global constraint (6.2.5).

However, we emphasize that the number of iterations required by the coordinator should be limited and that the procedure, if necessary, must provide a whole system feasible resource repartition. To meet these requirements let us first decompose the centralized problem 6.2 and introduce some notations and assumptions.

6.3.1 Problem Decomposition

Let $J_{\ell,k}(\mathbf{r}_{\ell,k})$ denotes the achieved optimal value achieved by subsystem ℓ for a given resource allocation $\mathbf{r}_{\ell,k}$:

$$J_{\ell,k}(\mathbf{r}_{\ell,k}) := L_{\ell}(\mathbf{x}_{\ell,k}^*, \mathbf{u}_{\ell,k}^*) \quad (6.3.1)$$

Moreover, consider that the (sub)gradient $\mathbf{g}_{\ell,k}(\mathbf{r}_{\ell,k})$ of the $J_{\ell,k}$ is available, namely:

$$\mathbf{g}_{\ell,k}(\mathbf{r}_{\ell,k}) \in \partial J_{\ell,k}(\mathbf{r}_{\ell,k}) \quad (6.3.2)$$

where $\partial J_{\ell,k}(\mathbf{r}_{\ell,k})$ is the subdifferential set of the function $J_{\ell,k}$ at $\mathbf{r}_{\ell,k}$.

Furthermore, assume that:

Assumption 6.1. For all ℓ and all k , the function $J_{\ell,k}(\mathbf{r}_{\ell,k})$ is convex, and its subgradient $\mathbf{g}_{\ell,k}(\mathbf{r}_{\ell,k}) \in \partial J_{\ell,k}(\mathbf{r}_{\ell,k})$ is available. \diamond

Assumption 6.2. The local subproblems 6.1 are feasible $\forall \mathbf{r}_{\ell,k} \in \mathcal{F}_{\ell,k}$. Moreover, the domains $\mathcal{F}_{\ell,k}, \forall \ell \in \mathcal{S}$ are known by the coordinator. \diamond

Remark 6.2.

Note that the local problems 6.1 are not always feasible if the condition $\mathbf{r}_{\ell,k} \in \mathcal{F}_{\ell,k}$ is not verified. Indeed, even if availability of the sets $\mathcal{F}_{\ell,k}$ for all the subsystems $\ell \in \mathcal{S}$ appears to be a quite strong assumption (assumption 6.2) in the general case, this assumption is realistic for the BEMS problem as will be shown in the next chapter. \diamond

Based on the previous definitions and assumptions, the optimization problem (6.2) can be rewritten as follows:

$$\underset{\{\mathbf{r}_{\ell,k} \in \mathcal{F}_{\ell,k}\}_{\ell \in \mathcal{S}}}{\text{Minimize}} \quad J(\mathbf{r}_{\cdot,k}) := \sum_{\ell \in \mathcal{S}} J_{\ell,k}(\mathbf{r}_{\ell,k}) \quad (6.3.3a)$$

$$\text{Subject to} \quad \mathbf{H}(\mathbf{r}_{\cdot,k}) \leq 0 \quad (6.3.3b)$$

where:

$$\mathbf{r}_{\cdot,k} := [\mathbf{r}_{1,k}^T, \dots, \mathbf{r}_{N_s,k}^T]^T \quad (6.3.4)$$

or more briefly:

Optimization Problem 6.3. Master problem

$$\underset{\mathbf{r}_{\cdot,k} \in \mathcal{D}}{\text{Minimize}} \quad J(\mathbf{r}_{\cdot,k}) \quad (6.3.5)$$

The notation $\mathbf{r}_{\cdot,k} \in \mathcal{D}$ means the fulfilment of both the feasibility conditions $\{\mathbf{r}_{\ell,k} \in \mathcal{F}_{\ell,k}\}_{\ell \in \mathcal{S}}$ and the global resources constraints (6.3.3b).

The optimization problem 6.3 is referred to as the master problem, and its solution is performed at the coordinator layer as explained in the following section.

6.4 Solving the master problem

In this section, the algorithm used to solve the master problem (6.3.3) is presented.

6.4.1 Disaggregated bundle method

To solve the master problem, the coordinator needs, at each decision instant, to approximate the function $J = \sum_{\ell \in \mathcal{S}} J_{\ell,k}$ as a function of the allowable resource profiles $\mathbf{r}_{\ell,k}$. It is worth reminding that the coordinator possesses no knowledge regarding the dynamics of the subsystems and their respective current states.

Nevertheless, the coordinator agent is able to affect any resource $\mathbf{r}_{\ell,k}$ to the subsystems $\ell \in \mathcal{S}$ and to requests the values of the objective function of each subsystem ℓ as well as their corresponding subgradients (assumption 6.1).

For this kind of problems, bundle method [Frangioni 2002] appears to be an interesting choice as it will be argued in the sequel. Bundle method relies on iteratively approximating the function to be minimized (here $J = \sum_{\ell \in \mathcal{S}} J_{\ell,k}$) by a so called *cutting plane model*. Since the objective function J is separable, a *disaggregated* approximation is built up, i.e., an individual *cutting plane model* \check{J}_ℓ of each function $J_{\ell,k}$ is constructed.

This section provides a presentation of the bundle method is given. However, readers with particular interests may refer to [Frangioni 2002] for more details regarding this optimization technique.

To be concise, the time index k is dropped in the notations (e.g. $\mathbf{r}_\ell \equiv \mathbf{r}_{\ell,k}$) since the procedure described here takes place at a given instant k .

The bundles

In disaggregated bundle method individual cutting plane approximations of the functions $\{J_\ell\}_{\ell \in \mathcal{S}}$ are built-up thanks to a memory $\mathfrak{B}_\ell^{(s)}$ dedicated to each subfunction ℓ , updated at each iteration s and defined as follows:

$$\mathfrak{B}_\ell^{(s)} := \{\mathbf{s}_\ell^{(i)}, \epsilon_\ell^{(i)}\}_{i=1, \dots, n_{\mathfrak{B}}} \quad (6.4.1)$$

The (sub)gradients $\mathbf{s}_\ell^{(i)}$ and their corresponding *linearization errors* $\epsilon_\ell^{(i)}$ (see (6.4.2b)), are computed thanks to the values of the function $J_\ell(\mathbf{r}_\ell^{(s)})$ and (sub)gradients $\mathbf{g}_\ell^{(s)}$ returned by each agent ℓ when the coordinator requests an evaluation at the current iterate $\mathbf{r}_\ell^{(s)}$. Namely, the first element of the bundle (corresponding to the current iteration s) $\{\mathbf{s}_\ell^{(1)}, \epsilon_\ell^{(1)}\}$ is defined as follows:

$$\mathbf{s}_\ell^{(1)} := \mathbf{g}_\ell^{(s)} \quad (6.4.2a)$$

$$\epsilon_\ell^{(1)} := J_\ell(\mathbf{r}_\ell^{(s)}) - \langle \mathbf{g}_\ell^{(s)}, \mathbf{r}_\ell^{(s)} \rangle \quad (6.4.2b)$$

Indeed, each bundle $\mathfrak{B}_\ell^{(s)}$ retains only the $n_{\mathfrak{B}}$ last elements and behaves like a FIFO register in which the first element ($i = 1$) of the bundle is updated at the current iterate s after the whole bundle has been shifted and its last element dropped, namely:

$$\mathfrak{B}_\ell^{(s)} = \text{Update}(\mathfrak{B}_\ell^{(s-1)}, J_\ell(\mathbf{r}_\ell^{(s)}), \mathbf{g}_\ell^{(s)}, \mathbf{r}_\ell^{(s)}) \quad (6.4.3)$$

where the function Update is defined by the algorithm (6.1).

Algorithm 6.1 Bundle update

- 1: **for** $i \leftarrow n_{\mathfrak{B}} - 1, \dots, 1$ **do** \triangleright Shift the bundle memory
 - 2: $\mathbf{s}_\ell^{(i+1)}, \epsilon_\ell^{(i+1)} \leftarrow \mathbf{s}_\ell^{(i)}, \epsilon_\ell^{(i)}$
 - 3: **end for**
 - 4: $\mathbf{s}_\ell^{(1)} \leftarrow \mathbf{g}_\ell^{(s)}$
 - 5: $\epsilon_\ell^{(1)} \leftarrow J_\ell(\mathbf{r}_\ell^{(s)}) - \langle \mathbf{g}_\ell^{(s)}, \mathbf{r}_\ell^{(s)} \rangle$
-

The bundles $\mathfrak{B}_\ell^{(s)}$ enable the so called *cutting plane approximation* $\check{J}_\ell^{(s)}(\cdot)$ to be defined according to:

$$\check{J}_\ell^{(s)}(\mathbf{r}_\ell) := \text{Max}_{i=1, \dots, n_{\mathfrak{B}}} \langle \mathbf{s}_\ell^{(i)}, \mathbf{r}_\ell \rangle + \epsilon_\ell^{(i)} \quad (6.4.4)$$

where each linear piece $Cut^{(i)}$ defines a half space as depicted on figure 6.2.

$$Cut^{(i)} : \langle \mathbf{s}_\ell^{(i)}, \mathbf{r}_\ell \rangle + \epsilon_\ell^{(i)}, i = 1, \dots, n_{\mathfrak{B}} \quad (6.4.5)$$

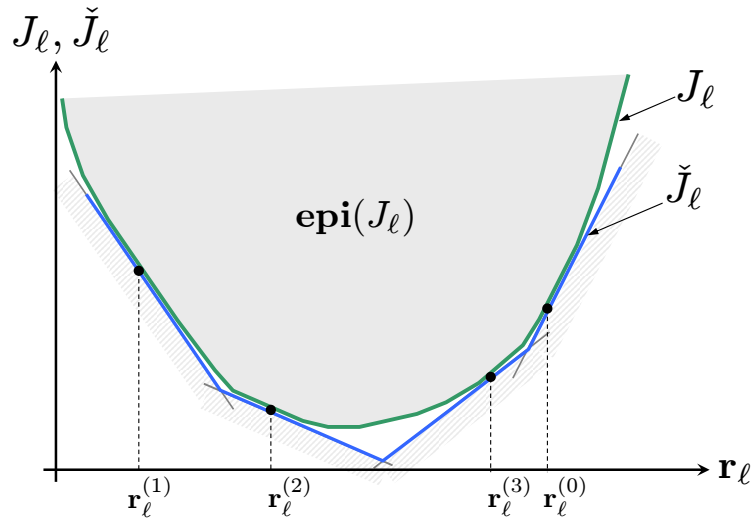


Figure 6.2 Representation of J_ℓ and its piece-wise linear approximation $\check{J}_\ell^{(3)}$ at the third iteration. The approximate function is a global under-estimator of J_ℓ .

Indeed, each *cutting plane* $Cut^{(i)}$ is a supporting hyperplane of the epigraph³ $\text{epi}(J_\ell)$ of the function J_ℓ and constitutes, since J_ℓ is assumed to be convex, a global under-estimator of J_ℓ .

³region over the function J_ℓ

The stabilized approximated master problem

Given the approximations $\check{J}_\ell^{(s)}, \ell \in \mathcal{S}$, an approximation $\check{J}^{(s)}$ of the centralized cost function can be obtained according to:

$$\check{J}^{(s)}(\mathbf{r}) := \sum_{\ell \in \mathcal{S}} \check{J}_\ell^{(s)}(\mathbf{r}_\ell) \quad (6.4.6)$$

One would simply use its minimizer as a next optimal resource candidate, namely:

Optimization Problem 6.4. Master problem -Cutting plane algorithm

$$\mathbf{r}^{(s+1)} := \underset{\mathbf{r} \in \mathcal{D}}{\text{Argmin}} [\check{J}^{(s)}(\mathbf{r})] \quad (6.4.7)$$

however, this may result in some instability [Bacaud et al. 2001] particularly at the first iterations since only few cuts are available leading to poor performances. This is actually the Kelley cutting plane algorithm [Kelley 1960]⁴.

In bundle methods [Lemaréchal 1974], instead of minimizing $\check{J}^{(s)}(\cdot)$ (optimization problem 6.4), the following *stabilized* optimization problem, denoted $\text{Master}^{(s)}$, is considered:

Optimization Problem 6.5. Stabilized master problem

$$\text{Master}^{(s)} : \quad \mathbf{r}^{(s+1)} := \underset{\mathbf{r} \in \mathcal{D}}{\text{Argmin}} [\check{J}^{(s)}(\mathbf{r}) + D^{\gamma^{(s)}}(\mathbf{r} - \bar{\mathbf{r}}^{(s)})] \quad (6.4.8)$$

where the stabilization term $D^{\gamma^{(s)}}(\mathbf{r} - \bar{\mathbf{r}}^{(s)})$ is introduced to prevent any drastic movement from the current best candidate point $\bar{\mathbf{r}}^{(s)}$, which is called the stability center (or central point).

Quite weak assumptions on the properties of $D^{\gamma^{(s)}}(\cdot)$ are necessary to ensure the convergence of the algorithm [Frangioni 2002]. However the most common choice is a the euclidean measure:

$$D^{\gamma^{(s)}}(\mathbf{r} - \bar{\mathbf{r}}^{(s)}) := \frac{1}{2 \cdot \gamma^{(s)}} \|\mathbf{r} - \bar{\mathbf{r}}^{(s)}\|_2 \quad (6.4.9)$$

Figure 6.3 depicts some of the most commonly used stabilization terms [Frangioni 2002].

⁴See also Bender's method [Dantzig & Thapa 1997b] for the linear programming case.

Remark 6.3.

More explicitly, the problem 6.5 is formulated as follows:

Optimization Problem 6.6. Master problem- explicit form

$$\text{Master}^{(s)} : \quad \mathbf{r}^{(s+1)} := \underset{\mathbf{r} \in \mathcal{D}, \{\mu_\ell\}_{\ell \in \mathcal{S}}}{\text{Argmin}} \left[\sum_{\ell \in \mathcal{S}} \mu_\ell + D^{\gamma^{(s)}}(\mathbf{r} - \bar{\mathbf{r}}^{(s)}) \right] \quad (6.4.10a)$$

Subject to:

$$\mathbf{S}_\ell^{(s)} \cdot \mathbf{r}_\ell - \mathbf{1}_{n_{\mathcal{B}} \times 1} \cdot \mu_\ell \leq \mathcal{E}_\ell^{(s)}, \quad \ell \in \mathcal{S} \quad (6.4.10b)$$

where $\mathbf{S}_\ell^{(s)}$ and $\mathcal{E}_\ell^{(s)}$ are defined as follows:

$$\mathbf{S}_\ell^{(s)} := \left[\mathbf{s}_\ell^{(1)}, \dots, \mathbf{s}_\ell^{(n_{\mathcal{B}})} \right]^T \quad (6.4.11a)$$

$$\mathcal{E}_\ell^{(s)} := \left[\epsilon_\ell^{(1)}, \dots, \epsilon_\ell^{(n_{\mathcal{B}})} \right]^T \quad (6.4.11b)$$

Actually, note that each inequality $\mathbf{S}_\ell^{(s)} \cdot \mathbf{r}_\ell - \mathbf{1}_{n_{\mathcal{B}} \times 1} \cdot \mu_\ell \leq \mathcal{E}_\ell^{(s)}$ in the optimization problem 6.6 is related to a subfunction $\ell \in \mathcal{S}$. It reflects the fact that the variable μ_ℓ has to be larger than all the linear pieces constituting the current polyhedral approximation $\check{J}_\ell^{(s)}(\mathbf{r}_\ell)$ (see (6.4.4)). This explains the inequalities (6.4.10b). \diamond

Remark 6.4.

Note that if \mathcal{D} was a polyhedron, then the optimization problem 6.6 is either a Quadratic Programming problem (in the case of quadratic stabilization term) or a Linear Programming problem if a stabilized trust region or a trust region stabilization function is used (see stabilization terms in figure 6.3). \diamond

The parameter $\gamma^{(s)} > 0$ is the proximity parameter and is updated at each iteration s . The stability center $\bar{\mathbf{r}}^{(s)}$ plays a crucial role in the bundle method since, contrary

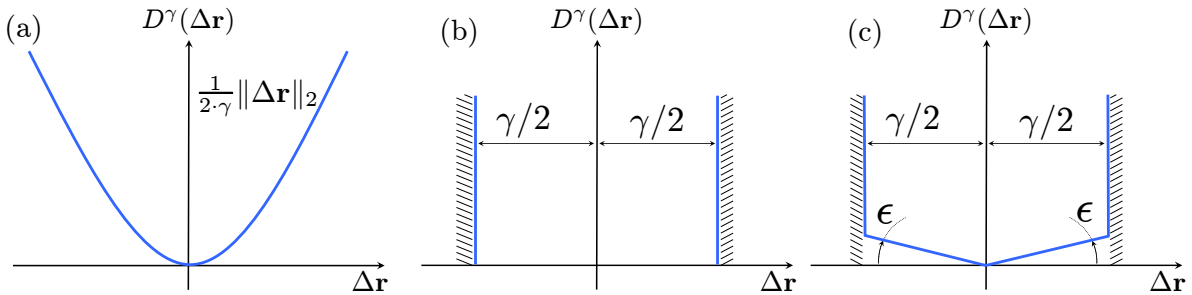


Figure 6.3 Stabilization terms. (a): quadratic stabilization term. (b): trust region. (c): stabilized trust region.

to pure cutting planes techniques [Briant et al. 2008], it keeps track of the best known solution until iteration s while avoiding oscillations resulting from a potentially poor approximation of J_ℓ .

Updating the parameter γ and the stability center $\bar{\mathbf{r}}^{(s)}$

To derive updating rules for the stability center $\bar{\mathbf{r}}^{(s)}$ and the parameter $\gamma^{(s)}$, let us define on the one hand the predicted decrease at iteration s :

$$\hat{d}^{(s)} := J(\bar{\mathbf{r}}^{(s)}) - \check{J}^{(s)}(\mathbf{r}^{(s+1)}) \geq 0 \quad (6.4.12)$$

on the other the real decrease $d^{(s)}$:

$$d^{(s)} := J(\bar{\mathbf{r}}^{(s)}) - J(\mathbf{r}^{(s+1)}) \quad (6.4.13)$$

If the real decrease is greater than a certain fraction $f \in [0, 1]$ of the predicted decrease then the current iterate s is called a *Serious Step*. In this case the coordinator enhanced the current solution: the central point $\bar{\mathbf{r}}^{(s)}$ is updated, and the trust region parameter γ is increased.

Otherwise, one has an insufficient decrease, namely $d^{(s)} \leq f \cdot \hat{d}^{(s)}$ and step s is called a *Null Step*: the central point is kept unchanged and the trust region parameter $\gamma^{(s)}$ is decreased. Note however, that in both situations the accuracy of the approximation $\check{J}^{(s)}$ is enhanced each time a new element is incorporated in the bundle (6.4.3).

The algorithm achieves the optimal solution with an accuracy ϵ_J when the predicted decrease $\hat{d}^{(s)}$ is lower than a predefined accuracy on the objective function $\hat{d}^{(s)} \leq \epsilon_J$. Since the number of iterations allowed in our framework is very limited, the condition $\hat{d}^{(s)} \leq \epsilon_J$ is rarely achieved. Therefore, the algorithm is generally stopped if the iteration counter s reaches the maximum number of iterations allowed s_{max} .

Let us finally emphasize that all iterates are feasible in that they respect all global and also local constraints. This feature is very interesting since the algorithm can be stopped, if necessary, at any iteration. To find a feasible starting point, a projection of the best known solution at instant k , denoted $\mathbf{r}^\#$ on the domain \mathcal{D} is performed at the initialization phase. The initialization function is noted Init , namely:

$$\mathbf{r}^{(0)} = \text{Init}(\mathbf{r}^\#) := \underset{\mathbf{r} \in \mathcal{D}}{\text{Argmin}} \|\mathbf{r} - \mathbf{r}^\#\| \quad (6.4.14)$$

Some other technical details regarding bundle compression techniques, updating strategies of parameter $\gamma^{(s)}$ have been omitted but are available in [Frangioni 2002].

	Aggregated model	Disaggregated model
Stabilized	Bundle-Agg	Bundle-Dis
Non stabilized	CP-Agg	CP-Dis

Table 6.1 Summary of optimization variants based on aggregation or not of the bundles and stabilization or not of the master problem.

Remark 6.5.

In this section a fully disaggregated variant of the bundle algorithm has been presented. It is worth underlining that a fully aggregated variant is also possible, i.e. where a unique (and subsequently less precise) approximation of the function J is constructed. This is achieved by forming a unique bundle for the function J , namely:

$$\mathfrak{B}^{(s)} := \left\{ \left[\begin{array}{c} \mathbf{s}_1^{(i)} \\ \vdots \\ \mathbf{s}_{N_s}^{(i)} \end{array} \right], \sum_{\ell \in \mathbf{S}} \epsilon_\ell^{(i)} \right\}_{i=1, \dots, n_{\mathfrak{B}}} \quad (6.4.15)$$

Therefore, one should distinguish four cases based on the stabilization or not of the master problem and aggregation or not of the bundles (table 6.1). These four variants will be assessed further in chapter 7, section 7.6.

◇

Remark 6.6.

In this work, an implicit assumption on synchronous communication is made. This essential assumption in the framework can be however avoided using some incremental-like bundle methods [Emiel & Sagastizábal 2008]. This has not been studied in the context of the present work.

◇

6.5 Distributing optimization over time

Ideally, all the iterations described in the previous section should take place during the sampling period $[k \cdot \tau, (k + 1) \cdot \tau]$. Moreover, many of these iterations have to be performed in order to achieve a sufficiently good approximation of cost functions $J_{\ell,k}$ (and therefore, a sufficiently good optimal solution). This may be incompatible with the sampling period or the communication capabilities.

The idea is then to still use a modified version of the past information contained in the previous bundles $\{\mathfrak{B}_{\ell,k-1}\}_{\ell \in \mathbf{S}}$. This operation relies on the assumption that

the functions $J_{\ell,k}(\cdot)$ do not change drastically and therefore the approximations of these functions, stored in the bundles:

$$\{\mathfrak{B}_{\ell,k-1} = \{\mathbf{s}_{\ell}^{(i)}, \epsilon_{\ell}^{(i)}\}_{i=1,\dots,n_{\mathfrak{B}}}\}_{\ell \in \mathcal{S}} \quad (6.5.1)$$

can be used as an initialization at instant k of the bundle but "corrected" in the following way :

$$\mathfrak{B}_{\ell,k}^{(0)} = \{m_{\ell,k} \cdot \overleftarrow{\mathbf{s}}_{\ell}^{(i)}, m_{\ell,k} \cdot \epsilon_{\ell}^{(i)}\}_{i=1,\dots,n_{\mathfrak{B}}} \quad (6.5.2)$$

where:

- the approximated (sub)gradient $\overleftarrow{\mathbf{s}}_{\ell}^{(i)}$ is obtained by conveniently shifting and completing the (sub)gradient vectors obtained over the last instants. The operator shift $\overleftarrow{\mathbf{v}}$ of any predicted profile of the vector $v \in \mathbb{R}^{n_v}$ is defined by:

$$\overleftarrow{\mathbf{v}} := [\Pi_1(\mathbf{v})^T, \dots, \Pi_{N-1}(\mathbf{v})^T, \Pi_{N-1}(\mathbf{v})^T]^T \quad (6.5.3)$$

- The positive parameter $m_{\ell,k} \in [0, 1 - \varepsilon]$ ($0 < \varepsilon \ll 1$) is the memory factor. It plays a central role in the scheme enabling a certain part of the information to be "forgotten".

The memory parameter expresses a trade-off between the quantity of information that one wants to keep and the fact the cuts used as initialization for the bundle at instant k should be under-estimators of the function $J_{\ell,k}$ in order to prevent the optimal solution from being excluded from the current search domain.

Remark that when $m_{\ell,k} = 0$, no information related the past is kept at the current instant, and the whole bundle information is equivalent to $J_{\ell,k} > 0$ (meaning that the whole information gathered during previous decision instants has been forgotten).

For these reasons, the memory factors $m_{\ell,k}$ are adjusted in accordance with the quality of the initial approximation $\check{J}_{\ell,k}^{init}$ computed at the initial point $\mathbf{r}_{\ell,k}^{(0)}$ and generalized to the whole bundle (figure 6.4).

$$m_{\ell,k} := 1 - \text{Sat}_{[0, 1-\varepsilon]} \left(\frac{[\check{J}_{\ell,k}^{init}(\mathbf{r}_{\ell,k}^{(0)}) - J_{\ell,k}(\mathbf{r}_{\ell,k}^{(0)})]^2}{[J_{\ell,k}(\mathbf{r}_{\ell,k}^{(0)})]^2} \right) \quad (6.5.4)$$

where the initial approximation $\check{J}_{\ell,k}^{init}$ results from the bundle $\mathfrak{B}_{\ell,k}^{(0)} | m_{\ell,k} = 1$ (with no forgetting factor). The function $\text{Sat}_{[a,b]}(\cdot)$ is the saturation function.

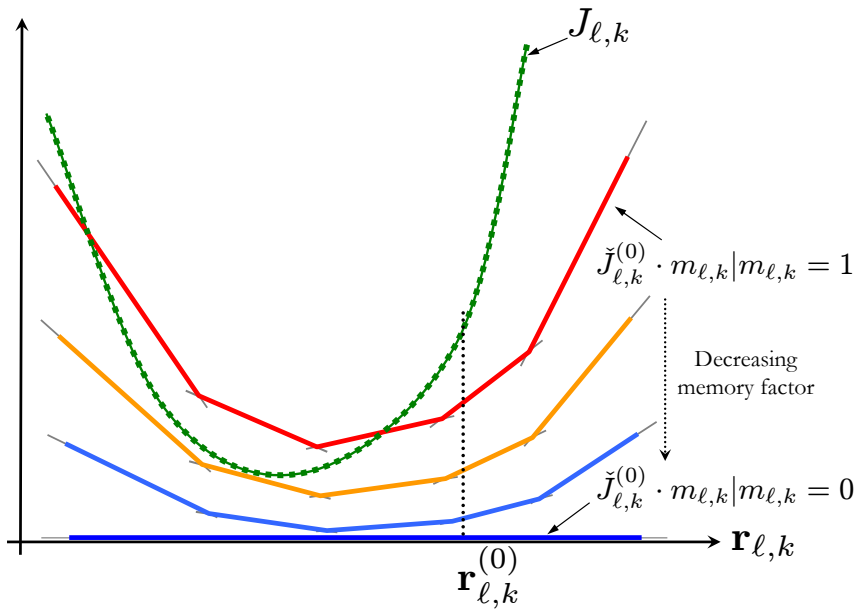


Figure 6.4 Effect of the memory factor on the first approximation of the function. For decreasing memory factors the initial approximation $J_{l,k}^{(0)}$ keeps less information but on the other hand prevents the optimal solution from being excluded from the search domain.

6.5.1 The correction mechanism

It is essential to understand that memory capability is based on the assumption that the functions $J_{l,k}$ from one decision instant to the next one are assumed to change *slowly*.

In such conditions, the initial approximation (6.5.2) is supposed to give a rough yet valuable starting approximation at instant k . However, it should be pointed out that this assumption is, in practice, very hard to check. Moreover, note that:

- The gradient approximation \overleftarrow{s}_l introduced previously introduces an intrinsic error,
- No knowledge about the subsystems respective states and/or disturbances is neither available nor taken into account by the coordination layer.

This is why a correction mechanism must be introduced to ensure *a priori* that the linear piece $i = 1, \dots, n_{\mathcal{S}}$ remains an under-estimator of the functions $l \in \mathcal{S}$. This is crucial in order to prevent the optimal point to be excluded from the current search domain.

More precisely, each time a new evaluation of the function $J_{\ell,k}(\mathbf{r}_{\ell,k}^{(s)})$ is performed, it is easy to check that each linear piece composing the current approximation of the function $\check{J}_{\ell}^{(s)}$ still under estimates the function at the given evaluation point. Basically if no error corrupted the approximation, the condition:

$$\check{J}_{\ell,k}(\mathbf{r}_{\ell,k}^{(s)}) \leq J_{\ell,k}(\mathbf{r}_{\ell,k}^{(s)}) \quad (6.5.5)$$

is always satisfied (see figure 6.2). Therefore, the differences $\beta^{(i)}$ can simply be computed:

$$\beta^{(i)} = J_{\ell,k}(\mathbf{r}_{\ell,k}^{(s)}) - (\langle \mathbf{s}_{\ell}^{(i)}, \mathbf{r}_{\ell,k}^{(s)} \rangle + \epsilon_{\ell}^{(i)}) \quad i = 1, \dots, n_{\mathfrak{B}} \quad (6.5.6)$$

Each $\beta^{(i)}$ represents the difference between the certain value of the function at the current iterate s (returned by agents) and the value of the linear piece i evaluated at the same point.

If $\beta^{(i)} \geq 0$, then the linear piece i is *a priori* a valid under-estimator of the function and remains unchanged in the bundle, since no reason indicated that it is *corrupted*. Otherwise ($\beta^{(i)} < 0$) the linear piece i in the bundle has to be vertically translated in order to correct its position and then to fulfil the condition (6.5.5), namely:

$$\text{if } \beta^{(i)} < 0 \quad \text{then } \epsilon_{\ell}^{(i)} = \epsilon_{\ell}^{(i)} + 1.1 \cdot \beta^{(i)} \quad (6.5.7)$$

Remark 6.7.

The correction mechanism enables on one hand to correct the information gathered in the bundle as explained before and on other to introduce a certain immunity against uncertainty on (sub)gradient information itself, since local solvers may return (sub)gradient values corrupted with some errors due the quality of their local solvers. Moreover, analogous techniques for non-convex function optimization are employed in bundle techniques [Grothey 2001]. \diamond

For clarity's sake, the correction mechanism is defined as a function:

$$\text{Correct}(\mathfrak{B}_{\ell,k}^{(s)}, J_{\ell,k}(\mathbf{r}_{\ell,k}^{(s)}), \mathbf{r}_{\ell,k}^{(s)}) \quad (6.5.8)$$

where the function $\text{Correct}(\cdot)$ given by the algorithm 6.2.

Memory mechanism principle is illustrated on figure 6.6 (see page 129).

Finally, to present the technique as clearly as possible, the complete framework is presented on figure 6.5, in which the elements $\{\text{BM}_{\ell}\}_{\ell \in \mathcal{S}}$ are the Bundle Manager units, performing the operations related to bundle storage, correction and memory described previously. The algorithm 6.3 (page 128) provides a full summary of the proposed framework ⁵.

⁵In the algorithm 6.3 (page 128), contraction and dilatation parameters of $\gamma^{(s)}$, here 1.1 and 0.8 are provided as indications.

Algorithm 6.2 Bundle correction mechanism

```

1: for  $i \leftarrow 1, \dots, n_{\mathfrak{B}}$  do
2:    $\beta^{(i)} = J_{\ell,k}(\mathbf{r}_{\ell,k}^{(s)}) - (\langle \mathbf{s}_{\ell}^{(i)}, \mathbf{r}_{\ell,k}^{(s)} \rangle + \epsilon_{\ell}^{(i)})$ 
3:   if  $\beta^{(i)} < 0$  then
4:      $\epsilon_{\ell}^{(i)} = \epsilon_{\ell}^{(i)} + 1.1 \cdot \beta^{(i)}$ 
5:   end if
6:    $\mathfrak{B}_{\ell,k}^{(s)} = \{\mathbf{s}_{\ell}^{(i)}, \epsilon_{\ell}^{(i)}\}_{i=1, \dots, n_{\mathfrak{B}}}$   $\triangleright$  Bundle update
7: end for

```

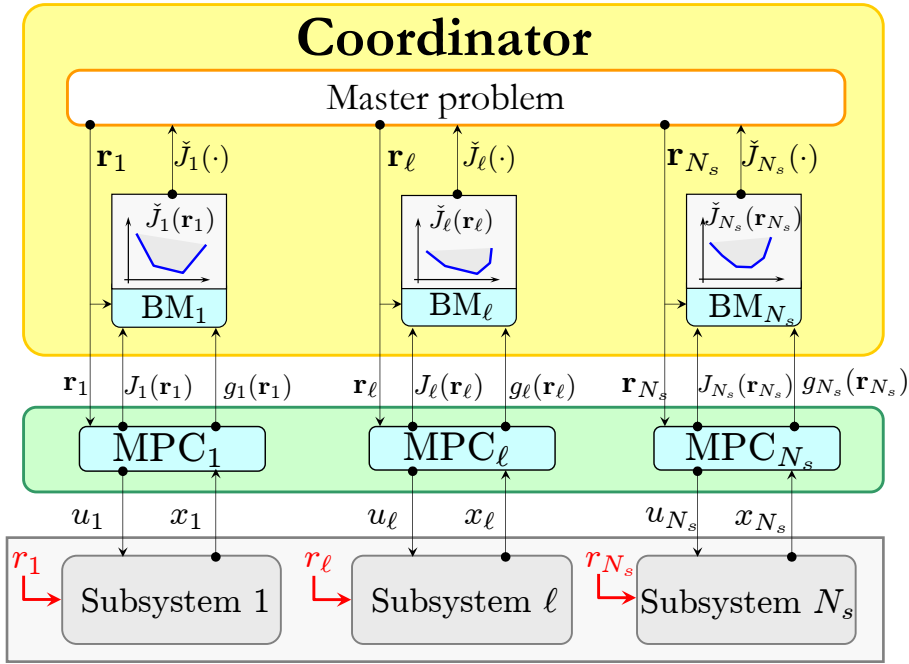


Figure 6.5 Hierarchical Distributed Model Predictive Control scheme.

6.6 Theoretical results availability

Convergence results for the classical bundle method (for an optimization problem defined once and for all) can be found in [Frangioni 2002] when the cost function is convex. The difficulties (in carrying the convergence analysis) associated with the dynamic character of the problem (that changes because of the state variation during a sampling period) can be overcome following the same guidelines recently used in [Alamir 2011]. Roughly speaking, it can be shown that the decrease in the cost function guaranteed in the ideal static case are disturbed by a term which is $O(\tau^2)$ where τ is the control updating period. As the latter is precisely decreased by the *distributed-in-time* scheme (requiring fewer iterations at each updating period), a sort of virtuous circle in favor of stability assessment takes place.

Algorithm 6.3 Bundle method based DMPC with memory

```

1: for each decision instant  $k$  do
2:    $s \leftarrow 0$  ▷ Initialize iteration counter
3:    $\mathbf{r}_{\cdot,k}^{(0)} \leftarrow \text{Init}(\overleftarrow{\mathbf{r}_{\cdot,k-1}^*})$  ▷ Send feasible candidate profiles to subsystems
4:   for  $\ell \leftarrow 1, \dots, N_s$  do ▷ Parallel operation performed by the subsystems
5:      $J_{\ell,k}(\mathbf{r}_{\ell,k}^{(0)}), \mathbf{g}_{\ell,k}^{(0)} \leftarrow \text{MPC}_\ell(\mathbf{r}_{\ell,k}^{(0)})$  ▷ Subsystems solve local problems
6:      $u_{\ell,k}^\# \leftarrow (u_{\ell,k}^*)^{(0)}$  ▷ Subsystems store their current optimal solution
7:      $m_{\ell,k} := 1 - \text{Sat}_{[0,1-\epsilon]} \left( \left[ \check{J}_\ell^{\text{init}}(\mathbf{r}_{\ell,k}^{(0)}) - J_{\ell,k}(\mathbf{r}_{\ell,k}^{(0)}) \right]^2 / [J_{\ell,k}(\mathbf{r}_{\ell,k}^{(0)})]^2 \right)$ 
8:      $\mathfrak{B}_{\ell,k}^{(0)} = \{m_{\ell,k} \cdot \overleftarrow{\mathfrak{s}}_\ell^{(i)}, m_{\ell,k} \cdot \epsilon_\ell^{(i)}\}_{i=1, \dots, n_{\mathfrak{B}}}$  ▷ Forgetting operation
9:      $\mathfrak{B}_{\ell,k}^{(0)} \leftarrow \text{Update}(\mathfrak{B}_{\ell,k}^{(0)}, J_{\ell,k}(\mathbf{r}_{\ell,k}^{(0)}), \mathbf{g}_{\ell,k}^{(0)}, \mathbf{r}_{\ell,k}^{(0)})$  ▷ Update bundles
10:     $\mathfrak{B}_{\ell,k}^{(0)} \leftarrow \text{Correct}(\mathfrak{B}_{\ell,k}^{(0)}, J_{\ell,k}(\mathbf{r}_{\ell,k}^{(0)}), \mathbf{r}_{\ell,k}^{(0)})$  ▷ Correct bundles
11:  end for
12:   $\bar{\mathbf{r}}^{(0)} \leftarrow \mathbf{r}_{\cdot,k}^{(0)}, \hat{d}^{(0)} \leftarrow \infty$  ▷ Initialize stability center
13:  while  $s \leq s_{\max}$  and  $\hat{d}^{(s)} \geq \eta_J$  do
14:     $\mathbf{r}_{\cdot,k}^{(s+1)} \leftarrow \text{Master}^{(s)}$  ▷ Coordinator solves master problem
15:     $\hat{d}^{(s)} = J(\bar{\mathbf{r}}_{\cdot,k}^{(s)}) - \check{J}^{(s)}(\mathbf{r}_{\cdot,k}^{(s+1)})$ 
16:    for  $\ell \leftarrow 1, \dots, N_s$  do
17:       $J_{\ell,k}(\mathbf{r}_{\ell,k}^{(s+1)}), \mathbf{g}_{\ell,k}^{(s+1)} \leftarrow \text{MPC}_\ell(\mathbf{r}_{\ell,k}^{(s+1)})$  ▷ Subsystems solve local opt. probs.
18:       $d^{(s)} = J(\bar{\mathbf{r}}_{\cdot,k}^{(s)}) - \check{J}^{(s)}(\mathbf{r}_{\cdot,k}^{(s+1)})$  ▷ Compute real decrease
19:      if  $\hat{d}^{(s)} > f \cdot d^{(s)}$  then ▷ Serious step
20:         $\gamma^{(s+1)} \leftarrow 1.1 \cdot \gamma^{(s)}, \bar{\mathbf{r}}_{\cdot,k}^{(s+1)} \leftarrow \mathbf{r}_{\cdot,k}^{(s+1)}$  ▷ Increase  $\gamma$ , update stab. center
21:         $u_{\ell,k}^\# \leftarrow (u_{\ell,k}^*)^{(s+1)}$  ▷ Subsystems update optimal solutions
22:      else ▷ Null step
23:         $\gamma^{(s+1)} \leftarrow 0.8 \cdot \gamma^{(s)}, \bar{\mathbf{r}}_{\cdot,k}^{(s+1)} \leftarrow \bar{\mathbf{r}}_{\cdot,k}^{(s)}$  ▷ Decrease  $\gamma$ , stab. cent. unchanged
24:      end if
25:       $\mathfrak{B}_{\ell,k}^{(s+1)} \leftarrow \text{Update}(\mathfrak{B}_{\ell,k}^{(s)}, J_{\ell,k}(\mathbf{r}_{\ell,k}^{(s+1)}), \mathbf{g}_{\ell,k}^{(s+1)}, \mathbf{r}_{\ell,k}^{(s+1)})$  ▷ Update bundles
26:       $\mathfrak{B}_{\ell,k}^{(s+1)} \leftarrow \text{Correct}(\mathfrak{B}_{\ell,k}^{(s+1)}, J_{\ell,k}(\mathbf{r}_{\ell,k}^{(s+1)}), \mathbf{r}_{\ell,k}^{(s+1)})$  ▷ Correct bundles
27:    end for
28:     $s \leftarrow s + 1$  ▷ Increment iteration counter
29:  end while
30:   $\mathbf{r}_{\cdot,k}^* \leftarrow \bar{\mathbf{r}}_{\cdot,k}^{(s+1)}$ 
31:  for  $\ell \leftarrow 1, \dots, N_s$  do ▷ Parallel operations performed by subsystems
32:    Subsystem  $\ell$  Applies  $u_{\ell,k}^\#$ 
33:  end for
34: end for

```

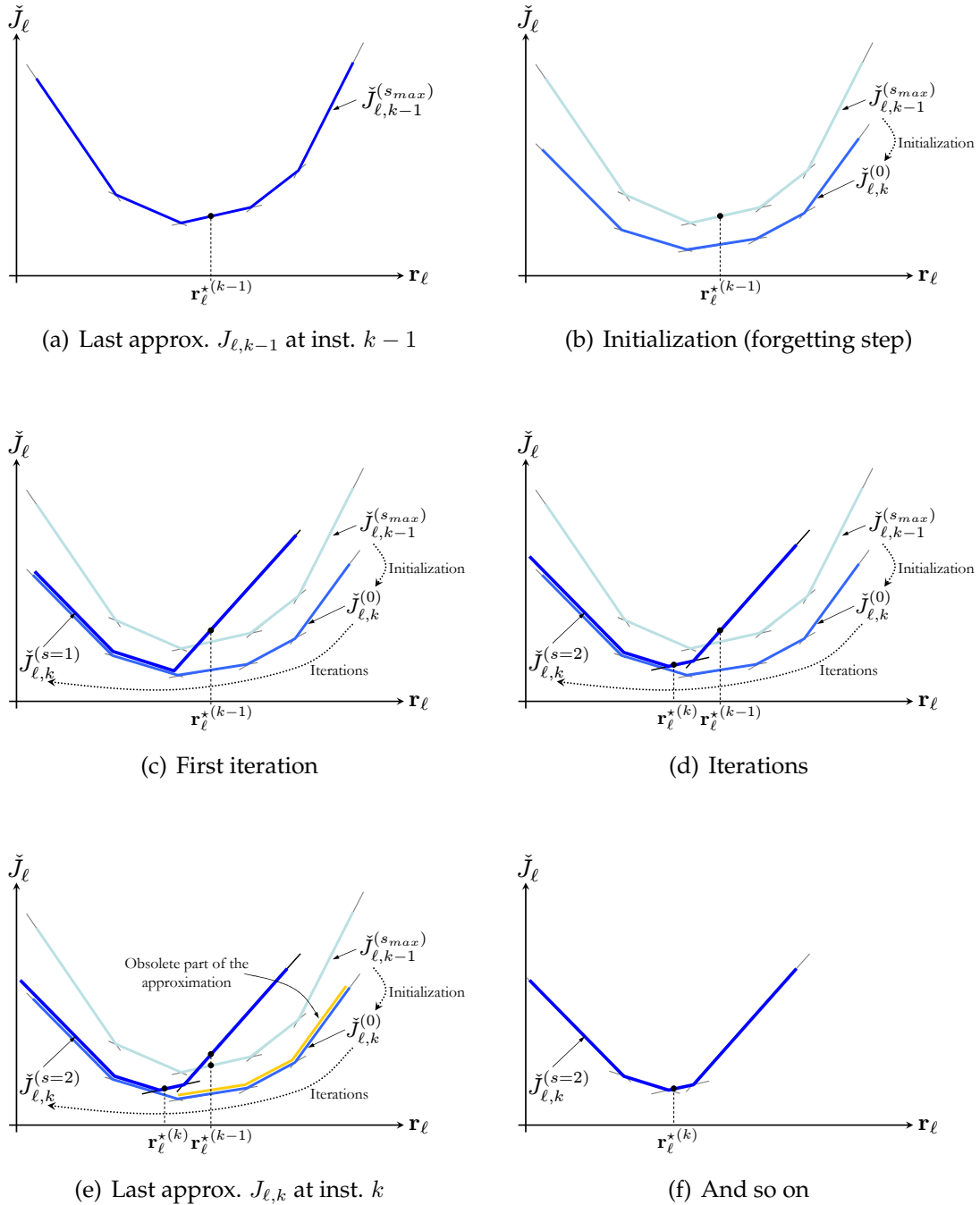


Figure 6.6 Illustration of the DMPC algorithm with memory-based mechanism.

6.7 Conclusion

In this chapter, a new *distributed-in-time* algorithm for distributed model predictive control has been presented. Its main advantage lies in decreasing the number negotiation iterations required in order to achieve a relevant solution at each decision instant. The scheme is particularly adapted to situations in which the computation units at the subsystem layer are much more ineffective compared to the one at coordination layer.

In future, the investigation of the effects of adjustment of the bundle size as well as the number of iterations will be carried out. This with a deeper theoretical study regarding convergence as well as theoretical performances.

In the next chapter the scheme presented in this chapter is tailored to the BEMS case. Indeed, a coordinator is introduced to manage the zone controllers designed in part II to handle global power consumption limitations in a multi-source context. This issue is deeply explained in chapter 7.

Chapter 7

Constrained DMPC for building energy management

Abstract

In this chapter, a DMPC approach for handling power limitations, shared inputs and a shared storage device in a multi-zone building is presented. The scheme, based on the distributed approach presented previously in chapter 6, is tailored to this issue.

7.1 Context and motivations

Model Predictive Control (MPC) is becoming a crucial paradigm for energy management in buildings. This fact results from its ability to manage constrained MIMO systems while taking into account weather forecast, energy tariffs, occupancy schedule etc.

As it has been pointed out in section 2.4.1, instead of managing buildings internal parameters, a crucial benefit of the usage of predictive strategies in buildings lies also in their ability to take into account some market conditions imposed by the utility.

In that sense, the objective of the chapter is to design a coordination mechanism able to manage the zone controllers in order to:

1. Make the building *smart grid ready* (this will be explained hereafter),
2. Handle power resources constraints, shared inputs as well as energy storage capability.

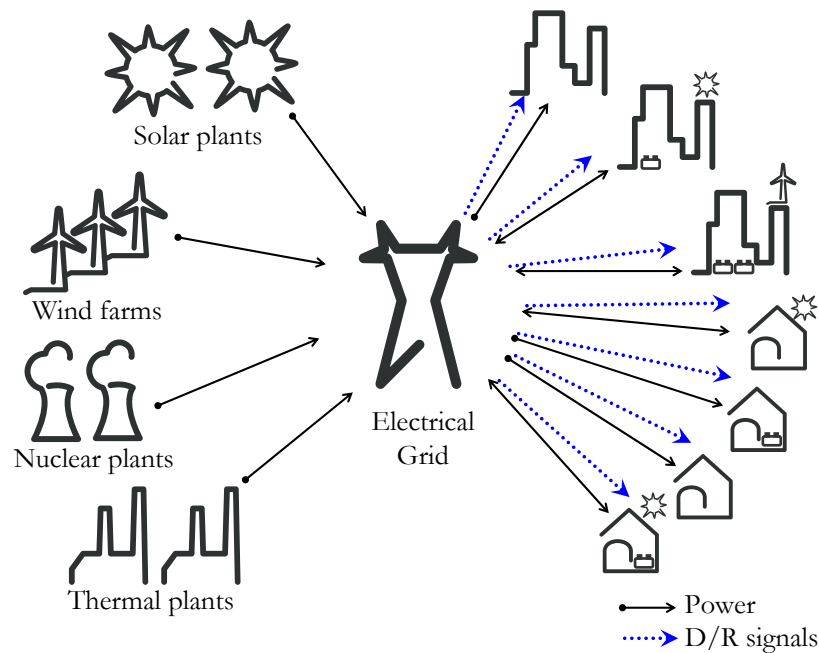


Figure 7.1 Illustration of the current electricity grid.

Smart grid ready buildings - demand responsive buildings

One of the major issues facing electricity providers lies in reducing supply-consumption imbalances in the electricity grid. This task is, on one hand, particularly critical since it ensures the consistency of the electrical grid and therefore sustainability of energy provisioning and, on the other hand, becoming extremely challenging with the increased penetration of renewable energy and the future massive introduction of electrical vehicles.

In this context, the conventional grid initially optimized to deliver energy from controlled centralized generation stations to end-users, in a one-way transmission line, is no longer adapted. In fact, the context calls for smarter grids able to manage heterogeneous distributed generation/consumption systems, which are moreover partially controllable (see [Chen et al. 2012, Saad et al. 2012, Koutsopoulou & Tassiulas 2010] and the references therein for deeper explanations).

Demand/Response (D/R) is an approach in which the market conditions are adjusted according to the status of the grid. Basically, end electricity users are requested to adjust their consumptions to *help* the electrical grid. Electricity grid managers achieve this objective by sending D/R signals (see figure 7.1) that may take several forms:

a. Time varying electricity rating

b. Maximal power consumption adjustment

c. Power dependant energy rating (see figure 7.2)

It goes without saying that electricity end-users should be *responsive* and therefore able to adapt their consumptions according to the market conditions. In fact, D/R strategies are nowadays in almost situations *manual*, this means that an operator in the building is responsible for adjusting the building consumption, by acting on building set-points or directly by switching-off some equipment when required. It is then quite obvious that:

1. the decisions to be undertaken by an operator become particularly difficult when rating conditions are complex and/or local production and/or storage capability (that may take several forms) are available,
2. large scale deployment and effectiveness of D/R strategies in such conditions is unreliable.

These only reasons fully justify the introduction of *automated* D/R capabilities for buildings. Indeed, automated D/R is a core component of the so called *smart grid*, since it enables electricity grid managers to make use of a huge energetic buffer (buildings) in order to:

- Maintain production-consumption equilibrium,
- *Shift* energy consumption to more appropriate periods during which energy is less carbonated for instance,
- Reduce peak power consumption and therefore avoid heavy investments in additional power plants [Chen et al. 2012]¹.

Constrained DMPC for buildings

Although a lot of effort has been deployed in designing MPC strategies for Building Energy Management Systems (BEMS), limitations have been pointed out in some previous studies (e.g. [Moroşan et al. 2010a, Ma et al. 2011]) when the dimension of the building increases.

In the case of large buildings, a centralized approach is too expensive (or even impossible) from a computational point of view. In addition to non scalability, non

¹Depending on estimations 100 hours during the whole year ($\approx 1\%$ of the time) are responsible for 10-20 % of the whole US investment in electric sector, see [Chen et al. 2012] and the references therein.

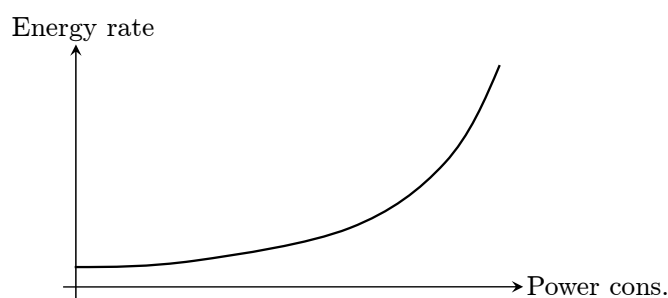


Figure 7.2 Power dependant energy rating: this means that energy rate depends on power consumption - the convex shape of the electricity rate is introduced to reduce excessive peak consumption.

modular schemes are generally inappropriate both for maintainability and safety reasons but also for extensibility concerns.

As discussed earlier (chapter 6), the principle of Distributed Model Predictive Control (DMPC) is to design local predictive controllers responsible of local decision making that have to come up with an agreement on the best system-wide strategy to implement.

For building application, this approach has been studied before². In [Moroşan et al. 2011, Moroşan et al. 2010b], DMPC strategies have been designed to handle a global power limitation or a centralized heating system using either a dual decomposition (Dantzig-Wolfe) or a primal decomposition (Bender) technique (see [Dantzig & Thapa 1997b]) to tackle the encountered issues. Nevertheless, the schemes handle either shared variables between zones or power limits but not these two features simultaneously.

In [Ma et al. 2011, Ma et al. 2012] the management of the thermal regulation of a multi-zone building is performed in a distributed fashion. A modified SQP method is combined to a dual decomposition of the centralized problem. The master problem is then solved thanks to a fast gradient technique. In this case, the authors report an important number of iterations to achieve a relevant sub-optimal solution (few hundreds), such a communication rate represents a serious drawback.

Furthermore, these works focus exclusively on the thermal aspect. Even if, from a purely conceptual point of view, the management of the other zone-relevant quantities (CO₂ and indoor illuminance) has no impact on the proposed schemes, complexity of the local sub-problems is increased and may affect their performances.

²see also [Dounis & Caraiscos 2009, Abras 2009] for other non-predictive multi-agent control systems in buildings

In chapters 4 and 5, a nonlinear MPC strategy has been proposed to manage zone relevant quantities to ensure occupants comfort at a minimal operational cost. In this chapter, these local controllers are used in a global DMPC framework to handle simultaneously:

- Limitations on power sources,
- Shared inputs between zones,
- Shared energy storage equipment (local battery).

This is the main originality of the work reported in the present chapter.

Furthermore, let us highlight the fact that a great attention is given to the communication rate. Indeed, the proposed mechanism exhibits good performances even when the number of allowed iterations is extremely low.

This chapter is organized as follows: in section 7.2 a schematic description of the problem is given. After a brief recall of zone model predictive control in section 7.3, the global multi-zone problem is formulated in section 7.4. The DMPC framework is derived and assessed on a 20 zones building in section 7.5. In section 7.6, assessment of the bundle method is provided. Section 7.7 present the simulation results. Finally, section 7.8 concludes the chapter and gives directions for further investigations.

7.2 Problem description

In this chapter, a multi-zone building is considered. The building is able to store electrical energy in batteries in order to redistribute it to zones. This storage capability offers the benefit of:

- i. shifting energy consumption of the building to periods in which electricity is cheaper,
- ii. storing energy to redistribute it to the zones in order to prevent any power constraint violation since the power provided by the grid to the building is limited.

Thus, the building should take into account this power limitation in advance to store energy in an electrical form or a thermal form in the zones in order to maintain occupants comfort within the prescribed level. Moreover, the amount of thermal energy stored in each zone should be adapted regarding the *thermal storage efficiency* of each zone.

Chapter 7. Constrained DMPC for building energy management

The aim of this study is to design a coordination mechanism able to address this issue (figure 7.3). In the next section, a brief recall on zone model predictive control which has been designed in chapters 4 and 5 is given since these zone MPC controllers are then integrated in the DMPC architecture.

It is important to highlight that physical couplings between zones are not explicitly taken into account in the control procedure. Indeed, as it has been discussed in chapter 4, dedicated observers have been designed to recover them. They are, therefore seen as disturbances and no cooperation mechanism addressing the physical couplings between zones is implemented³.

Before going further, let us first introduce some necessary complements to the zones controllers, by making each zone able to manage some local constraints. This is precisely the aim of the next section.

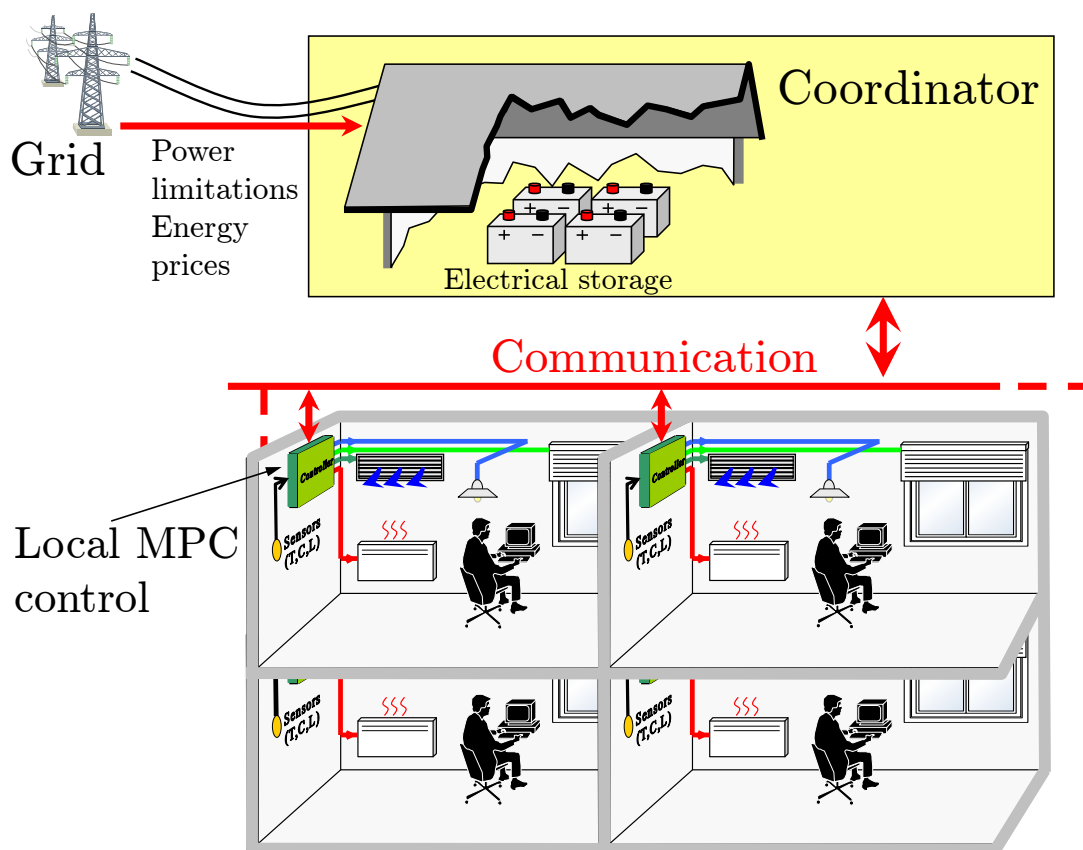


Figure 7.3 Constrained distributed Model Predictive in a multi-zone building. The coordinator gathers global information and ensures coordination of local controllers beside battery management.

³interested reader may refer to [Moroşan et al. 2010a] for some DMPC strategies enabling to take into account heat exchanges between zones explicitly.

7.3 Zone controllers

In this section, a brief recall on the previously designed zone model predictive controllers⁴ is given. As it will be discussed, slight modifications will be introduced in the zone-related optimization problems to handle local power limitations and shared inputs.

7.3.1 Zone models

Consider a building with n_z zones, where $\ell \in \mathbf{Z} = \{1, \dots, n_z\}$ is the zone index and let the following nonlinear state space representations describe the dynamical behavior of each zone $\ell \in \mathbf{Z}$:

$$\begin{cases} x_\ell^+ &= A_\ell \cdot x_\ell + [B_\ell(y_\ell, w_\ell)] \cdot u_\ell + G_\ell \cdot w_\ell \\ y_\ell &= C_\ell \cdot x_\ell + [D_\ell(w_\ell)] \cdot u_\ell + F_\ell \cdot w_\ell \end{cases} \quad (7.3.1)$$

where: $x_\ell \in \mathbb{R}^{n_x}$, $u_\ell \in \mathbb{R}^{n_u}$, $w_\ell \in \mathbb{R}^{n_w}$, $y_\ell \in \mathbb{R}^{n_y}$ are respectively the state, input, disturbance and output vectors related to the zone ℓ .

Further discussion regarding this model can be found in chapter 3. Nevertheless, let us recall some necessary elements to understand the sequel:

- The model (7.3.1) is a nonlinear model;
- Depending on the configuration of each zone ℓ , the vector u_ℓ gathers control of local equipment (HVAC⁵, lighting, shading) that may differ between zones. Normalized inputs are considered, i.e $u_\ell \in [0, 1]^{n_u}$.
- The output vector $y_\ell = [T_\ell, C_\ell, L_\ell]^T$ includes indoor air temperature, CO₂ level and illuminance in the zone ℓ .
- $w_\ell = [\phi_\ell^1, \dots, \phi_\ell^{n_f}, T_{ex}, \text{Occ}_\ell, C_{ex}]^T$ is the disturbance vector. More precisely: $\phi_\ell^1, \dots, \phi_\ell^{n_f}$ are the global irradiance fluxes on each of the n_f^f facades of the zone ℓ , T_{ex} is the outdoor temperature, Occ_ℓ is the number of occupants and C_{ex} is the outdoor CO₂ level.

⁴see chapters 4 and 5

⁵ HVAC: Heating, Ventilation and Air Conditioning

7.3.2 Zone Model Predictive Control

The objective of each zone model predictive controller is to keep the outputs of the system $y_\ell \in \mathbb{R}^3$ in their respective comfort range (chapter 4) at a minimum energetic cost, which may refer to a pure energetic criterion or a an invoice criterion in the case of varying energy tariff.

The comfort bounds related to outputs are obviously linked to the occupancy of the zone. The model (7.3.1) of each zone as well as prediction on disturbances, power costs and occupancy are jointly used in order to formulate the following optimization problem which has to be solved at each decision instant:

$$\underset{\mathbf{u}_\ell \in \mathbf{U}_\ell}{\text{Minimize}} \quad J^E(\mathbf{p}_\ell) + J^C(\mathbf{y}_\ell) + J^F(\mathbf{y}_\ell) + J^D(\mathbf{y}_\ell) \quad (7.3.2)$$

where:

- J^E, J^C, J^F, J^D stand respectively for energy cost, discomfort cost, final cost and actuators variations cost (see chapter 4),
- Recall that the boldfaced vector indicate predicted profiles (e.g. \mathbf{u}_ℓ is the predicted profile of the input vector u_ℓ over the prediction horizon).
- $\mathbf{p}_\ell \in \mathbb{R}^{n_e \cdot N}$ stands for predicted power consumption profile, where n_e is the total number of power sources.

One is interested in the case where the zone has access to several power sources, that may be moreover of the same type (several electrical sources for example), each power source being characterized by its related cost (and upper limit as it will explained after). More precisely, one considers that each of the n_e power sources belongs to one of the n_s types consumed by the zone.

Let \mathbf{b}_ℓ denotes the correspondence between sources and types. More precisely, each element $\mathbf{b}_\ell(i, j)$ of the matrix $\mathbf{b}_\ell \in \mathbb{R}^{n_s \times n_e}$ takes the value 1 iff the power source $j = 1, \dots, n_e$ is of type $i = 1, \dots, n_s$.

example:

Assume a zone equipped with a fan coil unit (chapter 5). The zone consumes electrical and thermal energy (there exists two power types $n_s = 2$). Moreover, the zone has access to three different electrical sources and one thermal source ($n_e = 3 + 1$). In this case:

$$\mathbf{b}_\ell := \begin{bmatrix} 1 & 1 & 1 & 0 \\ 0 & 0 & 0 & 1 \end{bmatrix} \in \mathbb{R}^{2 \times 4} \quad (7.3.3)$$

◇

According to the previous discussion, the power profile \mathbf{p}_ℓ is linked to the control variables by the following relation:

$$\mathcal{B}_\ell \cdot \mathbf{p}_\ell = \mathbf{E}_\ell \cdot \mathbf{u}_\ell \quad (7.3.4)$$

The matrix $\mathbf{E}_\ell \in \mathbb{R}^{n_s \cdot N \times n_u^\ell \cdot N}$ is suitably constructed to gather the power consumptions related to each actuator with respect to each power source (see (5.3.5)). The matrix \mathcal{B}_ℓ is given by:

$$\mathcal{B}_\ell := \mathbf{I}_N \otimes \mathbf{b}_\ell \quad (7.3.5)$$

- J^E corresponds to the integral energy criterion over the horizon. It depends on the predicted consumed power profile \mathbf{p} and the power costs Γ . Therefore:

$$J^E := \Gamma^T \cdot \mathbf{p} \quad (7.3.6)$$

The components of the vector $\Gamma \in \mathbb{R}^{n_e}$ correspond to the cost of the available power sources of zone ℓ .

- $J^C(\mathbf{y})$ is the discomfort criterion. It expresses the discomfort related to thermal, air quality and lighting aspects in a building and can be defined in terms of lower and upper bounds $\bar{\mathbf{y}}_\ell, \underline{\mathbf{y}}_\ell$. These bounds are linked to the predicted occupancy of each zone, (section 4.3).

7.3.3 Introducing local constraints

Let us assume that each zone $\ell \in \mathbf{Z}$ is submitted to two types of resource constraints:

- Upper limit resources constraints $\mathbf{r}_\ell^{\text{up}}$, that refer to upper constraints on local power consumption, namely:

$$\mathbf{p}_\ell \leq \mathbf{r}_\ell^{\text{up}} \quad (7.3.7)$$

- Shared inputs $r_\ell^{\text{eq}} \in \mathbb{R}^{n_{sh}^\ell}$ which are the inputs shared by the zone ℓ with other zones or some subset of zones (an example is given further). Namely, the following local constraint holds:

$$\Lambda_\ell \cdot \mathbf{u}_\ell = r_\ell^{\text{eq}} \quad (7.3.8)$$

where each element $\Lambda_\ell(i, j)$ of the matrix $\Lambda_\ell \in \mathbb{R}^{n_{sh}^\ell \times n_u^\ell}$ designates the shared input $j = 1, \dots, n_{sh}$ corresponding to the input $i = 1, \dots, n_u^\ell$ of the zone ℓ , namely:

$$\Lambda_\ell(i, j) = 1, \quad \text{if the shared input } j \text{ corresponds to input } i \text{ of zone } \ell \quad (7.3.9)$$

$$\Lambda_\ell(i, j) = 0, \quad \text{otherwise} \quad (7.3.10)$$

Furthermore, let us introduce the matrix Λ_ℓ :

$$\Lambda_\ell := \mathbf{I}_N \otimes \Lambda_\ell \quad (7.3.11)$$

Hence, the optimization problem 4.2 related to each zone $\ell \in \mathbf{Z}$ becomes:

Optimization Problem 7.1.

$$\text{NLP}_\ell: \underset{\mathbf{u}_\ell, \mathbf{p}_\ell, \mathbf{y}_\ell, \delta_1, \delta_2, \delta_d}{\text{Minimize}} J(\mathbf{u}_\ell, \mathbf{p}_\ell, \mathbf{y}_\ell, \Gamma_k) \quad (7.3.12a)$$

Subject To :

$$[\Phi_\ell(\mathbf{y}_\ell, \mathbf{w}_\ell)] \cdot \mathbf{u}_\ell + \delta_0^- + \delta_1^- \geq \underline{\mathbf{y}}_\ell - \Psi_\ell \cdot x_\ell - \Xi_\ell \cdot \mathbf{w}_\ell \quad (7.3.12b)$$

$$[\Phi_\ell(\mathbf{y}_\ell, \mathbf{w}_\ell)] \cdot \mathbf{u}_\ell - \delta_0^+ - \delta_1^+ \leq \bar{\mathbf{y}}_\ell - \Psi_\ell \cdot x_\ell - \Xi_\ell \cdot \mathbf{w}_\ell \quad (7.3.12c)$$

$$\mathbf{D} \cdot \mathbf{u}_\ell - \delta_d^+ + \delta_d^- = \mathbf{a} \quad (7.3.12d)$$

$$\mathbf{0} \leq \mathbf{u}_\ell \leq \mathbf{1} \quad (7.3.12e)$$

$$\mathcal{B}_\ell \cdot \mathbf{p}_\ell = \mathbf{E}_\ell \cdot \mathbf{u}_\ell \quad (7.3.12f)$$

$$\delta_1 \geq \mathbf{0}, \delta_d \geq \mathbf{0}, \mathbf{0} \leq \delta_2 \leq \begin{bmatrix} \delta_y \\ \delta_y \end{bmatrix} \quad (7.3.12g)$$

$$\Lambda_\ell \cdot \mathbf{u}_\ell = \mathbf{r}_\ell^{\text{eq}} \quad (7.3.12h)$$

$$\mathbf{p}_\ell \leq \mathbf{r}_\ell^{\text{up}} \quad (7.3.12i)$$

Note that, in the case of multi-source buildings, with several power sources of the same nature (previous example), the variables \mathbf{p}_ℓ need to be added to the set of decision variables \mathbf{z}_ℓ related to the zone ℓ (gathering all the decision variables involved in the optimization problem):

$$\mathbf{z}_\ell := \begin{bmatrix} \mathbf{u}_\ell^T & \mathbf{p}_\ell^T & \delta_0^T & \delta_1^T & \delta_d^T \end{bmatrix}^T \quad (7.3.13)$$

Following the guidelines presented in chapter 4, it can be shown that the MPC related optimization problem is a nonlinear optimization problem that can be solved thanks to the resolution of a sequence of LPs. Defining the local resource vector related to each zone r_ℓ by:

$$r_\ell := \begin{bmatrix} r_\ell^{\text{up}} \\ r_\ell^{\text{eq}} \end{bmatrix} \quad (7.3.14)$$

At each iteration i of the fixed-point algorithm, the following LP has to be solved:

Optimization Problem 7.2. Zone related optimization problem (nonlinear)

$$J_\ell(\mathbf{r}_\ell) := \underset{\mathbf{z}_\ell \leq \mathbf{z}_\ell \leq \bar{\mathbf{z}}_\ell}{\text{Minimize}} \mathbf{L}_\ell^{(i)} \cdot \mathbf{z}_\ell \quad (7.3.15)$$

Subject To :

$$\mathbf{A}_\ell^{(i)} \cdot \mathbf{z}_\ell \leq \mathbf{b}_\ell \quad (7.3.16)$$

$$\underline{\mathbf{e}}_\ell(\mathbf{r}_\ell) \leq \mathbf{A}'_\ell \cdot \mathbf{z}_\ell \leq \bar{\mathbf{e}}_\ell(\mathbf{r}_\ell) \quad (7.3.17)$$

$\underline{\mathbf{e}}_\ell(\mathbf{r}_\ell)$ and $\bar{\mathbf{e}}_\ell(\mathbf{r}_\ell)$ are affine in their arguments. They are introduced only to render the optimization problem writing compact.

In order to keep the formulation simple. It is assumed in the remainder that the MPC-related optimization problem takes the form of a linear programming problem at each decision instant. Actually, this is achieved by limiting the number of iterations to only one iteration.

Thus, assuming \mathbf{r}_ℓ given, the following LP has to be solved by each zone ℓ at each decision instant:

Optimization Problem 7.3. Zone optimization problem- $\text{MPC}_\ell(\mathbf{r}_\ell)$

$$J_\ell(\mathbf{r}_\ell) := \underset{\mathbf{z}_\ell \leq \mathbf{z}_\ell \leq \bar{\mathbf{z}}_\ell}{\text{Minimize}} \mathbf{L}_\ell \cdot \mathbf{z}_\ell \quad (7.3.18)$$

Subject To :

$$\mathbf{A}_\ell \cdot \mathbf{z}_\ell \leq \mathbf{b}_\ell \quad (7.3.19)$$

$$\underline{\mathbf{e}}_\ell(\mathbf{r}_\ell) \leq \mathbf{A}'_\ell \cdot \mathbf{z}_\ell \leq \bar{\mathbf{e}}_\ell(\mathbf{r}_\ell) \quad (7.3.20)$$

In the optimization problem 7.3, the optimal value of the objective function for some resource allocation \mathbf{r}_ℓ is abusively denoted $J_\ell(\mathbf{r}_\ell)$.

Note that since the optimization problem 7.3 is an LP problem, a subgradient $\mathbf{g}_\ell(\mathbf{r}_\ell) \in \partial J_\ell(\mathbf{r}_\ell)$ is given by dual variables corresponding to the constraints (7.3.20) [Dantzig & Thapa 1997a, Dantzig & Thapa 1997b]. This enables the methodology developed in chapter 6 to be used as shown in the following section.

7.4 DMPC - the control problem

In order to clarify the presentation, this section treats increasingly complex situations. Firstly, considering that a global power limitation \bar{p}_g on the total power consumption of the building holds, then that an electrical battery is available. Finally that, in addition, some inputs are shared between zones.

As it will be shown, in these three cases, the final forms of the master problems (solved by the coordinator) are similar. With this respect, only the formulation are proposed in this section, the adaptation of the bundle algorithm seen in chapter 6 are proposed in the next section.

7.4.1 Global power limitation

Consider that a global power limitation holds on the total consumed power of the building, denoted hereafter by p_g (see figure 7.4), namely:

$$p_g \leq \bar{p}_g \quad (7.4.1)$$

where \bar{p}_g is the maximum power consumption of the whole building. In this case, the global constraint 7.4.1 is equivalent to:

$$\sum_{\ell \in \mathbf{Z}} p_\ell \leq \bar{p}_g \quad (7.4.2)$$

Hence, the centralized open-loop optimization problem is given by:

Optimization Problem 7.4.

$$\underset{\mathbf{z}_1, \dots, \mathbf{z}_{n_z}, \mathbf{r}_1, \dots, \mathbf{r}_{n_z}}{\text{Minimize}} \quad \sum_{\ell \in \mathbf{Z}} L_\ell \cdot \mathbf{z}_\ell \quad (7.4.3a)$$

Subject To :

$$\sum_{\ell \in \mathbf{Z}} \mathbf{r}_\ell \leq \bar{\mathbf{p}}_g \quad (7.4.3b)$$

$$\mathbf{A}_\ell \cdot \mathbf{z}_\ell \leq \mathbf{b}_\ell, \quad \ell \in \mathbf{Z} \quad (7.4.3c)$$

$$\underline{\mathbf{e}}_\ell(\mathbf{r}_\ell) \leq \mathbf{A}'_\ell \cdot \mathbf{z}_\ell \leq \bar{\mathbf{e}}_\ell(\mathbf{r}_\ell), \quad \ell \in \mathbf{Z} \quad (7.4.3d)$$

$$\underline{\mathbf{z}}_\ell \leq \mathbf{z}_\ell \leq \bar{\mathbf{z}}_\ell, \quad \ell \in \mathbf{Z} \quad (7.4.3e)$$

which induces the following master problem:

Optimization Problem 7.5. Master problem - global power limitation

$$\underset{\mathbf{r}_1, \dots, \mathbf{r}_{n_z}}{\text{Minimize}} \quad \sum_{\ell \in \mathbf{Z}} J_\ell(\mathbf{r}_\ell) \quad (7.4.4a)$$

Subject To :

$$\sum_{\ell \in \mathbf{Z}} \mathbf{r}_\ell \leq \bar{\mathbf{p}}_g \quad (7.4.4b)$$

Note concerning the constraint (7.4.4b), that an inequality is used instead of an equality to prevent infeasibility in the case where no power limitation holds ($\bar{p}_g = \infty$).

Remark 7.1.

Note that the optimization problem 7.4 can be put in another form. Basically, one can consider that local equality constraints hold on power consumptions by imposing equality constraints instead of power limitation consumption:

$$\mathbf{p}_\ell = \mathbf{r}_\ell \tag{7.4.5}$$

However, since the optimization problem 7.4 is intended to be solved in a distributed fashion, the formulation 7.4 is better. This results from the fact that the local problems 7.3 are less constrained leading to simpler approximations \check{J}_ℓ . \diamond

7.4.2 Global power limitation and shared energy storage

Consider now that, in addition, an electrical storage capability is available. In order to formulate the centralized optimization problem, let us first introduce the battery model.

Electrical battery model

The simplified electrical battery model is given by the following switched system:

$$b^+ = b + \tau \cdot \eta(p_b) \cdot p_b \tag{7.4.6a}$$

with:

$$\eta(p_b) = \begin{cases} \eta^+ & \text{if } p_b \geq 0 \\ 1/\eta^- & \text{if } p_b < 0 \end{cases} \tag{7.4.6b}$$

where:

- p_b is the battery power ($p_b > 0$: charge) ($p_b < 0$: discharge), it is limited in charge and discharge, hence $|p_b| \leq \bar{p}_b$,
- τ is the sampling period,
- $(\eta^+, \eta^-) \in]0, 1]^2$ represent respectively the charge and discharge efficiency of the battery,
- b represents the battery state of charge in [kWh] and is also limited: $\underline{b} \leq b \leq \bar{b}$.

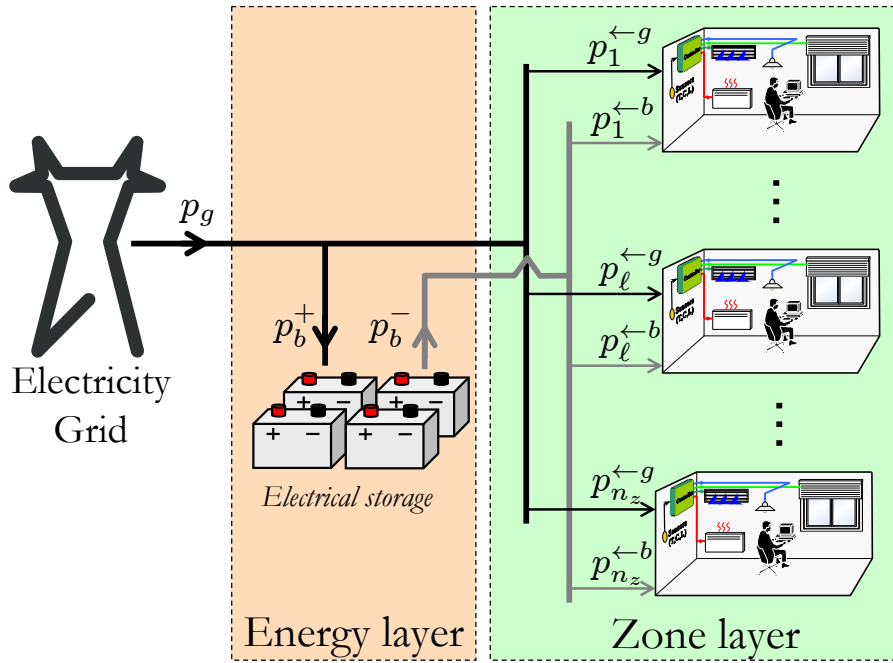


Figure 7.4 Zone layer and Energy layer. Each zone ℓ has access virtually to two power sources $p_\ell^{<g>}$ and $p_\ell^{}$.

To derive the control problem, it is necessary to define an equivalent model of the model (7.4.6) by introducing p_b^+ and p_b^- standing respectively for charge and discharge battery powers:

$$p_b = p_b^+ - p_b^-, \quad p_b^+, p_b^- \geq 0 \quad (7.4.7)$$

Thus, it is possible to state that the battery model defined by (7.4.6) is equivalent to:

$$\begin{cases} b^+ = b + (\tau \cdot \eta^+) \cdot p_b^+ - (\tau/\eta^-) \cdot p_b^- \\ p_b^+ \cdot p_b^- = 0, \quad p_b^+, p_b^- \geq 0 \end{cases} \quad (7.4.8)$$

The constraint $p_b^+ \cdot p_b^- = 0$ means that the battery is either charged or discharged.

Centralized optimization problem

Consider now that one is able to virtually split the power consumption of each zone p_ℓ distinguishing $p_\ell^{<g>}$ which is the amount of power consumed by the zone ℓ from grid and $p_\ell^{}$ which is the amount of power consumed from the battery. One can easily see

that fulfilment of the set of the following linear constraints ensures the respect of the global power constraint (7.4.1) on the building (see figure 7.4).

$$\sum_{\ell=1}^{\ell=n_z} p_{\ell}^{\leftarrow g} + p_b^+ \leq \bar{p}_g \quad (7.4.9a)$$

$$\sum_{\ell=1}^{\ell=n_z} p_{\ell}^{\leftarrow b} = p_b^- \quad (7.4.9b)$$

Note at this step that the energy layer (see figure 7.4) is, from a zone perspective, a resource provider which provides two types of electrical powers:

- Grid power: its predicted tariff profile is given by Γ_g ,
- Battery power: it is provided by the energy layer and its tariff profile is given by $\Gamma_b = \mathbf{0}$.

Defining now zone resources related to each zone ℓ by:

$$r_{\ell} = \begin{bmatrix} r_{\ell}^{\leftarrow g} \\ r_{\ell}^{\leftarrow b} \end{bmatrix} \quad (7.4.10)$$

the centralized optimization problem can be formulated on the following form:

Optimization Problem 7.6. Centralized optimization problem

$$\underset{\mathbf{p}_b^+, \mathbf{p}_b^-, \mathbf{z}_1, \dots, \mathbf{z}_{n_z}, \mathbf{r}_1, \dots, \mathbf{r}_{n_z}}{\text{Minimize}} \quad \Gamma_g \cdot \mathbf{p}_b^+ + \sum_{\ell \in \mathbf{Z}} \mathbf{L}_{\ell} \cdot \mathbf{z}_{\ell} \quad (7.4.11a)$$

Subject To :

$$\underline{\mathbf{b}} - b_0 \leq \tau \cdot \eta^+ \cdot \Phi_e \cdot \mathbf{p}_b^+ + \frac{\tau}{\eta^-} \cdot \Phi_e \cdot \mathbf{p}_b^- \leq \bar{\mathbf{b}} - b_0 \quad (7.4.11b)$$

$$\mathbf{0} \leq \mathbf{p}_b^+, \mathbf{p}_b^- \leq \bar{\mathbf{p}}_b \quad (7.4.11c)$$

$$\mathbf{p}_b^+ \odot \mathbf{p}_b^- = \mathbf{0} \quad (7.4.11d)$$

$$\sum_{\ell \in \mathbf{Z}} \mathbf{r}_{\ell}^{\leftarrow g} + \mathbf{p}_b^+ \leq \bar{\mathbf{p}}_g \quad (7.4.11e)$$

$$\sum_{\ell \in \mathbf{Z}} \mathbf{r}_{\ell}^{\leftarrow b} = \mathbf{p}_b^- \quad (7.4.11f)$$

$$\mathbf{A}_{\ell} \cdot \mathbf{z}_{\ell} \leq \mathbf{b}_{\ell}, \quad \ell \in \mathbf{Z} \quad (7.4.11g)$$

$$\underline{\mathbf{z}}_{\ell} \leq \mathbf{z}_{\ell} \leq \bar{\mathbf{z}}_{\ell}, \quad \ell \in \mathbf{Z} \quad (7.4.11h)$$

$$\underline{\mathbf{e}}_{\ell}(\mathbf{r}_{\ell}) \leq \mathbf{A}'_{\ell} \cdot \mathbf{z}_{\ell} \leq \bar{\mathbf{e}}_{\ell}(\mathbf{r}_{\ell}), \quad \ell \in \mathbf{Z} \quad (7.4.11i)$$

where:

- b_0 is initial state of charge of the battery at the current decision instant,
- \odot is the element-wise product,
- $\Phi_e \in \mathbb{R}^{N \times N}$ is a triangular matrix given by:

$$\Phi_e := \begin{bmatrix} 1 & 0 & 0 & \dots & 0 \\ 1 & 1 & 0 & \dots & 0 \\ \vdots & \dots & \dots & \dots & \dots \\ 1 & 1 & 1 & \dots & 1 \end{bmatrix} \quad (7.4.12)$$

- Note that the equality (7.4.11f) implies that the whole discharged power will be used by the zones. Namely imposing the inequality (7.4.11f) is sufficient to impose the relation:

$$\sum_{\ell \in \mathbf{Z}} \mathbf{r}_\ell^{\leftarrow b} = \mathbf{p}_b^- \Rightarrow \sum_{\ell \in \mathbf{Z}} \mathbf{p}_\ell^{\leftarrow b} = \mathbf{p}_b^- \quad (7.4.13)$$

which basically means that there is no reason to discharge the battery if the discharged power is not consumed.

Notice that the optimization problem 7.6 is not an LP due the presence of the product terms (7.4.11d), meaning that the battery can not be charged and discharged simultaneously.

Actually, even if not imposed, the constraint (7.4.11d) is always fulfilled provided that charging and discharging the battery simultaneously is never interesting when minimizing an economical objective is involved (one can refer to [Mattingley et al. 2010] for a simple example). This last property is of great importance since it enables to consider the system (7.4.6) as a simple linear system with two inputs p_b^+ , p_b^- in which it is not mandatory to consider explicitly the switched property of the system.

Hence, the master problem in this case is the following LP where the constraint (7.4.11d) does not appear in the optimization problem 7.7 as it has been explained before:

Optimization Problem 7.7. Master problem - pow. limit and battery management

$$\underset{\mathbf{p}_b^+, \mathbf{p}_b^-, \mathbf{r}_1, \dots, \mathbf{r}_{n_z}}{\text{Minimize}} \quad \Gamma_g \cdot \mathbf{p}_b^+ + \sum_{\ell \in \mathbf{Z}} J_\ell(\mathbf{r}_\ell) \quad (7.4.14a)$$

Subject To :

$$\underline{\mathbf{b}} - b_0 \leq \tau \cdot \eta^+ \cdot \Phi_e \cdot \mathbf{p}_b^+ - \frac{\tau}{\eta^-} \cdot \Phi_e \cdot \mathbf{p}_b^- \leq \bar{\mathbf{b}} - b_0 \quad (7.4.14b)$$

$$\mathbf{0} \leq \mathbf{p}_b^+, \mathbf{p}_b^- \leq \bar{\mathbf{p}}_b \quad (7.4.14c)$$

$$\sum_{\ell \in \mathbf{Z}} \mathbf{r}_\ell^{\leftarrow g} + \mathbf{p}_b^+ \leq \bar{\mathbf{p}}_g \quad (7.4.14d)$$

$$\sum_{\ell \in \mathbf{Z}} \mathbf{r}_\ell^{\leftarrow b} = \mathbf{p}_b^- \quad (7.4.14e)$$

7.4.3 Global power limitation, shared energy storage and shared inputs

Suppose that some shared inputs between zones exist. Namely, some centralized actuator(s) has an impact on some subset(s) of zones. Each element of $r^{\text{eq}} \in \mathbb{R}^{n_{sh}}$ represents a shared actuator. Let us note the power consumption of the total shared actuators by p_e :

$$\mathbf{p}_e := \mathbf{E}_e \cdot \mathbf{r}^{\text{eq}} \quad (7.4.15)$$

where \mathbf{E}_e groups the maximal power consumption of the shared actuators (similarly to \mathbf{E}_ℓ in the zone). In this case:

$$\mathbf{p}_e = \mathbf{p}_e^{\leftarrow b} + \mathbf{p}_e^{\leftarrow g} \quad (7.4.16)$$

where $\mathbf{p}_e^{\leftarrow g}$ and $\mathbf{p}_e^{\leftarrow b}$ are respectively the parts of power consumed from grid and from battery by the shared actuators.

Recalling the explanations concerning local constraints (see subsection 7.3.3) and that:

$$r_\ell = \begin{bmatrix} r_\ell^{\leftarrow g} \\ r_\ell^{\leftarrow b} \\ r_\ell^{\text{eq}} \end{bmatrix} \quad (7.4.17)$$

deduction of the master problem is straightforward by considering that these actuators are managed by the coordinator.

Optimization Problem 7.8.

$$\underset{\mathbf{p}_b^+, \mathbf{p}_b^-, \mathbf{r}_1, \dots, \mathbf{r}_{n_z}}{\text{Minimize}} \quad \Gamma_g \cdot \mathbf{p}_b^+ + \sum_{\ell \in \mathbf{Z}} J_\ell(\mathbf{r}_\ell) \quad (7.4.18a)$$

Subject To :

$$\underline{\mathbf{b}} - b_0 \leq \tau \cdot \eta^+ \cdot \Phi_e \cdot \mathbf{p}_b^+ - \frac{\tau}{\eta^-} \cdot \Phi_e \cdot \mathbf{p}_b^- \leq \bar{\mathbf{b}} - b_0 \quad (7.4.18b)$$

$$\mathbf{p}_e^{\leftarrow g} + \mathbf{p}_e^{\leftarrow b} = \mathbf{E} \cdot \mathbf{p}_e \quad (7.4.18c)$$

$$\mathbf{0} \leq \mathbf{p}_b^+, \mathbf{p}_b^- \leq \bar{\mathbf{p}}_b \quad (7.4.18d)$$

$$\sum_{\ell \in \mathbf{Z}} \mathbf{r}_\ell^{\leftarrow g} + \mathbf{p}_b^+ + \mathbf{p}_e^{\leftarrow g} \leq \bar{\mathbf{p}}_g \quad (7.4.18e)$$

$$\sum_{\ell \in \mathbf{Z}} \mathbf{r}_\ell^{\leftarrow b} + \mathbf{p}_e^{\leftarrow b} \leq \mathbf{p}_b^- \quad (7.4.18f)$$

Note that the shared actuators do not appear explicitly in the minimization arguments of the problem 7.8 since they are included in local resources $\mathbf{r}_\ell^{\text{eq}}$ related to each zone (see relation (7.4.17)).

Remark 7.2.

Following the same guidelines presented in the section. It can be also shown that the scheme can be extended to handle local energy production. \diamond

7.5 Distributed Model Predictive Control

In this section, the coordination mechanism presented in chapter 6 is tailored to the present application. As discussed in section 7.4, the centralized optimization problem reduces to:

Optimization Problem 7.9. Master problem

$$\underset{\mathbf{z}_e, \mathbf{r}}{\text{Minimize}} \quad \mathbf{L}_e \cdot \mathbf{z}_e + \sum_{\ell \in \mathbf{Z}} J_\ell(\mathbf{r}_\ell) \quad (7.5.1a)$$

Subject To :

$$\mathbf{A}_e \cdot \mathbf{z}_e + \sum_{\ell \in \mathbf{Z}} \mathbf{D}_\ell \cdot \mathbf{r}_\ell \leq \mathbf{b}_e \quad (7.5.1b)$$

$$\mathbf{0} \leq \mathbf{r}_\ell^{\text{up}} \leq \bar{\mathbf{p}}_\ell, \ell \in \mathbf{Z} \quad (7.5.1c)$$

$$\mathbf{0} \leq \mathbf{r}^{\text{eq}} \leq \mathbf{1} \quad (7.5.1d)$$

where:

- The vector of variables \mathbf{z}_e gathers all the variables related to the energy layer,

- The matrices $\mathbf{A}_e, \mathbf{b}_e, \{\mathbf{D}_\ell\}_{\ell \in \mathbf{Z}}$ can be easily defined (see optimization problem 7.8).

To sum-up, in the optimization problem 7.9:

- The first constraint (7.5.1b) is the power coupling constraint,
- The constraints (7.5.1c) and (7.5.1d) are introduced in order to:
 - a. Ensure the feasibility of the local subproblems 7.3 by explicitly imposing positiveness of maximal limitations on zones powers (which is actually the assumption on availability of feasibility sets $\mathcal{F}_{\ell,k}$ (assumption 6.2);
 - b. Reduce the search domain by imposing explicitly that resource cannot exceed the amount of power that the zone can consume.

In the sequel, the master problem 7.9 is shortly denoted as follows:

Optimization Problem 7.10. Master problem

$$\underset{(\mathbf{z}_e, \mathbf{r}) \in \mathcal{D}}{\text{Minimize}} \quad J := \left[J_E(\mathbf{z}_e) + \sum_{\ell \in \mathbf{Z}} J_\ell(\mathbf{r}_\ell) \right] \quad (7.5.2)$$

The expression $(\mathbf{z}_e, \mathbf{r}) \in \mathcal{D}$ indicates the fulfilment of the constraints (7.5.1b)-(7.5.1d).

7.5.1 Solving the master problem

As discussed in chapter 6, in bundle method the function to be minimized is approximated by a cutting plane model, here the objective function J is separable since:

$$J = J_E + \sum_{\ell \in \mathbf{Z}} J_\ell \quad (7.5.3)$$

It is important to highlight that only the unknown functions $\{\check{J}_\ell\}_{\ell \in \mathbf{Z}}$ need to be approximated given that the function J_E is perfectly known at the master level.

Thus, at each iteration s of the bundle algorithm (chapter 6) the approximation $\check{J}^{(s)}$ can be obtained by summing all contributions:

$$\check{J}^{(s)}(\mathbf{z}_e, \mathbf{r}) := J_E(\mathbf{z}_e) + \sum_{\ell \in \mathbf{Z}} \check{J}_\ell^{(s)}(\mathbf{r}_\ell) \quad (7.5.4)$$

resulting in the following stabilized optimization problem:

Optimization Problem 7.11. Stabilized master problem

$$\underset{(\mathbf{z}_e, \mathbf{r}_1, \dots, \mathbf{r}_{n_z}) \in \mathcal{D}}{\text{Minimize}} \quad [\check{J}^{(s)}(\mathbf{z}_e, \mathbf{r}) + D^{\gamma^{(s)}}(\mathbf{r} - \bar{\mathbf{r}}^{(s)})] \quad (7.5.5)$$

The stabilization function $D^{\gamma^{(s)}}$ is defined hereafter.

7.5.2 The stabilization term

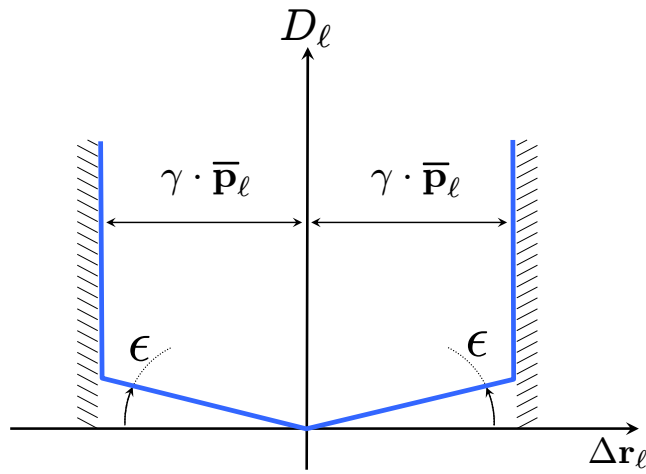


Figure 7.5 Stabilization term ($\Delta \mathbf{r}_\ell = \mathbf{r}_\ell - \bar{\mathbf{r}}_\ell^{(s)}$).

Recall that the stabilization term $D^{\gamma^{(s)}}(\mathbf{r} - \bar{\mathbf{r}}^{(s)})$ is introduced in order to prevent *drastic* variation from the current stability center $\bar{\mathbf{r}}^{(s)}$ which is the best known solution at iteration s . The stabilization term $D^{\gamma^{(s)}}(\mathbf{r} - \bar{\mathbf{r}}^{(s)})$ used in the sequel is chosen of the following form:

$$D^{\gamma^{(s)}}(\mathbf{r} - \bar{\mathbf{r}}^{(s)}) := \sum_{\ell \in \mathbf{Z}} D_\ell^\gamma(\mathbf{r}_\ell - \bar{\mathbf{r}}_\ell^{(s)}) \quad (7.5.6)$$

where each profile $\bar{\mathbf{r}}_\ell^{(s)}$ designates the part of the stability center corresponding to the zone $\ell \in \mathbf{Z}$. Namely:

$$\bar{\mathbf{r}}^{(s)} = \begin{bmatrix} \bar{\mathbf{r}}_1^{(s)} \\ \vdots \\ \bar{\mathbf{r}}_{N_s}^{(s)} \end{bmatrix} \quad (7.5.7)$$

Here, a *stabilized* trust region is used (see figure 7.5). The benefit of such distance measure lies in the fact that the stabilized master problem 7.11 remains a linear programming problem which is not the case for general proximal bundle methods based on quadratic stabilization term leading to QPs which are more computationally demanding especially if the size of the problem is quite large.

The parameter $\epsilon > 0$ (see figure 7.5) is fixed a priori but needs to be chosen small enough to ensure good performance of the scheme (see [Frangioni 2002]).

The trust region parameter $\gamma^{(s)} \in [\underline{\gamma}, \bar{\gamma}]$ is updated at each iteration s . Notice that the two thresholds $\underline{\gamma}$ and $\bar{\gamma}$ designate respectively minimum and maximum movement from the current stability center relatively to the maximum value that r_ℓ can take.

Remark 7.3.

Stabilization terms related to \mathbf{r}^{eq} are similar to those presented here except that their maximum values is always 1 (normalized control inputs on actuators). ◇

Finally, the coordination mechanism is summarized on figure 7.6 (page 152).

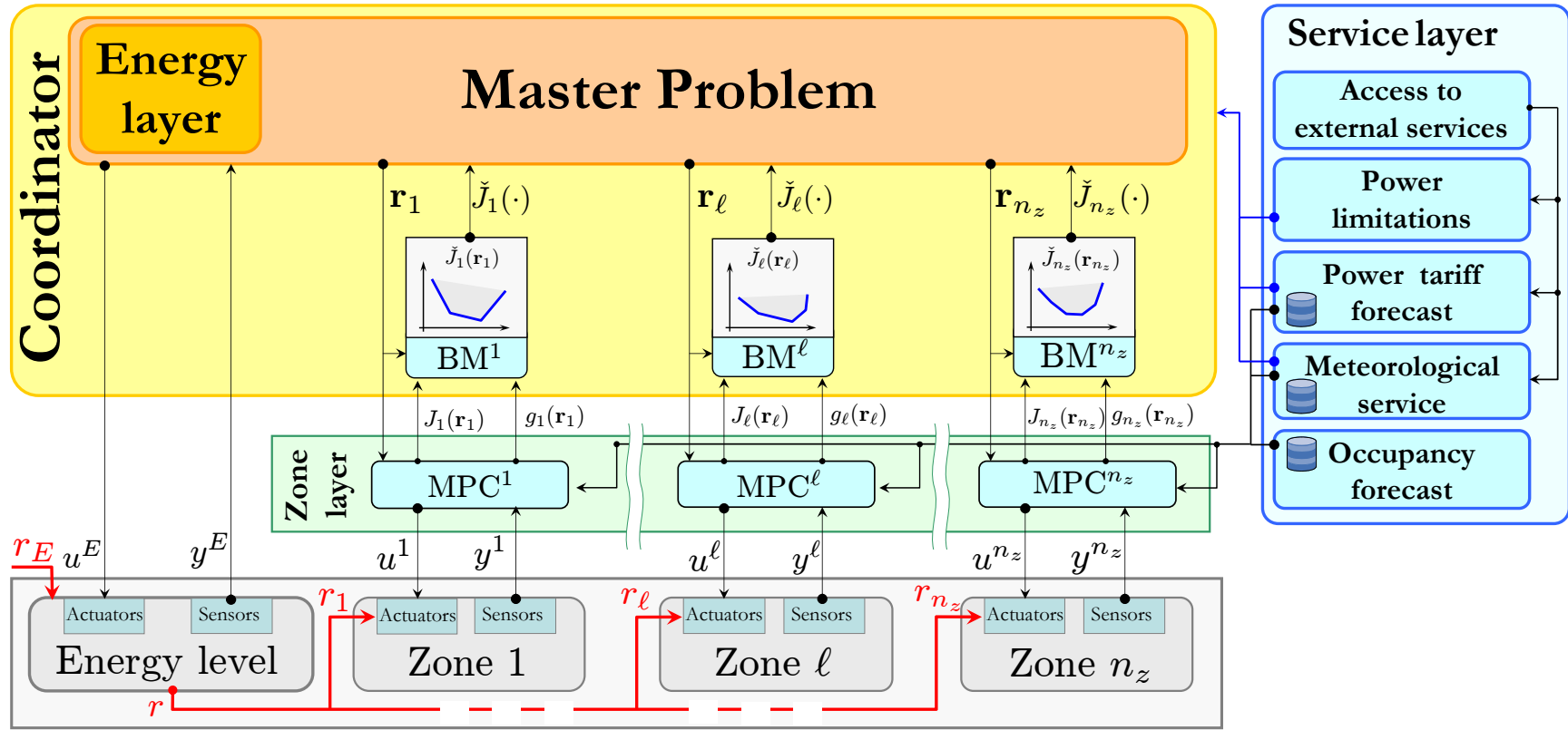


Figure 7.6 Illustration of the coordination mechanism in the building. Each $MPC_{\ell \in Z}$ aims to minimize its local objective given some restrictions r_ℓ on power consumption. The coordinator gathers sub-gradients $g_{\ell \in Z}$ and functions values $J_{\ell \in Z}$ to solve the master problem by forming $\check{J}(\cdot)$ and resend new resources restriction $r_{\ell \in Z}$, and so on until convergence.

Remark 7.4.

Note that, since a trust region is employed, the master problem 7.11 may become infeasible if starting from a non feasible initial solution. Moreover, starting from a feasible initial solution ensures the successive feasibility of the problems 7.11 which is crucial. Note also that this fact is not linked to the feasibility of the centralized problem, which is always feasible. \diamond

7.6 Assessment of the bundle method

In this section, a numerical study of the bundle algorithm is proposed. Here, one is only interested in solving one given optimization problem at a fixed decision instant. In order to assess the proposed solution, the four algorithms (or variants) discussed previously in chapter 6 (see remark 6.5) are compared:

1. *Disaggregated* bundle method,
2. *Aggregated* bundle method,
3. Cutting plane algorithm with (*disaggregated model*),
4. Cutting plane algorithm with (*aggregated model*),

Assessment approach

In the following case study, a 20-zone building is submitted to a power limitation \bar{p}_g and equipped with an electrical battery. The electricity rate is time varying. Let us introduce the sub-optimality (S-O) measure:

$$\text{S-O}[\%] := 100 \cdot \frac{J - J^*}{J^*}, \quad \text{where: } J^* \text{ is the optimal function value} \quad (7.6.1)$$

which simply indicates the gap between the current best function value obtained by the algorithm at the current iterate and the real optimal value (J^*), computed by solving the centralized optimization problem.

In this case study, the prediction horizon is 24 hours. As a parametrization of the inputs trajectory is implemented with $N_{par}^u = 20$, $\mathbf{r} \in \mathbb{R}^{2880}$, $\mathbf{r}_\ell \in \mathbb{R}^{144}$ (see section 4.7 in chapter 4 for explanations on the parametrization used in this work). In this case the centralized optimization problem is an LP with ≈ 22000 decision variables and ≈ 16000 constraints.

The algorithms are assessed on increasingly *difficult* problems. This is achieved by decreasing the power limitation \bar{p}_g . In this case study, $\bar{p}_g \in \{40, 35, 25, 20\} [kW]$.

Note that, the more \bar{p}_g is reduced, the more difficult is the problem. The results are reported on figure 7.7.

Discussion

- (a) $\bar{p}_g = 40$: note in this case that the four methods present quite similar results even if the pure cutting plane algorithm with aggregated model is slower and does not converge to optimal solution (S-O \approx 0.5 %),
- (b) $\bar{p}_g = 35$: in this case the bundle algorithm (the two variants) outperform the pure cutting plane techniques. Moreover, the disaggregated version of the cutting plane algorithm is much more effective. However, aggregation in the case of the bundle method does not improve performance.
- (c) $\bar{p}_g = 25$: the pure cutting plane algorithm fails to achieve the optimal solution (S-O \approx 20% after 150 iterations). Note that the bundle algorithm achieves the optimal solution after 20 iterations for disaggregated version and 35 iterations in the aggregated one.
- (d) $\bar{p}_g = 20$: cutting plane methods are totally ineffective when the problem becomes much more constrained. With disaggregated bundle method, the optimal solution is achieved after approximatively 50 iterations.

The results show clearly that the bundle algorithm outperforms classical cutting plane techniques. It has to be noticed that disaggregation enhances considerably the performance of schemes. In the following section, closed-loop simulation are performed.

7.7 Simulations

In this section some simulations are performed to illustrate the proposed DMPC strategy.

7.7.1 Battery management and global power limitation

In this section, a 48 hours simulation is performed on a 20-zone building. The zones are equipped with electrical heaters. The capacity of the battery is 10 [kWh] ($0 \leq b \leq 10$), its efficiency $\eta^+ = \eta^- = 0.9$, its maximal charge and discharge power $p_b \leq 5$ [kW]. The maximal total power allowed to the building is $\bar{p}_g = 25$ [kW]. Moreover, electricity

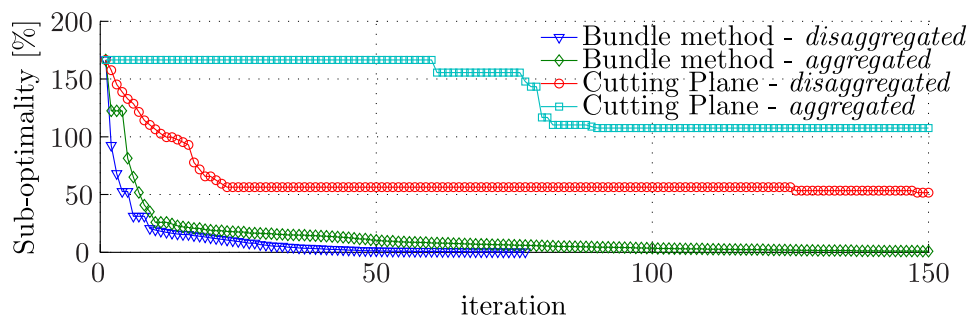
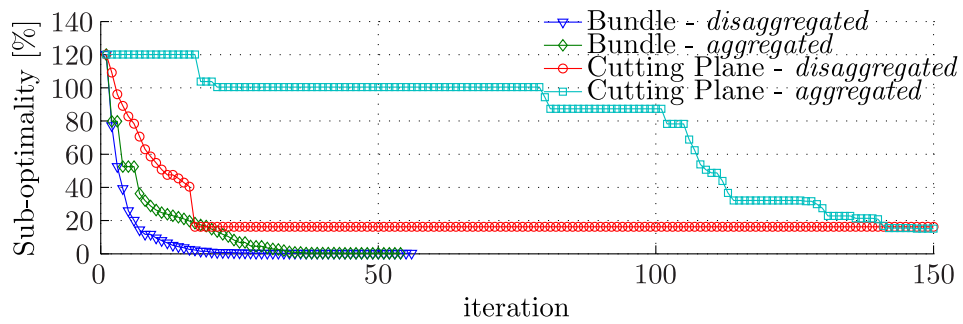
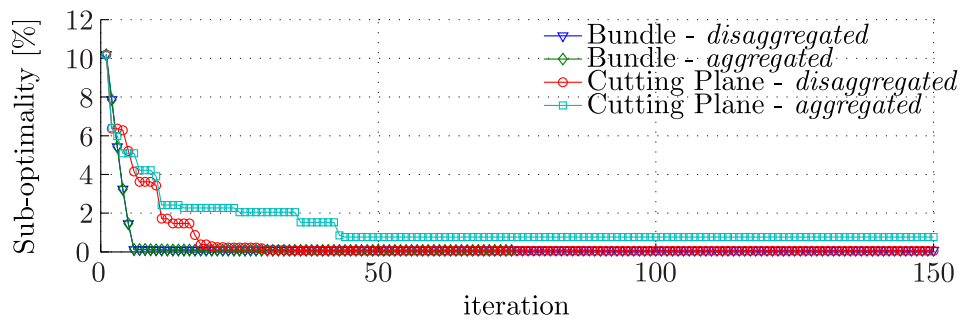
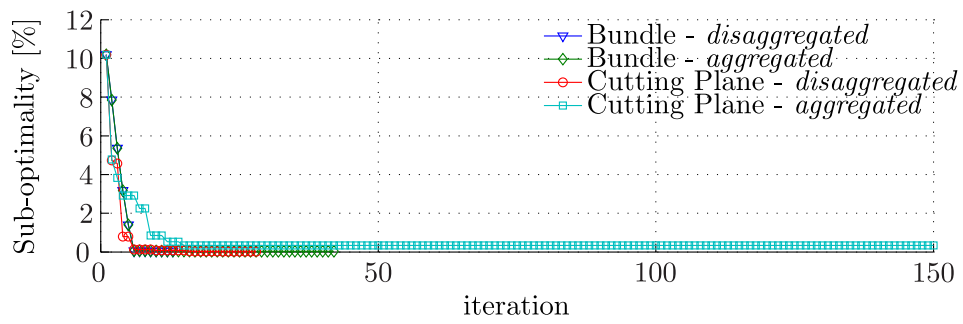


Figure 7.7 Illustration of the bundle algorithm effectiveness for increasingly constrained optimization problems.

tariff is time varying, during on-peak hours (6 a.m. → 10 p.m) its cost is 11.54 c€, during off-peak hours its cost is 6.66 c€. The prediction horizon is 12 hours and the control refreshing period is 5 minutes. Moreover, all the zone occupancy profiles are perfectly known and identical.

First, let us investigate the effect of introducing the distributed-in-time feature memory feature (section 6.5). Recall that this basically consists of keeping a certain amount of the past information from one decision instant to the other. The results are shown on figure 7.8. Notice, that the introduction of memory clearly enables a faster decrease of the cost function. For instance, 5 iterations with memory enables nearly the same performances as with 15 iterations without memory in terms of cost function decrease. Nevertheless, in this case even if the decrease is faster, the closed performances are quasi similar for all these configurations concerning invoice as well as comfort requirements.

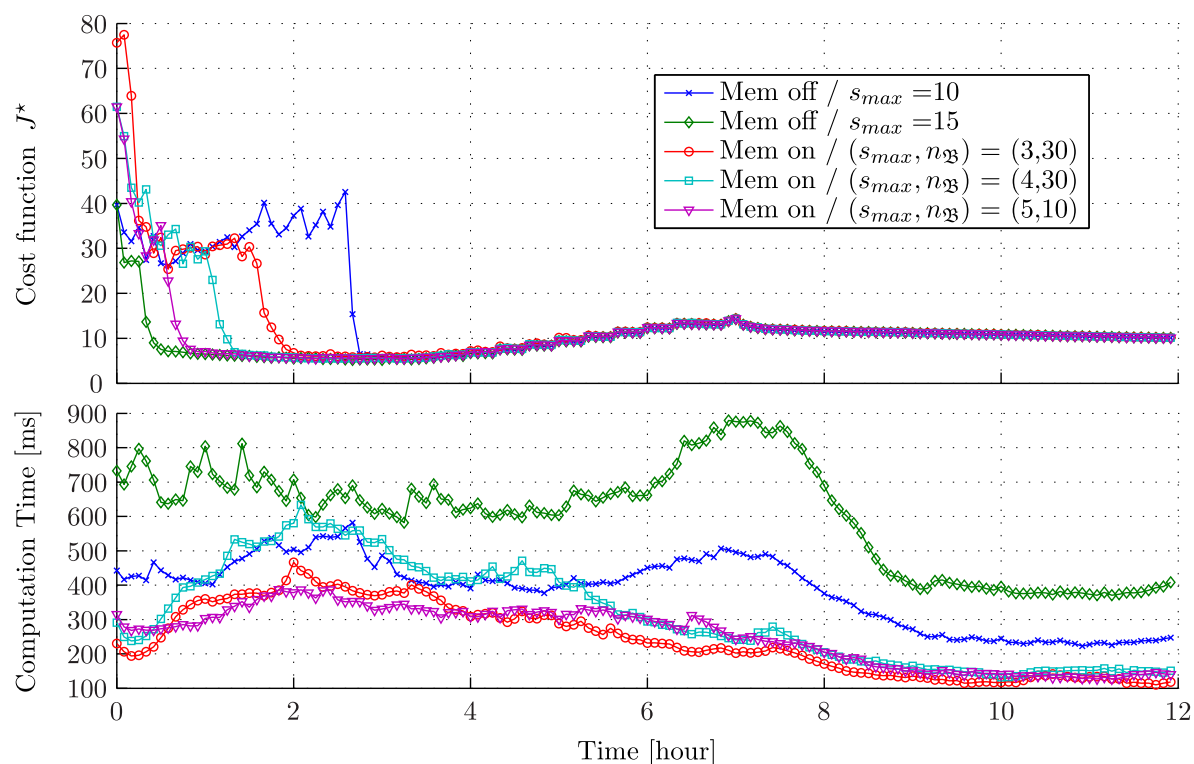


Figure 7.8 Comparison of performance of the DMPC algorithm with and without distributed-in-time feature during the first 12 [h]: in the presented case study, this enables to reduce the computational time by more than 60 % for quite similar performances in terms of cost function decrease. The mean computational time of the centralized solution is in this case 1.23[s].

Figure 7.9 (page 158) shows the simulation results obtained for this scenario when

the number of allowed iterations is 3 ($s_{max} = 3$). Notice that:

- The first sub-plot shows the global consumption of the building which never exceeds the maximum allowed level (25 [kWh]). This limit is obviously respected since it is explicitly imposed.
- On the second sub-plot, it can be noticed that the battery is used as an energetic buffer, storing energy during off-peak periods (red surface) in order to give it back to the zones during on-peak periods (blue surface). It can also be noticed that the battery charging is always performed before zones consumption is started (sub-plot 3) -this is clearer on the second day-, this is because an energy storage is also performed in the zones. Nevertheless, given heat losses in the zones, it is more beneficial to start storing heat in the zone after storing it in the battery (optimal start like behavior).
- Note that some zones are much more preheated than others (see the grey and dark blue temperature curves). This behavior results from the optimal power dispatch performed by the coordinator. Indeed, much more heat is stored in the zones dissipating less energy (see temperatures decreases during the night).
- The fourth sub-plot shows temperatures of the zones in the buildings⁶, note that the upper and lower limits (20 [°C]/24 [°C]) during the occupied period are respected. Note however that the anticipative effect of MPC is clear since the zones are preheated before occupied hours in order to reach the desired temperature.

Figure 7.10 (page 159) shows the simulation results obtained when applying a centralized control (optimal solution). Notice that the behavior is basically similar (one can note for instance that the preheated zones are the same ones in the two cases).

⁶CO₂ level and indoor lighting have been omitted since the main interest here is related to temperature, nevertheless CO₂ and lighting constraints are also respected.

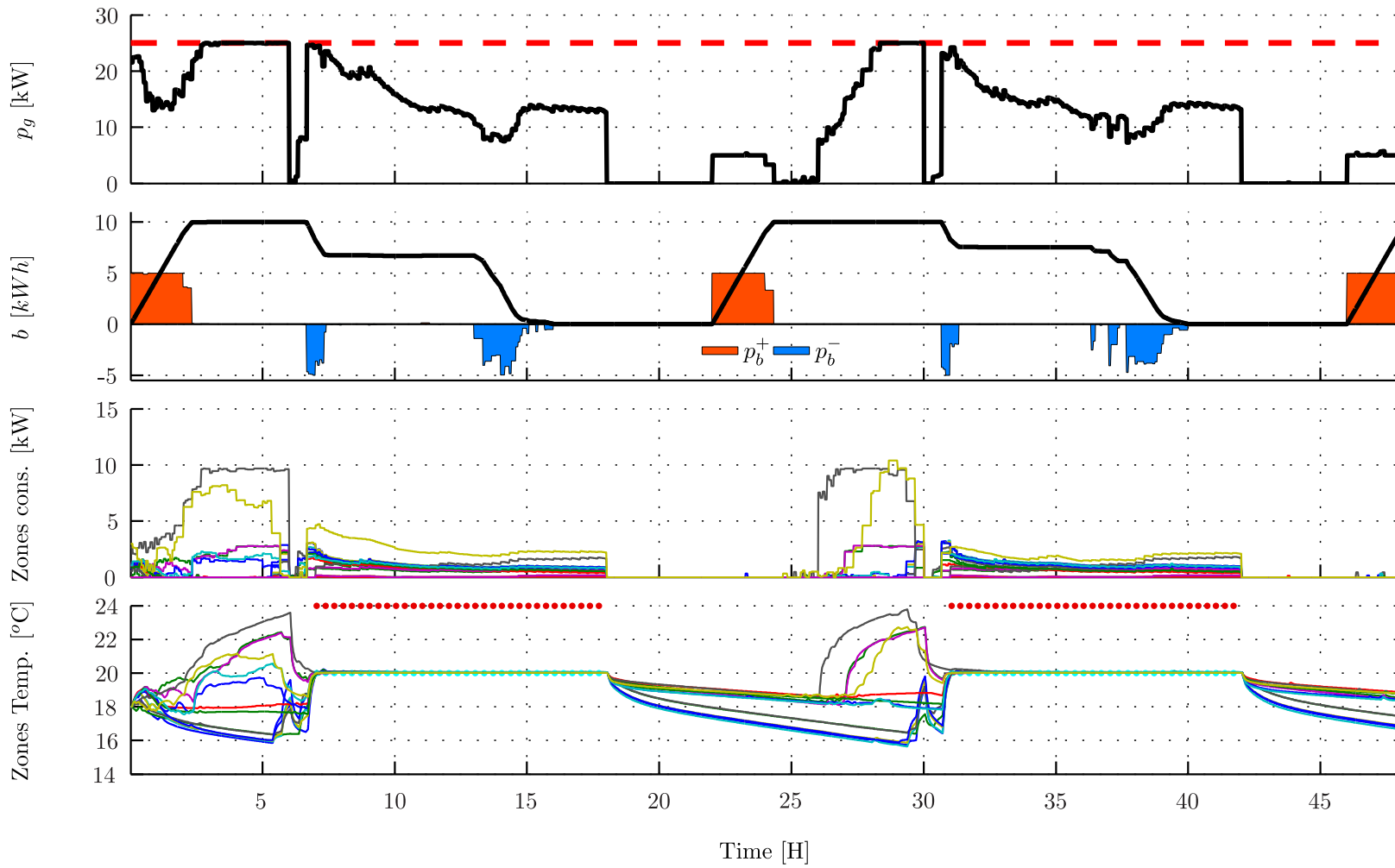


Figure 7.9 DMPC ($s_{max} = 3$ iterations with memory) with battery management and power limitation for a 20 zones building. Note that the closed-loop profiles are slightly different from those obtained with a centralized control (figure 7.10). However, invoice and comfort are quasi-similar.

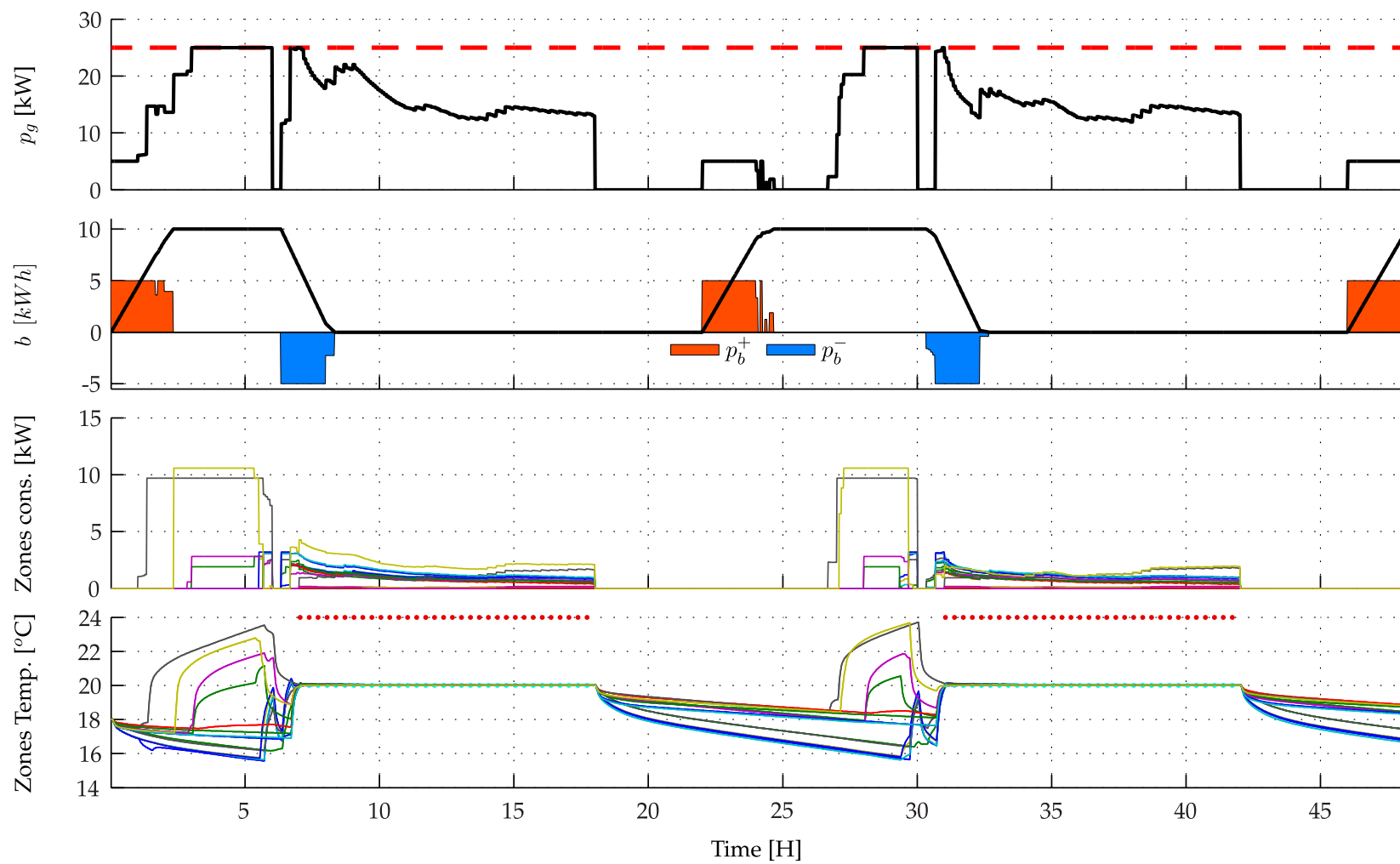


Figure 7.10 Centralized control with battery management and power limitation on a 20-zone building. These results have to be compared with those obtained using the DMPC algorithm (figure 7.9)

7.7.2 Computational time

Figure 7.11 shows the computational time required by the coordinator and the zones for 3 iterations and $n_{\text{zb}} = 30$ (number of elements stored in each bundle). Notice that the average time spent by the coordinator (for all iterations) T_c^C is 100 [ms]. Moreover, it appears that most of the time is spent solving the master problem (coordinator). The total computation time is equal to $T_c^C + \max(T_c^Z)$ (since the zones compute their respective optimal solutions in parallel) is in average equal to 149 [ms]. Note that the computational time is negligible compared to the refreshing period (5 min.) enabling real-time implementability even for a far higher number of zones in the building.

Remark 7.5.

Solving the centralized problem, in this case (20 zones), takes in average 1.23 [s] using CPLEX and 4.5[s] using GLPK. The linear programming Matlab solver (simplex) failed in all cases after few tens of seconds and is inefficient for this kind of problems. Moreover, as it has been noted in [Moroşan et al. 2011], the solver performance largely determines the computational load and reliability of the centralized solution. Increasing the number of zones to 40, the computational time of CPLEX is in average equal to 20[s] and GLPK fails to achieve the optimal solution after more than 2 minutes. When increasing, the number of zones to 100, it becomes difficult even for CPLEX to find a solution. This takes approximately one minute and crashes after few time steps due to memory problems (that may be related also to the interface between CPLEX and Matlab). ◇

7.7.3 Handling shared variables

In this case, one considers that there exists a shared actuator in the building. Here, a single actuator in the whole building is assumed available for ventilation. Namely, one considers that zones dumpers responsible for adjusting the airflow injected in each zone are not available and that only a global airflow supply in the whole building exists. This is illustrated on figure 7.12.

Moreover, the price signal is time varying (see the first subplot, figure 7.13), it is assumed known in advance. Moreover a power limitation on the whole building exists. The results are presented on figure 7.13), note that in this case (as it was the case previously) the closed-loop performances are quasi-similar when using a centralized control or a distributed approach (similarly to the first case study).

Notice that the most pertinent behavior that has to be underlined is that the ventilation is adjusted to meet CO₂ requirements on all the zones of the building (see subplot 6 figure 7.13).

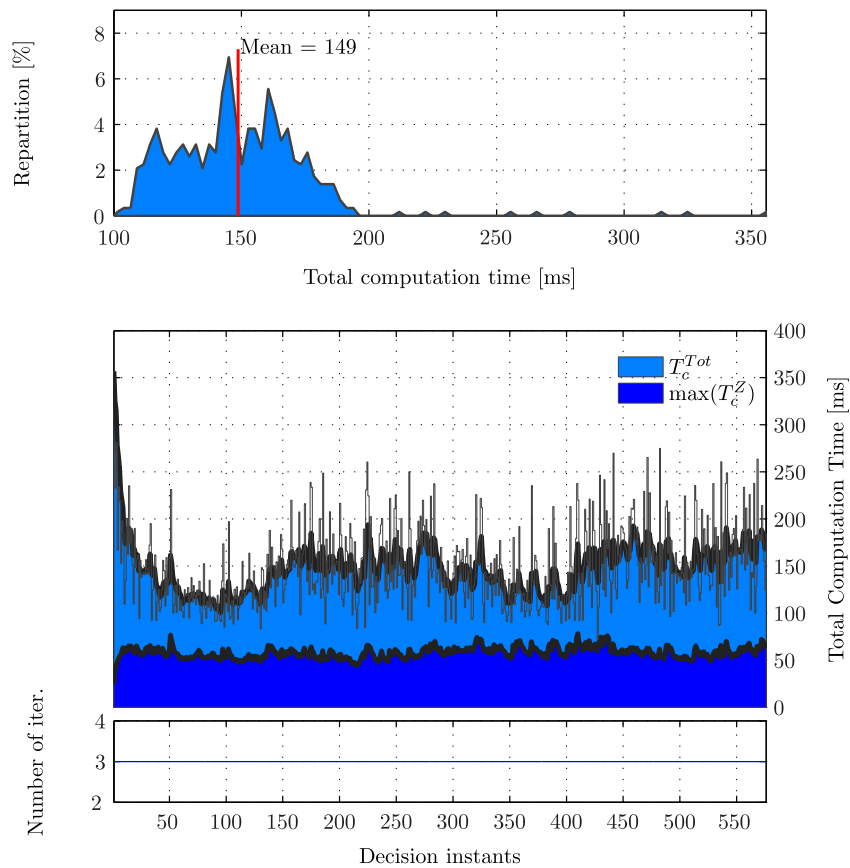


Figure 7.11 Computation time. Results obtained on an Intel® Core™ i7 CPU X920 @ 2.00 GHz, 3.23 Go RAM. ILOG CPLEX 12.1 solver was used.

7.7.4 Introducing uncertainty

In this last simulation, a weekly simulation is performed in a quite more realistic case, it is assumed that:

- Zone occupancy profiles are different from one zone to the other and moreover only occupancy schedules are available (the number of occupants is unknown).
- Energy tariff is time-varying (off-peak, on-peak periods).
- Weather is uncertain. Uncertainty is introduced using the mechanism described in section 4.9.4.
- Power limitation is set to 20 [kW] (5 [kW] less than the first case study).

One is interested in comparing the performances of DMPC scheme with and without introducing the memory mechanism (see section 6.5 for a description of

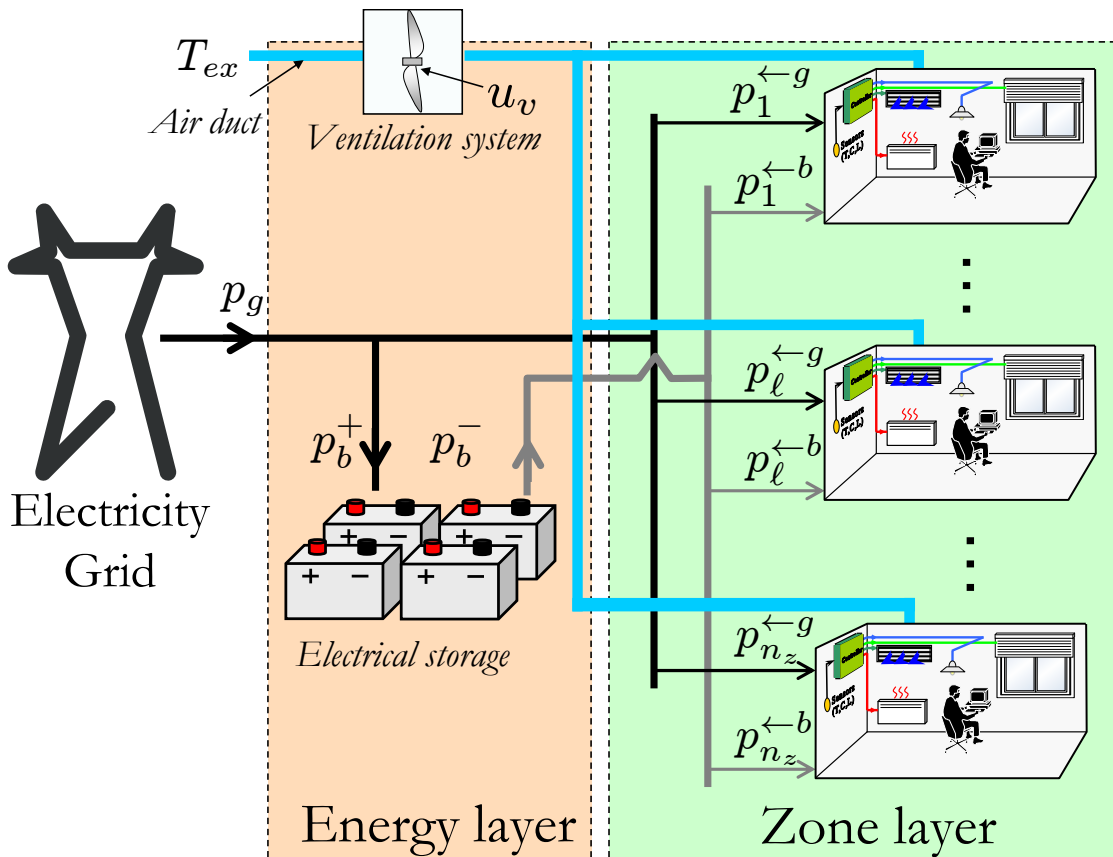


Figure 7.12 Handling shared actuators between zones with DMPC. The ventilation system impacts all the zones simultaneously, therefore its management should take into account all the zones needs in terms of fresh air. The simulation results are reported in figure 7.13

the distributed-in-time optimization) for different maximum number of iterations $s_{max} \in \{1, 3, 5, 10, 20\}$. The maximum number of elements of the bundle is constant in all cases $n_{\text{sg}} = 30$.

The closed-loop performances are presented on figure 7.14. Namely, the invoice (figure 7.14.(a)), the thermal constraint violation (TCV [$^{\circ}\text{C}\cdot\text{h}$]) on figure 7.14.(b) (which is the integral over time over all zones of thermal constraint violation) as well as the illuminance constraint violation (LCV [$\text{Lux}\cdot\text{h}$]) on figure 7.14.(c). Concerning the CO_2 level constraint violation, it is not presented as the results were quite similar in all cases (the constraint is very rarely violated in all the cases). The red curves represents the results obtained with a centralized control (optimal) which is the baseline.

Note first that introducing memory clearly enhances the performance of the scheme. Actually, in all the cases, except for $s_{max} = 1$, the invoice is lower and the constraints especially on lighting are much less violated. Concerning the thermal

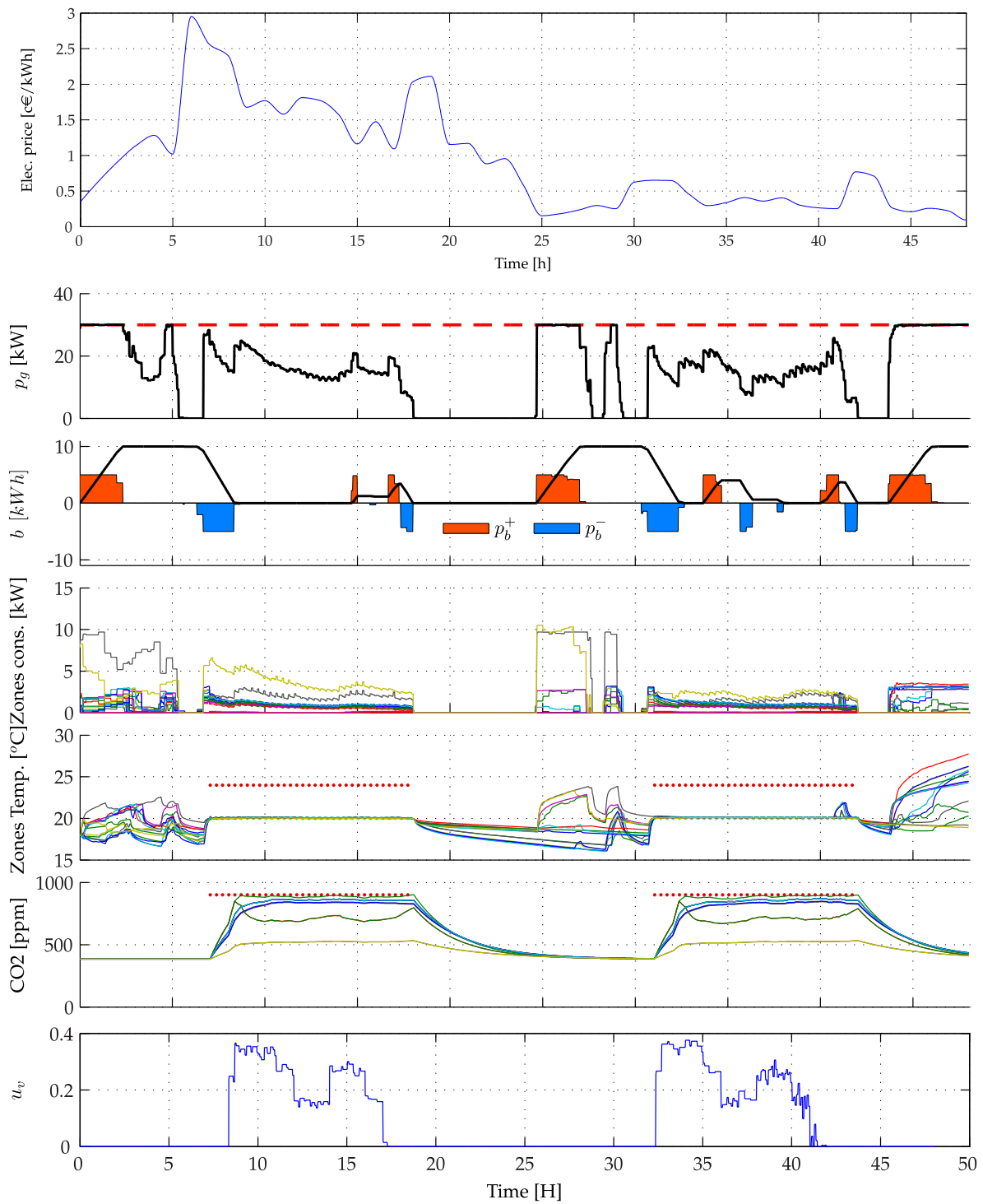


Figure 7.13 DMPC with a shared input actuator. Notice that the CO_2 level is decreased in some zones to meet the requirements on other zones (since a unique actuator affects the whole zones). Notice also that the battery is basically used to store energy during low price periods in order to redistribute it to the zones when energy price is higher.

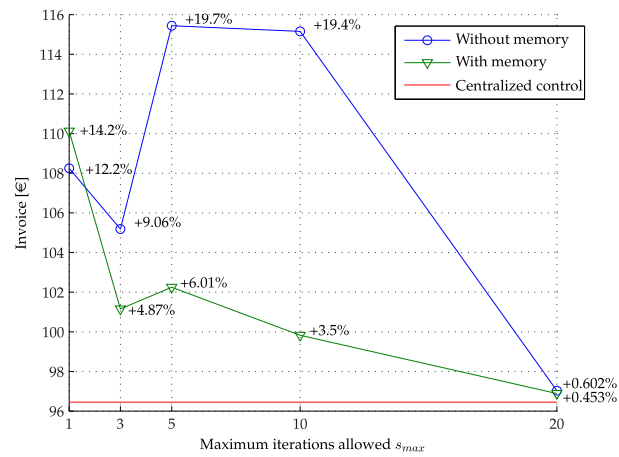
constraint violation (figure 7.14.(b)), note that it is less violated than the case in which a centralized solution is applied. Actually, this is explained by the fact that thermal violations are very small in all cases (TCV=1 [$^{\circ}\text{C}\cdot\text{h}$] implies that a mean temperature constraint violation of 0.01 [$^{\circ}\text{C}$] is observed in the each zone), which simply means that in all cases the temperature is rarely violated in average.

Hence, increasing the number of iterations may lead, if no memory mechanism is implemented, to worst results from the energetic point of view. This is to reduce in this case the constraint violation on indoor illuminance. Note that rather similar performances are achieved with 20 iterations. Nevertheless, introducing a memory mechanism enables in this case better performances as for the same number of allowed iterations, the scheme performance is better. This illustrates the fact that limiting the number of iterations would lead to undesirable behavior and that introducing memory prevents, in this case, this behavior. Note finally that, even for very low allowed number of iterations, the scheme still exhibits fairly good performance.

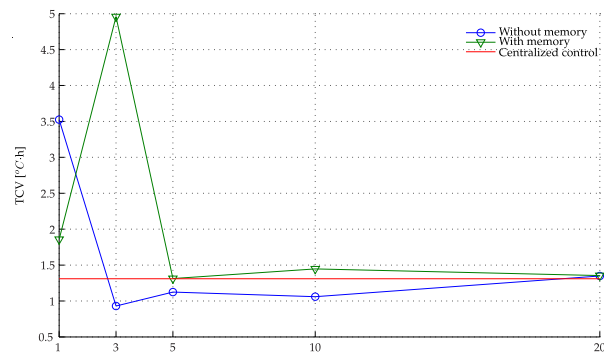
7.8 Conclusion

In this chapter, a distributed model predictive control framework has been proposed in order to tackle the complexity issue in a multi-zone building submitted to power limitation and equipped with an electrical battery and facing varying energy tariff. The proposed DMPC exhibits good performance beside a low computational burden enabling real-time implementation for a realistic number of zones.

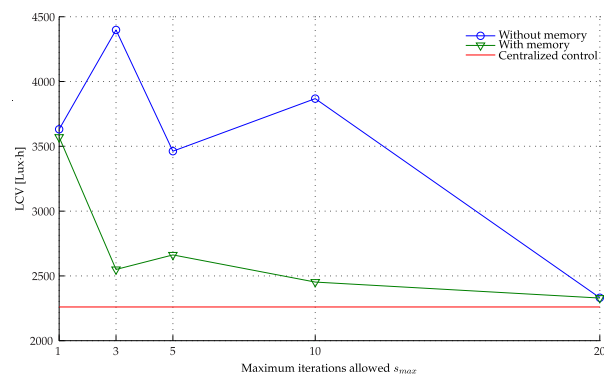
Note that introducing the memory mechanism enabled to enhance the performance of the scheme as it enables better performances for the same number of iterations. The natural extension of the current work is a real-time implementation in a demonstrator building.



(a) Invoice



(b) Thermal Constraint violation



(c) Lighting constraint violation

Figure 7.14 Performance comparison between DMPC with and without memory for different values of maximum number of iterations.

General conclusion

General conclusion

This work was fully dedicated to the design of Model Predictive Control (MPC) algorithms for energy management in buildings.

In part I, brief recalls on building simulation and control techniques used in energy management systems have been provided as well as an introduction to MPC.

In part II, a zone predictive controller has been developed to control the occupant comfort parameters (temperature, CO₂ level as well as indoor illuminance) in each zone of the building beside minimizing energy consumption (or invoice in the case of varying energy rate). As it has been shown, the underlying optimization problem is, in this case, a nonlinear optimization problem that has been solved efficiently thanks to a fixed-point algorithm. It has been shown that the controller can be extended to handle fan coil unit and include readily in the LP formulation a PWA approximation of their heat emission characteristic. Moreover, **an implementation of the algorithm has been conducted on a Schneider-Electric controller (Roombox), showing the compatibility of the control algorithm with the currently commercialized controllers.** Furthermore, on the proposed building, **simulations showed that an energy saving of 14 % can be achieved compared to a well tuned rule-based control strategy on the investigated case study.**

In part III, the zone controllers have been used in a **distributed framework to handle power limitations, multi-source buildings as well as power storage and shared actuators.** This has been performed by introducing a coordinator able to manage the shared resources between the zones. As discussed, the distributed solution offers the benefit of breaking the complexity of the underlying centralized optimization problem as well as preserving the modularity of the scheme. Moreover, **to limit communication rate and computational load on the local controllers, a distributed-in-time optimization technique has been introduced.**

The whole work presented in this thesis as well as the large number of identified works using predictive strategies, showed the diversity of features that can be handled transparently in buildings thanks to the use of predictive strategies: coupled dynamics in a zone, power limitations, local storage, variable energy prices, multi-

sources.

This thesis focused on the development of predictive control strategies as well as implementation and efficiency of the optimization algorithms used to solve the underlying optimization problems by employing several techniques to reduce their complexity (parametrization of optimal solution, distribution of the optimization task among agents, distribution of the optimization over time), while providing illustrative examples in each case. Nevertheless, large scale simulations should be conducted to assess the proposed predictive controller in the diversity of scenarios that can be encountered (buildings, climates, occupancies, HVAC systems, etc.). Moreover, assessment of the control strategy in real-life situations must be also be conducted in future studies.

The challenges

Many challenges condition the implementation of MPC-based solutions in buildings, they represent the main issues that have to be treated in future works. The following summarizes these issues and proposes some references for interested readers:

1. The need for a model: availability of a model of the building is a crucial requirement and represents the main drawback of the technique. However, assuming this model available, much more capabilities and much more flexibility regarding the situations that may occur (varying energy prices, power limitations, etc.) are possible. This critical issue could be basically treated in two ways:
 - 1.a Starting from a physical description of the building: for instance, [Coffey et al. 2010] proposes using a TRNSYS model of the building as a black box model. An optimization algorithm is then designed to find the optimal control sequence based on this model (Clean Urban Energy ⁷ includes this approach in its commercial solution). Another example of using first principle models can be found in [Romanos 2007]. The main disadvantage of this approach lies in the important number of physical parameters related to the building on one hand and the fact that it is very difficult to calibrate a building modeled on some simulation software given experimental data on the other.
 - 1.b Model identification (self-adaptive models): in this case, there is no description of physical phenomena except for the establishment of the general structure of the model. The model is derived from data set in-situ and can be adapted over

⁷www.cleanurbanenergy.com

time. For instance, Building-IQ⁸ uses this approach in its commercialized solution. Furthermore, one can use some grey-box approach as proposed in [Bacher & Madsen 2011] (basically, finding the values of the resistors and capacitances composing the RC network) or a black-box approach as presented in [Malisani et al. 2010].

2. In this work, assumption is made on availability of inputs (heating, ventilation, blinds, etc.). Even if this assumption appears to be quite realistic when using some RoomBox-like controller, it is not in most cases. Actually, buildings inputs are not available. Basically, one has only access to set-points (temperature references for example) since equipment are generally provided with their own control-loops. It is therefore necessary to characterize the building model in closed-loop (building + controller). The controllers may be complex to describe since internal regulators are generally not described by manufacturers and may include their own functioning logic. This problem is described and partially treated in [Baltensperger & Ullmann 2009].
3. The need for reliable weather forecast: this point is addressed by [Henze et al. 2004] for instance. It is attempted to find the best predictor of local weather. Other approaches, like those presented in [Stauch et al. 2010], lie on local weather correction by a Kalman filter.
4. Computation resources: solving the underlying optimization problems resulting from the implementation of predictive controllers may become problematic in some situations. This can be performed locally or using some *could* computation service.
 - 4.a Local calculation: either centrally on one physical machine or in a distributed manner on multiple controllers, as it has been proposed in this work.
 - 4.b Delocalized calculation: the resolution of the optimization problems is not performed within the building, the problem is formulated locally and then transmitted via Internet to a computation server for resolution.
5. Evaluating the energy impact: even if many studies provide energy saving estimations (among which this one), providing an energy potential saving is generally complex in practice. This is basically due to the fact that the initial reference may vary according to the situation. In this work the initial reference was a well tuned rule-based strategy. In other works, or in real life a clear definition of the initial strategy and baseline may be problematic.

⁸www.buildingiq.com

Appendices

Appendix A

Résumé en français

Résumé

Cette partie est un résumé en français du manuscrit de thèse. Le résumé ne prétendant pas être exhaustif, le lecteur est prié de se reporter à la version anglaise pour plus de détails techniques.

A.1 Introduction

L'intérêt grandissant pour l'efficacité énergétique des bâtiments s'est traduit par la recherche de méthodes de contrôle de plus en plus performantes (et le plus souvent de plus en plus sophistiquées) pour l'amélioration de la gestion de l'énergie dans le bâtiment. [Dounis & Caraiscos 2009] argumente ce constat et présente les principales techniques de commande avancées élaborées pour les **BEMS**¹.

À l'heure actuelle, les stratégies de gestion de l'énergie pour les bâtiments sont principalement basées sur une *concaténation de règles logiques*. Bien que cette approche offre des avantages certains, particulièrement lors de sa mise en œuvre sur des automates programmables, elle peine à traiter la diversité de *situations complexes* rencontrées (prix variables de l'énergie, limitations de puissance, capacité de stockage d'énergie, bâtiments de grandes dimension). En outre, les principaux inconvénients de cette approche peuvent être résumés dans ce qui suit:

- La concaténation d'un nombre élevé de règles conduit à un arbre de décision de taille importante, il devient dès-lors difficile d'assurer la cohérence du système expert proposé.
- Le nombre de paramètres de réglage est très élevé, ce qui a pour effet de com-

¹BEMS: Building Energy Management System

plier l'étape de commissioning pendant d'installation.

- Les bâtiments sont amenés à se complexifier, en intégrant de plus en plus des systèmes/possibilités de production/stockage/revente, et ce dans un contexte probable de haute volatilité du prix de l'énergie. Pour ces situations de plus en plus complexes, une logique basée sur des règles expertes atteint ses limites étant donné le caractère à la fois "quantitatif" et "anticipatif" des décisions.

Pour palier à ces limitations, nombre d'auteurs préconisent d'aborder la problématique sous un angle radicalement différent. Le principe consiste non plus à imaginer la meilleure action (règle) à entreprendre dans un cas de figure déterminé, mais à modéliser le "système bâtiment" tout en exprimant un objectif (minimiser l'énergie, minimiser le coût, ...) ainsi que l'ensemble des contraintes opérationnelles sous forme d'un problème d'optimisation qu'il reste à résoudre.

La résolution de ce dernier problème conduit à un plan optimal d'actions, ce plan est régulièrement remis en question, conférant au système bouclé un caractère à la fois anticipatif et réactif.

Il s'avère que ce paradigme dit **MPC**² (commande prédictive) est particulièrement adapté à notre problématique, tel qu'attesté par la multitude de travaux entrepris autour de ce sujet.

A.2 Commande prédictive non linéaire - rappels³

Cette section propose une brève introduction à la commande prédictive non linéaire, le lecteur intéressé peut se reporter à [Mayne et al. 2000] pour plus d'informations.

A.2.1 Notations

Soit le système dynamique non linéaire donné sous sa forme discrète:

$$x_{k+1} = f(x_k, u_k, w_k) \tag{A.1a}$$

$$y_k = h(x_k, u_k, w_k) \tag{A.1b}$$

Avec:

²**MPC**: Model Predictive Control

³ Résumé de la partie I du manuscrit.

A.2. Commande prédictive non linéaire - rappels

- $(x, u, w, y) \in \mathbb{R}^{n_x} \times \mathbb{R}^{n_u} \times \mathbb{R}^{n_w} \times \mathbb{R}^{n_y}$ sont respectivement les vecteurs d'état, entrée, perturbation et sortie du système (A.1),
- $x_k \equiv x(k \cdot \tau)$, où τ est la période d'échantillonnage et k le temps,
- $x^+ \equiv x_{k+1}$ est le vecteur d'état à l'instant suivant.

Notons la trajectoire prédite du vecteur $v \in \mathbb{R}^{n_v}$ à l'instant k sur l'horizon de prédiction de longueur N par:

Notation A.1. Trajectoire prédite

$$\mathbf{v}_k := [v_{k|k}^T, v_{k+1|k}^T, \dots, v_{k+N-1|k}^T]^T \in \mathbb{R}^{N \cdot n_v} \quad (\text{A.2})$$

exemple: $\mathbf{u}_k = [u_{k|k}^T, u_{k+1|k}^T, \dots, u_{k+N-1|k}^T]^T \in \mathbb{R}^{N \cdot n_u}$ est la trajectoire d'entrée prédite à l'instant k sur l'horizon de prédiction $[k, k + N - 1]$.

Si aucune ambiguïté ne résulte, \mathbf{v}_k est notée \mathbf{v} . ◇

Définissons de plus l'opérateur *sélection* $\Pi_j(\mathbf{v}_k)$ comme suit:

Notation A.2. Opérateur sélection

$$\Pi_j(\mathbf{v}_k) := v_{k+j|k} \quad (\text{A.3})$$

L'opérateur $\Pi_j(\cdot)$ sélectionne le $(j + 1)^{\text{ème}}$ vecteur v dans la séquence \mathbf{v}_k (ex.: $\Pi_0(\mathbf{v}_k) = v_{k|k}$).

De plus, notons:

$$\Pi_{[j_0:j_1]}(\mathbf{v}_k) := [v_{k+j_0|k}^T, \dots, v_{k+j_1|k}^T]^T, \quad j_1 > j_0 \quad (\text{A.4})$$

◇

A.2.2 Commande prédictive non linéaire

En commande prédictive non linéaire, le modèle (A.1) ainsi que le vecteur de perturbation prédit w_k sont utilisés à l'instant de décision k afin de trouver la séquence d'entrée optimale notée \mathbf{u}_k^* , minimisant le critère J . Ainsi à chaque instant k , le problème d'optimisation suivant doit être résolu:

Problème d'optimisation A.1. Problème d'optimisation générique

$$\mathbf{u}_k^* = \underset{\mathbf{u}}{\text{Argmin}} J(\mathbf{u}, \mathbf{y}) \quad (\text{A.5a})$$

avec:

$$\begin{cases} \forall j = 0, \dots, N - 1 \\ \Pi_{j+1}(\mathbf{x}) = f(\Pi_j(\mathbf{x}), \Pi_j(\mathbf{u}), \Pi_j(\mathbf{w})) \\ \Pi_j(\mathbf{y}) = h(\Pi_j(\mathbf{x}), \Pi_j(\mathbf{u}), \Pi_j(\mathbf{w})) \end{cases} \quad (\text{A.5b})$$

$$\Pi_0(\mathbf{x}) = x_k \quad (\text{A.5c})$$

$$\mathcal{C}^{\text{st}}(\mathbf{y}, \mathbf{w}, \mathbf{u}, \mathbf{x}) \leq 0 \quad (\text{A.5d})$$

Une fois le problème (A.1) résolu, seul le premier élément de la séquence $\Pi_0(\mathbf{u}_k^*) = u_{k|k}^*$ est appliqué au système durant l'intervalle de temps $[k \cdot \tau, (k + 1) \cdot \tau]$. Toute la procédure est ainsi répétée à chaque instant de décision, en se basant sur une nouvelle mesure ou estimation de l'état courant du système x ainsi que sur de nouvelles prédictions de perturbation w . Ceci aboutit à une commande dite en *horizon glissant* (figure A.1).

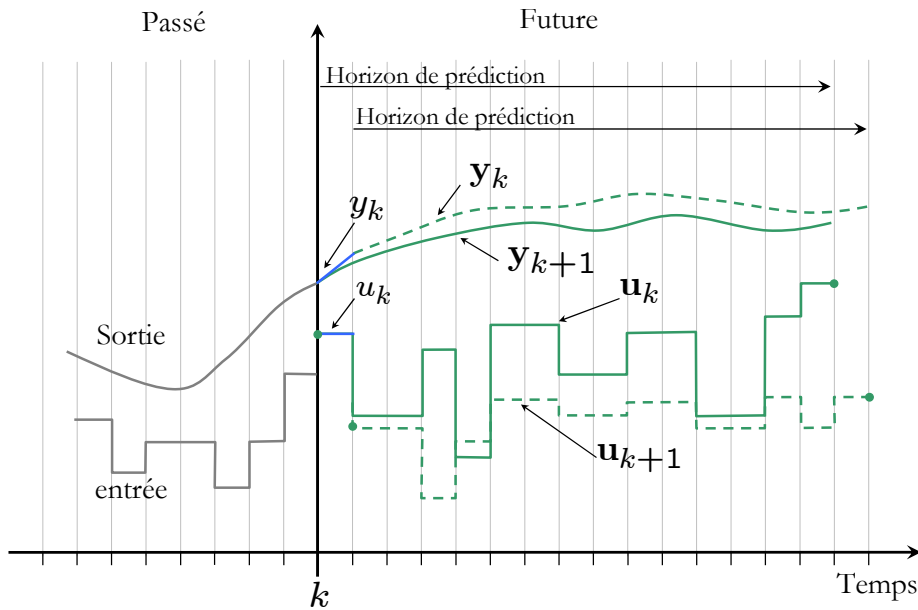


Figure A.1 Commande à horizon glissant: à chaque instant de décision une nouvelle séquence de commande \mathbf{u}_k est calculée, seul le premier élément de la séquence (u_k) est mis en œuvre.

Il s'avère que l'un des principaux avantages découlant de l'utilisation de la commande prédictive réside dans son caractère intuitif. En effet, le problème de con-

trôle est réduit à un problème d'optimisation, faisant de ce paradigme un outil d'abstraction puissant qui permet de traiter des process de natures très différentes sous réserve bien sur de disposer des outils d'optimisation adéquats pour résoudre les problèmes d'optimisation résultants, et les résoudre dans les délais impartis.

D'autre part, notons que le traitement des systèmes multi-entrées/multi-sorties est l'autre point fort découlant de ce paradigme. Rappelons néanmoins que le prix de la performance est intimement liée à l'exactitude du modèle de commande, en effet sa concordance avec la réalité détermine en grande partie les caractéristiques du système bouclé. Nous pouvons résumer les principaux avantages de cette technique par:

- 1- Manipulation de système multi-entrées/multi-sorties de manière transparente.
- 2- Traitement explicite des saturations sur les entrées et/ou les états du système.
- 3- Traitement explicite des coûts économiques.

Dans la pratique, certaines difficultés de mise en oeuvre liées essentiellement aux :

- 1- Temps de calcul d'une solution optimale (qui découle de la complexité du problème à résoudre);
- 2- Nécessite de disposer d'un modèle de commande.

nécessitent certaines simplifications et adaptations au problème réel, ces simplifications s'opèrent essentiellement à plusieurs niveaux:

- 1- Sur le modèle de commande à intégrer: ce dernier doit distiller l'essentiel du comportement dynamique du système sans pour autant en négliger les phénomènes les plus prépondérant.
- 2- Sur le problème à résoudre: en tentant de trouver la formulation la plus simple qui exprime toute-fois le vrai problème que l'on a à résoudre.
- 3- Sur la solution du problème d'optimisation: il n'est parfois pas possible de trouver la solution optimale du problème à résoudre dans les délais impartis, dans ce cas on se contente d'une solution sous-optimale en prenant certaines précautions.

A.2.3 La commande prédictive dans le bâtiment

Nombre d'applications de la commande prédictive ont été investiguées dans la littérature. Chaque auteur a, par une application judicieuse de la commande prédictive, apporté une réponse à une partie de la problématique qui nous concerne en se

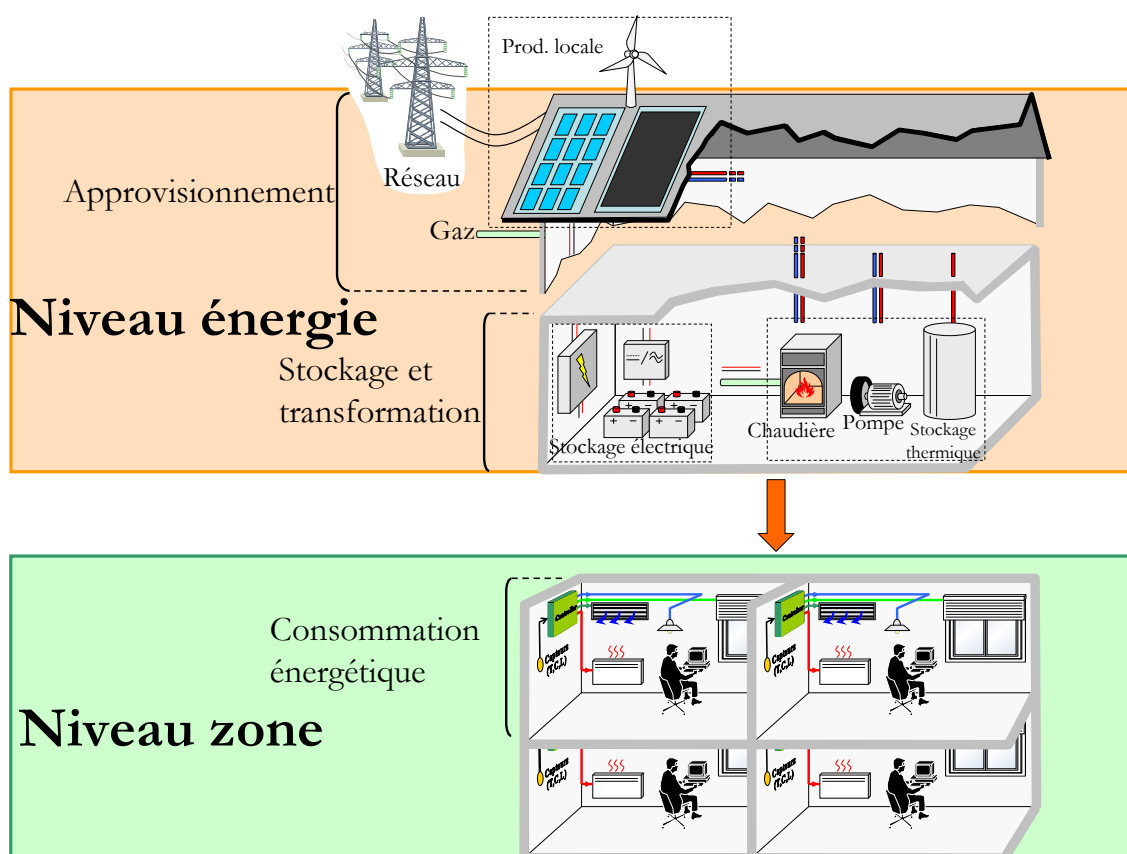


Figure A.2 Décomposition du bâtiment- niveau énergie et niveau zone

focalisant généralement sur l'un des deux périmètres suivants (voir figure A.2):

- 1- **Contrôleur de Zone:** nous entendons par zone une partie contigu d'un bâtiment disposant de ses propres actionneurs et au sein de laquelle doivent être maintenues des conditions environnementales satisfaisantes.
- 2- **Gestion de flux énergétiques globaux:** il est question ici de s'intéresser au problème d'approvisionnement d'énergie et de balance entre différentes sources d'énergie dans le bâtiment sans agir sur la consommation mais en la considérant comme donnée.

Notons toutefois que la distinction ci-dessus a uniquement pour but de structurer la présentation, certaines études échappant à cette catégorisation. En fait, cette distinction exprime le fait que l'étude en question se focalise sur l'un des deux périmètres en simplifiant (parfois excessivement) l'autre. Par exemple: [Siroky et al. 2010] utilise la description d'une seule zone qu'il prend en tant que zone référence pour la commande des systèmes de chauffage de tout le bâtiment, certains auteurs ne s'attachent



Figure A.3 Commande prédictive dans le bâtiment - principaux ingrédients

pas à spécifier un périmètre d'application et/ou allient la commande prédictive à d'autres approches [Abrás 2009].

Il est de plus à noter que certains auteurs incluent explicitement les incertitudes sur les prévisions météorologiques dans le problème d'optimisation à résoudre [Oldewurtel et al. 2010].

La figure A.3 illustre les principaux ingrédients nécessaires à la mise en œuvre de la commande prédictive pour la gestion de l'énergie dans le bâtiment.

A.3 Commande prédictive de zone⁴

Le tableau A.1 reprend l'ensemble des entrées/sorties et perturbations liées à une zone du bâtiment.

Dans cette partie, le problème d'optimisation lié à une zone du bâtiment est formulé. Rappelons tout d'abord la structure du modèle d'une zone du bâtiment donnée sous sa forme de représentation d'état (bilinéaire):

$$\begin{cases} x^+ &= A \cdot x + [B(y, w)] \cdot u + F \cdot w \\ y &= C \cdot x + D(w) \cdot u \end{cases} \quad (\text{A.1})$$

La forme simulateur équivalente au système (A.1) notée \mathcal{Z} est définie par:

$$y_k := \mathcal{Z}(\mathbf{u}_k, \mathbf{w}_k, x_k) \quad (\text{A.2})$$

qui signifie simplement que le profil y_k est obtenu lorsque le système part de l'état x_k et lorsque les profils d'entrée \mathbf{u}_k et perturbation \mathbf{w}_k lui sont appliqués.

⁴Résumé de la partie II du manuscrit.

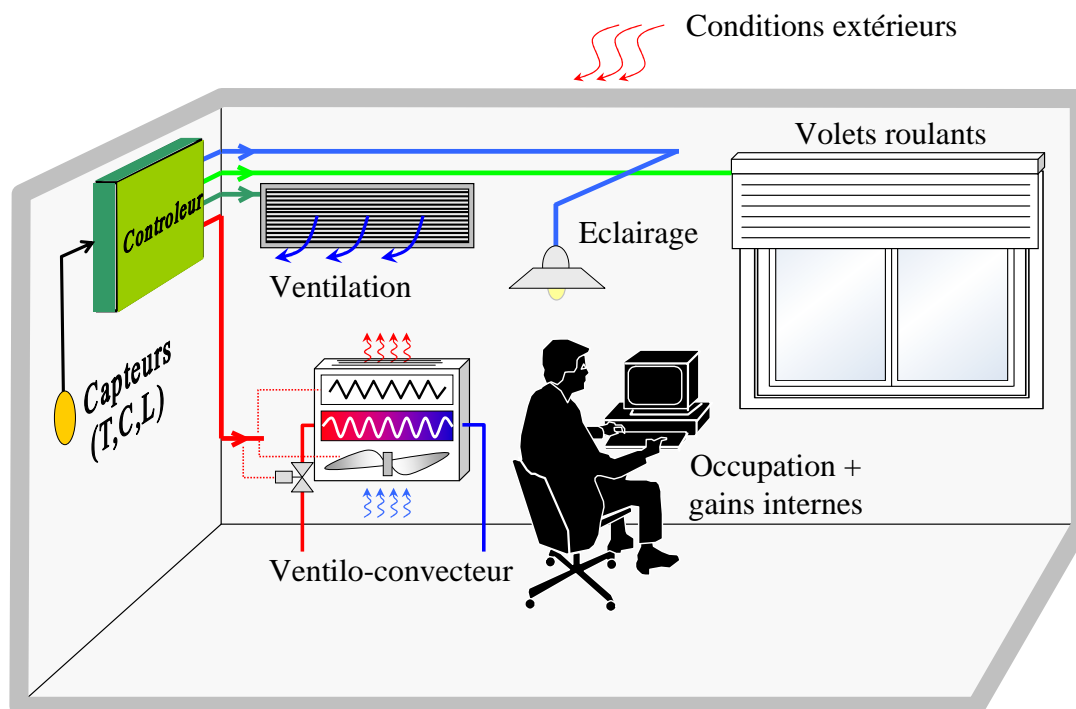


Figure A.4 Représentation d'une zone du bâtiment: une zone est espace contigu du bâtiment disposant d'un certain nombre d'actionneurs (chauffage, ventilation, volets roulants, éclairage artificiel, ...) ainsi que de capteurs d'ambiance.

Dans la suite, les quantités suivantes sont supposées connues:

Hypothèse A.3.1.

- L'état courant x_k (obtenu par observation),
- Les prédictions tarifaires sur le prix de l'énergie Γ ,
- Les prédictions sur le vecteur de perturbation w_k ,
- Les bornes de confort haute (\underline{y}_k) et basse (\bar{y}_k) implicitement liées à l'occupation prédite de la zone Occ_k .

Supposons de plus que la consommation des équipements électriques est linéaire⁵

⁵Le lecteur peut se reporter au chapitre 5 pour la prise en compte d'actionneurs disposant de caractéristiques non linéaires. Il y est question de la gestion des ventilo-convecteurs. Ceci n'est pas détaillé dans le cadre de ce résumé.

	Variables	Description	Unit
Commandes	u_h	commande de chauffage électrique	[–]
	u_v	position du registre	[–]
	u_l	commande d'éclairage	[–]
	$\{u_b^i\}_{i=1,\dots,N_f}$	commande de volet roulant (façade i)	[–]
Perturbations	T_{ex}	Température externe	[°C]
	$\{T_{adj}^i\}_{i \in N_{adj}}$	Température des zones adjacentes	[°C]
	$\{\phi_g^i\}_{i=1,\dots,N_f}$	Flux solaire global sur la façade i	[W/m ²]
	Occ	Nombre d'occupants	[–]
	C_{ex}	Taux de CO ₂ externe	[ppm]
Sorties	T	Température	[°C]
	C	Taux de CO ₂	[ppm]
	L	Eclairage	[Lux]

Table A.1 Entrées/Sorties et perturbations liées à une zone du bâtiment.

par rapport à la commande u . En notant $p_k \in \mathbb{R}$ la consommation électrique totale de la zone à l'instant k , il résulte que:

$$p_k = E \cdot u_k \in \mathbb{R} \quad (\text{A.3})$$

où la matrice $E \in \mathbb{R}^{1 \times n_u}$ regroupe les consommations électriques maximales de tous les équipements (correspondants à u):

$$E := \begin{bmatrix} \alpha_h & \alpha_v & \alpha_l & 0 & \dots & 0 \end{bmatrix} \quad (\text{A.4})$$

les scalaires α_h , α_v and α_l correspondent respectivement aux consommations induites par le chauffage électrique, le système de ventilation et l'éclairage artificiel.

Le profil prédit de consommation de puissance est ainsi donné par:

$$\mathbf{p}_k = \mathbf{E} \cdot \mathbf{u}_k, \quad \mathbf{p}_k \in \mathbb{R}^N \quad (\text{A.5})$$

avec:

$$\mathbf{E} := \mathbf{I}_N \otimes E \quad (\text{A.6})$$

En considérant que les commandes des actionneurs sont normées ($u_k \in [0, 1]^{n_u}$), le problème d'optimisation résultant est donné par:

Problème d'optimisation A.2. Problème d'optimisation - niveau zone

$$\mathbf{u}_k^* = \underset{0 \leq \mathbf{u} \leq \mathbf{1}}{\text{Argmin}} \quad J^E(\mathbf{\Gamma}_k, \mathbf{p}_k) + J^C(\mathbf{y}_k) + J^D(\mathbf{u}_k) + J_F(\Pi_{(N-1)}(\mathbf{y}_k)) \quad (\text{A.7})$$

avec:

$$\mathbf{p}_k = \mathbf{E} \cdot \mathbf{u}_k \quad (\text{A.8})$$

$$\mathbf{y}_k = \mathcal{Z}(\mathbf{u}_k, \mathbf{w}_k, x_k) \quad (\text{A.9})$$

où:

- J^E est le critère énergétique:

$$J^E(\mathbf{\Gamma}_k, \mathbf{p}_k) = (\mathbf{\Gamma}_k^T \cdot \mathbf{E})^T \cdot \mathbf{u}_k \quad (\text{A.10})$$

- $J^C(\mathbf{y}_k)$ est le critère d'inconfort \mathbf{y}_k . La fonction d'inconfort force la sortie du système à appartenir à la région de confort lorsque une occupation est détectée. La fonction est paramétrisée par les scalaires positifs ρ_0, ρ_1 and le vecteur $\delta_y \in \mathbb{R}^{n_y \cdot N}$ (voir figures A.6 et A.5).

- $J^D(\mathbf{u}_k)$ pondère les vitesses de variation des commandes:

$$J^D(\mathbf{u}_k) = \langle \Delta, |\Pi_0(\mathbf{u}_k) - u_{k-1}| \rangle + \sum_{j=1}^{j=N} \langle \Delta, |\Pi_j(\mathbf{u}_k) - \Pi_{(j-1)}(\mathbf{u}_k)| \rangle \quad (\text{A.11})$$

Rappelons que $\Pi_j(\mathbf{u}_k)$ sélectionne le j^{eme} composant du profil prédit \mathbf{u}_k . $|\cdot|$ est la valeur absolue par élément.

- $J_F(\Pi_{(N-1)}(\mathbf{y}_k))$ est un coût final, indiquant ici que la zone doit être à même de retrouver un niveau de confort à la fin de l'horizon de prédiction.

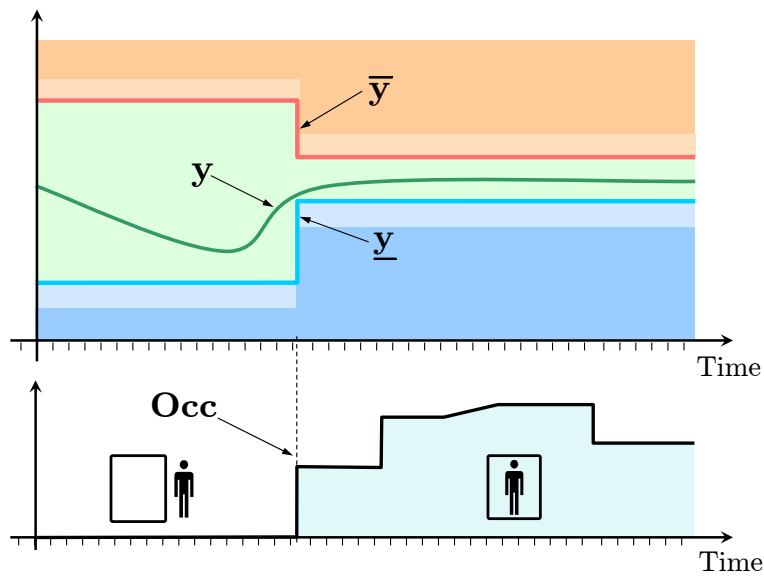


Figure A.5 Borne de confort. Les bornes de confort sont liées à l'occupation de la zone.

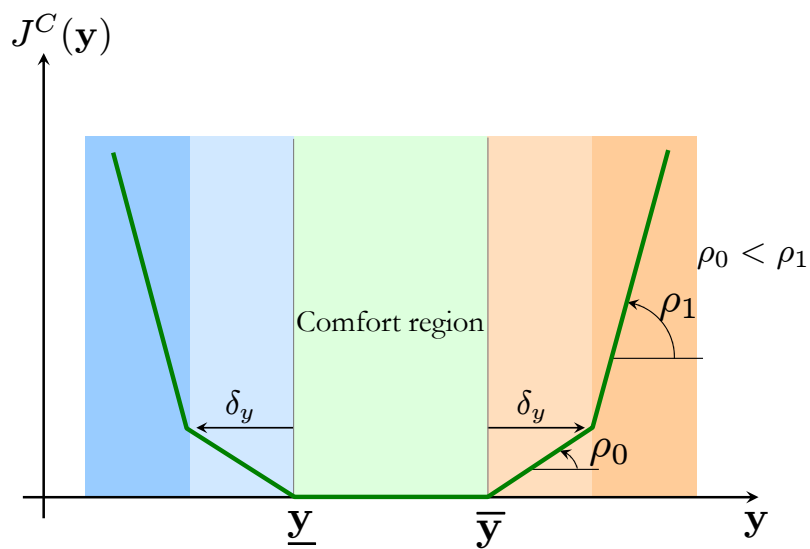


Figure A.6 Fonction d'inconfort. La fonction d'inconfort pénalise toute violations inférieure ou supérieure sur les limites de confort.

Le problème d'optimisation A.2 peut être exprimé sous la forme suivante:

Problème d'optimisation A.3.

$$\text{NLP}_k: \underset{\mathbf{u}_k, \delta_0, \delta_1, \delta_d, \mathbf{y}_k}{\text{Minimize}} J(\mathbf{u}_k, \mathbf{y}_k, \Gamma_k) \quad (\text{A.12a})$$

avec :

$$[\Phi(\mathbf{y}_k, \mathbf{w}_k)]\mathbf{u}_k + \delta_0^- + \delta_1^- \geq \underline{\mathbf{y}}_k - \Psi x_k - \Xi \mathbf{w}_k \quad (\text{A.12b})$$

$$[\Phi(\mathbf{y}_k, \mathbf{w}_k)]\mathbf{u}_k - \delta_0^+ - \delta_1^+ \leq \bar{\mathbf{y}}_k - \Psi x_k - \Xi \mathbf{w}_k \quad (\text{A.12c})$$

$$\mathbf{D} \cdot \mathbf{u}_k - \delta_d^+ + \delta_d^- = \mathbf{a} \quad (\text{A.12d})$$

$$\mathbf{0} \leq \mathbf{u}_k \leq \mathbf{1} \quad (\text{A.12e})$$

$$\delta_0 \geq \mathbf{0}, \delta_d \geq \mathbf{0}, \mathbf{0} \leq \delta_1 \leq \begin{bmatrix} \delta_y \\ \delta_y \end{bmatrix} \quad (\text{A.12f})$$

$$\mathbf{y}_k = \mathcal{Z}(\mathbf{u}_k, \mathbf{w}_k, x_k) \quad (\text{A.12g})$$

Avec:

- $\delta_0 := \begin{bmatrix} \delta_0^+ \\ \delta_0^- \end{bmatrix} \in \mathbb{R}^{2 \cdot N \cdot n_y}$, $\delta_1 := \begin{bmatrix} \delta_1^+ \\ \delta_1^- \end{bmatrix} \in \mathbb{R}^{2 \cdot N \cdot n_y}$ sont des variables complémentaires introduites pour décrire la fonction $J^C(\mathbf{y})$ (figure A.6);
- $\delta_d := \begin{bmatrix} \delta_d^+ \\ \delta_d^- \end{bmatrix} \in \mathbb{R}^{2 \cdot N \cdot n_u}$ sont des variables complémentaires introduites pour décrire la fonction $J^D(\mathbf{y})$;
- Les notations $\mathbf{1}$ et $\mathbf{0}$ indiquent des vecteurs (ou matrices) de 1 et de 0 de tailles appropriées,
- $\Phi(\mathbf{y}_k, \mathbf{w}_k)$, Ψ and Ξ sont les matrices de prédiction définies comme suit:

$$\Psi := \begin{bmatrix} C \\ CA \\ CA^2 \\ \cdot \\ CA^{N-1} \end{bmatrix}, \quad \Phi(\mathbf{y}_k, \mathbf{w}_k) := \begin{bmatrix} D_k & \mathbf{0} & \cdot & \mathbf{0} \\ CB_k & D_{k+1} & \cdot & \cdot \\ CAB_k & CB_{k+1} & \cdot & \cdot \\ \cdot & \cdot & \cdot & \mathbf{0} \\ CA^{N-2}B_k & CA^{N-3}B_{k+1} & \cdot & D_{k+N-1} \end{bmatrix} \quad (\text{A.13})$$

où: $B_k := B(y_k, w_k)$ and $D_k := D(w_k)$.

- Les matrices \mathbf{D} et \mathbf{a} sont définies comme suit:

$$\mathbf{D} := \begin{bmatrix} \mathbf{I}_{n_u} & \mathbf{0} & \mathbf{0} & \dots & \dots & \mathbf{0} \\ \mathbf{I}_{n_u} & -\mathbf{I}_{n_u} & \mathbf{0} & \dots & \dots & \mathbf{0} \\ \mathbf{0} & \mathbf{I}_{n_u} & -\mathbf{I}_{n_u} & \dots & \dots & \mathbf{0} \\ \dots & \dots & \dots & \dots & \dots & \dots \\ \mathbf{0} & \dots & \dots & \mathbf{0} & \mathbf{I}_{n_u} & -\mathbf{I}_{n_u} \end{bmatrix}, \mathbf{a} := \begin{bmatrix} u_{k-1} \\ \mathbf{0} \\ \mathbf{0} \\ \dots \\ \mathbf{0} \end{bmatrix}, \quad (\text{A.14})$$

En définissant la variable de décision \mathbf{z} qui regroupe toutes les variables de décision liées à la zone par:

$$\mathbf{z} := \left[\mathbf{u}_k^T \quad \delta_0^T \quad \delta_1^T \quad \delta_d^T \right]^T \quad (\text{A.15})$$

le problème d'optimisation A.3 peut être mis sous la forme:

Problème d'optimisation A.4.

$$\underset{\mathbf{z} \leq \mathbf{z} \leq \bar{\mathbf{z}}, \mathbf{y}_k}{\text{Minimize}} \mathbf{L} \cdot \mathbf{z} \quad (\text{A.16})$$

avec:

$$\mathbf{A}(\mathbf{y}_k) \cdot \mathbf{z} \leq \mathbf{b} \quad (\text{A.17})$$

$$\mathbf{y}_k = \mathcal{Z}(\mathbf{u}_k, \mathbf{w}_k, x_k) \quad (\text{A.18})$$

Les matrices \mathbf{L} , $\mathbf{A}(\mathbf{y})$, \mathbf{b} , $\bar{\mathbf{z}}$, \mathbf{z} sont données par B.

Le problème d'optimisation A.3 est un problème d'optimisation non linéaire (non convexe). Ceci résulte de la présence de produits entre les variables \mathbf{y} and \mathbf{z} . Afin de le résoudre, il est proposé d'utiliser un algorithme de point fixe, présenté dans ce qui suit.

A.3.1 Résolution du problème d'optimisation

Une procédure itérative est mise en œuvre afin de résoudre le problème d'optimisation A.4. A l'itération s de l'algorithme du point fixe, une trajectoire $\mathbf{y}_k^{(s)}$ est donnée à priori. Ainsi, on peut former le système linéaire temps variant *fictif* suivant:

$$\text{LTV}^{(s)} : \begin{cases} x^+ &= A \cdot x + \left[B(\mathbf{y}^{(s)}, \mathbf{w}) \right] \cdot u + F \cdot w \\ y &= C \cdot x + D(\mathbf{w}) \cdot u \end{cases} \quad (\text{A.19})$$

Il en découle le problème de programmation linéaire suivant, dans lequel la trajectoire \mathbf{y} n'est pas une variable de décision puisque donnée à priori:

Problème d'optimisation A.5. Programmation linéaire

$$\underset{\underline{\mathbf{z}} \leq \mathbf{z} \leq \bar{\mathbf{z}}}{\text{Minimize}} \mathbf{L} \cdot \mathbf{z} \quad \text{s.t.} : \quad \mathbf{A}(\mathbf{y}_k^{(s)}) \cdot \mathbf{z} \leq \mathbf{b} \quad (\text{A.20})$$

La solution du problème A.5 donne la trajectoire optimale $\mathbf{u}_k^{(s)}$ correspondant au système (A.19):

$$\mathbf{u}_k^{(s)} \leftarrow \text{LP}_k^{(s)} \quad (\text{A.21})$$

celle-ci est réinjectée dans le système non linéaire, résultant en une nouvelle trajectoire $\mathbf{y}_k^{(s+1)}$ à l'itération $s + 1$:

$$\mathbf{y}_k^{(s+1)} = \mathcal{Z}(\mathbf{u}_k^{(s)}, \mathbf{w}_k, x_k) \quad (\text{A.22})$$

où \mathcal{Z} est la forme simulateur de la zone (voir eq. (A.2)). Ces deux étapes ((A.21) et (A.22)) sont répétées jusqu'à ce que la différence entre deux itérés successifs $e^{(s)} := \text{Max}(\|\mathbf{y}_k^{(s+1)} - \mathbf{y}_k^{(s)}\|_\infty, \|\mathbf{u}_k^{(s+1)} - \mathbf{u}_k^{(s)}\|_\infty)$ soit inférieure à une certaine précision $e^{(s)} \leq \eta$ ou que le nombre d'itération maximale s_{max} soit atteint. Ceci est résumé par l'algorithme A.1.

Algorithm A.1 Algorithme du point-fixe

- 1: $s \leftarrow 1$
 - 2: $\mathbf{u}_k^{(0)} \leftarrow [\Pi_1(\mathbf{u}_{k-1}^*)^T, \dots, \Pi_{(N-1)}(\mathbf{u}_{k-1}^*)^T, \Pi_{(N-1)}(\mathbf{u}_{k-1}^*)^T]^T \quad \triangleright \text{Initialisation}$
 - 3: $\mathbf{y}_k^{(1)} \leftarrow \mathcal{Z}(\mathbf{u}_k^{(0)}, \mathbf{w}_k, x_k)$
 - 4: $e^{(0)} \leftarrow \infty$
 - 5: **Tant que** $e^{(s-1)} \geq \eta$ **et** $s \leq s_{max}$ **faire**
 - 6: $\mathbf{u}_k^{(s)} \leftarrow \text{LP}_k^{(s)}$
 - 7: $\mathbf{y}_k^{(s+1)} = \mathcal{Z}(\mathbf{u}_k^{(s)}, \mathbf{w}_k, x_k)$
 - 8: $e^{(s)} \leftarrow \text{Max}(\|\mathbf{y}_k^{(s+1)} - \mathbf{y}_k^{(s)}\|_\infty, \|\mathbf{u}_k^{(s+1)} - \mathbf{u}_k^{(s)}\|_\infty)$
 - 9: $s \leftarrow s + 1$
 - 10: **Fin tant que**
 - 11: $\mathbf{u}_k^* \leftarrow \mathbf{u}_k^{(s-1)}$
-

A.3.2 Simulations

La figure A.7 présente une simulation sur une zone sur une durée de 48 [h]. Nous pouvons constater que la bornes de confort sont toujours respectées pendant les horaires d'occupation des locaux. De plus notons concernant la commande de chauffage

u_h le démarrage optimal, celui-ci permet d'enclencher le chauffage le plus tard possible afin d'économiser l'énergie tout en démarrant suffisamment tôt pour permettre à la température d'atteindre la zone de confort à l'arrivée des occupants.

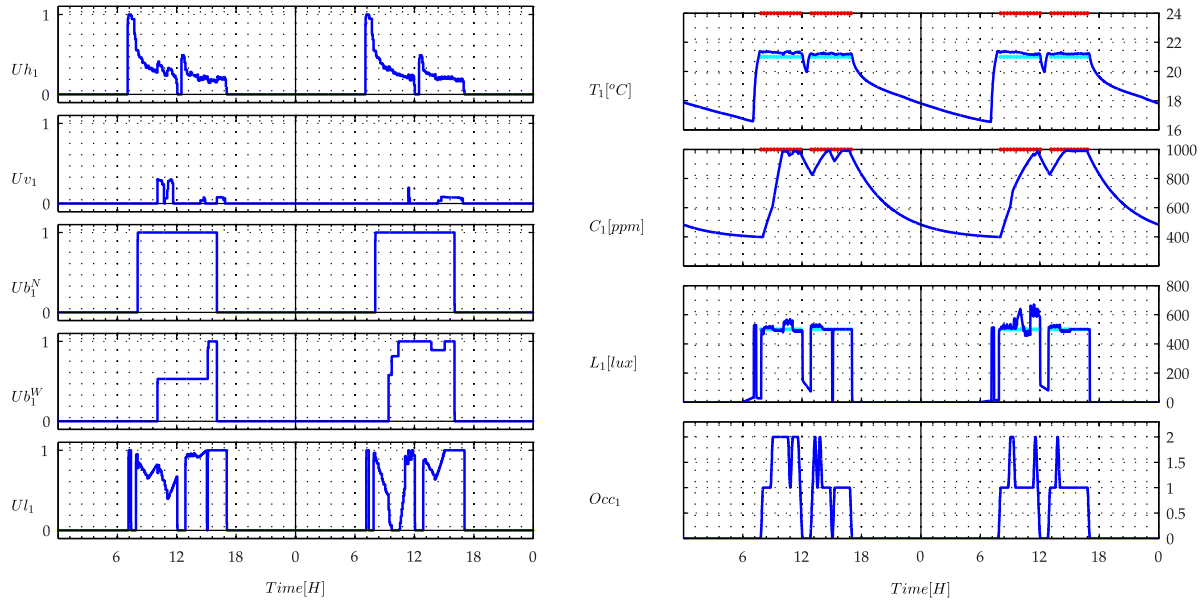


Figure A.7 Validation du contrôleur prédictif de zone

Lorsque nous mettons en place ce procédé sur un bâtiment disposant de plusieurs zones (20 zones dans ce cas de figure), les gains d'énergie s'élèvent à approximativement 15 % comparé à une commande classique (règles expertes) bien réglée (développée dans le cadre du programme HOMES). Les résultats de simulation annuelle reportés sur le tableau A.2 comparent les résultats obtenus par une commande prédictive lorsque les prévisions météorologiques sont parfaites ($\alpha = 0$) et lorsqu'elles sont entachées d'erreurs. CTG [%] est une mesure en pourcentage du temps passé en condition de confort thermique et VCT [$k \cdot ^\circ C \cdot h$] est l'intégral des violations sur les contraintes de température.

	Cons. énergétique [kWh/m^2]	CTG [%]	VCT [$k \cdot ^\circ C \cdot h$]
Rule based	142	91.6	322
MPC ($\alpha = 1$)	119 (-16%)	91.8	295
MPC ($\alpha = 0$)	122 (-14%)	88.1	310

Table A.2 Consommation énergétique/ Confort - Règles expertes vs. MPC

A.3.3 Implémentation sur contrôleurs temps-réel

L'algorithme de commande prédictive de zone ayant été développé en Matlab a été mis en œuvre sur un contrôleur temps réel commercialisé par Schendier-Electric: la RoomBox (voir figure A.8). Afin de l'implanter sur cette cible, l'algorithme a été traduit manuellement en C/C++ à l'aide d'une librairie de calcul matriciel développée au sein du Gipsa-lab. Il a été constaté lors des tests que le temps de calcul moyen était de l'ordre de 10[s] et qu'il était largement en dessous de la période d'échantillonnage (une à plusieurs minutes). La même constatation peut être faite concernant l'occupation mémoire, l'algorithme utilise 10[Mo] sur les 128[Mo] disponible dans une RoomBox. Ceci démontre la compatibilité de l'algorithme de commande prédictive avec le type de cible.



Figure A.8 Le contrôleur de zone office Roombox (Schneider-Electric)

A.4 Commande prédictive distribuée ⁶

Tel qu'indiqué dans l'introduction, l'un des principaux avantages de la commande prédictive dans le bâtiment réside dans sa capacité à prendre en compte des conditions de marché de l'énergie imposées par le fournisseur d'énergie. Celles-ci, en plus de prendre la forme de signaux tarifaires, peuvent aussi être traduites en termes de limitations de puissance. Plus explicitement, le fournisseur d'énergie impose une limite supérieure de puissance consommée.

Il est question dans cette partie du travail d'étendre le schéma de contrôle mis en œuvre pour une zone du bâtiment à un bâtiment dans son intégralité pour prendre en charge d'une part des limitations de puissance globales mais aussi une ressource

⁶Résumé de la partie III du manuscrit.

de stockage partagée entre les zones du bâtiment (ici une batterie électrique)⁷. Il est proposé d'adopter une approche dite "distribuée", dans laquelle chaque zone garde un degré d'autonomie en actionnant elle-même ses propres actionneurs locaux mais soumise à un ensemble de contraintes ajustées par un étage de commande supérieur (coordinateur).

L'approche distribuée offre des avantages quant à la mise à l'échelle de la solution⁸ ainsi que pour des raisons de maintenabilité et d'extensibilité de la solution.

A.4.1 Mise en œuvre de la commande prédictive distribuée

Considérons un bâtiment de n_z zones, où $\ell \in \mathbf{Z} = \{1, \dots, n_z\}$ désigne l'indice de chaque zone représentée par le système non linéaire suivant:

$$\begin{cases} x_\ell^+ &= A_\ell \cdot x_\ell + [B_\ell(y_\ell, w_\ell)] \cdot u_\ell + G_\ell \cdot w_\ell \\ y_\ell &= C_\ell \cdot x_\ell + [D_\ell(w_\ell)] \cdot u_\ell + F_\ell \cdot w_\ell \end{cases} \quad (\text{A.1})$$

où $x_\ell \in \mathbb{R}^{n_x}$, $u_\ell \in \mathbb{R}^{n_u}$, $w_\ell \in \mathbb{R}^{n_w}$, $y_\ell \in \mathbb{R}^{n_y}$ désignent respectivement l'état, l'entrée, la sortie et la perturbation liés à la zone ℓ .

L'objectif de chaque contrôleur de zone est de maintenir les sorties $y_\ell \in \mathbb{R}^3$ dans les bornes de confort au moindre coût énergétique. Ceci est réalisé par la résolution du problème d'optimisation suivant (à chaque instant de décision):

$$\underset{u_\ell \in \mathbf{U}_\ell}{\text{Minimize}} \quad J^E(\mathbf{p}_\ell) + J^C(\mathbf{y}_\ell) + J^F(\mathbf{y}_\ell) + J^D(\mathbf{y}_\ell) \quad (\text{A.2})$$

Dans le problème d'optimisation (A.2) J^E , J^C , J^F et J^D représentent respectivement les coûts liés à l'énergie, l'inconfort, le coût final et le coût sur le mouvement des actionneurs.

Le bâtiment est de plus équipé d'une batterie électrique dont le modèle est donné par:

$$b^+ = b + \tau \cdot \eta(p_b) \cdot p_b \quad (\text{A.3a})$$

avec:

$$\eta(p_b) = \begin{cases} \eta^+ & \text{if } p_b \geq 0 \\ 1/\eta^- & \text{if } p_b < 0 \end{cases} \quad (\text{A.3b})$$

⁷La démarche présentée ici permet de plus de prendre en charge des actionneurs communs entre les zones. Cette fonctionnalité n'est pas présentée dans ce résumé. Le lecteur est prié de se reporter au chapitre 7 pour plus d'explications.

⁸la taille des problèmes d'optimisation dans une approche centralisée peut être prohibitive à sa mise en œuvre sur des bâtiments de grande taille.

Où:

- p_b est la puissance de charge/décharge de la batterie électrique ($p_b > 0$: charge) ($p_b < 0$: décharge), $|p_b| \leq \bar{p}_b$,
- τ est la période d'échantillonnage,
- $(\eta^+, \eta^-) \in]0, 1[^2$ représentent respectivement l'efficacité de charge et de décharge,
- b est l'état de charge de la batterie exprimé en [kWh], $\underline{b} \leq b \leq \bar{b}$.

Ainsi, l'introduction d'une contrainte de puissance globale (sur tout le bâtiment) \bar{p}_g se traduit par les contraintes suivantes:

$$\sum_{\ell \in \mathbf{Z}} p_{\ell}^{\leftarrow g} + p_b^+ \leq \bar{p}_g \quad (\text{A.4a})$$

$$\sum_{\ell \in \mathbf{Z}} p_{\ell}^{\leftarrow b} = p_b^- \quad (\text{A.4b})$$

$p_{\ell}^{\leftarrow g}$ et $p_{\ell}^{\leftarrow b}$ représentent les puissances reçues par la zone ℓ à partir du réseau électrique et de la batterie (voir figure A.9). De ce fait, le niveau énergie est perçu par les zones comme un fournisseur d'énergie mettant à disposition deux types de ressources: l'une émanant du réseau électrique et l'autre de la batterie, les deux caractérisées par leur propre prix et limites.

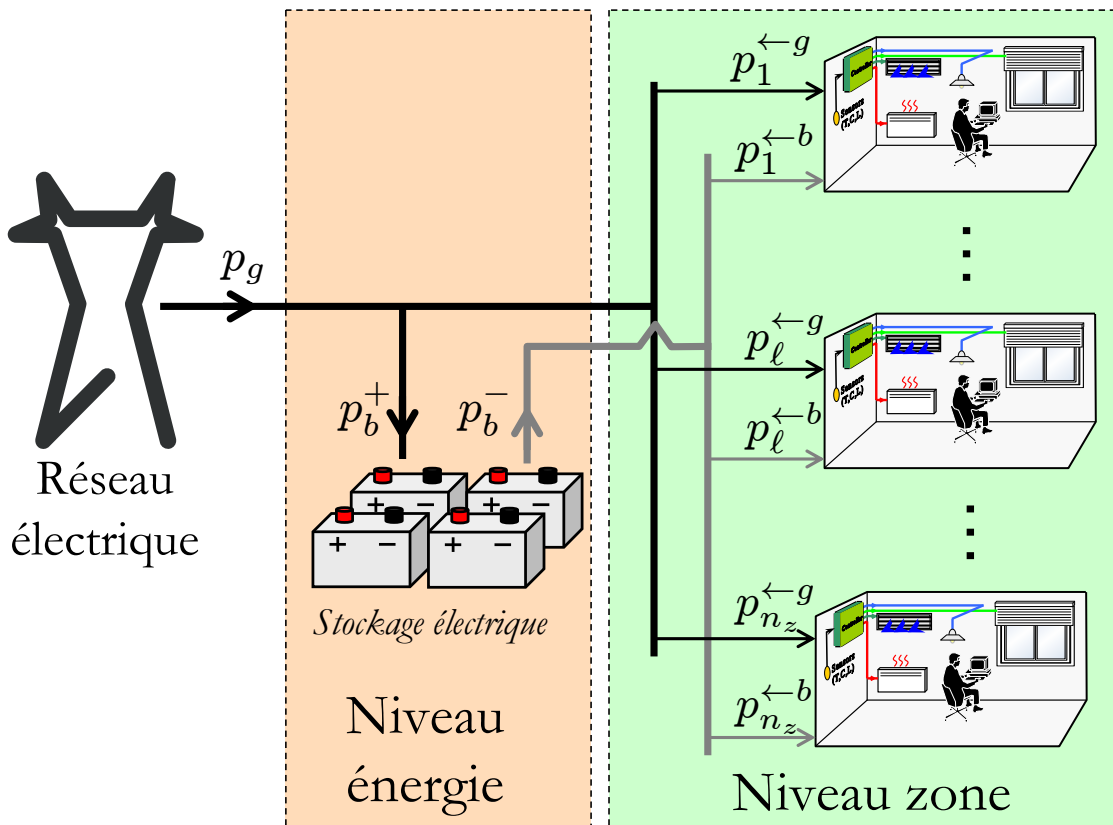


Figure A.9 Commande prédictive distribuée - Mise en œuvre sur un bâtiment multizone équipé d'un système de stockage électrique et soumis à une contrainte de puissance consommée.

A.4.2 Introduction de contraintes de ressources locales

Introduisons les variables "ressources" $\mathbf{r} := \{\mathbf{r}_\ell\}_{\ell \in \mathbf{Z}}$, où chaque \mathbf{r}_ℓ représente une limite supérieure de ressources. Ainsi, chaque problème d'optimisation (résolu par chaque zone) est modifié comme suit:

Problème d'optimisation A.6. Problème d'optimisation local (zone)

$$\text{MPC}_\ell(\mathbf{r}_\ell) : \underset{\mathbf{z}_\ell \leq \mathbf{z}_\ell \leq \bar{\mathbf{z}}_\ell}{\text{Minimize}} \mathbf{L}_\ell^{(i)} \cdot \mathbf{z}_\ell \quad (\text{A.5})$$

Subject To :

$$\mathbf{A}_\ell \cdot \mathbf{z}_\ell \leq \mathbf{b}_\ell \quad (\text{A.6})$$

$$\mathbf{A}'_\ell \cdot \mathbf{z}_\ell \leq \mathbf{r}_\ell \quad (\text{A.7})$$

\mathbf{z}_ℓ inclut toutes les variables de décision internes impliquées dans le problème d'optimisation locale lié à la zone ℓ (voir le problème d'optimisation A.3).

$$\mathbf{z}_\ell := \left[\mathbf{u}_\ell^T \quad \mathbf{p}_\ell^T \quad \delta_0^T \quad \delta_1^T \quad \delta_d^T \right]^T \quad (\text{A.8})$$

Il est important de noter que pour une affectation de ressource donnée \mathbf{r}_ℓ , la résolution du problème d'optimisation A.6 fournit une information par rapport à la valeur de la fonction objectif $J_\ell(\mathbf{r}_\ell)$ ainsi qu'une information de sensibilité (sous-gradient) notée $g_\ell(\mathbf{r}_\ell)$.

$$(J_\ell(\mathbf{r}_\ell), \mathbf{g}_\ell(\mathbf{r}_\ell)) \leftarrow \text{MPC}_\ell(\mathbf{r}_\ell) \quad (\text{A.9})$$

A.4.3 Introduction du mécanisme de coordination

Au niveau du bâtiment, le problème d'optimisation prend la forme suivante:

Problème d'optimisation A.7. Problème maitre

$$\underset{\mathbf{p}_b^+, \mathbf{p}_b^-, \mathbf{r}_1, \dots, \mathbf{r}_{n_z}}{\text{Minimize}} \quad J := \Gamma_g \cdot \mathbf{p}_b^+ + \sum_{\ell \in \mathbf{Z}} J_\ell(\mathbf{r}_\ell) \quad (\text{A.10a})$$

Subject To :

$$\underline{\mathbf{b}} - b_0 \leq \tau \cdot \eta^+ \cdot \Phi_e \cdot \mathbf{p}_b^+ - \frac{\tau}{\eta^-} \cdot \Phi_e \cdot \mathbf{p}_b^- \leq \bar{\mathbf{b}} - b_0 \quad (\text{A.10b})$$

$$\mathbf{p}_e^{\leftarrow g} + \mathbf{p}_e^{\leftarrow b} = \mathbf{E} \cdot \mathbf{p}_e \quad (\text{A.10c})$$

$$\mathbf{0} \leq \mathbf{p}_b^+, \mathbf{p}_b^- \leq \bar{\mathbf{p}}_b \quad (\text{A.10d})$$

$$\sum_{\ell \in \mathbf{Z}} \mathbf{r}_\ell^{\leftarrow g} + \mathbf{p}_b^+ + \mathbf{p}_e^{\leftarrow g} \leq \bar{\mathbf{p}}_g \quad (\text{A.10e})$$

$$\sum_{\ell \in \mathbf{Z}} \mathbf{r}_\ell^{\leftarrow b} + \mathbf{p}_e^{\leftarrow b} \leq \mathbf{p}_b^- \quad (\text{A.10f})$$

que l'on peut mettre sous le forme suivante:

Problème d'optimisation A.8. Problème maitre -forme générale

$$\underset{(\mathbf{z}_e, \mathbf{r}) \in \mathcal{D}}{\text{Minimize}} \quad J := \left[J_E(\mathbf{z}_e) + \sum_{\ell \in \mathbf{Z}} J_\ell(\mathbf{r}_\ell) \right] \quad (\text{A.11})$$

où \mathbf{z}_e inclut toutes les variables de décision liées au niveau énergie. Φ_e est une matrice adéquatement construite (dynamique de la batterie, voir équation (7.4.12)). L'expression $(\mathbf{z}_e, \mathbf{r}) \in \mathcal{D}$ équivaut à la validité de l'ensemble des contraintes (A.10b)-(A.10f).

Le problème A.8 met en jeu les variables ressources \mathbf{r}_ℓ relatives à chaque zone ainsi que les variables \mathbf{z}_e relatives au niveau énergie. Ce problème est résolu par le

coordinateur qui, rappelons-le, ne dispose que d'informations par rapport à la valeur de la fonction J_ℓ ainsi que de son gradient \mathbf{g}_ℓ pour affectation de ressource \mathbf{r}_ℓ donnée (voir (A.9)). Ainsi, le coordinateur ne dispose d'aucune mesure d'état local x_ℓ ou emprise sur les actionneurs des zones u_ℓ .

Afin de résoudre ce problème d'optimisation, il est nécessaire de mettre au point un mécanisme permettant d'approximer les fonctions locales J_ℓ . Ceci est expliqué dans ce qui suit.

A.4.4 Algorithme des plans coupants stabilisé⁹

Afin de résoudre le problème d'optimisation A.8, il est proposé d'employer un algorithme de plans coupants stabilisé. La méthode se base sur des approximations successives des fonctions J_ℓ (inconnues par le coordinateur). Ces approximations \check{J}_ℓ sont illustrées sur la figure A.10.

Il est possible de construire ces approximations car pour une affectation de ressource donnée \mathbf{r}_ℓ le coordinateur dispose d'informations relatives à la valeur de la fonction ainsi qu'à son sous-gradient.

Dans notre cas, la fonction J est séparable. Il est donc possible de construire une approximation pour chaque sous-fonction J_ℓ puis de les sommer:

$$J = J_E + \sum_{\ell \in \mathbf{Z}} J_\ell \quad (\text{A.12})$$

Ainsi, à chaque itération s de l'algorithme, une nouvelle approximation $\check{J}^{(s)}$ est générée:

$$\check{J}^{(s)}(\mathbf{z}_e, \mathbf{r}) := J_E(\mathbf{z}_e) + \sum_{\ell \in \mathbf{Z}} \check{J}_\ell^{(s)}(\mathbf{r}_\ell) \quad (\text{A.13})$$

Au lieu de minimiser $\check{J}^{(s)}$, ce qui risquerait d'induire une certaine instabilité [Briant et al. 2008], une forme stabilisée de la fonction (A.13) est minimisée autour de la meilleure solution connue à l'itération s :

⁹Une explication générale de la méthode est proposée dans cette sous-section. Néanmoins, des détails importants sont omis, le lecteur est donc prié de se reporter au chapitre 6, section 6.4 pour plus d'explications.

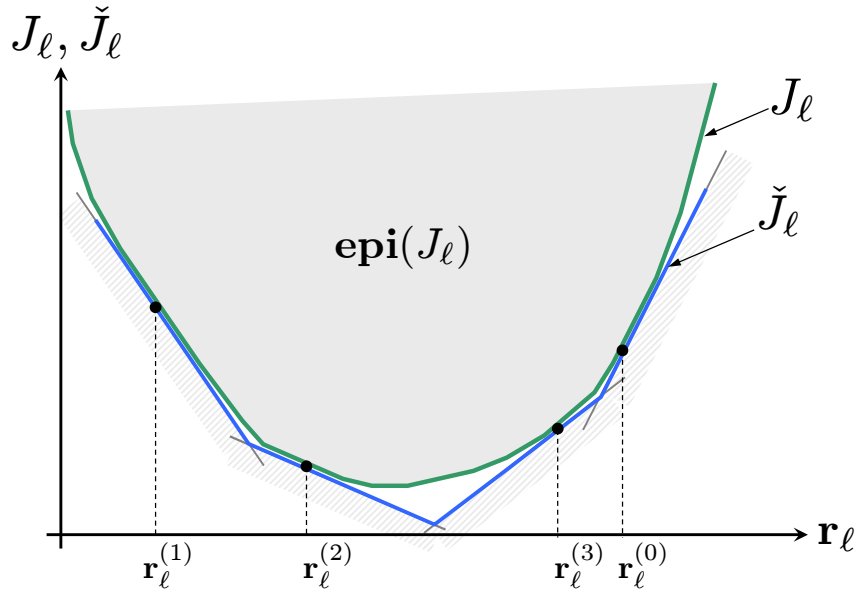


Figure A.10 Approximation par plans coupants de la fonction J_ℓ

Problème d'optimisation A.9. Problème maître stabilisé

$$\mathbf{r}^{(s+1)} \leftarrow \underset{(\mathbf{z}_e, \mathbf{r}_1, \dots, \mathbf{r}_{n_z}) \in \mathcal{D}}{\text{Argmin}} [\check{J}^{(s)}(\mathbf{z}_e, \mathbf{r}) + D^{\gamma^{(s)}}(\mathbf{r} - \bar{\mathbf{r}}^{(s)})] \quad (\text{A.14})$$

Où:

- $\bar{\mathbf{r}}^{(s)}$ est le centre de stabilité qui n'est autre que la meilleure solution obtenue à l'itération s ,
- $D^{\gamma^{(s)}}$ est une fonction distance paramétrisée par le scalaire $\gamma^{(s)}$. Plus précisément $\gamma^{(s)}$ définit une région de confiance autour de laquelle le prochain itéré $\mathbf{r}^{(s+1)}$ doit appartenir (voir figure A.11). Cette région de confiance est augmentée si une amélioration est constatée et diminuée dans le cas contraire.

Dans notre cas, $D^{\gamma^{(s)}}$ est de la forme suivante:

$$D^{\gamma^{(s)}}(\mathbf{r} - \bar{\mathbf{r}}^{(s)}) := \sum_{\ell \in \mathbf{Z}} D_\ell^\gamma(\mathbf{r}_\ell - \bar{\mathbf{r}}_\ell^{(s)}) \quad (\text{A.15})$$

où chaque profil $\bar{\mathbf{r}}_\ell^{(s)}$ désigne la partie du centre de stabilité liée à la zone $\ell \in \mathbf{Z}$.

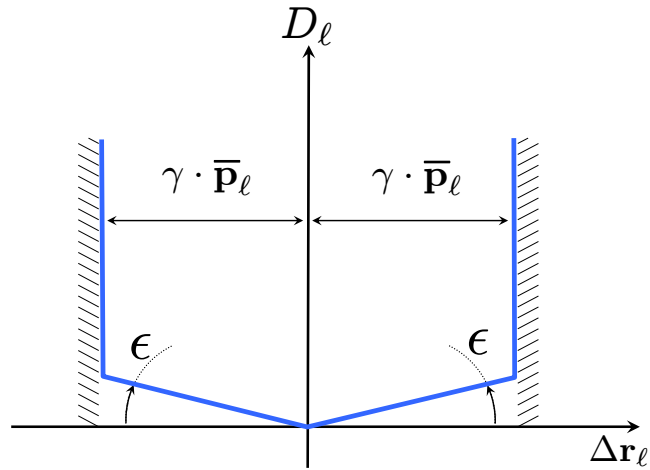


Figure A.11 Stabilization term ($\Delta r_\ell = r_\ell - \bar{r}_\ell^{(s)}$).

Plus précisément:

$$\bar{\mathbf{r}}^{(s)} = \begin{bmatrix} \bar{\mathbf{r}}_1^{(s)} \\ \vdots \\ \bar{\mathbf{r}}_{N_s}^{(s)} \end{bmatrix} \quad (\text{A.16})$$

Le paramètre $\epsilon > 0$ (voir figure A.11) est fixé a priori. Néanmoins, il doit être choisi suffisamment petit pour assurer la convergence de l'algorithme [Frangioni 2002]. \bar{p}_ℓ est la valeur maximale que peut atteindre la puissance consommée par la zone ℓ .

En conclusion, le schéma fonctionnel de commande distribué est illustré figure A.12.

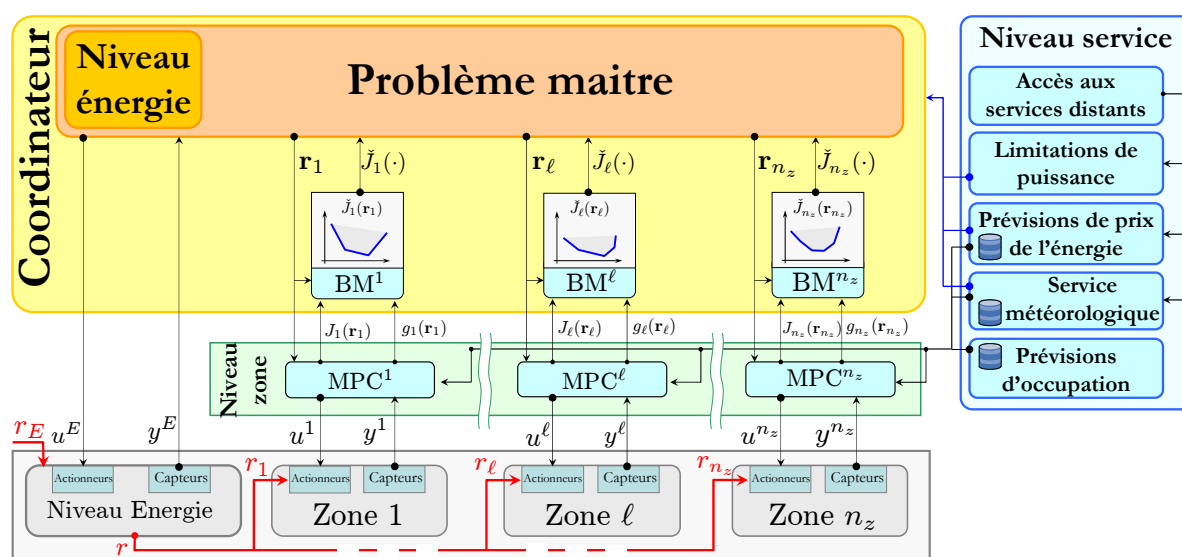


Figure A.12 Commande prédictive distribuée - schéma fonctionnel

A.4.5 Résultats de simulations

La figure A.13 illustre un résultat de simulation sur un bâtiment de 20 zones soumis à une limitation de puissance de 25 [kW] et disposant d'une batterie électrique pouvant stocker 10 [kWh] d'énergie électrique. De plus, il est à noter que le prix de l'énergie est variable, ainsi l'énergie fournie par le réseau est approximativement deux fois moins chère pendant les périodes creuses (22[h] → 6[h] (le lendemain)).

Notons, que le comportement optimal dans ce cas de figure consiste à stocker de l'énergie sous forme électrique pendant les heures creuses afin de le restituer au bâtiment ainsi que de stocker de l'énergie sous forme thermique pendant les périodes (surchauffer le bâtiment) pendant les heures creuses. Constatons tout de plus que ce stockage thermique n'est pas effectué de manière uniforme sur tout le bâtiment, seules les zones disposant d'une meilleure isolation sont surchauffées illustrant ainsi la répartition optimale de ressources mise en œuvre par le coordinateur.

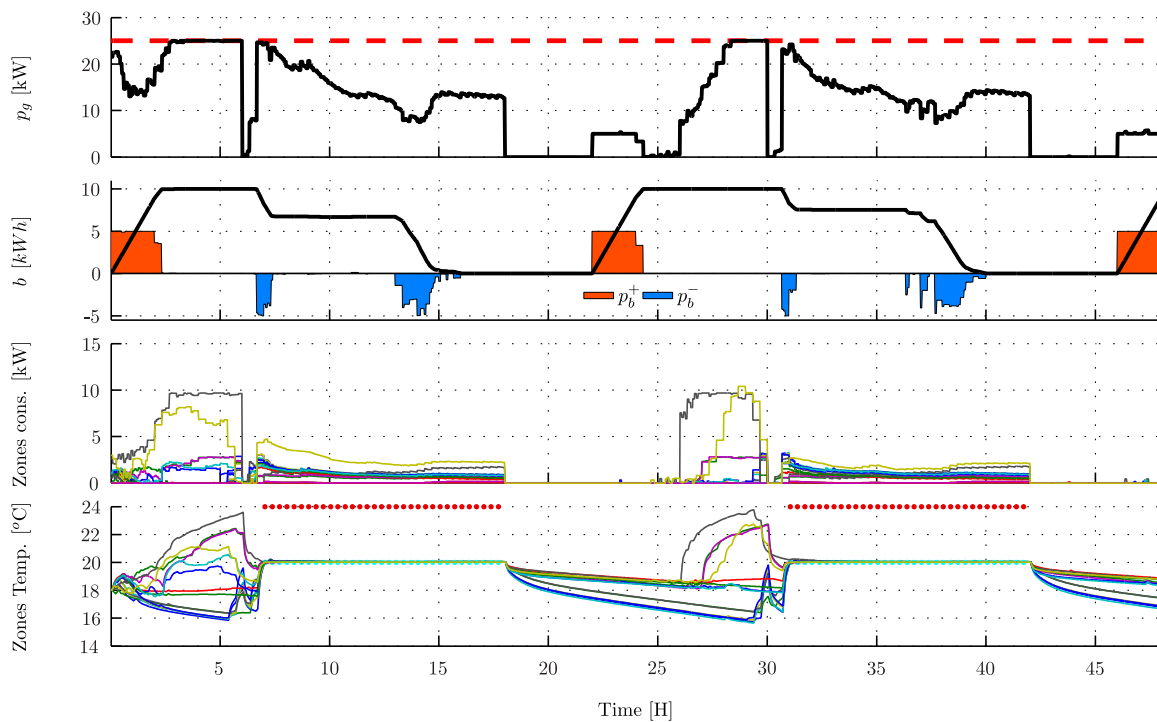


Figure A.13 Simulation de la commande distribuée sur un bâtiment de 20 zones disposant d'une batterie électrique sur 48 [h]. Le nombre d'itérations à chaque instant de décision est de 3.

A.5 Conclusion générale

Cette thèse a été dédiée au développement et l'évaluation d'une commande prédictive distribuée pour la gestion de l'énergie dans le bâtiment ainsi que l'étude de l'embarcabilité de l'algorithme de contrôle sur une cible temps-réel (Roombox - Schneider-Electric).

Il a été proposé l'élaboration d'un schéma de commande distribué pour contrôler les conditions climatiques dans chaque zone du bâtiment. L'objectif étant de contrôler simultanément: la température intérieure, le taux de CO_2 ainsi que le niveau d'éclairage dans chaque zone en agissant sur les équipements présents (CVC, éclairage, volets roulants). Il a été constaté en simulation que celle-ci pouvait générer sur notre cas d'étude approximativement 15 % d'économie d'énergie pour un niveau de confort analogue.

Par ailleurs, le cas des bâtiments multi-sources (par exemple: réseau électrique + production locale solaire), dans lequel chaque source d'énergie est caractérisée par

son propre prix et une limitation de puissance, est pris en compte. Dans ce contexte, les décisions relatives à chaque zone ne peuvent plus être effectuées de façon indépendante. Pour résoudre ce problème, un mécanisme de coordination basé sur une décomposition du problème d'optimisation centralisé a été mis en œuvre. Ce mécanisme permet en un nombre restreint d'itérations d'aboutir à des performances comparables à celle d'une approche centralisée tout en préservant une structure modulaire.

Appendix B

Linear programming problem matrices

$$\mathbf{L} = [(\mathbf{\Gamma}_k^T \cdot \mathcal{A})^T, \rho_0 \cdot \mathbf{1}_{2N \cdot n_y \times 1}, \rho_1 \cdot \mathbf{1}_{2N \cdot n_y \times 1}, \rho_D \cdot \mathbf{1}_{2N \cdot n_u \times 1}]^T \quad (\text{B.1})$$

$$\mathbf{A} = \begin{bmatrix} \Phi(\mathbf{y}_k, \mathbf{w}_k) & -\mathbf{I} & \mathbf{0} & -\mathbf{I} & \mathbf{0} & \mathbf{0} & \mathbf{0} \\ -\Phi(\mathbf{y}_k, \mathbf{w}_k) & \mathbf{0} & \mathbf{I} & \mathbf{0} & \mathbf{I} & \mathbf{0} & \mathbf{0} \\ \mathbf{D} & \mathbf{0} & \mathbf{0} & \mathbf{0} & \mathbf{0} & \mathbf{I} & -\mathbf{I} \\ -\mathbf{D} & \mathbf{0} & \mathbf{0} & \mathbf{0} & \mathbf{0} & -\mathbf{I} & \mathbf{I} \end{bmatrix} \quad (\text{B.2})$$

$$\mathbf{b} = \begin{bmatrix} \bar{\mathbf{y}}_k - \Psi x_k - \Xi \mathbf{w}_k \\ \underline{\mathbf{y}}_k - \Psi x_k - \Xi \mathbf{w}_k \\ \mathbf{a} \\ -\mathbf{a} \end{bmatrix} \quad (\text{B.3})$$

$$\bar{\mathbf{z}} = \begin{bmatrix} \mathbf{1}_{N \cdot n_u \times 1} \\ \infty_{N \cdot n_u \times 1} \\ \infty_{N \cdot n_y \times 1} \\ \delta_y \\ \infty_{N \cdot n_y \times 1} \\ \delta_y \\ \infty_{N \cdot n_u \times 1} \end{bmatrix} \quad (\text{B.4})$$

$$\bar{\mathbf{z}} = \begin{bmatrix} \mathbf{0} \end{bmatrix} \quad (\text{B.5})$$

Appendix C

Prediction errors on d^C and d^L

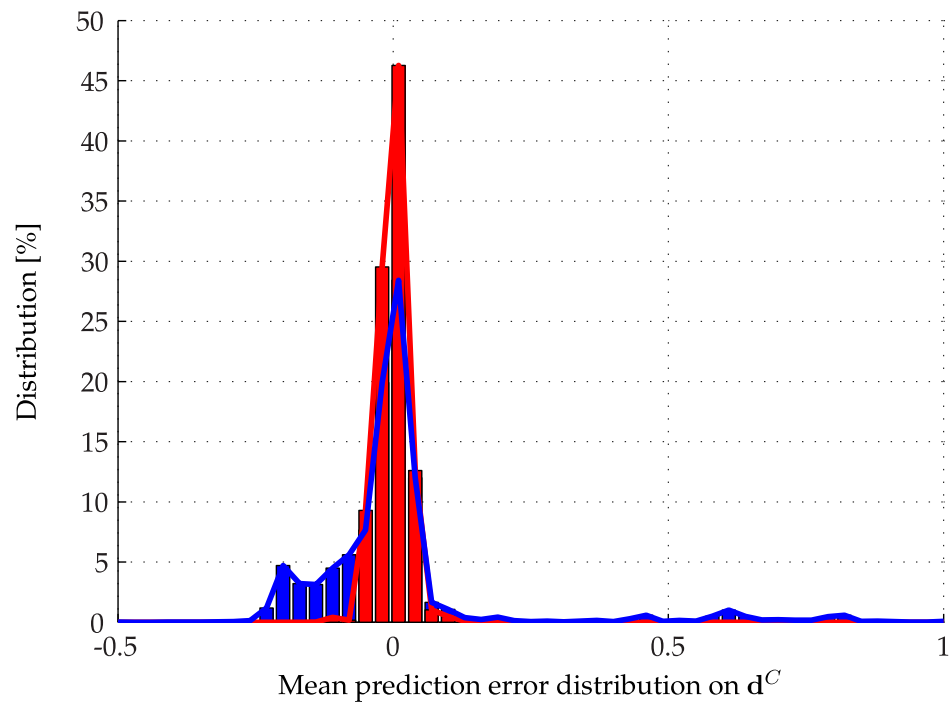


Figure C.1 Prediction errors comparison on d^C between the proposed prediction mechanism (red) and employing the current observed value over the whole prediction horizon ($d^+ = d$) in blue.

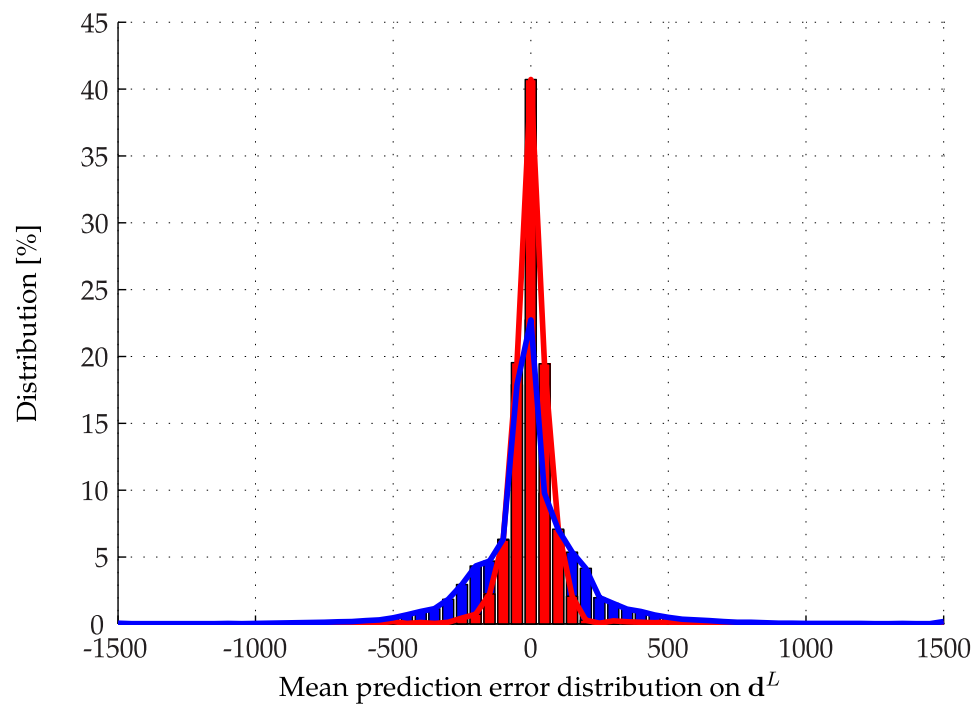


Figure C.2 Prediction errors comparison on d^L between the proposed prediction mechanism (red) and employing the current observed value over the whole prediction horizon ($d^+ = d$) in blue.

Appendix D

Yearly estimated disturbances

On figure D.1, the estimated disturbances obtained for a yearly simulation are presented. Recall that these estimated disturbances represent the errors between the *real* building (Simbad) and the control model embedded in the zone controllers.

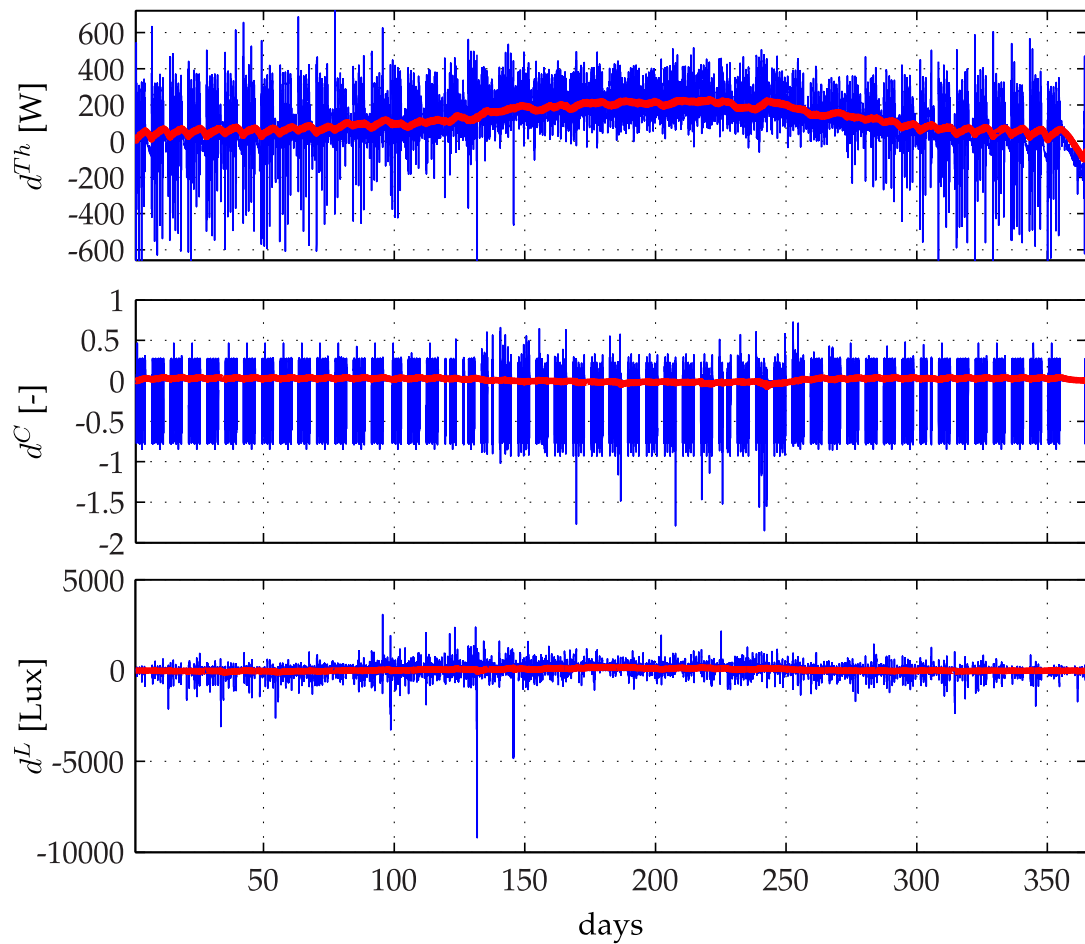


Figure D.1 Estimated disturbances during one year (blue: estimated, red: filtered). Note that the estimated heat flux d^{Th} increases during summer due to the fact that adjacent zones temperatures are larger (which results in receiving more heat).

Appendix E

Computational time for the 20 zones of the building

See figure E.1 (page 208).

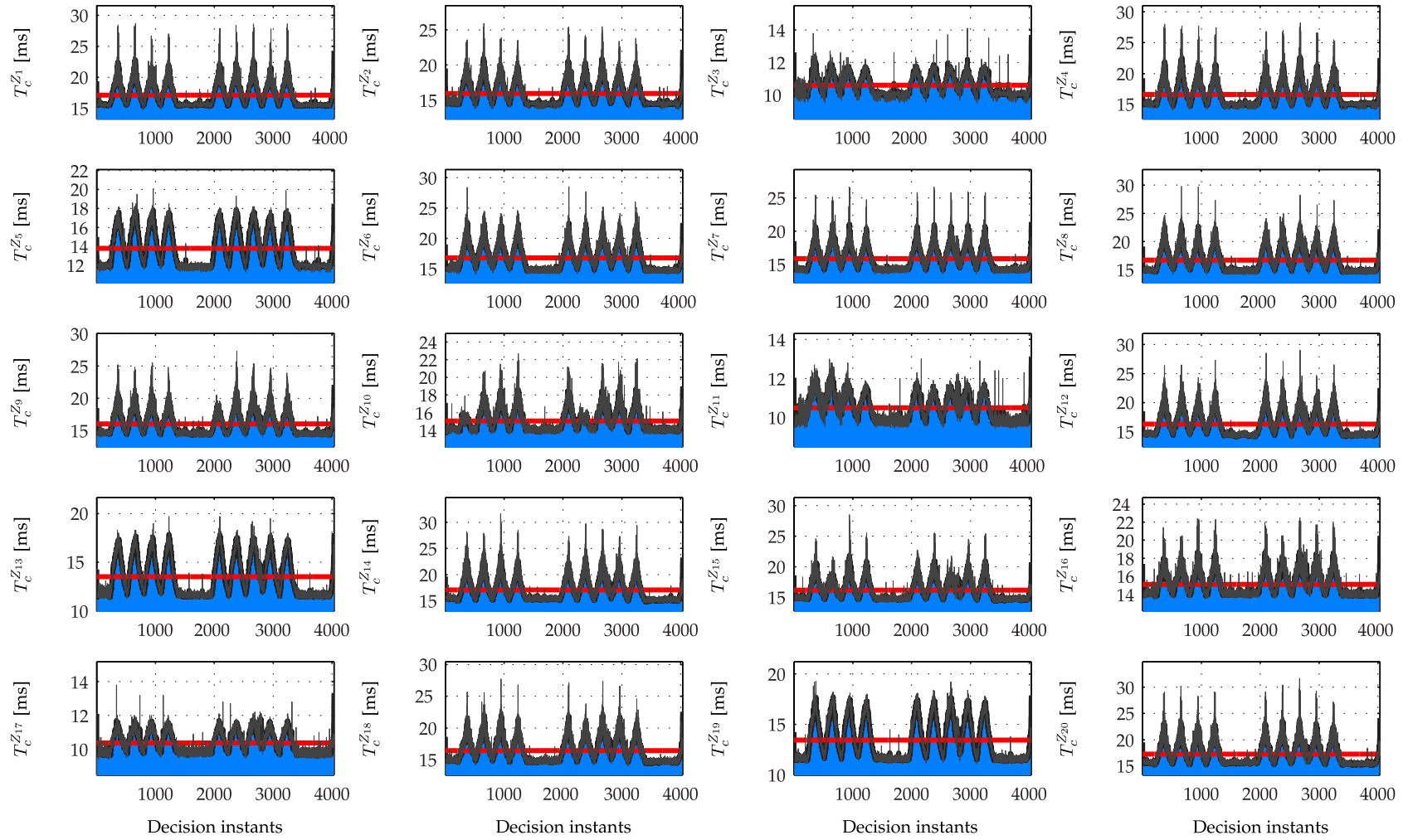


Figure E.1 Computational burden - 20 zones

Appendix F

C code and equivalent M code

Matlab code

```
14 %% Input vector length + 1
15 Nu=size(S.SysB,2);
16 %% Output vector length
17 Ny=length(Z.Outputs);
18 %% State vector length
19 Nx=length(S.InitialState);
20 %% Compute Phi
21 A= S.A;
22 C= S.C;
23 if length(Z.OPToptions.T_Par)==1,
24     Z.OPToptions.T_Par=Z.OPToptions.T_Par:Z.OPToptions.T_Par:Z.OPToptions.H;
25 end
26 if length(Z.OPToptions.T_Con)==1,
27     Z.OPToptions.T_Con=Z.OPToptions.T_Con:Z.OPToptions.T_Con:Z.OPToptions.H;
28 end
29 Phi_yC=zeros(Ny*Z.OPToptions.H,Nx);
30 Phi_yC(1:Ny,1:Nx)=C;
31 for k=2:Z.OPToptions.H,
32     Phi_yC((k-1)*Ny+1:k*Ny,1:Nx)=Phi_yC((k-2)*Ny+1:(k-1)*Ny,1:Nx)*A;
33 end
34 Z.Phi_y=Phi_yC;
```

Appendix F. C code and equivalent M code

```
C++ code
18 // Input vector length + 1
19 int Nu = size(S.SysB, 2);
20 // Output vector length
21 int Ny = length(*Z.Satisfaction(1)) / 2;
22 // state vector length
23 int Nx = length(S.InitialState);
24 // Compute Phi
25 Matrix A = S.A;
26 Matrix C = S.C;
27 if (length(Z.OPToptions.T_Par) == 1)
28     Z.OPToptions.T_Par = IntMatrix(Z.OPToptions.T_Par(1),
29                                     Z.OPToptions.T_Par(1), Z.OPToptions.H);
30 if (length(Z.OPToptions.T_Con) == 1)
31     Z.OPToptions.T_Con = IntMatrix(Z.OPToptions.T_Con(1),
32                                     Z.OPToptions.T_Con(1), Z.OPToptions.H);
33 Matrix Phi_yC = zeros(Ny * Z.OPToptions.H, Nx);
34 Phi_yC.Set(1, 1, C);
35 for (int k = 2; k <= Z.OPToptions.H; k++) {
36     Matrix m = Phi_yC.GetRows((k - 2) * Ny + 1, 1, (k-1) * Ny) * A;
37     Phi_yC.Set((k - 1) * Ny + 1, 1, m); }
38 Z.Phi_y = Phi_yC;
```

Bibliography

- Abras, S. [2009], *Système domotique Multi-Agents pour la gestion de l'énergie dans l'habitat*, PhD thesis, Institut polytechnique de Grenoble.
- Abras, S., Ploix, S., Pesty, S. & Jacomino, M. [2007], A multi-agent home automation approach for power management, *in 'Proceedings of the 1st IFAC Workshop on Convergence of Information Technologies and Control Methods with Power Plants and Power Systems'*, Cluj-Napoca, Romania, pp. 93–98.
- Alamir, M. [2011], 'A framework for real-time implementation of low dimensional parameterized NMPC', *Automatica* **48**, 198 – 204.
- ASHRAE55 - ANSI/ASHRAE Standard 55-2004 - *Thermal Environmental Conditions for Human Occupancy* [2004]. Standard.
- Awad, B., Chaudry, M., Wu, J. & Jenkins, N. [2009], Integrated optimal power flow for electric power, *in '20th International Conference on Electricity Distribution'*.
- Bacaud, L., Lemaréchal, C., Renaud, A. & Sagastizábal, C. [2001], 'Bundle methods in stochastic optimal power management: A disaggregated approach using preconditioners', *Computational Optimization and Applications* **20**, 227–244.
- Bacher, P. & Madsen, H. [2011], 'Identifying suitable models for the heat dynamics of buildings', *Energy & Buildings* **43**, 1511–1522.
- Balan, R., Cooper, J., Chao, K.-M., Stan, S. & Donca, R. [2011], 'Parameter identification and model based predictive control of temperature inside a house', *Energy and Buildings* **43**(2-3), 748 – 758.
- Baltensperger, T. & Ullmann, F. [2009], *Embedding predictive control in hierarchical integrated room automation systems*, Master's thesis, Automatic Control Laboratory (IFA), ETH Zurich and Siemens Building Technologies.
- Bemporad, A. & Morari, M. [1999], 'Control of systems integrating logic, dynamics and constraints', *Automatica* **35**, 497–427.

Bibliography

- Borrelli, Y. M., Hancey, F. & B. Packard, A. B. [2009], Model predictive control of thermal energy storage in building cooling systems, *in* 'Proceedings of the 48th IEEE Conference on Decision and Control, Shanghai, China', pp. 392 – 397.
- Briant, O., Lemaréchal, C., Meurdesoif, P., Michel, S., Perrot, N. & Vanderbeck, F. [2008], 'Comparison of bundle and classical column generation', *Mathematical programming* **113(2)**, 299–344.
- Camponogara, E., Jia, D., Krogh, B. H. & Talukdar, S. [2002], 'Distributed model predictive control', *IEEE Control Systems Magazine* **February**, 44–52.
- Candanedo, J. & Athienitis, A. K. [2009], Application of predictive control strategies in a net zero energy solar house, *in* 'PLEA2009 - 26th Conference on Passive and Low Energy Architecture, Quebec City, Canada'.
- Chen, S., Tsui, K., Wu, H., Hou, Y., Wu, Y.-C. & Wu, F. F. [2012], 'Load/ price forecasting and managing demand response for smart grids', *IEEE Signal Processing Magazine* **68**, 68–84.
- Chen, T. [2001], 'Real-time predictive supervisory operation of building thermal systems with thermal mass', *Energy & Buildings* **33**, 141–150.
- Chen, T. [2002], 'Application of adaptive predictive control to a floor heating system with a large thermal lag', *Energy & Buildings* **34**, 45–51.
- Coffey, B., Haghghat, F., Morofsky, E. & Kutrowski, E. [2010], 'A software framework for model predictive control with genopt', *Energy and Buildings* **42(7)**, 1084 – 1092.
- Collazos, A., Maréchal, F. & Gähler, C. [2009], 'Predictive optimal management method for the control of polygeneration systems', *Computers & Chemical Engineering* **33**, 1584–1592.
- Cooperman, A., Dieckmann, J. & Brodrick, J. [2010], 'using weather data for predictive control', *Ashrae journal* pp. 130–132.
- Dantzig, G. B. & Thapa, M. N. [1997a], *Dantzig G., Thapa M. Linear programming. Vol.1 -Introduction*, Springer.
- Dantzig, G. B. & Thapa, M. N. [1997b], *Dantzig G., Thapa M. Linear programming. Vol.2 -Theory and extensions*, Springer.
- Deng, K., Barooah, P., Mehta, P. G. & Meyn, S. P. [2010], Building thermal model reduction via aggregation of states, *in* 'American Control Conference, Baltimore, MD'.

- Diehl, M. [2009], Report of literature survey, analysis, and comparison of on-line optimization methods for hierarchical and distributed MPC, Hierarchical and Distributed Model Predictive Control of Large-Scale Systems-Deliverable Number: 4.1.1/ Seventh Framework programme theme -ICT.
- Doan, D., Keviczky, T. & Schutter, B. D. [2009], Overview, toolbox and tutorial manual of existing state-of-the-art distributed optimization algorithms, Hierarchical and Distributed Model Predictive Control of Large-Scale Systems-Deliverable Number: 4.1.2/ Seventh Framework programme theme -ICT.
- Dounis, A. & Caraiscos, C. [2009], 'Advanced control systems engineering for energy and comfort management in a building environment-a review', *Energy Conversion & Management* **13**, 1246–1261.
- Emiel, G. & Sagastizábal, C. [2008], Incremental bundle methods for mid-term power planning, in 'International Conference on Engineering Optimization Rio de Janeiro, Brazil'.
- EN15251 -*Indoor environmental input parameters for design and assessment of energy performance of buildings addressing indoor air quality, thermal environment, lighting and acoustics* [2005]. Standard.
- EN ISO 7730 -*Ergonomics of the thermal environment. Analytical determination and interpretation of thermal comfort using calculation of the PMV and PPD indices and local thermal comfort criteria* [2006]. Standard.
- European Commission [2003], *The energy challenge of the 21st century : the role of nuclear energy*, Scientific and Technical Committee Euratom (STC).
- European Commission [2010], *Directive 2010/31/EU of the European Parliament and of The Council of 19 May 2010 on the energy performance of buildings (recast)*, Official Journal of the European Union.
- EuroStat [2010], *Energy, transport and environment indicators*, number ISSN 1725-4566.
- Frangioni, A. [2002], 'Generalized bundle methods', *SIAM Journal of Optimization* **13** (1), 117–156.
- Freire, R. Z., Oliveira, G. H. C. & Mendes, N. [2005], Development of single-zone predictive equations using linear regression for advanced controllers synthesis, in 'Building Simulation, Montréal, Canada'.
- Freire, R. Z., Oliveira, G. & Mendes, N. [2008], 'Predictive controllers for thermal comfort optimization and energy savings', *Energy & Buildings* **40**, 1353–1365.

Bibliography

- Griffith, R. E. & Stewart, R. A. [1961], 'A nonlinear programming technique for the optimization of continuous processing systems', *Management Science* 7, 379–392.
- Grothey, A. [2001], *Decomposition Methods for Nonlinear Nonconvex Optimization Problems*, PhD thesis, The University of Edinburgh.
- Gwerder, M. & Tödli, J. [2007], 'Patent, device for controlling the room temperature in building using a predictive control device'.
- Gwerder, M. & Tödli, J. [2009], 'Patent, system for controlling room temperature in building using predictive control'.
- Gyalistras, D. & Gwerder, M. [2010], *Use of weather and occupancy forecasts for optimal building climate control (opticontrol): Two years progress report*.
- Gyalistras, D. & Team, T. O. [2010], *Use of weather and occupancy forecasts for optimal building climate control- opticontrol, final report*.
- Ha, L. D., Ploix, S., Zamaï, E. & Jacomino, M. [2008], 'Realtimes dynamic optimization for demand-side load management', *International Journal of Management Science and Engineering Management* 3(4), 243–252.
- Henze, G. P., Kalz, D. E., Felsmann, C. & Knabe, G. [2004], 'Impact of forecasting accuracy on predictive optimal control of active and passive building thermal storage inventory', *HVAC & R Research* 10 (2), 153–178.
- Henze, G. P. & Krarti, M. [2005], *Predictive optimal control of active and passive building thermal storage inventory-final report, Cooperative Agreement DE-FC26-01NT41255/ University of Nebraska-Lincoln and University of Colorado at Boulder*.
- Houwing, M., Negenborn, R., Heijnen, P., Schutter, B. D. & Hellendoorn, H. [2007], *Least-cost model predictive control of residential energy resources when applying micro chp*, in 'Power Tech, Lausanne, Switzerland', number 291.
- IEA [2011a], *Key world energy statics*. International Energy Agency.
- IEA [2011b], *World energy outlook*. International Energy Agency.
- Jaluria, Y. [2007], *Design and Optimization of Thermal Systems - Second Edition*, number ISBN 978-0-8493-3753-6, CRC press.
- Jung, O. [2009], *Approche Multicritère numérique et expérimentale de la ventilation et rafraîchissement d'un multizone par controle de composants de façade*, PhD thesis, Institut National des sciences appliquées de Lyon.

- Kelley, J. E. [1960], 'The cutting plane method for solving convex programs', *Journal of the SIAM* **8**, 703–712.
- Kolokotsa, D., Pouliezos, A., Stavrakakis, G. & Lazos, C. [2009], 'Predictive control techniques for energy and indoor environmental quality management in buildings', *Building and Environment* **44**, 1850–1863.
- Koutsopoulou, I. & Tassioulas, L. [2010], Control and optimization meet the smart power grid: Scheduling of power demands for optimal energy management, in 'arXiv:1008.3614v1'.
- Landau, I. D. & Zito, G. [2006], *Digital Control Systems Design, Identification and Implementation*, number ISBN-10: 1846280559, Springer.
- Le, K. [2008], Gestion optimale des consommations d'énergie dans les bâtiments, PhD thesis, Institut Polytechnique de Grenoble et Université de Danang.
- Lemaréchal, C. [1974], An algorithm for minimizing convex functions, in 'Information Processing '74, North Holland', pp. 552–556.
- Ma, Y., Anderson, G. & Borrelli, F. [2011], A distributed predictive control approach to building temperature regulation, in 'American Control Conference (ACC), San Francisco, CA', pp. 2089 – 2094.
- Ma, Y., Borrelli, F. & Richter, S. [2012], *Distributed Model Predictive Control for building thermal regulation*, SIAM Book on Control and Optimization with Differential-Algebraic Constraints.
- Mahdavi, A. & Pröglhöf, C. [2009], Toward empirically-based models of people's presence and actions in buildings, in 'IBPSA Conference', IBPSA, pp. 537–544.
- Malisani, P., Chaplais, F., Petit, N. & Feldmann, D. [2010], Thermal building model identification using time-scaled identification methods, in '49th IEEE Conference on Decision and Control, Atlanta, USA'.
- Maor, I. & Reddy, A. [2008], Near-optimal scheduling control of combined heat and power systems for buildings / ASHRAE research project 1340-rp-final report.
- Mattingley, J., Wang, Y. & Boyd, S. [2010], Code generation for receding horizon control, in 'IEEE international symposium on computer-aided control system design. Yokohama, Japan'.
- Mayne, D. Q., Rawlings, J. B., Rao, C. V. & Sokaert, P. O. M. [2000], 'Constrained model predictive control: Stability and optimality', *Automatica* **36**, 789–814.

Bibliography

- Moroşan, D.-P., Bourdais, R., Dumur, D. & Buisson, J. [2011], Distributed MPC for multi-zone temperature regulation with coupled constraints, *in '18th IFAC World Congress, Milano, Italy'*.
- Moroşan, P.-D., Bourdais, R., Dumur, D. & Buisson, J. [2010a], 'Building temperature regulation using a distributed model predictive control', *Energy & Buildings* **42**, 1445 – 1452.
- Moroşan, P.-D., Bourdais, R., Dumur, D. & Buisson, J. [2010b], Distributed model predictive control based on Benders' decomposition, *in '49th IEEE Conference on Decision and Control, Atlanta, USA'*.
- Mustafaraja, G., Chena, J. & Lowry, G. [2010], 'Development of room temperature and relative humidity linear parametric models for an open office using BMS data', *Energy & Buildings* **42**, 348–356.
- Negenborn, R., Houwing, M., De Schutter, B. & Hellendoorn, J. [2009], Model predictive control for residential energy resources using a mixed-logical dynamic model, *in 'IEEE International Conference on Networking, Sensing and Control, Okayama, Japan'*.
- Negenborn, R., Schutter, B. D. & Hellendoorn, J. [2004], Multi-agent model predictive control: A survey, *in 'Technical report 04-010 -Delft Center for Systems and Control -Delft University of Technology'*.
- Nygård-Ferguson, A.-M. [1990], Predictive Thermal Control Of Building Systems, PhD thesis, Ecole Polytechnique Federale de Lausanne.
- Oldewurtel, F. [2011], Stochastic Model Predictive Control for Energy Efficient Building Climate Control, PhD thesis, ETH Zurich.
- Oldewurtel, F., Gyalistras, D., Gwerder, M., Jones, C. N., Parisio, A., Stauch, V., Lehmann, B. & Morari, M. [2010], Increasing energy efficiency in building climate control using weather forecasts and model predictive control, *in '10th REHVA World Congress Clima', Antalya, Turkey*.
- Oldewurtel, F., Jones, C. N. & Morari, M. [2008], A tractable approximation of chance constrained stochastic MPC based on affine disturbance feedback, *in '47th IEEE Conference on Decision and Control', Cancun, Mexico*.
- Page, J. [2007], Simulating occupant presence and behaviour in buildings, PhD thesis, Ecole Polytechnique Fédérale de Lausanne.
- Parisio, A. [2009], Handling Uncertainty with Application to Indoor Climate Control and Resource Allocation Planning, PhD thesis, University of Sannio.

- Qin, S. J. & Badgwell, T. A. [2003], 'A survey of industrial model predictive control technology', *Control Engineering Practice* **11**, 733–764.
- Rao, C. & Rawlings, J. [2000], 'Linear programming and model predictive control', *Journal of Process Control* **10**, 283–289.
- Rawlings, J. B. & Stewart, B. T. [2008], 'Coordinating multiple optimization-based controllers: New opportunities and challenges', *8th International IFAC Symposium on Dynamics and Control of Process Systems. Cancun, Mexico*. **18**, 839–845.
- Riederer, P. [2001], Thermal Room Modeling Adapted To The Test Of HVAC Control Systems, PhD thesis, Ecole des Mines de Paris.
- Riederer, P., Marchio, D., Visier, J. C., Husaunndee, A. & Lahrech, R. [2001], Influence of sensor position in building thermal control: development and validation of an adapted zone model, in 'Seventh International IBPSA Conference, Rio de Janeiro, Brazil.'
- Riederer, P., Marchio, D., Visier, J., Husaunndee, A. & Lahrech, R. [2002], 'Room thermal modelling adapted to the test of hvac control systems', *Building & Environment* **37**, 777–790.
- Riederer, P., Marchio, Visier, P. G. J., Lahrech, R. & Husaunndee, A. [2000], Building zone modeling adapted to the study of temperature control systems, in 'ASHRAE/CIBSE conference, Dublin, Ireland.'
- Romanos, P. [2007], Thermal Model Predictive Control for Demand Side Management for Cooling Strategies, PhD thesis, University of Kassel.
- Saad, W., Han, Z., Poor, V. & T., B. [2012], 'Game-theoretic methods for the smart grid', *IEEE Signal Processing Magazine* **68**, 86–104.
- Scheu, H., Calderon, J. C., Doan, D., Garcia, J. F., Negenborn, R., Tarau, A., Arroyave, F. V., Schutter, B. D., Espinosa, J. J. & Marquardt, W. [2009], Report on assessment of existing coordination mechanisms for simple case studies, and on possible options for improving and extending these coordination mechanisms, Hierarchical and Distributed Model Predictive Control of Large-Scale Systems-Deliverable Number: 3.3.1/ Seventh Framework programme theme -ICT.
- Scheu, H. & Marquardt, W. [2009], Report on literature survey on hierarchical and distributed nonlinear MPC, including analysis and comparison, and description of the resulting methodological framework, Hierarchical and Distributed Model Predictive Control of Large-Scale Systems-Deliverable Number: 3.1.1/ Seventh Framework programme theme -ICT.

Bibliography

- Scheu, H., Marquardt, W., Doan, M., Keviczky, T., Schutter, B. D., Moroşan, P.-D., Bourdais, R., Dumur, D., Buisson, J., Limon, D., Maestre, J., de la Pena, D. M., Camacho, E., Espinosa, J., Marquez, A., Garcia, J. & Arroyave, F. V. [2010], Report on new methods for complex control problems (nonlinear, dynamic, constrained), Hierarchical and Distributed Model Predictive Control of Large-Scale Systems-Deliverable Number: 3.1.3/ Seventh Framework programme theme - ICT.
- Siroky, J., Privara, S. & Ferkl, L. [2010], Model predictive control of building heating system, *in* '10th REHVA World Congress Clima'.
- Stauch, V., Hug, C., Schubiger, F. & Steiner, P. [2010], Weather forecasts, observations and algorithms for building simulation and predictive control (contributions by meteoswiss for the 3rd year of opticontrol).
- U.S. Congress [1992], *Building Energy Efficiency*, Washington, DC: U.S. Government Printing Office.
- Virk, G. & J.Y.M.Cheung [1995], 'Practical stochastic multivariate identification for buildings', *Appl. Math. Modeling* **19**, 622–636.
- Zavala, V., Constantinescu, E., Krause, T. & Anitescu, M. [2009], Report: Weather forecast-based optimization of integrated energy systems, *in* 'Argonne National Laboratory'.

"Distributed Model Predictive Control for energy management in buildings"

Ph.D. thesis - Grenoble University

Mohamed Yacine LAMOUDI

Buildings represent more than 40 % of world-wide energy consumption. Even if several control strategies have been proposed to enhance energy management systems in buildings, this issue remains essentially open.

This thesis is concerned with the development and assessment of Model Predictive Control (MPC) algorithms for energy management in buildings. In this work, a study of implementability of the control algorithm on a real-time hardware target is conducted beside yearly simulations showing a substantial energy saving potential. The thesis explores also the ability of MPC to deal with the diversity of *complex* situations that could be encountered (varying energy price, power limitations, local storage capability, large scale buildings).

This thesis proposes the design of a distributed predictive control scheme to control the indoor conditions in each zone of the building and manage resource constraints in the context of multi-source buildings. This CIFRE Ph.D. thesis was prepared within the Gipsa-lab laboratory in partnership with Schneider-Electric in the scope of the HOMES program (www.homesprogramme.com).

"Commande prédictive distribuée pour la gestion de l'énergie dans les bâtiments"

Thèse de Doctorat - Université de Grenoble

Mohamed Yacine LAMOUDI

Les bâtiments consomment plus de 40 % de l'énergie mondiale. Bien que nombre de propositions pour améliorer la gestion de l'énergie dans les bâtiments aient été avancées, cette problématique demeure essentiellement ouverte.

Cette thèse porte sur le développement et l'évaluation d'une commande prédictive pour la gestion de l'énergie dans le bâtiment ainsi que l'étude de l'embarcabilité de l'algorithme de contrôle sur une cible temps-réel (Roombox - Schneider-Electric). En plus des divers simulations montrant l'intérêt d'une telle approche, ce travail explore aussi la capacité de la commande prédictive à s'adapter à des scénarii *complexes* (prix variable de l'énergie, bâtiments multi-sources, contraintes de ressources, stockage d'énergie, ...).

Ce travail propose l'élaboration d'une architecture de commande distribuée pour contrôler les paramètres de confort dans chaque zone du bâtiment sous respect de contraintes de ressources globales. Cette thèse CIFRE a été préparée au sein du laboratoire Gipsa-lab en partenariat avec Schneider-Electric dans le cadre du programme HOMES (www.homesprogramme.com).
